UNIVERSITY OF CALIFORNIA,
IRVINE

Design and Development of Isobactins: Prodrugs of Teixobactin and Teixobactin Derivatives

DISSERTATION

submitted in partial satisfaction of the requirements
for the degree of

DOCTOR OF PHILOSOPHY

in Chemistry

by

Chelsea Rae Jones

Dissertation Committee:
Professor James S. Nowick, Chair
Professor Elizabeth N. Bess
Professor David L. Van Vranken

2024

DEDICATION

To

my family and my friends,

I don’t know how I would have done it without your love and support

you are what kept me going

TABLE OF CONTENTS

LIST OF FIGURES

LIST OF TABLES

LIST OF SCHEMES

ACKNOWLEDGEMENTS

I would not have been able to make it through my graduate school career without the help and support from so many beautiful people. I would first like to express my appreciation to my advisor, Professor James S. Nowick. James, I am grateful for your support on my project and all the advice you provided to my research. Your enthusiasm towards my research helped keep me focused and determined even when the research was tough. I will always be grateful for the guidance you provided, the freedoms you gave me, and the knowledge you passed along to me.

To the members of the Nowick lab, both past and present, thank you for all that you have done for me. To my mentors and friends who have graduated, you all taught me skills that have carried me through my graduate career. To Tuan, Xing, Gretchen, Maj, and Chelsea, thank you for being dear friends during your time here and all your support. Our lunch time breaks, long weekends in lab, and everything in between, will always be treasured memories. To Sarah, we joined this lab together and now we leave it together and I'm grateful to have been on this journey with you. To my friends still in the lab, Jason and Sophie, I thank you both for your patience and friendship through some of my most trying times in my graduate career. Sophie, our constant banter, mental health walks, funny videos, and more, always lifted me up when I was down. I know you both will continue to succeed during your time in grad school, and I am excited to hear about all your accomplishments. To my friends in other labs, especially Nadia, I thank you for always providing an outlet and keeping me positive. Our game nights, breakfast dates, Angels games, and all other activities help me escape from the lab and focus on taking care of myself. Nadia, I first met you during our visit weekend and on the first day of orientation you came up to me and helped me feel a little less alone. We joined neighboring labs, and even though we didn't talk every day, you were always there to be a sounding board during the tough times. I am forever grateful to you all for your friendship and support and I am so excited for our futures.

I also need to acknowledge Grant Lai, my undergraduate student who played one of the greatest roles in my graduate career. You joined me as a freshman, without even having taken your first college organic chemistry class. The way you stepped up and took initiative to learn the fundamentals to understand my research will always impress me. You helped me complete so much in my time here and took on projects of your own to support my work. Thank you for all your hard work, I will forever be grateful, and I know you will succeed at anything you do in life.

To my family, I could not have done any of this without you, all of you. Mom and Dad, your unwavering support in my decision to pursue a Ph.D. along with your advice and random text messages of love always helped me keep my head up. To Ryan, Jaquel, and the kiddos, your kind words, updates on Vi and Hugh, and the time I got to spend with you all every Christmas will always hold a special place in my heart. To Caitlin (and Oly), our random FaceTime calls while I was at work to our snail mail always helped me laugh through the pain and reminded me, I mattered. You have always been one on of my biggest cheerleaders in life. Your support and love are endless, and I am so lucky to have parents and siblings like you all. I cannot express how deeply appreciative I am of you all. To Eric, although you aren't technically family, you will always be my dearest friend. Your visits and constant affirmation always helped me keep one foot in front of the other. And to Matt, you entered my life like a blazing star during a dark time and guided me back to the light. Our weekend adventures from errands, coffee dates, outdoor excursions, and more, helped me remember what is important in life. Your support is steadfast, your patience endless, and I am profoundly appreciative of you. I love and appreciate you all and thank you from the bottom of my heart!

VITA

Chelsea Rae Jones

Education

University of California, Irvine (Irvine, CA) 2019–2024
Ph.D. Candidate, Chemistry

University of Utah (Salt Lake City, UT) 2014–2018
Bachelor of Science, Chemistry – Biology Emphasis

Skills

Chemical Biology and Organic Chemistry:

- Solid-phase peptide synthesis, HPLC purification of peptides, bacterial and mammalian cell culture, minimum inhibitory concentration (MIC) assay, cytotoxicity assay, hemolytic assay, liposome preparation and dye leakage assay, serum stability studies, small molecule synthesis.

Analytical Chemistry:

- Agilent analytical HPLC 1200 and 1260 use and maintenance, Shimadzu and Rainin Dynamax preparative HPLC use and maintenance, Biotage Isolera One system use, mass spectrometry (Sciex MALDI TOF/TOF 5800, Waters QDa, LCT Premier, Xevo G2-XS, QQQ MS Systems), 1D (^{1}H, ^{13}C, ^{19}F, ^{31}P) NMR spectroscopy.

Professional Experience

Graduate Student Researcher – University of California, Irvine 2020–2024
Professor James S. Nowick

- Spearheaded the design, synthesis, and evaluation of teixobactin prodrug analogues.
- Executed the solid-phase synthesis, HPLC purification, and chemical and biological analysis of numerous peptide antibiotics including teixobactin analogues, fluorescent teixobactin analogues, and novel peptide antibiotics.
- Synthesis and evaluation of small molecules used in peptide synthesis and the synthesis of a noncanonical amino acid.

Post-Baccalaureate & Undergraduate Researcher – University of Utah 2017–2019
Synthetic & Medicinal Chemistry Core, Dr. Paul Sebahar & Dr. Ryan Looper

- Participated in research for the development of a TRPV4 antagonist through synthetic organic chemistry.
- Synthesis of several small molecules using a variety of synthetic routes and reactions.
- Purification of molecules through both column chromatography and flash chromatography on a Teledyne ISCO CombiFlash system.
- Analysis of organic molecules through 1D NMR and LCMS.

Spectral TA – University of Utah 2018–2019

- Ran NMR samples for multiple undergraduate labs.
- Obtained training on three NMR instruments including Varian Unity 300 Spectrometer, Inova 400 Spectrometer, and Varian VXR 500 Spectrometer.
- Obtained ^{1}H, ^{13}C, ^{19}F, and paramagnetic NMR spectra and processed in both Mestrenova and ACD Labs NMR software.

Publications and Patents

Jones, C. R.; Lai, G. H.; Padilla, M. S. T. L.; Nowick, J. S. Investigation of Isobactin Analogues of Teixobactin. **Manuscript submitted**.

Jones, C. R.; Guaglianone, G.; Lai, G. H.; Nowick, J. S. Isobactins: *O*-Acyl Isopeptide Prodrugs of Teixobactin and Teixobactin Derivatives. *Chem. Sci.*, **2022**, *13*, 13110–13116.

Krumberger, M.[*]; Li, X.[*]; Kreutzer, A. G.; Peoples, A. J.; Nitti, A. G.; Cunningham, A. M.; **Jones, C. R.**; Achorn, C.; Ling, L. L.; Hughes, D. E.; Nowick, J. S. Synthesis and Stereochemical Determination of the Peptide Antibiotic Novo29. *J. Org. Chem.*, **2023**, *88*, 2214–2220.
[*]These authors contributed equally

Shukla, R.; Lavore, F.; Maity, S.; Derks, M. G. N.; **Jones, C. R.**; Vermeulen, B. J. A.; Melcrová, A.; Morris, M. A.; Becker, L. M.; Wang, X.; Kumar, R.; Medeiros-Silva, J.; van Beekveld, R. A. M.; Bonvin, A. M. J. J.; Lorent, J. H.; Lelli, M.; Nowick, J. S.; MacGillavry, H. D.; Peoples, A. J.; Spoering, A. L.; Ling, L. L.; Hughes, D. E.; Roos, W. H.; Breukink, E.; Lewis, K.; Weingarth, M. Teixobactin Kills Bacteria by a Two-Pronged Attack on the Cell Envelope. *Nature*, **2022**, *608*, 390–396.

Morris, M. A.; Vallmitjana, A.; Grein, F.; Schneider, T.; Arts, M.; **Jones, C. R.**; Nguyen, B. T.; Hashemian, M. H.; Malek, M.; Gratton, E.; Nowick, J. S. Visualizing the Mode of Action and Supramolecular Assembly of Teixobactin Analogues in Bacillus Subtilis. *Chem. Sci.*, **2022**, *13*, 7747–7754.

Morris, M. A.; **Jones, C. R.**; Nowick, J. S. Synthesis and Application of Fluorescent Teixobactin Analogues. *Method. Enzymol.*, **2022**, *665*, 233–258.

Samdin, T. D.; **Jones, C. R.**; Guaglianone, G.; Kreutzer, A. G.; Freites, J. A.; Wierzbicki, M.; Nowick, J. S. A β-Barrel-Like Tetramer Formed by a β-Hairpin Derived From Aβ. *Chem. Sci*.**, 2024,** *15,* 285–297.
Hurst, P. J.; Gassaway, K. J., Abouchaleh, M. F.; Idris, N. S.; **Jones, C. R.**; Dicksion, C. A.; Nowick, J. S.; Patterson, J. P. Drug Catalyzed Polymerization Yields One Pot Nanomedicines. *RSC Appl Polym.,* **2024.** *2*, 238-247.

"Prodrugs of Antibiotic Teixobactin", **Jones, C. R.**; Nowick, J. S. Provisional Patent Application No. 63/241,920 filed September 8, 2021. (UC Case # 2022-718).

"Prodrugs of Antibiotic Teixobactin", **Jones, C. R.**; Nowick, J. S. Provisional Patent Application No. 63/364,690 filed May 13, 2022. (UC Case # 2022-718-2).

Presentations

Jones, C. R.; Guaglianone, G.; Lai, G. H.; Nowick, J. S. Isobactins: *O*-Acyl Isopeptide Prodrugs of Teixobactin and Teixobactin Derivatives. October 2023
Presented at the 18th Annual Peptide Therapeutics Symposium Poster Session at the Scripps Seaside Forum, La Jolla, CA.

Jones, C. R.: Guaglianone, G.; Lai, G. H.; Nowick, J. S. Isobactins: *O*-Acyl Isopeptide Prodrugs of Teixobactin and Teixobactin Derivatives. June 2023
Presented at the 28th American Peptide Symposium Poster Session, Scottsdale, AZ.

Jones, C. R.; Guaglianone, G.; Lai, G. H.; Nowick, J. S. Isobactins: *O*-Acyl Isopeptide Prodrugs of Teixobactin and Teixobactin Derivatives. October 2022
Presented at the Gordon Research Seminar and the Gordan Research Conference Poster Sessions, Oxnard, CA.

Jones, C. R.; Guaglianone, G.; Lai, G. H.; Nowick, J. S. Isobactins: *O*-Acyl Isopeptide Prodrugs of Teixobactin and Teixobactin Derivatives. August 2022
Presented as an oral presentation at the AbbVie Scholars Symposium 2022 (virtual).

Jones, C. R.; Guaglianone, G.; Lai, G. H.; Nowick, J. S. Isobactins: *O*-Acyl Isopeptide Prodrugs of Teixobactin and Teixobactin Derivatives. June 2022
Presented at the 27th American Peptide Symposium Poster Session and Flash Talk, Whistler, BC.

Jones, C. R.; Nowick, J. S. Teixobactin *O*-acyl isopeptide prodrugs exhibit a reduced propensity to aggregate while maintaining comparable antibiotic activity. October 2021
Presented at the 16th Annual Peptide Therapeutics Symposium Poster Session and Flash Talk at The Salk Institute, La Jolla, CA.

Mentorship and Leadership

Chemistry Teaching Assistant Mentoring Program (Irvine, CA) 2021–2024

- Conducted orientation TA training and met with mentees twice a quarter to prepare for teaching assignments, set goals, develop good teaching practices, discuss mid-quarter feedback, and reflect on progress in teaching.
- Attended professional development training before training and guiding mentees.
- Participated in program as a mentee during 1st year of my graduate program.

Mentor to undergraduate research associate (Irvine, CA) 2022–2024

- Mentored an undergraduate student in the Nowick group. Supervised and taught solid-phase peptide synthesis, peptide purification, bacterial cell culture, mammalian cell culture, MIC assay, and analytical chemistry methods such as TLC, MS, NMR. This has guided the mentee to pursue an MD/Ph.D. program after graduation in Spring 2025.

Awards and Honors

- Recipient of the *2024 Contributions to the Chemistry Department Teaching Program by a TA – Continuing* Award, **2024**.
- Recipient of the *Allergan Graduate Fellowship in Organic Chemistry* in the UCI Department of Chemistry, **2023/24** (awarded to one graduate student annually and provides one quarter of funding).
- Selected as the *AbbVie Scholars Symposium nominee* from UCI, **August 2022**.
- Winner of *The Dr. Elizabeth A. Schram Award* for the 2022 Young Investigator Poster Competition at the 27th American Peptide Symposium, **2022**.
- Awarded several *Travel Grant Awards* to present my research at various conferences including: the 16th and 18th Annual Peptide Therapeutics Symposium in **2021** and **2023**, and the 27th American Peptide Symposium in **2022**.
- Member of the New University Scholars program where I received the *New University Scholars two-year scholarship*, **Fall 2014-Spring 2016**.
- Awarded the *BlockU Certificate in Medical Humanities*, **May 2015**.

Teaching

Teaching Assistant (Irvine, CA) 2019–2024

- Chem 51LD, Organic Chemistry Lab, Fall 2019
- Chem 51LB, Organic Chemistry Lab, Winter 2020, Winter 2022
- Chem 51LC, Organic Chemistry Lab, Spring 2020, Summer 2020, Fall 2020

Head Teaching Assistant/Developmental TA (Irvine, CA) 2020–2024

- Chem 51LC, Organic Chemistry Lab, Summer Session II 2020
- Chem M52LA, Majors Organic Chemistry Lab, Fall 2023. Developed an experiment for the M52LC course.
- Chem M52LB, Majors Organic Chemistry Lab, Winter 2024.

ABSTRACT OF THE DISSERTATION

Design and Development of Isobactins: Prodrugs of Teixobactin and Teixobactin Derivatives
by

Chelsea Rae Jones

Doctor of Philosophy in Chemistry

University of California, Irvine, 2024

Professor James S. Nowick, Chair

In my thesis I aim to develop novel antibiotics in the fight against Gram-positive bacteria. In Chapter 1, I summarize the outlook of antibiotic resistance and how a new antibiotic, teixobactin, serves as a promising antibiotic candidate for drug development. I provide a summary on the mechanism of action of teixobactin, structure-activity relationship studies of teixobactin, and the limitations of teixobactin as an antibiotic drug candidate. In the last section of Chapter 1, I review isoacyl motifs and their use in the development of prodrugs and in the synthesis of aggregation-prone peptide sequences.

In Chapter 2, I introduce my work in the design and development of *O*-acyl isopeptide prodrugs of teixobactin analogues, which we have termed *isobactins*, to overcome the limitations of teixobactin. The antibiotic teixobactin is a promising drug candidate against drug-resistance pathogens, such as MRSA and VRE, but forms insoluble gels that may limit intravenous administration. *O*-Acyl isopeptide prodrug analogues of teixobactin circumvent the problem of gel formation while retaining antibiotic activity. The teixobactin prodrug analogues contain ester linkages between Ile_6 and Ser_7, Ile_2 and Ser_3, or between both Ile_6 and Ser_7 and Ile_2 and Ser_3. Upon exposure to physiological pH, the prodrug analogues undergo clean conversion to the corresponding amides, with half-lives between 13 and 115 min. Prodrug analogues containing

lysine, arginine, or leucine at position 10 exhibit good antibiotic activity against a variety of Gram-positive bacteria while exhibiting little or no cytotoxicity or hemolytic activity. Because *O*-acyl isopeptide prodrug analogues of teixobactin exhibit clean conversion to the corresponding teixobactin analogues with a reduced propensity to form gels, it is anticipated that teixobactin prodrugs will be superior to teixobactin as drug candidates.

In Chapter 3, I present my work in the investigation of additional isobactin analogues of teixobactin. I present nine new isobactin analogues that exhibit a reduced propensity to form gels in aqueous conditions while maintaining potent antibiotic activity against MRSA, VRE, and other Gram-positive bacteria. These isobactin analogues contain commercially available amino acid residues at position 10, replacing the synthetically challenging L-*allo*-enduracididine residue that is present in teixobactin. The isobactins undergo clean conversion to their corresponding teixobactin analogues at physiological pH and exhibit little to no hemolytic activity or cytotoxicity. Because isobactin analogues exhibit enhanced solubility, delayed gel formation, and are more synthetically accessible, it is anticipated that isobactin prodrug analogues may be superior drug candidates to teixobactin.

In Chapter 4, I describe my efforts towards the synthesis of natural teixobactin and isobactins A, B, and C. The previous two chapters highlight the design of prodrugs of teixobactin analogues, which replace the synthetically challenging L-*allo*-enduracididine residue at position 10 with commercially available amino acids. Therefore, to obtain natural teixobactin and the prodrugs of teixobactin, isobactins A, B, and C, the native L-*allo*-enduracididine residue must be introduced. Chapter 4 describes the efforts in the synthesis of L-*allo*-enduracididine and the synthesis of natural teixobactin and isobactins A, B, and C. This chapter serves as the groundwork for future graduate students that may work on the synthesis of these isobactins.

Chapter 1

Antibiotic Resistance, The Antibiotic Teixobactin, and the Application of Isoacyl Motifs

INTRODUCTION

Antibiotics have transformed modern medicine, giving us the most powerful tools to combat life-threatening infections.[1] The modern world first saw an antimicrobial agent with Salvarsan, a synthetic antibiotic for the treatment of syphilis in the 1910s.[2] This research led to the discovery of new synthetic antibiotics inspired by dyes, sulfonamides. These sulfa drugs were the first truly effective, broad-spectrum antibiotics in clinical use and are still in use today.[2] Sulfa drugs were quickly superseded with the discovery of penicillin and its first successful clinical use in 1942. Before long, the market was flooded with new antibiotics with the "golden age" of antibiotic discovery occurring from the late 1940s to the early 1970s. But this rate of discovery fell dramatically from the 1970s onwards, leading to the current situation we are facing today: antibiotic-resistance and very few "new" antibiotics reaching the market today.[2,3]

Antibiotic resistance is a growing concern within the healthcare field as the number of deaths due to these infections increases and antibiotic efficacy decreases. Each year, antibiotic-resistant bacteria cause at least 2.8 million infections and more than 35,000 deaths in the United States each year and around 700,000 deaths worldwide each year.[1,4] Overuse and misuse of antibiotics in conjunction with the lack of new drug development have contributed to the rise in antibiotic resistance.[5–7] Gram-positive pathogens—including methicillin-resistant *Staphylococcus aureus* (MRSA), vancomycin-resistant *Enterococci* (VRE), and multidrug-resistant

Mycobacterium tuberculosis (MDR-TB)—cause more than 60% of the deaths related to antibiotic resistant infection.[1,5,8]

The emergence of antibiotic resistance isn't just one of the biggest global public health threats, but it also poses an extensive economic threat. The impact of antibiotic-resistant bacteria causing roughly 2.8 million infections and 35,000 deaths a year has led to losses of $20 billion in direct costs and $35 billion in indirect costs each year in the United States alone.[9] Antibiotic resistance also threatens modern medicine by complicating critical medical care.[1] Procedures such as surgery, cancer care, and organ transplants, are highly susceptible to bacterial infections and without effective antibiotics these bacterial infections can be fatal. As such, antibiotic resistance poses both a public health threat but also an economic burden on our society and will only worsen if new antibiotics are not developed.

Unfortunately, even as the threat of antibiotic resistance increases, the pipeline for innovative antibiotics is shrinking. Between 1962 and 2000, no new major classes of antibiotics were approved for the treatment of bacterial infections, with the majority of antimicrobial agents in clinical development being analogues of existing drugs.[1,10,11] Over the last two decades, roughly fifty new antibiotics have been approved for clinical use, with only five of these being first-in-class antibiotics including linezolid (2000), daptomycin (2003), retapamulin (2007), fidaxomicin (2011), and bedaquiline (2012).[12–15] Resistant bacteria have already been discovered to all five of these first-in-class antibiotics, with significant resistance developed against linezolid, daptomycin, and retapamulin.[16–20] Since 2017, six start-up companies have been awarded FDA approval for new antibiotics, but all of these companies have filed for bankruptcy, been acquired, or are shutting down antibiotic research altogether.[21] These factors combined highlight the critical need to expand the antibiotic pipeline to fight antibiotic resistance.

THE ANTIBIOTIC TEIXOBACTIN

In 2015, Lewis and coworkers discovered teixobactin, a new peptide antibiotic isolated from the Gram-negative bacterium *Eleftheria terrae.*[22] Teixobactin has generated considerable excitement as it kills Gram-positive bacteria—including ones considered to be urgent and serious threats by the CDC—without developing resistance.[1,22] Teixobactin has activity against many Gram-positive pathogens, including *Staphylococcus aureus*, MRSA, VRE, *Bacillus anthracis*, *Mycobacterium tuberculosis*, and *Clostridium difficile*, exhibiting remarkable potency (MIC values ranging from 0.005–0.5 μg/mL).[22] Teixobactin exhibits another noteworthy property in its *in vivo* activity, protecting mice against death from MRSA at 0.2 mg/kg, making it over an order of magnitude more effective than vancomycin, which requires 2.8 mg/kg to achieve comparable protection.[22] These findings suggest that teixobactin has the potential to be an effective antibiotic against drug-resistant pathogens and help combat the increasing threat of antibiotic resistance.

Teixobactin is a nonribosomal depsipeptide consisting of a linear tail (residues 1–7) and a macrolactone ring (residues 8–11) (Figure 1.1). Teixobactin contains five nonproteinogenic amino acids including *N*-Me-D-Phe$_1$, D-Gln$_4$, D-*allo*-Ile$_5$, D-Thr$_8$, and L-*allo*-enduracididine$_{10}$ (L-*allo*-End$_{10}$). The macrolactone of teixobactin is formed through the ester linkage of the β-hydroxy group of D-Thr$_8$ and the *C*-terminus of Ile$_{11}$.

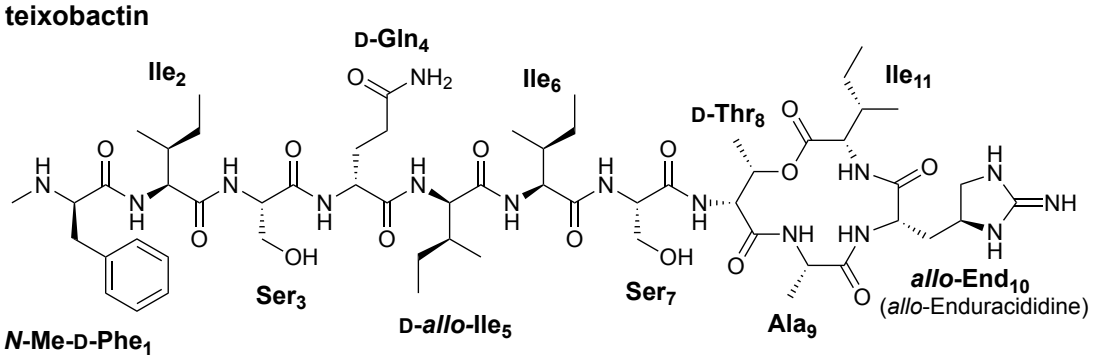

Figure 1.1. Structure of teixobactin.

Teixobactin has a unique mechanism of action compared to antibiotics currently approved for use in clinic. Teixobactin inhibits cell wall biosynthesis by binding to cell wall precursor molecules, which consequently leads to cellular lysis.[22–26] Teixobactin can recognize and bind several cell-wall building blocks and wall teichoic acid precursors, including lipid I, lipid II, lipid III, and undecaprenyl pyrophosphate (C_{55}-PP).[23] Specifically, teixobactin binds to the highly conserved prenyl-pyrophosphate moiety found in all these membrane-bound cell wall precursors.[22,23,26]

Recent studies have further elucidated the mechanism of action of teixobactin. Solid-state NMR structures of a teixobactin analogue and teixobactin bound to lipid II further confirms this binding mode and highlights the importance of the sequence of D- and L-amino acids in teixobactin.[23,26] The hydrophobic sidechains of *N*-Me-D-Phe$_1$, Ile$_2$, D-*allo*-Ile$_5$, and Ile$_6$ act as membrane-anchors whereas the hydrophilic sidechains of Ser$_3$, D-Gln$_4$, and Ser$_7$ are water exposed.[23,26] This allows for the alignment of the ring moiety of teixobactin to coordinate the pyrophosphate-sugar moiety of lipid II. Teixobactin then quickly forms antiparallel β-sheets upon binding of lipid II, sequestering it and preventing the biosynthesis of peptidoglycan as well as compromising the membrane integrity.[25–27] The ability of teixobactin to recognize several conserved, extracellular, and highly immutable precursor molecules, allows teixobactin to evade bacterial resistance decreasing the likelihood of teixobactin-resistant bacteria.[22,23,28–30]

Since the initial report of teixobactin in 2015, various research groups have made efforts to develop efficient synthetic routes, and thus enable the generation of analogues for structure–activity relationship (SAR) studies and optimization of its pharmacological properties. To date, five total syntheses of teixobactin have been reported.[31–35] This research has also enabled SAR studies of several hundred teixobactin analogues, in which residues in teixobactin were modified

to understand which residues are critical for antibiotic activity (Figure 1.2).[27,34,36–67] Collectively, these SAR studies have revealed which residues can tolerate modification and have led to teixobactin analogues that have comparable *in vitro* and *in vivo* activity to teixobactin against MRSA and VRE.

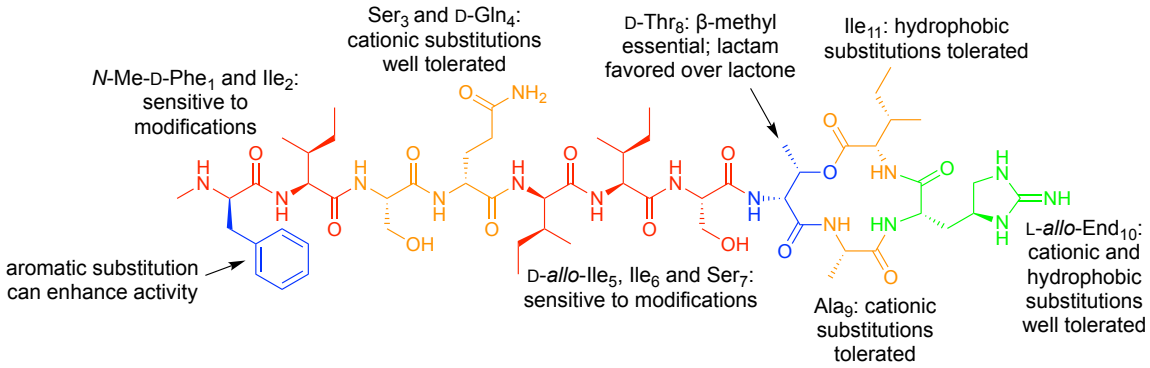

Figure 1.2. Summary of SAR for teixobactin. Green indicates substitutions well tolerated, orange indicates some substitutions tolerated, red indicates substitutions highly sensitive to modification, and blue highlights that some modifications that can enhance activity. This figure was adapted from Karas *et al.*[68]

Although teixobactin is such a promising antibiotic drug candidate, there are limitations of teixobactin. These include the commercially unavailable, difficult to synthesis L-*allo*-End and the gel formation of teixobactin in serum or buffer, impeding its intravenous use at higher concentrations. SAR studies have provided insight into potent analogues of teixobactin that don't require the complex L-*allo*-End, but unfortunately work to develop more soluble analogues has not been successful. In performing SAR studies with teixobactin analogues, the Nowick lab found that modifications that eliminated the propensity of teixobactin to form gels in aqueous solutions also eliminated its potent antibiotic activity.[40,42,49] With the limitation of the L-*allo*-End addressed through SAR, the poor solubility and propensity of teixobactin to form gels still highlights the need for teixobactin analogues with improved pharmacological properties. Overcoming this

obstacle would be a significant advance towards realizing the promise of teixobactin as a new antibiotic for the treatment of Gram-positive infections.

THE APPLICATION OF ISOACYL MOTIFS

Intramolecular acyl transfers, *O*-to-*N* and *N*-to-*O* acyl migrations have been explored since the early 1920s. The *N*-to-*O* acyl shift takes place under strongly acidic conditions whereas the *O*-to-*N* acyl shift occurs under neutral or basic conditions (Figure 1.3). In recent decades, both acyl transfers have witnessed several applications in both medicinal chemistry and peptide chemistry. Specifically, the *O*-to-*N* acyl transfer has attracted considerable attention for its use in various research areas, including establishing new peptide segment ligation methods; the facilitation of synthesizing, handling, and investigating difficult peptide sequences; and the development of prodrugs.[69]

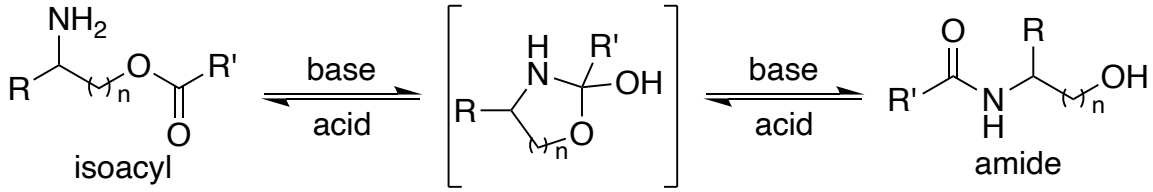

Figure 1.3. The *O*-to-*N* and *N*-to-*O* acyl migration. This figure was adapted from Mailig and Liu.[69]

Prodrugs are biologically inactive compounds that after administration must undergo either chemical or enzymatic transformations to release the active drug compound.[69,70] Prodrugs are a well-established strategy used to improve the properties of the parent drug, such as permeability, solubility, half-life, and bioavailability. There are many prodrug approaches reported in literature, but in recent decades isoacyl prodrugs have gained traction in this field. The isoacyl prodrug free amine group can be stabilized in a salt form, allowing the prodrug to be chemically stable while also providing a protonated amine in a previously uncharged molecule, enhancing solubility. The

isoacyl prodrug can then undergo the *O*-to-*N* acyl transfer under physiological conditions to provide the fully active parent drug. Many applications of the isoacyl prodrug have been seen in literature from HIV-1 inhibitors to cancer drugs, where the isoacyl motif allows for improved aqueous solubility, enhanced bioavailability, and even increased tissue specificity.[71–78]

Not only does the isoacyl motif enhance solubility of prodrugs, but it can also be used to enhance the solubility as well as biophysical properties of peptides. Various peptide sequences can be hydrophobic and aggregation prone and form insoluble secondary structures. The insertion of an isoacyl motif into the peptide backbone can significantly disrupt the secondary structure of the peptide, therefore significantly improving the peptides biophysical properties.[69] This application of incorporating the isoacyl motif into the synthesis of a peptide was first reported by Kiso and coworkers in 2004.[79] The addition of the isoacyl motif remarkably enhanced the efficiency of synthesizing the difficult peptide and this improvement was attributed to the ability of the isoacyl motif disrupting the secondary structure of the hydrophobic, aggregation prone sequence. This demonstrated the possible applications of the isoacyl motif, specifically *O*-acyl-Ser/Thr isopeptides, for the preparation of difficult peptide sequences.

Since this first application by Kiso and coworkers, the synthesis of many other complicated peptide sequences, including amyloid β, have been considerably improved. A notable example includes the design of an *O*-acyl isopeptide prodrug of human glucagon by the DiMarchi group.[78] Natural human glucagon is known for its poor solubility, substantially limiting its clinical use as an emergency treatment for severe hypoglycemia. The DiMarchi group discovered that the addition of a single *O*-acyl isopeptide bond into the sequence of synthetic glucagon could significantly improve the solubility and completely suppress aggregation of the peptide. Just as

other isoacyl prodrugs, the *O*-acyl isopeptide prodrug could undergo conversion to the biologically active glucagon, providing a route to a clinically relevant drug.

In 2006, both the Kiso and Carpino groups introduced the premade *O*-acyl-Ser/Thr isodipeptide building blocks that could be directly incorporated into solid-phase peptide synthesis (SPPS).[80–82] The creation of the *O*-acyl isodipeptides has promoted the use of the isoacyl motif in the synthesis of aggregation prone peptide sequences and drastically enhanced that ability to access these difficult sequences. Easy access to *O*-acyl isodipeptides allows for any difficult to synthesize and handle peptide sequences containing a serine or threonine to be improved upon. With the knowledge of teixobactin containing two serine residues, the application of the *O*-acyl isodipeptide motif could provide a route to a clinically useful drug that overcomes the solubility issues of teixobactin.

In my dissertation, I utilize the *O*-acyl isopeptide method to design prodrugs of teixobactin analogues. In Chapter 2, I describe the first synthesis of numerous *O*-acyl isopeptide prodrugs of teixobactin analogues, termed isobactins, to overcome the limitations of teixobactin and its propensity to form gels in aqueous conditions. In Chapter 3, I further explore the isobactin prodrug analogues of teixobactin through a small SAR study using commercially available amino acids. In Chapter 4, I summarize my efforts towards the synthesis of natural teixobactin and isobactins A, B, and C.

REFERENCES AND NOTES

1. Centers for Disease Control and Prevention (U.S.). *Antibiotic Resistance Threats in the United States, 2019*; Centers for Disease Control and Prevention (U.S.), 2019.

2. Hutchings, M. I.; Truman, A. W.; Wilkinson, B. Antibiotics: Past, Present and Future. *Curr. Opin. Microbiol.* **2019**, *51*, 72–80.

3. Home | AMR Review https://amr-review.org/ (accessed 2024 -03 -25).

4. New report calls for urgent action to avert antimicrobial resistance crisis https://www.who.int/news/item/29-04-2019-new-report-calls-for-urgent-action-to-avert-antimicrobial-resistance-crisis (accessed 2024 -03 -25).

5. Gould, I. M.; Bal, A. M. New Antibiotic Agents in the Pipeline and How They Can Help Overcome Microbial Resistance. *Virulence* **2013**, *4*, 185–191.

6. Ventola, C. L. The Antibiotic Resistance Crisis. *Pharm. Ther.* **2015**, *40*, 277–283.

7. Michael, C. A.; Dominey-Howes, D.; Labbate, M. The Antimicrobial Resistance Crisis: Causes, Consequences, and Management. *Front. Public Health* **2014**, *2*, 145.

8. Gross, M. Antibiotics in Crisis. *Curr. Biol.* **2013**, *23*, R1063–R1065.

9. Smith, R.; Coast, J. The True Cost of Antimicrobial Resistance. *BMJ* **2013**, *346*, f1493.

10. Jacobs, A. W.H.O. Warns That Pipeline for New Antibiotics Is Running Dry. *The New York Times*. January 17, 2020.

11. 2019 antibacterial agents in clinical development: an analysis of the antibacterial clinical development pipeline https://www.who.int/publications-detail-redirect/9789240000193 (accessed 2024 -03 -25).

12. Butler, M. S.; Blaskovich, M. A.; Cooper, M. A. Antibiotics in the Clinical Pipeline in 2013. *J. Antibiot. (Tokyo)* **2013**, *66*, 571–591.

13. Butler, M. S.; Paterson, D. L. Antibiotics in the Clinical Pipeline in October 2019. *J. Antibiot. (Tokyo)* **2020**, *73*, 329–364.

14. Butler, M. S.; Henderson, I. R.; Capon, R. J.; Blaskovich, M. A. T. Antibiotics in the Clinical Pipeline as of December 2022. *J. Antibiot. (Tokyo)* **2023**, *76*, 431–473.

15. Shi, Z.; Zhang, J.; Tian, L.; Xin, L.; Liang, C.; Ren, X.; Li, M. A Comprehensive Overview of the Antibiotics Approved in the Last Two Decades: Retrospects and Prospects. *Molecules* **2023**, *28*, 1762.

16. Eliopoulos, G. M.; Meka, V. G.; Gold, H. S. Antimicrobial Resistance to Linezolid. *Clin. Infect. Dis.* **2004**, *39*, 1010–1015.

17. Tran, T. T.; Munita, J. M.; Arias, C. A. Mechanisms of Drug Resistance: Daptomycin Resistance. *Ann. N. Y. Acad. Sci.* **2015**, *1354*, 32–53.

18. Goudarzi, M.; Khoshbayan, A.; Taheri, F. Retapamulin: Current Status and Future Perspectives. *Arch. Clin. Infect. Dis.* **2021**, *16*.

19. Marchandin, H.; Anjou, C.; Poulen, G.; Freeman, J.; Wilcox, M.; Jean-Pierre, H.; Barbut, F. In Vivo Emergence of a Still Uncommon Resistance to Fidaxomicin in the Urgent Antimicrobial Resistance Threat Clostridioides Difficile. *J. Antimicrob. Chemother.* **2023**, *78*, 1992–1999.

20. Günther, G.; Mhuulu, L.; Diergaardt, A.; Dreyer, V.; Moses, M.; Anyolo, K.; Ruswa, N.; Claassens, M.; Niemann, S.; Nepolo, E. Bedaquiline Resistance after Effective Treatment of Multidrug-Resistant Tuberculosis, Namibia - Volume 30, Number 3—March 2024 - Emerging Infectious Diseases Journal - CDC.

21. Mosbergen, D. The World Needs New Antibiotics. The Problem Is, No One Can Make Them Profitably. https://www.wsj.com/tech/biotech/antibiotics-drug-development-business-fda-aa5b4f00 (accessed 2024 -05 -07).

22. Ling, L. L.; Schneider, T.; Peoples, A. J.; Spoering, A. L.; Engels, I.; Conlon, B. P.; Mueller, A.; Schäberle, T. F.; Hughes, D. E.; Epstein, S.; Jones, M.; Lazarides, L.; Steadman, V. A.; Cohen, D. R.; Felix, C. R.; Fetterman, K. A.; Millett, W. P.; Nitti, A. G.; Zullo, A. M.; Chen, C.; Lewis, K. A New Antibiotic Kills Pathogens without Detectable Resistance. *Nature* **2015**, *517*, 455–459.

23. Shukla, R.; Medeiros-Silva, J.; Parmar, A.; Vermeulen, B. J. A.; Das, S.; Paioni, A. L.; Jekhmane, S.; Lorent, J.; Bonvin, A. M. J. J.; Baldus, M.; Lelli, M.; Veldhuizen, E. J. A.; Breukink, E.; Singh, I.; Weingarth, M. Mode of Action of Teixobactins in Cellular Membranes. *Nat. Commun.* **2020**, *11*, 2848.

24. Homma, T.; Nuxoll, A.; Gandt, A. B.; Ebner, P.; Engels, I.; Schneider, T.; Götz, F.; Lewis, K.; Conlon, B. P. Dual Targeting of Cell Wall Precursors by Teixobactin Leads to Cell Lysis. *Antimicrob. Agents Chemother.* **2016**, *60*, 6510–6517.

25. Öster, C.; Walkowiak, G. P.; Hughes, D. E.; Spoering, A. L.; Peoples, A. J.; Catherwood, A. C.; Tod, J. A.; Lloyd, A. J.; Herrmann, T.; Lewis, K.; Dowson, C. G.; Lewandowski, J. R. Structural Studies Suggest Aggregation as One of the Modes of Action for Teixobactin. *Chem. Sci.* **2018**, *9*, 8850–8859.

26. Shukla, R.; Lavore, F.; Maity, S.; Derks, M. G. N.; Jones, C. R.; Vermeulen, B. J. A.; Melcrová, A.; Morris, M. A.; Becker, L. M.; Wang, X.; Kumar, R.; Medeiros-Silva, J.; van Beekveld, R. A. M.; Bonvin, A. M. J. J.; Lorent, J. H.; Lelli, M.; Nowick, J. S.; MacGillavry, H. D.; Peoples, A. J.; Spoering, A. L.; Ling, L. L.; Hughes, D. E.; Roos, W. H.; Breukink, E.; Lewis, K.; Weingarth, M. Teixobactin Kills Bacteria by a Two-Pronged Attack on the Cell Envelope. *Nature* **2022**, *608*, 390–396.

27. Yang, H.; Wierzbicki, M.; Du Bois, D. R.; Nowick, J. S. X-Ray Crystallographic Structure of a Teixobactin Derivative Reveals Amyloid-like Assembly. *J. Am. Chem. Soc.* **2018**, *140*, 14028–14032.

28. Breukink, E.; de Kruijff, B. Lipid II as a Target for Antibiotics. *Nat. Rev. Drug Discov.* **2006**, *5*, 321–323.

29. de Kruijff, B.; van Dam, V.; Breukink, E. Lipid II: A Central Component in Bacterial Cell Wall Synthesis and a Target for Antibiotics. *Prostaglandins Leukot. Essent. Fatty Acids* **2008**, *79*, 117–121.

30. Lloyd, D. G.; Schofield, B. J.; Goddard, M. R.; Taylor, E. J. De Novo Resistance to Arg10-Teixobactin Occurs Slowly and Is Costly. *Antimicrob. Agents Chemother.* **2020**, *65*, e01152-20.

31. Jin, K.; Sam, I. H.; Po, K. H. L.; Lin, D.; Ghazvini Zadeh, E. H.; Chen, S.; Yuan, Y.; Li, X. Total Synthesis of Teixobactin. *Nat. Commun.* **2016**, *7*, 12394.

32. Giltrap, A. M.; Dowman, L. J.; Nagalingam, G.; Ochoa, J. L.; Linington, R. G.; Britton, W. J.; Payne, R. J. Total Synthesis of Teixobactin. *Org. Lett.* **2016**, *18*, 2788–2791.

33. Liu, L.; Wu, S.; Wang, Q.; Zhang, M.; Wang, B.; He, G.; Chen, G. Total Synthesis of Teixobactin and Its Stereoisomers. *Org. Chem. Front.* **2018**, *5*, 1431–1435.

34. Zong, Y.; Fang, F.; Meyer, K. J.; Wang, L.; Ni, Z.; Gao, H.; Lewis, K.; Zhang, J.; Rao, Y. Gram-Scale Total Synthesis of Teixobactin Promoting Binding Mode Study and Discovery of More Potent Antibiotics. *Nat. Commun.* **2019**, *10*, 3268.

35. Gao, B.; Chen, S.; Hou, Y. N.; Zhao, Y. J.; Ye, T.; Xu, Z. Solution-Phase Total Synthesis of Teixobactin. *Org. Biomol. Chem.* **2019**, *17*, 1141–1153.

36. Jad, Y. E.; Acosta, G. A.; Naicker, T.; Ramtahal, M.; El-Faham, A.; Govender, T.; Kruger, H. G.; de la Torre, B. G.; Albericio, F. Synthesis and Biological Evaluation of a Teixobactin Analogue. *Org. Lett.* **2015**, *17*, 6182–6185.

37. Abdel Monaim, S. A. H.; Jad, Y. E.; Ramchuran, E. J.; El-Faham, A.; Govender, T.; Kruger, H. G.; de la Torre, B. G.; Albericio, F. Lysine Scanning of Arg10–Teixobactin: Deciphering the Role of Hydrophobic and Hydrophilic Residues. *ACS Omega* **2016**, *1*, 1262–1265.

38. Monaim, S. A. H. A.; Jad, Y. E.; Acosta, G. A.; Naicker, T.; Ramchuran, E. J.; El-Faham, A.; Govender, T.; Kruger, H. G.; Torre, B. G. de la; Albericio, F. Re-Evaluation of the N-Terminal Substitution and the D-Residues of Teixobactin. *RSC Adv.* **2016**, *6*, 73827–73829.

39. Parmar, A.; Iyer, A.; Vincent, C. S.; Lysebetten, D. V.; Prior, S. H.; Madder, A.; Taylor, E. J.; Singh, I. Efficient Total Syntheses and Biological Activities of Two Teixobactin Analogues. *Chem. Commun.* **2016**, *52*, 6060–6063.

40. Yang, H.; Chen, K. H.; Nowick, J. S. Elucidation of the Teixobactin Pharmacophore. *ACS Chem. Biol.* **2016**, *11*, 1823–1826.

41. Abdel Monaim, S. A. H.; Ramchuran, E. J.; El-Faham, A.; Albericio, F.; de la Torre, B. G. Converting Teixobactin into a Cationic Antimicrobial Peptide (AMP). *J. Med. Chem.* **2017**, *60*, 7476–7482.

42. Chen, K. H.; Le, S. P.; Han, X.; Frias, J. M.; Nowick, J. S. Alanine Scan Reveals Modifiable Residues in Teixobactin. *Chem. Commun.* **2017**, *53*, 11357–11359.

43. Jin, K.; Po, K. H. L.; Wang, S.; Reuven, J. A.; Wai, C. N.; Lau, H. T.; Chan, T. H.; Chen, S.; Li, X. Synthesis and Structure-Activity Relationship of Teixobactin Analogues via Convergent Ser Ligation. *Bioorg. Med. Chem.* **2017**, *25*, 4990–4995.

44. Monaim, S. A. H. A.; Noki, S.; Ramchuran, E. J.; El-Faham, A.; Albericio, F.; Torre, B. G. de la. Investigation of the N-Terminus Amino Function of Arg10-Teixobactin. *Molecules* **2017**, *22*, 1632.

45. Parmar, A.; Iyer, A.; Prior, S. H.; Lloyd, D. G.; Goh, E. T. L.; Vincent, C. S.; Palmai-Pallag, T.; Bachrati, C. Z.; Breukink, E.; Madder, A.; Lakshminarayanan, R.; Taylor, E. J.; Singh, I. Teixobactin Analogues Reveal Enduracididine to Be Non-Essential for Highly Potent Antibacterial Activity and Lipid II Binding. *Chem. Sci.* **2017**, *8*, 8183–8192.

46. Parmar, A.; Prior, S. H.; Iyer, A.; Vincent, C. S.; Lysebetten, D. V.; Breukink, E.; Madder, A.; Taylor, E. J.; Singh, I. Defining the Molecular Structure of Teixobactin Analogues and Understanding Their Role in Antibacterial Activities. *Chem. Commun.* **2017**, *53*, 2016–2019.

47. Schumacher, C. E.; Harris, P. W. R.; Ding, X.-B.; Krause, B.; Wright, T. H.; Cook, G. M.; Furkert, D. P.; Brimble, M. A. Synthesis and Biological Evaluation of Novel Teixobactin Analogues. *Org. Biomol. Chem.* **2017**, *15*, 8755–8760.

48. Wu, C.; Pan, Z.; Yao, G.; Wang, W.; Fang, L.; Su, W. Synthesis and Structure–Activity Relationship Studies of Teixobactin Analogues. *RSC Adv.* **2017**, *7*, 1923–1926.

49. Yang, H.; Bois, D. R. D.; Ziller, J. W.; Nowick, J. S. X-Ray Crystallographic Structure of a Teixobactin Analogue Reveals Key Interactions of the Teixobactin Pharmacophore. *Chem. Commun.* **2017**, *53*, 2772–2775.

50. Girt, G. C.; Mahindra, A.; Jabri, Z. J. H. A.; Croix, M. D. S.; Oggioni, M. R.; Jamieson, A. G. Lipopeptidomimetics Derived from Teixobactin Have Potent Antibacterial Activity against Staphylococcus Aureus. *Chem. Commun.* **2018**, *54*, 2767–2770.

51. Guo, C.; Mandalapu, D.; Ji, X.; Gao, J.; Zhang, Q. Chemistry and Biology of Teixobactin. *Chem. – Eur. J.* **2018**, *24*, 5406–5422.

52. Jin, K.; Po, K. H. L.; Kong, W. Y.; Lo, C. H.; Lo, C. W.; Lam, H. Y.; Sirinimal, A.; Reuven, J. A.; Chen, S.; Li, X. Synthesis and Antibacterial Studies of Teixobactin Analogues with Non-Isostere Substitution of Enduracididine. *Bioorg. Med. Chem.* **2018**, *26*, 1062–1068.

53. Malkawi, R.; Iyer, A.; Parmar, A.; Lloyd, D. G.; Leng Goh, E. T.; Taylor, E. J.; Sarmad, S.; Madder, A.; Lakshminarayanan, R.; Singh, I. Cysteines and Disulfide-Bridged Macrocyclic Mimics of Teixobactin Analogues and Their Antibacterial Activity Evaluation against Methicillin-Resistant Staphylococcus Aureus (MRSA). *Pharmaceutics* **2018**, *10*, 183.

54. Mandalapu, D.; Ji, X.; Chen, J.; Guo, C.; Liu, W.-Q.; Ding, W.; Zhou, J.; Zhang, Q. Thioesterase-Mediated Synthesis of Teixobactin Analogues: Mechanism and Substrate Specificity. *J. Org. Chem.* **2018**, *83*, 7271–7275.

55. Ng, V.; Kuehne, S. A.; Chan, W. C. Rational Design and Synthesis of Modified Teixobactin Analogues: In Vitro Antibacterial Activity against Staphylococcus Aureus, Propionibacterium Acnes and Pseudomonas Aeruginosa. *Chem. – Eur. J.* **2018**, *24*, 9136–9147.

56. Parmar, A.; Lakshminarayanan, R.; Iyer, A.; Mayandi, V.; Leng Goh, E. T.; Lloyd, D. G.; Chalasani, M. L. S.; Verma, N. K.; Prior, S. H.; Beuerman, R. W.; Madder, A.; Taylor, E. J.; Singh, I. Design and Syntheses of Highly Potent Teixobactin Analogues against Staphylococcus Aureus, Methicillin-Resistant Staphylococcus Aureus (MRSA), and Vancomycin-Resistant Enterococci (VRE) in Vitro and in Vivo. *J. Med. Chem.* **2018**, *61*, 2009–2017.

57. Ramchuran, E. J.; Somboro, A. M.; Abdel Monaim, S. A. H.; Amoako, D. G.; Parboosing, R.; Kumalo, H. M.; Agrawal, N.; Albericio, F.; Torre, B. G. de L.; Bester, L. A. In Vitro Antibacterial Activity of Teixobactin Derivatives on Clinically Relevant Bacterial Isolates. *Front. Microbiol.* **2018**, *9*, 1535.

58. Zong, Y.; Sun, X.; Gao, H.; Meyer, K. J.; Lewis, K.; Rao, Y. Developing Equipotent Teixobactin Analogues against Drug-Resistant Bacteria and Discovering a Hydrophobic Interaction between Lipid II and Teixobactin. *J. Med. Chem.* **2018**, *61*, 3409–3421.

59. Gunjal, V. B.; Reddy, D. S. Total Synthesis of Met10-Teixobactin. *Tetrahedron Lett.* **2019**, *60*, 1909–1912.

60. Velkov, T.; Swarbrick, J. D.; Hussein, M. H.; Schneider-Futschik, E. K.; Hoyer, D.; Li, J.; Karas, J. A. The Impact of Backbone N-Methylation on the Structure-Activity Relationship of Leu10-Teixobactin. *J. Pept. Sci.* **2019**, *25*, e3206.

61. Chiorean, S.; Antwi, I.; Carney, D. W.; Kotsogianni, I.; Giltrap, A. M.; Alexander, F. M.; Cochrane, S. A.; Payne, R. J.; Martin, N. I.; Henninot, A.; Vederas, J. C. Dissecting the Binding Interactions of Teixobactin with the Bacterial Cell-Wall Precursor Lipid II. *ChemBioChem* **2020**, *21*, 789–792.

62. Morris, M. A.; Malek, M.; Hashemian, M. H.; Nguyen, B. T.; Manuse, S.; Lewis, K.; Nowick, J. S. A Fluorescent Teixobactin Analogue. *ACS Chem. Biol.* **2020**, *15*, 1222–1231.

63. Yang, H.; Pishenko, A. V.; Li, X.; Nowick, J. S. Design, Synthesis, and Study of Lactam and Ring-Expanded Analogues of Teixobactin. *J. Org. Chem.* **2020**, *85*, 1331–1339.

64. Yim, V. V.; Cameron, A. J.; Kavianinia, I.; Harris, P. W. R.; Brimble, M. A. Thiol-Ene Enabled Chemical Synthesis of Truncated S-Lipidated Teixobactin Analogs. *Front. Chem.* **2020**, *8*.

65. Wu, Q.; Mishra, B.; Wang, G. Linearized Teixobactin Is Inactive and after Sequence Enhancement, Kills Methicillin-Resistant Staphylococcus Aureus via a Different Mechanism. *Pept. Sci.* **2022**, *114*, e24269.

66. Parmar, A.; Lakshminarayanan, R.; Iyer, A.; Goh, E. T. L.; To, T. Y.; Yam, J. K. H.; Yang, L.; Newire, E.; Robertson, M. C.; Prior, S. H.; Breukink, E.; Madder, A.; Singh, I. Development of Teixobactin Analogues Containing Hydrophobic, Non-Proteogenic Amino Acids That Are Highly Potent against Multidrug-Resistant Bacteria and Biofilms. *Eur. J. Med. Chem.* **2023**, *261*, 115853.

67. Scioli, G.; Marinaccio, L.; Bauer, M.; Kamysz, W.; Parmar, A.; Newire, E.; Singh, I.; Stefanucci, A.; Mollica, A. New Teixobactin Analogues with a Total Lactam Ring. *ACS Med. Chem. Lett.* **2023**, *14*, 1827–1832.

68. Karas, J. A.; Chen, F.; Schneider-Futschik, E. K.; Kang, Z.; Hussein, M.; Swarbrick, J.; Hoyer, D.; Giltrap, A. M.; Payne, R. J.; Li, J.; Velkov, T. Synthesis and Structure−activity Relationships of Teixobactin. *Ann. N. Y. Acad. Sci.* **2020**, *1459*, 86–105.

69. Mailig, M.; Liu, F. The Application of Isoacyl Structural Motifs in Prodrug Design and Peptide Chemistry. *ChemBioChem* **2019**, *20*, 2017–2031.

70. Wu, K.-M. A New Classification of Prodrugs: Regulatory Perspectives. *Pharmaceuticals* **2009**, *2*, 77–81.

71. Hurley, T. R.; Colson, C. E.; Hicks, G.; Ryan, M. J. Orally Active Water-Soluble N,O-Acyl Transfer Products of a .Beta.,.Gamma.-Bishydroxyl Amide Containing Renin Inhibitor. *J. Med. Chem.* **1993**, *36*, 1496–1498.

72. Kiso, Y.; Matsumoto, H.; Yamaguchi, S.; Kimura, T. Design of Small Peptidomimetic HIV-1 Protease Inhibitors and Prodrug Forms. *Lett. Pept. Sci.* **1999**, *6*, 275–281.

73. Kazmierski, W. M.; Bevans, P.; Furfine, E.; Spaltenstein, A.; Yang, H. Novel Prodrug Approach to Amprenavir-Based HIV-1 Protease Inhibitors via O→*N Acyloxy* Migration of P1 Moiety. *Bioorg. Med. Chem. Lett.* **2003**, *13*, 2523–2526.

74. Subbaiah, M. A. M.; Meanwell, N. A.; Kadow, J. F.; Subramani, L.; Annadurai, M.; Ramar, T.; Desai, S. D.; Sinha, S.; Subramanian, M.; Mandlekar, S.; Sridhar, S.; Padmanabhan, S.; Bhutani, P.; Arla, R.; Jenkins, S. M.; Krystal, M. R.; Wang, C.; Sarabu, R. Coupling of an

Acyl Migration Prodrug Strategy with Bio-Activation To Improve Oral Delivery of the HIV-1 Protease Inhibitor Atazanavir. *J. Med. Chem.* **2018**, *61*, 4176–4188.

75. Skwarczynski, M.; Sohma, Y.; Kimura, M.; Hayashi, Y.; Kimura, T.; Kiso, Y. O–N Intramolecular Acyl Migration Strategy in Water-Soluble Prodrugs of Taxoids. *Bioorg. Med. Chem. Lett.* **2003**, *13*, 4441–4444.

76. Hayashi, Y.; Skwarczynski, M.; Hamada, Y.; Sohma, Y.; Kimura, T.; Kiso, Y. A Novel Approach of Water-Soluble Paclitaxel Prodrug with No Auxiliary and No Byproduct: Design and Synthesis of Isotaxel. *J. Med. Chem.* **2003**, *46*, 3782–3784.

77. Li, B. X.; Xie, F.; Fan, Q.; Barnhart, K. M.; Moore, C. E.; Rheingold, A. L.; Xiao, X. Novel Type of Prodrug Activation through a Long-Range O,N-Acyl Transfer: A Case of Water-Soluble CREB Inhibitor. *ACS Med. Chem. Lett.* **2014**, *5*, 1104–1109.

78. Mroz, P. A.; Perez-Tilve, D.; Liu, F.; Mayer, J. P.; DiMarchi, R. D. Native Design of Soluble, Aggregation-Resistant Bioactive Peptides: Chemical Evolution of Human Glucagon. *ACS Chem. Biol.* **2016**, *11*, 3412–3420.

79. Sohma, Y.; Sasaki, M.; Hayashi, Y.; Kimura, T.; Kiso, Y. Novel and Efficient Synthesis of Difficult Sequence-Containing Peptides through O–N Intramolecular Acyl Migration Reaction of O-Acyl Isopeptides. *Chem. Commun.* **2004**, No. 1, 124–125.

80. Yoshiya, T.; Taniguchi, A.; Sohma, Y.; Fukao, F.; Nakamura, S.; Abe, N.; Ito, N.; Skwarczynski, M.; Kimura, T.; Hayashi, Y.; Kiso, Y. "O-Acyl Isopeptide Method" for Peptide Synthesis: Synthesis of Forty Kinds of "O-Acyl Isodipeptide Unit" Boc-Ser/Thr(Fmoc-Xaa)-OH. *Org. Biomol. Chem.* **2007**, *5*, 1720–1730.

81. Sohma, Y.; Taniguchi, A.; Skwarczynski, M.; Yoshiya, T.; Fukao, F.; Kimura, T.; Hayashi, Y.; Kiso, Y. 'O-Acyl Isopeptide Method' for the Efficient Synthesis of Difficult Sequence-Containing Peptides: Use of 'O-Acyl Isodipeptide Unit.' *Tetrahedron Lett.* **2006**, *47*, 3013–3017.

82. Coin, I.; Dölling, R.; Krause, E.; Bienert, M.; Beyermann, M.; Sferdean, C. D.; Carpino, L. A. Depsipeptide Methodology for Solid-Phase Peptide Synthesis: Circumventing Side Reactions and Development of an Automated Technique via Depsidipeptide Units,. *J. Org. Chem.* **2006**, *71*, 6171–6177.

Chapter 2[a]

Isobactins: *O*-Acyl Isopeptide Prodrugs of Teixobactin and Teixobactin Derivatives

Prologue to Chapter 2

Chapter 2 describes a project that aimed to develop prodrugs of teixobactin and teixobactin derivatives to overcome a solubility limitation of teixobactin and teixobactin derivatives. This project could not have been achieved without the support of my collaborators. Prof. James S. Nowick and I collaborated on the conception of the project with Prof. Nowick proposing the A-series prodrugs and myself proposing the B- and C-series of prodrugs. I synthesized peptides along with the assistance of my undergraduate student, Grant Lai. All peptide characterization and purifications were completed by me. I also performed all the conversion kinetic, minimum inhibitory concentration (MIC), gelation, and hemolytic experiments. Dr. Gretchen Guaglianone taught me the skills of mammalian cell culture and cytotoxicity assays and provided her expertise and assistance with performing these experiments. Dr. Tim Murphy and NeoSome Life Sciences, LLC provided guidance in the design and execution of the *in vivo* efficacy experiments, contributing greatly to this project. Our collaborators at NovoBiotic Pharmaceuticals, LLC provided natural teixobactin that was used as a control in the experiments described in chapter 2. I am grateful to all my collaborators who supported this project and helped see it to the end.

In the original report on teixobactin, the authors performed the MIC assays in the presence of 0.002% polysorbate 80. It is believed the polysorbate 80 prevents teixobactin from sticking to

[a]This chapter is taken verbatim from Jones, C. R.; Guaglianone, G.; Lai, G. H.; Nowick, J. S. Isobactins: *O*-Acyl Isopeptide Prodrugs of Teixobactin and Teixobactin Derivatives. *Chem. Sci.*, **2022**, *13*, 13110–13116.

the plastic surfaces of the polystyrene plates used in this assay. Our laboratory has previously found that addition of polysorbate 80 can have dramatic effects upon the measured MIC values. Therefore, for the MIC assays as well as the hemolytic assays, all assays were performed in both the absence and presence of polysorbate 80 to observe any effects.

INTRODUCTION

In 2015, teixobactin was reported as a promising new antibiotic candidate.[1] This non-ribosomal depsipeptide has excellent antibiotic activity against Gram-positive bacteria, including drug-resistant strains such as MRSA, VRE, and MDR-TB (Figure 2.1). The macrocyclic ring of teixobactin binds to the highly conserved prenyl-pyrophosphate-saccharide regions of lipid II and related membrane-bound cell wall precursors.[1–5] These targets are extracellular and immutable, making it almost impossible for bacteria to develop resistance.[3,6–8] For these reasons, teixobactin has generated considerable excitement as a promising new candidate for antibiotic drug development.

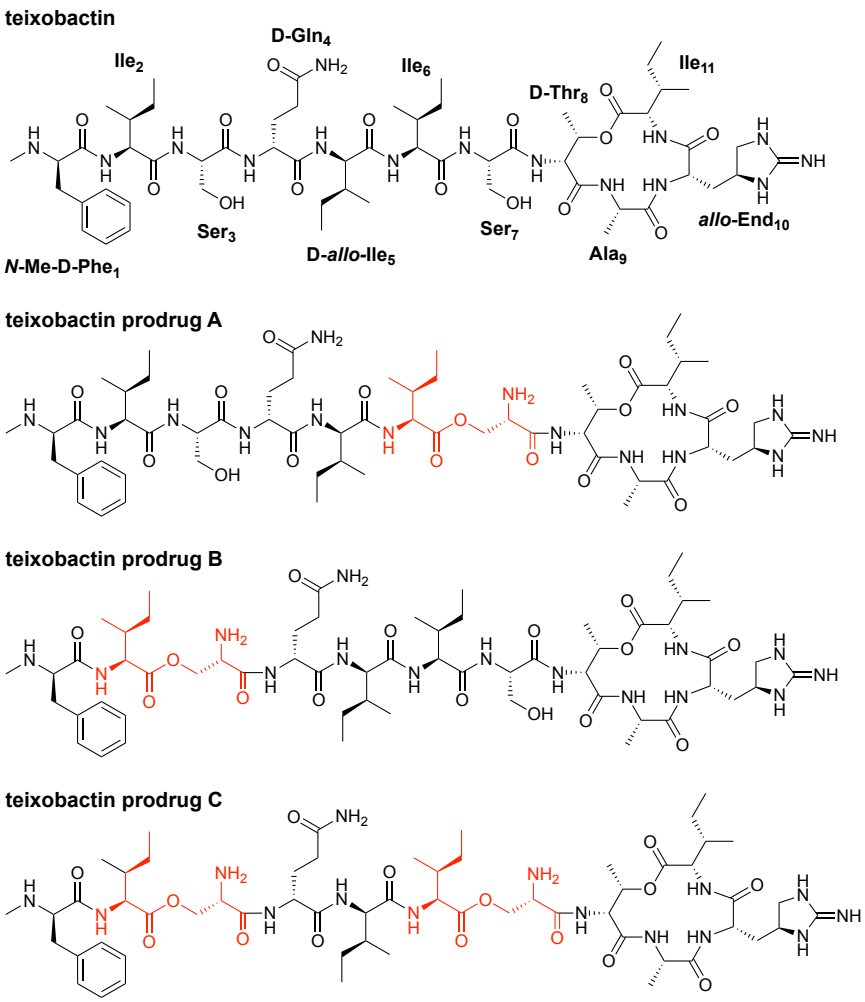

Figure 2.1. Structures of teixobactin and the teixobactin prodrugs.

Unfortunately, teixobactin aggregates to form gels in the physiological conditions needed for intravenous administration. In performing structure-activity relationship studies with teixobactin analogues, our laboratory found that modifications of teixobactin that eliminated the propensity to form gels also eliminated its potent antibiotic activity.[9–11] We further found that teixobactin and active teixobactin analogues assemble to form amyloid-like fibrils and that this mode of supramolecular assembly appears to be inherently connected to both the potent antibiotic activity and the formation of gels.[2,12] The propensity of teixobactin to form gels has the potential

to jeopardize its promise as a clinically useful intravenous antibiotic against drug-resistant Gram-positive pathogens by limiting dosing to low concentrations that do not form gels or aggregates.

In the current paper, we introduce *O*-acyl isopeptide prodrug analogues of teixobactin that are stable and non-gelating in acidic solution but gradually convert to the corresponding active teixobactin analogue at neutral pH (Figure 2.2). We envision that prodrugs of native teixobactin (Figure 2.1) and teixobactin prodrug analogues should thus circumvent the problem of gel formation and facilitate intravenous administration. The *O*-acyl isopeptide prodrug analogues undergo clean conversion to the corresponding teixobactin analogues at physiological pH. The prodrug analogues exhibit comparable or slightly improved antibiotic activity to the corresponding teixobactin analogues. The prodrug analogues also exhibit improved solubility in aqueous conditions and do not gelate immediately upon exposure to physiological conditions. Hemolytic assays with human red blood cells show little to no hemolytic activity, and cytotoxicity assays with HeLa cells show no significant cytotoxicity. A mouse thigh infection model against MRSA demonstrates *in vivo* efficacy. These findings suggest that teixobactin prodrugs and teixobactin prodrug analogues may be attractive alternatives to teixobactin as antibiotic drug candidates that circumvent the gelation problem of teixobactin.

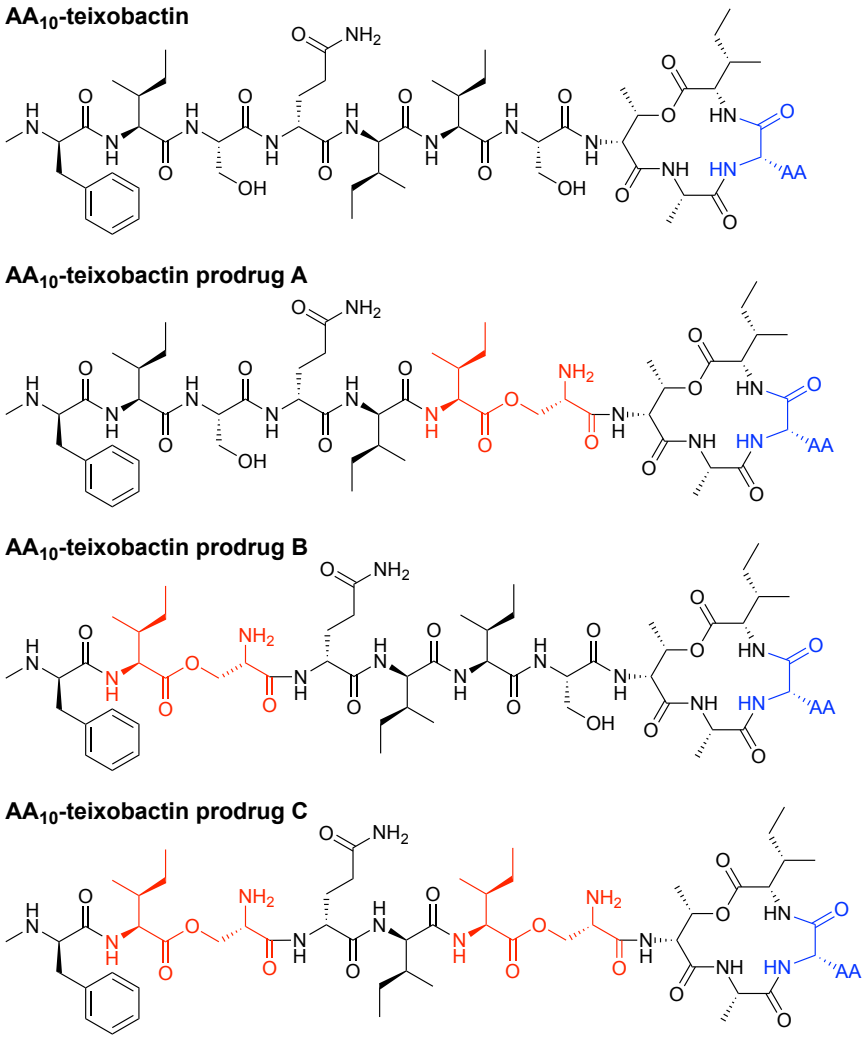

Figure 2.2. Structures of teixobactin analogues and *O*-acyl isopeptide prodrugs of teixobactin analogues. AA is lysine, arginine, or leucine.

RESULTS AND DISCUSSION

We envisioned that the *O*-acyl isopeptide strategy that Kiso and coworkers developed to facilitate the synthesis of aggregation-prone peptide sequences could be adapted to circumvent the propensity of teixobactin to aggregate under conditions needed for intravenous administration.[13–17] In the *O*-acyl isopeptide strategy, a native amide bond is replaced with an ester linkage to serine or threonine to disrupt β-sheet formation by an aggregation-prone sequence. The resulting *O*-acyl

isopeptide also has an additional positive charge which further enhances solubility. Upon exposure to neutral or basic conditions, the *O*-acyl isopeptide rearranges to form the native amide bond (Figure 2.3).

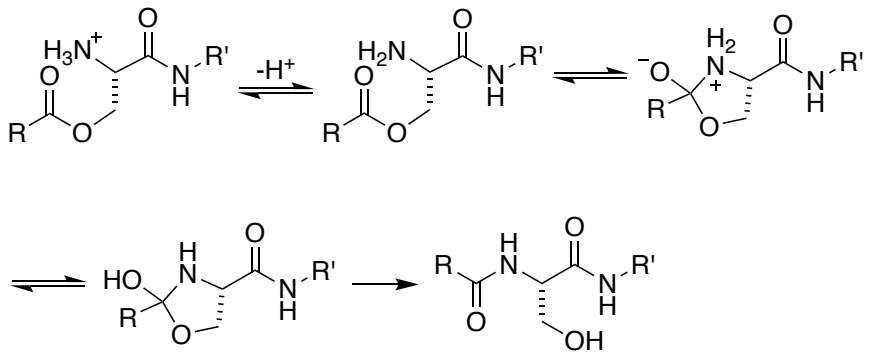

Figure 2.3. Mechanism of the conversion of *O*-acyl isopeptides to peptides.

Synthesis of Teixobactin *O*-acyl Isopeptide Prodrug Analogues

We adapted the synthesis of teixobactin analogues that our laboratory previously developed to permit the synthesis of *O*-acyl isopeptide prodrugs of teixobactin analogues.[11] We synthesized the teixobactin *O*-acyl isopeptide prodrug analogues by Fmoc-based solid-phase peptide synthesis (SPPS) using the commercially available Boc-Ser(Fmoc-Ile)-OH *O*-acyl isodipeptide building block in place of Ile_2 and Ser_3, Ile_6 and Ser_7, or both Ile_2 and Ser_3 and Ile_6 and Ser_7. We used this approach to synthesize prodrugs of the teixobactin analogues, Lys_{10}-teixobactin, Arg_{10}-teixobactin, and Leu_{10}-teixobactin. The Arg_{10} analogue replaces the cyclic guanidinium group of *allo*-enduracididine (*allo*-End) with an acyclic guanidinium group and exhibits good antibiotic activity, albeit not as good as the native antibiotic.[11,18–20] The Lys_{10} analogue also contains a positively charged residue and exhibits good antibiotic activity.[11,20] The Leu_{10} analogue is especially interesting, because it contains an uncharged residue, yet exhibits good antibiotic activity.[20–22] Although the lack of commercial sources of *allo*-enduracididine makes it more

difficult to access the corresponding prodrugs of teixobactin, we anticipate that the synthetic route described here should also allow the synthesis of teixobactin prodrugs.

The synthesis of these *O*-acyl isopeptide prodrugs begins by attaching Fmoc-Lys(Boc)-OH, Fmoc-Arg(Pbf)-OH, or Fmoc-Leu-OH to 2-chlorotrityl chloride resin. Residues 9 through 1 are then introduced by standard Fmoc-based SPPS using HCTU as the coupling reagent.[11] Boc-Ser(Fmoc-Ile)-OH is coupled in place of the desired Ile and Ser residues to provide an ester linkage in place of an amide linkage. Ile_{11} is then introduced through an esterification using DIC and DMAP.[11] Fmoc deprotection followed by cleavage of the peptide from resin with 20% hexafluoroisopropanol (HFIP) in CH_2Cl_2 affords the selectively deprotected uncyclized peptide. Solution-phase macrolactamization with HATU and HOAt, followed by global deprotection with trifluoroacetic acid (TFA) and RP-HPLC purification affords the desired *O*-acyl isopeptide prodrug analogue of teixobactin as the trifluoroacetate salt. Scheme 2.1 illustrates this route with the synthesis of Lys_{10}-teixobactin prodrug A. Synthesis on a 0.1 mmol scale typically yields ca. 10 mg of the *O*-acyl isopeptide prodrug.

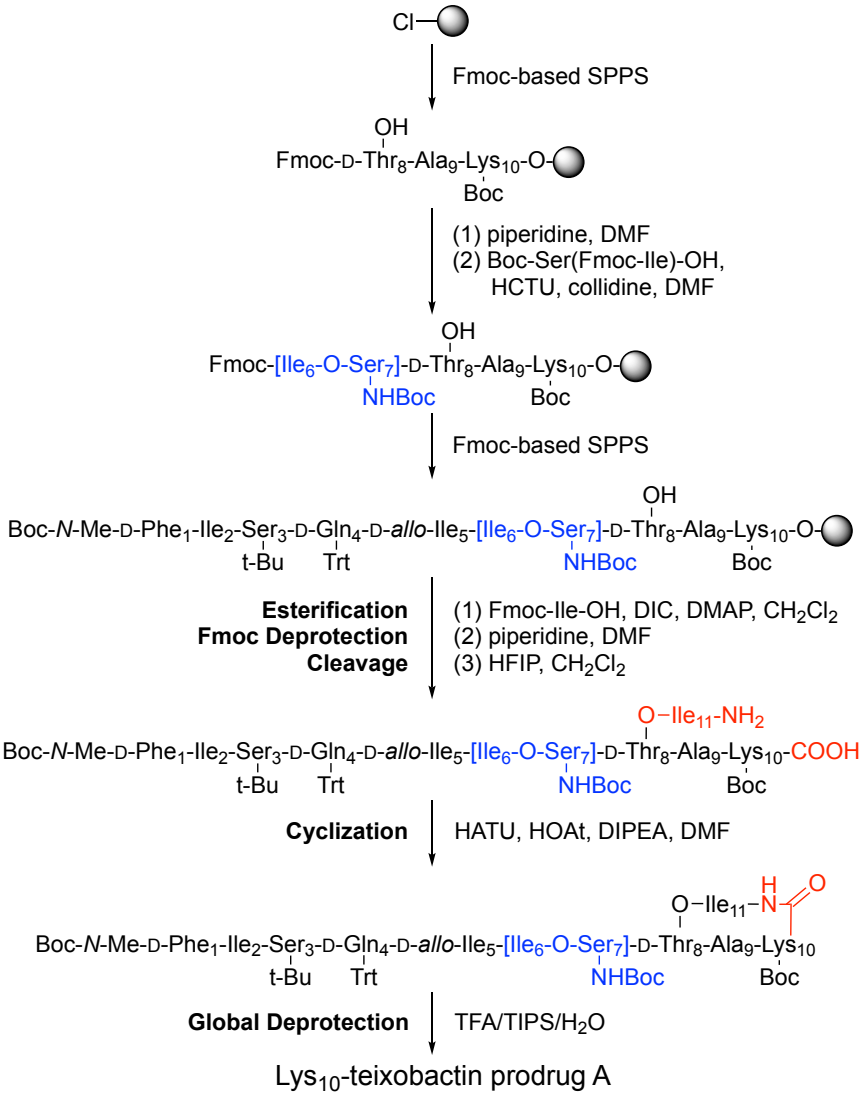

Scheme 2.1. Synthesis of Lys_{10}-teixobactin prodrug A.

The trifluoroacetate salts of the *O*-acyl isopeptide teixobactin analogues are more soluble and easier to handle than the corresponding teixobactin analogues. When synthesizing active teixobactin analogues, we routinely have to dissolve the compounds in 30–40% aqueous acetonitrile for preparative HPLC injection, while only 10–20% acetonitrile is required for the *O*-acyl isopeptide teixobactin prodrug analogues. We routinely handle the *O*-acyl isopeptide teixobactin prodrug analogues as 10 mg/mL aqueous solutions, while the corresponding teixobactin analogues are not soluble at this concentration and form gels (Figure S2.1). The

introduction of the *O*-acyl isopeptide linkage thus improves the solubility and handling of the prodrugs by reducing their propensity to aggregate in aqueous solutions.

Conversion of the Prodrugs to Teixobactin Analogues

Each of the teixobactin prodrugs undergoes clean conversion to the corresponding teixobactin analogue at physiological pH. When each of the A and B series of prodrugs was incubated in 50 mM phosphate buffer at pH 7.4 and the conversion reaction was monitored by HPLC, a new peak appeared in the HPLC trace corresponding to the teixobactin analogue. Figure 2.4A illustrates the clean conversion of Lys_{10}-teixobactin prodrug A to Lys_{10}-teixobactin. No intermediates were observed, and the conversion was complete within 12–24 h at 23 ± 2 °C (Figure S2.2 and S2.3). When each of the C series of prodrugs was incubated in 50 mM phosphate buffer under similar conditions, two intermediates were observed, and conversion to the corresponding teixobactin analogue was complete within 12–24 h (Figure S2.4). The intermediates correspond to the A and B series prodrugs, which form upon isomerization of the Ile_2–Ser_3 and Ile_6–Ser_7 isopeptide linkages.

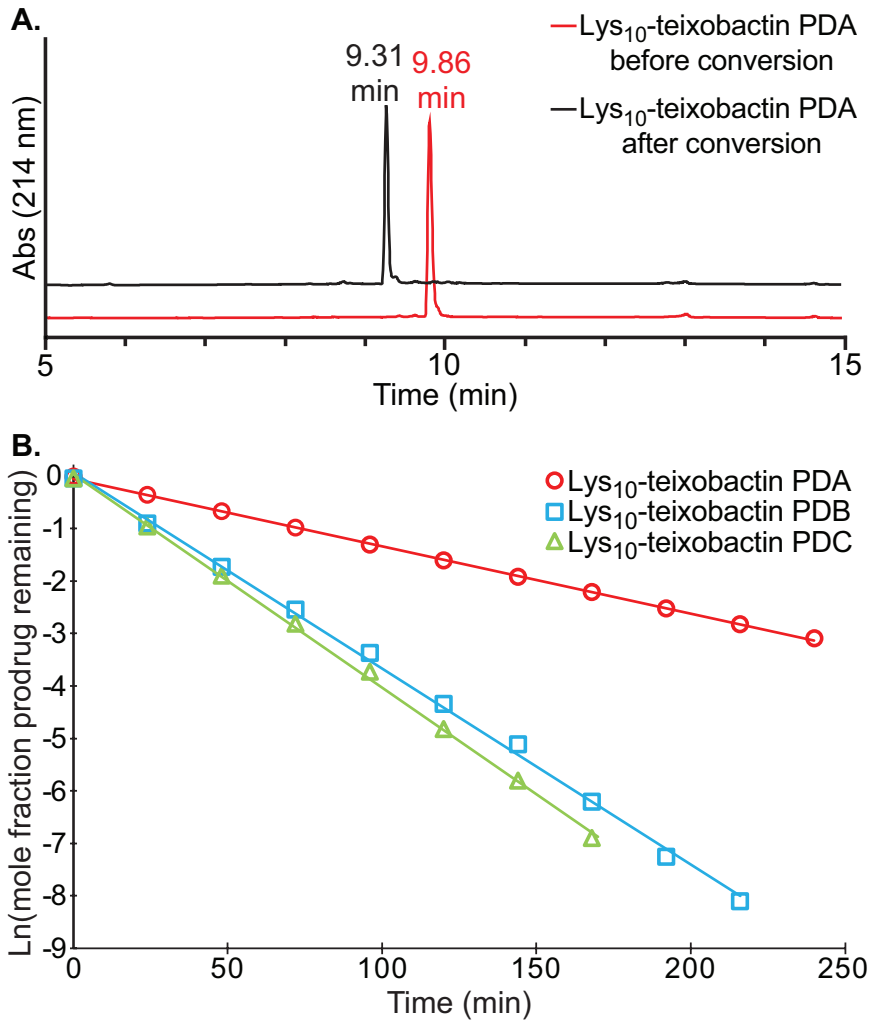

Figure 2.4. (A) Analytical RP-HPLC trace showing clean conversion of Lys_{10}-teixobactin prodrug A (red) to Lys_{10}-teixobactin (black). HPLC was run on a C18 column with a gradient of 5–100% acetonitrile over 20 min. (B) Conversion kinetics of Lys_{10}-teixobactin prodrugs A, B, and C, illustrating the disappearance of the prodrug over time. All reactions were run at 23 ± 2 °C in 50 mM phosphate buffer at pH 7.4 and monitored by HPLC analysis on a C18 column with a gradient of 5–67% acetonitrile over 15 min.

The conversion of the A and B series of prodrugs to the corresponding teixobactin analogues shows clean first-order kinetics for the disappearance of the prodrugs and the appearance of the corresponding teixobactin analogues. The conversion of the C series of prodrugs also shows clean first-order kinetics for the disappearance of the prodrugs (Figures S2.5 and S2.6). The A- and B-series prodrugs form as intermediates during conversion of the C series and then

undergo subsequent conversion to the corresponding teixobactin analogues (Figures S2.7–S2.9). Figure 2.4B illustrates the conversion kinetics for the disappearance of Lys_{10}-teixobactin prodrugs A, B, and C. The A-series prodrugs exhibited half-lives of 54–115 minutes in phosphate buffer at 23 ± 2 °C, while the B- and C-series prodrugs exhibited half-lives of 13–36 minutes (Table 2.1). The shorter half-lives of the B- and C-series prodrugs may reflect effects of the *N*-terminal methylammonium group on the pK_a of the proximal Ser_3 ammonium group in the B- and C-series *O*-acyl isopeptides.

Table 2.1. Half-lives of teixobactin *O*-acyl isopeptide prodrug analogues.[a]

	half-life (min)
Lys_{10}-teixobactin Prodrug A	54
Lys_{10}-teixobactin Prodrug B	18
Lys_{10}-teixobactin Prodrug C	15
Arg_{10}-teixobactin Prodrug A	65
Arg_{10}-teixobactin Prodrug B	25
Arg_{10}-teixobactin Prodrug C	13
Leu_{10}-teixobactin Prodrug A	115
Leu_{10}-teixobactin Prodrug B	36
Leu_{10}-teixobactin Prodrug C	19

[a]All half-lives were determined at 23 ± 2 °C in 50 mM phosphate buffer at pH 7.4.

Conversion of the prodrugs to the corresponding teixobactin analogues occurs more rapidly at 37 °C. When the Lys_{10}-teixobactin series of prodrugs was incubated at 37 °C in 100 mM phosphate buffer at pH 7.4, conversion to Lys_{10}-teixobactin occurred 3–5 times faster, with half-lives of 4–10 minutes (Figures S2.10 and S2.11).

Antibiotic Activity

The *O*-acyl isopeptide prodrugs exhibit comparable or slightly improved antibiotic activity compared to the corresponding teixobactin analogues (Table 2.2). We evaluated the antibiotic activity of the teixobactin *O*-acyl isopeptide prodrugs using minimum inhibitory concentration (MIC) assays with four Gram-positive bacteria and compared the MIC values to those of the parent

teixobactin analogues. We used methicillin-susceptible and methicillin-resistant *S. aureus* as representative pathogens and *B. subtilis* and *S. epidermidis* as additional Gram-positive bacteria, and we used *E. coli* as a Gram-negative control. We compared the activities of the teixobactin analogues and prodrugs to those of teixobactin and vancomycin.

The Lys_{10}-teixobactin prodrugs showed slightly improved activity compared to Lys_{10}-teixobactin. Thus, the Lys_{10}-teixobactin prodrugs exhibited MICs of 0.5–2 μg/mL, while Lys_{10}-teixobactin exhibited MICs of 2–4 μg/mL. The Arg_{10}-teixobactin prodrugs showed comparable antibiotic activity to Arg_{10}-teixobactin, with MICs of 1–2 μg/mL. The Leu_{10}-teixobactin prodrugs showed equal or slightly improved antibiotic activity compared to Leu_{10}-teixobactin, with MICs of 0.5–2 μg/mL.

In the original report on teixobactin, the authors performed MIC assays in the presence of 0.002% polysorbate 80, with the rationale that the polysorbate 80 prevented teixobactin from sticking to plastic surfaces.[1,23,24] Our laboratory has previously found that addition of polysorbate 80 can have dramatic effects upon the measured MIC value.[11] When we performed MIC assays with the Lys_{10}-, Arg_{10}-, and Leu_{10}-teixobactin analogues of teixobactin and the corresponding prodrugs A, B, and C in the presence of polysorbate 80, we also observed enhanced antibiotic activity. Lys_{10}-teixobactin exhibited MICs of 0.25–2 μg/mL, and the Lys_{10}-teixobactin prodrugs exhibited MICs of 0.125–2 μg/mL. Arg_{10}-teixobactin and the Arg_{10}-teixobactin prodrugs exhibited MICs of 0.25–2 μg/mL. Leu_{10}-teixobactin exhibited MICs of 0.25–1 μg/mL, and the Leu_{10}-teixobactin prodrugs exhibited MICs of 0.0625–0.5 μg/mL.

Although the prodrugs themselves are not expected to exhibit antibiotic activity, conversion under the 37 °C assay conditions should be rapid enough to prevent the bacteria from propagating. The greater activity observed for some of the prodrugs may reflect higher effective

drug concentrations resulting from complete dispersion of the prodrugs within the media. In the presence of 0.002% polysorbate 80, the Leu_{10}-teixobactin prodrugs (MIC 0.0625–0.5 μg/mL) are somewhat more active than vancomycin (MIC 0.125–2 μg/mL), although somewhat less active than teixobactin itself (MIC 0.0078–1 μg/mL).

Table 2.2. MIC values of teixobactin *O*-acyl isopeptide prodrug analogues and teixobactin analogues in μg/mL with 0% and 0.002% polysorbate 80.

	Bacillus subtilis ATCC 6051	*Staphylococcus epidermidis* ATCC 14990	*Staphylococcus aureus* (MSSA) ATCC 29213	*Staphylococcus aureus* (MRSA) ATCC 700698	*Escherichia coli* ATCC 10798
Lys_{10}-teixobactin	2[a] 0.25[b]	2–4[a] 2[b]	4[a] 2[b]	4[a] 2[b]	>32[a] >8[b]
Lys_{10}-teixobactin Prodrug A	1[a] 0.125–0.25[b]	2[a] 1[b]	2[a] 1–2[b]	2[a] 1[b]	>32[a] >8[b]
Lys_{10}-teixobactin Prodrug B	0.5–1[a] 0.25[b]	2[a] 1[b]	2[a] 1–2[b]	2[a] 1[b]	>32[a] >8[b]
Lys_{10}-teixobactin Prodrug C	0.5–1[a] 0.125–0.25[b]	2[a] 1[b]	2[a] 1[b]	2[a] 1[b]	>32[a] >8[b]
Arg_{10}-teixobactin	1[a] 0.5[b]	1[a] 1[b]	2[a] 1[b]	2[a] 1[b]	>32[a] >8[b]
Arg_{10}-teixobactin Prodrug A	1[a] 0.25[b]	2[a] 1[b]	2[a] 1[b]	1[a] 1[b]	>32[a] >8[b]
Arg_{10}-teixobactin Prodrug B	1[a] 0.25[b]	2[a] 1[b]	2[a] 2[b]	2[a] 1[b]	>32[a] >8[b]
Arg_{10}-teixobactin Prodrug C	1[a] 0.25[b]	2[a] 0.5–1[b]	2[a] 1[b]	2[a] 1[b]	>32[a] >8[b]
Leu_{10}-teixobactin	2[a] 0.5–1[b]	2[a] 2[b]	2[a] 0.25–0.5[b]	2[a] 0.5–1[b]	>32[a] >8[b]
Leu_{10}-teixobactin Prodrug A	1[a] 0.125[b]	1[a] 0.5[b]	2[a] 0.5[b]	1[a] 0.5[b]	>32[a] >8[b]
Leu_{10}-teixobactin Prodrug B	0.5[a] 0.0625[b]	1[a] 0.25–0.5[b]	1[a] 0.25–0.5[b]	1[a] 0.5[b]	>32[a] >8[b]
Leu_{10}-teixobactin Prodrug C	1[a] 0.125[b]	2[a] 0.5[b]	2[a] 0.5[b]	1[a] 0.5[b]	>32[a] >8[b]
Teixobactin	0.0312[a] 0.0078[b]	1[a] 0.0078[b]	1[a] 0.5[b]	0.5[a] 0.25[b]	32[a] >8[b]
Vancomycin	0.125–0.25[a] 0.5[b]	1[a] 2[b]	0.5[a] 1[b]	2[a] 2[b]	>32[a] >8[b]

[a]Culture media containing 0% polysorbate 80. [b]Culture media containing 0.002% polysorbate 80.

Gel Formation

The *O*-acyl isopeptide prodrug analogues of teixobactin exhibit delayed gel formation at physiological pH. We compared gel formation of the teixobactin analogues to that of the *O*-acyl isopeptide prodrugs in a qualitative gelation assay. In this experiment, a 10 mg/mL stock solution of the peptide trifluoroacetate salt in DMSO is added to 1X PBS buffer at pH 7.4 and gel formation is observed over time.[9,12] Crystal violet is added to the PBS buffer to facilitate the visualization of the gels by providing contrast. When Lys_{10}-teixobactin is added to PBS, large gelatinous aggregates form immediately (Figure 2.5). Similar behavior is also observed for teixobactin (as the hydrochloride salt). In contrast, when the Lys_{10}-teixobactin prodrugs are added, no immediate gel formation occurs. After 5 mins, a few small gelatinous aggregates become visible, with Lys_{10}-teixobactin prodrug C showing the least amount of gel formation. After 15 mins, the number of aggregates increases but the size of the aggregates does not. By 60 mins, gel formation increases significantly, especially for Lys_{10}-teixobactin prodrugs A and B, which also begin to form gelatinous aggregates of larger size. The Arg_{10}-teixobactin prodrugs and Leu_{10}-teixobactin prodrugs show similar behavior, not immediately forming gels when added to PBS, and then forming aggregates over 60 minutes (Figures S2.12 and S2.13). In contrast, Arg_{10}-teixobactin and Leu_{10}-teixobactin form gels immediately upon addition to PBS.

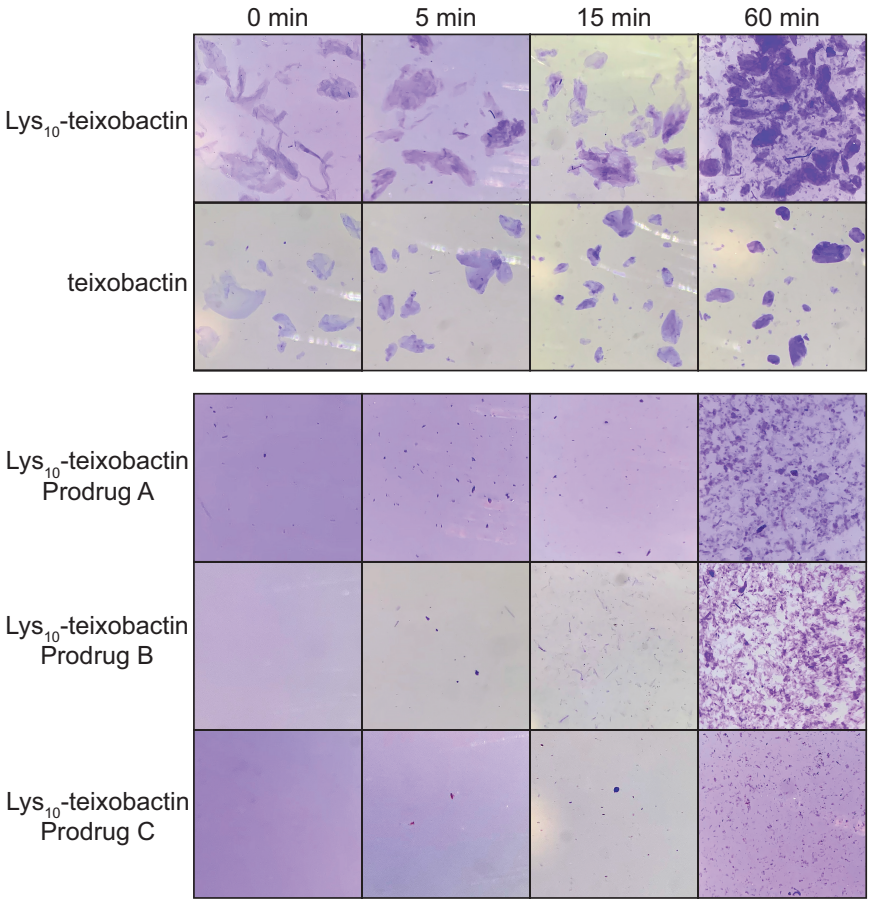

Figure 2.5. Gel formation of Lys_{10}-teixobactin and teixobactin and delayed gel formation of Lys_{10}-teixobactin prodrugs A, B, and C.

The gelation assays of the *O*-acyl isopeptide prodrugs demonstrate that these compounds do not gelate immediately upon exposure to buffer, unlike teixobactin and active teixobactin analogues. Thus, the prodrugs remain in solution and can be thoroughly dispersed in PBS. As the prodrugs gradually convert, they form aggregates that are smaller and more dispersed than those formed by teixobactin and the teixobactin analogues. The greater solubility of the prodrugs should impart better pharmacological properties than the parent analogues and may thus make them superior drug candidates.

Hemolytic and Cytotoxicity Assays

We evaluated the hemolytic activity of the *O*-acyl isopeptide prodrugs and the corresponding teixobactin analogues with human red blood cells (Figures S2.14–S2.21). We used Triton X-100 and melittin as positive controls and vancomycin and water (vehicle) as negative controls in the hemolysis assays.[9,25,26] The teixobactin analogues and corresponding *O*-acyl isopeptide prodrugs exhibited no hemolytic activity at concentrations up to 100 μg/mL in the absence of polysorbate 80. In the presence of 0.002% polysorbate 80, the Arg_{10}-teixobactin analogue and corresponding *O*-acyl isopeptide prodrugs exhibited modest hemolytic activity, with 7–10% hemolytic activity occurring at 100 μg/mL. In contrast, 0.002% polysorbate 80 had no effect on the hemolytic activity of Lys_{10}-teixobactin and Leu_{10}-teixobactin and little effect on the corresponding *O*-acyl isopeptide prodrug analogues. When we performed hemolysis assays with teixobactin, we observed no hemolysis up to 100 μg/mL without polysorbate 80 and modest hemolysis (4%) at 100 μg/mL with 0.002% polysorbate 80. We observed no hemolysis with vancomycin at concentrations up to 100 μg/mL, and we observed 26–30% hemolysis with 1.25 μg/mL melittin with and without 0.002% polysorbate 80. Collectively, these studies suggest the *O*-acyl isopeptide prodrug analogues should be suitable for intravenous administration at concentrations well above the MIC values.

To further assess the potential of the teixobactin *O*-acyl isopeptide prodrug analogues as potential drugs we performed cytotoxicity assays (Figures S2.22–S2.27). We evaluated the cytotoxicity of the teixobactin *O*-acyl isopeptide prodrugs and the corresponding teixobactin analogues on HeLa cells using a Promega Cytotox-Glo assay. In these experiments, the Lys_{10}- and Arg_{10}-teixobactin *O*-acyl isopeptide prodrugs exhibited no cytotoxicity at concentrations up to 50 μM (72–85 μg/mL). The Leu_{10}-teixobactin *O*-acyl isopeptide prodrugs exhibited no cytotoxicity

at concentrations up to 25 μM (33–39 μg/mL) and slight cytotoxicity at 50 μM (66–77 μg/mL). These studies further suggest that the *O*-acyl isopeptide prodrug analogues should be suitable for intravenous administration at concentrations well above the MIC values.

***In vivo* efficacy**

We evaluated the *in vivo* efficacy of the Leu_{10}-teixobactin *O*-acyl isopeptide prodrugs and Leu_{10}-teixobactin in a mouse thigh infection model against MRSA (Figure 2.6 and Figure S2.28). In this experiment, mice were rendered neutropenic and then infected with MRSA (ATCC BAA-1717). After 2 h, the mice were treated with the Leu_{10}-teixobactin prodrugs, Leu_{10}-teixobactin, or vancomycin with intravenous BID dosing at 1, 3.3, and 10 mg/kg. After an additional 24 h, the mice were euthanized and the bacterial loads of the treated mice were compared to those of the untreated mice at the 2- and 26-hour time points. At 10 mg/kg dosing, Leu_{10}-teixobactin and each of the Leu_{10}-teixobactin prodrugs lowered the bacterial loads by 3–4 orders of magnitude over the untreated mice at the 26-hour time point and also lowered the bacterial load below the untreated mice at the 2-hour time point. Leu_{10}-teixobactin prodrug A also substantially lowered the bacterial load at 3.3 mg/kg dosing and thus appeared to exhibit the greatest efficacy, demonstrating activity comparable to vancomycin.

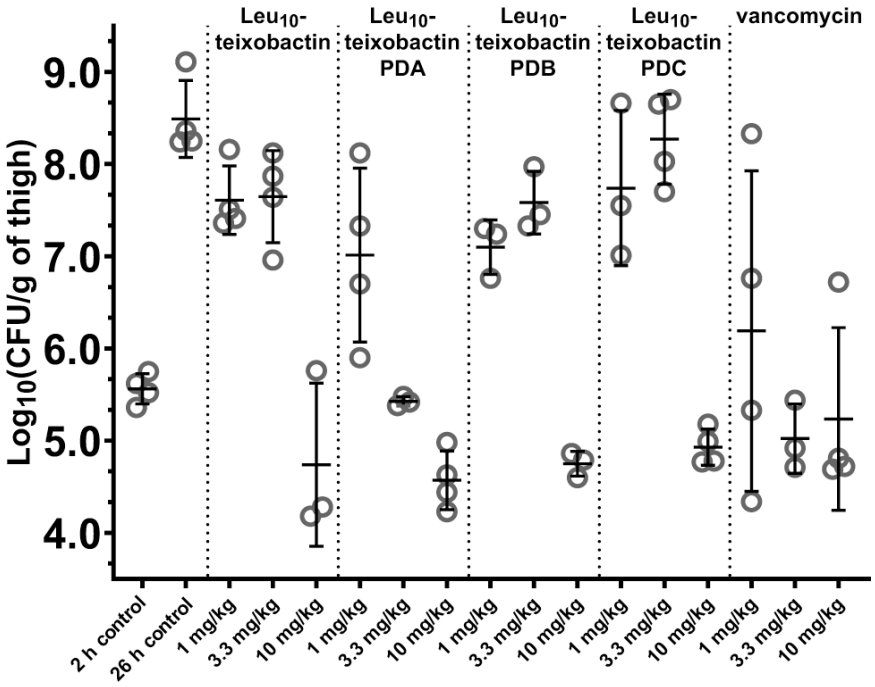

Figure 2.6. Neutropenic mouse thigh infection efficacy model against MRSA (ATCC BAA-1717) of the Leu_{10}-teixobactin prodrugs and Leu_{10}-teixobactin, with vancomycin as a positive control.

CONCLUSIONS

The propensity of teixobactin to aggregate and form gels in aqueous conditions may lead to limitations in dosing or formulation, or even the failure of teixobactin to advance to and succeed in clinical trials. Teixobactin prodrugs and prodrug analogues containing *O*-acyl isopeptide linkages may circumvent this problem. The compounds have a reduced propensity to aggregate and do not form gels immediately upon exposure to physiological pH. The prodrug analogues convert quantitatively and cleanly to the corresponding teixobactin analogues and exhibit conversion half-lives of 13–115 minutes at room temperature. The prodrug analogues exhibit comparable or slightly improved antibiotic activity against Gram-positive bacteria compared to the corresponding teixobactin analogues. The prodrug analogues have MIC values of 0.5–2 μg/mL without addition of polysorbate 80, and even lower MIC values in the presence of 0.002%

polysorbate 80. Furthermore, the prodrug analogues exhibit low hemolytic activity with or without polysorbate 80 and do not exhibit any significant cytotoxicity. The Leu_{10}-teixobactin series exhibited efficacy upon intravenous dosing in an *in vivo* infection model against MRSA.

We anticipate that intravenous administration of *O*-acyl isopeptide prodrugs of teixobactin and teixobactin analogues in human patients will allow thorough mixing and dilution in the bloodstream before conversion to the corresponding drugs. The mixing and dilution should mitigate the formation of gels and thus facilitate intravenous administration, providing a more straightforward path for teixobactin derivatives to progress to and succeed in clinical trials.

Teixobactin *O*-acyl isopeptide prodrug analogues containing leucine at position 10 exhibit comparable antibiotic activity to vancomycin. We expect that teixobactin *O*-acyl isopeptide prodrugs containing *allo*-enduracididine at position 10 will exhibit even better antibiotic activity. Because teixobactin *O*-acyl isopeptide prodrugs analogues exhibit clean conversion to the corresponding teixobactin analogues with reduced propensity to form gels, we anticipate that teixobactin prodrugs will be superior to teixobactin as drug candidates. Even the Lys_{10}-, Arg_{10}-, and Leu_{10}-teixobactin prodrug analogues reported here exhibit good antibiotic activity, with Leu_{10}-teiobactin prodrugs A, B, and C being especially noteworthy. We propose the term “isobactins” for teixobactin prodrugs and teixobactin prodrug analogues, to reflect that they isomerize to teixobactin and teixobactin analogues. We believe that the isobactins warrant further study, because the isobactins overcome a potential limitation in the intravenous dosing of teixobactin.

Epilogue to Chapter 2

After the publication of chapter 2, Prof. Nowick and I, along with our collaborators at NovoBiotic Pharmaceuticals, LLC, aimed to perform a small study to obtain a general indication of toxicity of Leu_{10}-teixobactin Prodrug A (PDA). Leu_{10}-teixobactin PDA was determined to be our lead compound from the *in vivo* efficacy study described in chapter 2. We aimed to obtain data on a repeat dose tolerability study in rats along with blood chemistries and histopathology. For these studies, NovoBiotic Pharmaceuticals, LLC provided natural teixobactin as a control and I provided Leu_{10}-teixobactin PDA. The rat repeat dose tolerability studies with histology, along with analysis and summary of the experiments, were performed by NeoSome Life Sciences, LLC.

To perform the rat repeat dose study, NeoSome Life Sciences, LLC required around 500 mg of the HCl salt of Leu_{10}-teixobactin PDA. To obtain this material, I had to scale up the synthesis of the peptide. Standardly, I synthesize the peptide on a 0.1 mmol scale using 300 mg of resin. For the synthesis of material for the toxicity study, I synthesized the peptide on a 0.2 mmol scale using 600 mg of resin. Over the course of one week, I performed five separate syntheses of Leu_{10}-teixobactin PDA on a 0.2 mmol scale, yielding roughly 1 g of crude peptide. After purifications and conversion of the material to the HCl salt as described in the supporting information of chapter 2, I provided NeoSome Life Sciences, LLC with 510 mg of peptide. I also still had roughly 350 mg of crude material that could be further purified out to obtain clean peptide.

In the rat repeat dose tolerability study, nine rats were used with three rats per group and three groups total. For the experiment, all test articles were formulated in dextrose 5% in water (D5W) just prior to each dose. The vehicle (teixobactin) and the test article (Leu_{10}-teixobactin PDA) were administered in a volume of 5 mL/kg via intravenous tail vein injection daily for 5 days. Dose volumes were adjusted daily based on animal body weight. Twenty-four hours after

the final dose administration, rats were euthanized, and blood was collected along with the spleens, kidneys, livers, hearts, and lungs. Clinical chemistries and gross necropsy were performed with observations recorded.

Group 1 received teixobactin as a 7.5 mg/kg dose via intravenous tail vein injection daily for 5 days with no observed difficulty. Group 2 received 20 mg/kg (4 mg/mL) dosing of Leu_{10}-teixobactin PDA daily for five days. Tail irritation was observed in group 2 beginning at the third dose administration, resulting in one rat in this group receiving its final dose administration via intraperitoneal injection. Group 3 was initially to received 80 mg/kg (16 mg/mL) dosing but due to solubility issues in the 5 mL/kg dosing used, the dose was initially dropped to 60 mg/kg. Unfortunately, the first rat dosed at 60 mg/kg (12 mg/mL) died immediately after dose administration. Therefore, the dose was dropped to 40 mg/kg (8 mg/mL) and the two remaining animals in the group were dosed. Unfortunately, both these animals died within two minutes of the dose administration.

At gross necropsy, the kidneys for one rat in group 1 (vehicle) did appear slightly pale and mottled. All other animal tissues did appear within the normal limits. The serum separation was clean with minimal cell lysis. Overall, it was concluded that the findings from the analysis of the blood chemistries and hematology as well as the histology performed all appeared within the range of normal and as expected for IV administration. Overall, it appears that a dose of 20 mg/kg of Leu_{10}-teixobactin PDA is tolerated in rats, but doses of 40 and 60 mg/kg are not tolerated. The rat repeated dose tolerability study did provide some insight onto the toxicity of Leu_{10}-teixobactin PDA and provides a steppingstone for possible future preclinical development of this peptide. We are grateful to NeoSome Life Science, LLC and Novobiotic Pharmaceuticals, LLC for their guidance, execution, and insights on the study and the corresponding data.

REFERENCES AND NOTES

1. Ling, L. L.; Schneider, T.; Peoples, A. J.; Spoering, A. L.; Engels, I.; Conlon, B. P.; Mueller, A.; Schäberle, T. F.; Hughes, D. E.; Epstein, S.; Jones, M.; Lazarides, L.; Steadman, V. A.; Cohen, D. R.; Felix, C. R.; Fetterman, K. A.; Millett, W. P.; Nitti, A. G.; Zullo, A. M.; Chen, C.; Lewis, K. A New Antibiotic Kills Pathogens without Detectable Resistance. *Nature* **2015**, *517*, 455–459.

2. Shukla, R.; Medeiros-Silva, J.; Parmar, A.; Vermeulen, B. J. A.; Das, S.; Paioni, A. L.; Jekhmane, S.; Lorent, J.; Bonvin, A. M. J. J.; Baldus, M.; Lelli, M.; Veldhuizen, E. J. A.; Breukink, E.; Singh, I.; Weingarth, M. Mode of Action of Teixobactins in Cellular Membranes. *Nat Commun* **2020**, *11*, 2848.

3. Homma, T.; Nuxoll, A.; Gandt, A. B.; Ebner, P.; Engels, I.; Schneider, T.; Götz, F.; Lewis, K.; Conlon, B. P. Dual Targeting of Cell Wall Precursors by Teixobactin Leads to Cell Lysis. *Antimicrob Agents Chemother* **2016**, *60*, 6510–6517.

4. Öster, C.; Walkowiak, G. P.; Hughes, D. E.; Spoering, A. L.; Peoples, A. J.; Catherwood, A. C.; Tod, J. A.; Lloyd, A. J.; Herrmann, T.; Lewis, K.; Dowson, C. G.; Lewandowski, J. R. Structural Studies Suggest Aggregation as One of the Modes of Action for Teixobactin. *Chem. Sci.* **2018**, *9*, 8850–8859.

5. Shukla, R.; Lavore, F.; Maity, S.; Derks, M. G. N.; Jones, C. R.; Vermeulen, B. J. A.; Melcrová, A.; Morris, M. A.; Becker, L. M.; Wang, X.; Kumar, R.; Medeiros-Silva, J.; van Beekveld, R. A. M.; Bonvin, A. M. J. J.; Lorent, J. H.; Lelli, M.; Nowick, J. S.; MacGillavry, H. D.; Peoples, A. J.; Spoering, A. L.; Ling, L. L.; Hughes, D. E.; Roos, W. H.; Breukink, E.; Lewis, K.; Weingarth, M. Teixobactin Kills Bacteria by a Two-Pronged Attack on the Cell Envelope. *Nature* **2022**, *608*, 390–396.

6. Breukink, E.; de Kruijff, B. Lipid II as a Target for Antibiotics. *Nat Rev Drug Discov* **2006**, *5*, 321–323.

7. de Kruijff, B.; van Dam, V.; Breukink, E. Lipid II: A Central Component in Bacterial Cell Wall Synthesis and a Target for Antibiotics. *Prostaglandins, Leukotrienes and Essential Fatty Acids* **2008**, *79*, 117–121.

8. Lloyd, D. G.; Schofield, B. J.; Goddard, M. R.; Taylor, E. J. De Novo Resistance to Arg10-Teixobactin Occurs Slowly and Is Costly. *Antimicrobial Agents and Chemotherapy* **2020**, *65*, e01152-20.

9. Chen, K. H.; Le, S. P.; Han, X.; Frias, J. M.; Nowick, J. S. Alanine Scan Reveals Modifiable Residues in Teixobactin. *Chem. Commun.* **2017**, *53*, 11357–11359.

10. Yang, H.; Bois, D. R. D.; Ziller, J. W.; Nowick, J. S. X-Ray Crystallographic Structure of a Teixobactin Analogue Reveals Key Interactions of the Teixobactin Pharmacophore. *Chem. Commun.* **2017**, *53*, 2772–2775.

11. Yang, H.; Chen, K. H.; Nowick, J. S. Elucidation of the Teixobactin Pharmacophore. *ACS Chem. Biol.* **2016**, *11*, 1823–1826.

12. Yang, H.; Wierzbicki, M.; Du Bois, D. R.; Nowick, J. S. X-Ray Crystallographic Structure of a Teixobactin Derivative Reveals Amyloid-like Assembly. *J. Am. Chem. Soc.* **2018**, *140*, 14028–14032.

13. Yoshiya, T.; Taniguchi, A.; Sohma, Y.; Fukao, F.; Nakamura, S.; Abe, N.; Ito, N.; Skwarczynski, M.; Kimura, T.; Hayashi, Y.; Kiso, Y. "O-Acyl Isopeptide Method" for Peptide Synthesis: Synthesis of Forty Kinds of "O-Acyl Isodipeptide Unit" Boc-Ser/Thr(Fmoc-Xaa)-OH. *Org. Biomol. Chem.* **2007**, *5*, 1720–1730.

14. Sohma, Y.; Taniguchi, A.; Skwarczynski, M.; Yoshiya, T.; Fukao, F.; Kimura, T.; Hayashi, Y.; Kiso, Y. 'O-Acyl Isopeptide Method' for the Efficient Synthesis of Difficult Sequence-Containing Peptides: Use of 'O-Acyl Isodipeptide Unit.' *Tetrahedron Letters* **2006**, *47*, 3013–3017.

15. Sohma, Y.; Yoshiya, T.; Taniguchi, A.; Kimura, T.; Hayashi, Y.; Kiso, Y. Development of O-Acyl Isopeptide Method. *Peptide Science* **2007**, *88*, 253–262.

16. Mroz, P. A.; Perez-Tilve, D.; Liu, F.; Mayer, J. P.; DiMarchi, R. D. Native Design of Soluble, Aggregation-Resistant Bioactive Peptides: Chemical Evolution of Human Glucagon. *ACS Chem. Biol.* **2016**, *11*, 3412–3420.

17. Mailig, M.; Liu, F. The Application of Isoacyl Structural Motifs in Prodrug Design and Peptide Chemistry. *ChemBioChem* **2019**, *20*, 2017–2031.

18. Parmar, A.; Iyer, A.; Vincent, C. S.; Lysebetten, D. V.; Prior, S. H.; Madder, A.; Taylor, E. J.; Singh, I. Efficient Total Syntheses and Biological Activities of Two Teixobactin Analogues. *Chem. Commun.* **2016**, *52*, 6060–6063.

19. Jad, Y. E.; Acosta, G. A.; Naicker, T.; Ramtahal, M.; El-Faham, A.; Govender, T.; Kruger, H. G.; de la Torre, B. G.; Albericio, F. Synthesis and Biological Evaluation of a Teixobactin Analogue. *Org. Lett.* **2015**, *17*, 6182–6185.

20. Karas, J. A.; Chen, F.; Schneider-Futschik, E. K.; Kang, Z.; Hussein, M.; Swarbrick, J.; Hoyer, D.; Giltrap, A. M.; Payne, R. J.; Li, J.; Velkov, T. Synthesis and Structure−activity Relationships of Teixobactin. *Annals of the New York Academy of Sciences* **2020**, *1459*, 86–105.

21. Parmar, A.; Iyer, A.; Prior, S. H.; Lloyd, D. G.; Goh, E. T. L.; Vincent, C. S.; Palmai-Pallag, T.; Bachrati, C. Z.; Breukink, E.; Madder, A.; Lakshminarayanan, R.; Taylor, E. J.; Singh, I. Teixobactin Analogues Reveal Enduracididine to Be Non-Essential for Highly Potent Antibacterial Activity and Lipid II Binding. *Chem. Sci.* **2017**, *8*, 8183–8192.

22. Parmar, A.; Lakshminarayanan, R.; Iyer, A.; Mayandi, V.; Leng Goh, E. T.; Lloyd, D. G.; Chalasani, M. L. S.; Verma, N. K.; Prior, S. H.; Beuerman, R. W.; Madder, A.; Taylor, E. J.; Singh, I. Design and Syntheses of Highly Potent Teixobactin Analogues against

Staphylococcus Aureus, Methicillin-Resistant Staphylococcus Aureus (MRSA), and Vancomycin-Resistant Enterococci (VRE) in Vitro and in Vivo. *J. Med. Chem.* **2018**, *61*, 2009–2017.

23. Arhin, F. F.; Sarmiento, I.; Belley, A.; McKay, G. A.; Draghi, D. C.; Grover, P.; Sahm, D. F.; Parr, T. R.; Moeck, G. Effect of Polysorbate 80 on Oritavancin Binding to Plastic Surfaces: Implications for Susceptibility Testing. *Antimicrob Agents Chemother* **2008**, *52*, 1597–1603.

24. Kavanagh, A.; Ramu, S.; Gong, Y.; Cooper, M. A.; Blaskovich, M. A. T. Effects of Microplate Type and Broth Additives on Microdilution MIC Susceptibility Assays. *Antimicrobial Agents and Chemotherapy* **2018**, *63*, e01760-18.

25. Evans, B. C.; Nelson, C. E.; Yu, S. S.; Beavers, K. R.; Kim, A. J.; Li, H.; Nelson, H. M.; Giorgio, T. D.; Duvall, C. L. Ex Vivo Red Blood Cell Hemolysis Assay for the Evaluation of pH-Responsive Endosomolytic Agents for Cytosolic Delivery of Biomacromolecular Drugs. *JoVE* **2013**, No. 73, 50166.

26. Oddo, A.; Hansen, P. R. Hemolytic Activity of Antimicrobial Peptides. In *Antimicrobial Peptides: Methods and Protocols*; Hansen, P. R., Ed.; Methods in Molecular Biology; Springer: New York, NY, 2017; pp 427–435.

Supporting Information for Chapter 2:

Isobactins: *O*-acyl isopeptide prodrugs of teixobactin and teixobactin derivatives

Table of Contents

Supplementary figures

Supplementary figures

Figure S2.1. Solubility of Lys_{10}-teixobactin prodrug A, B, and C and Lys_{10}-teixobactin in water. Well 1: 1.0 mg of Lys_{10}-teixobactin prodrug A TFA salt in 100 µL of water. Well 2: 1.0 mg of Lys_{10}-teixobactin prodrug B TFA salt in 100 µL of water. Well 3: Lys_{10}-teixobactin prodrug C TFA salt in 100 µL of water. Well 4: 1.0 mg of Lys_{10}-teixobactin TFA salt in 100 µL of water. Lys_{10}-teixobactin prodrugs A, B, and C have solubility of at least 10 mg/mL in water and form clear solutions, while Lys_{10}-teixobactin is considerably less soluble and forms a gel.

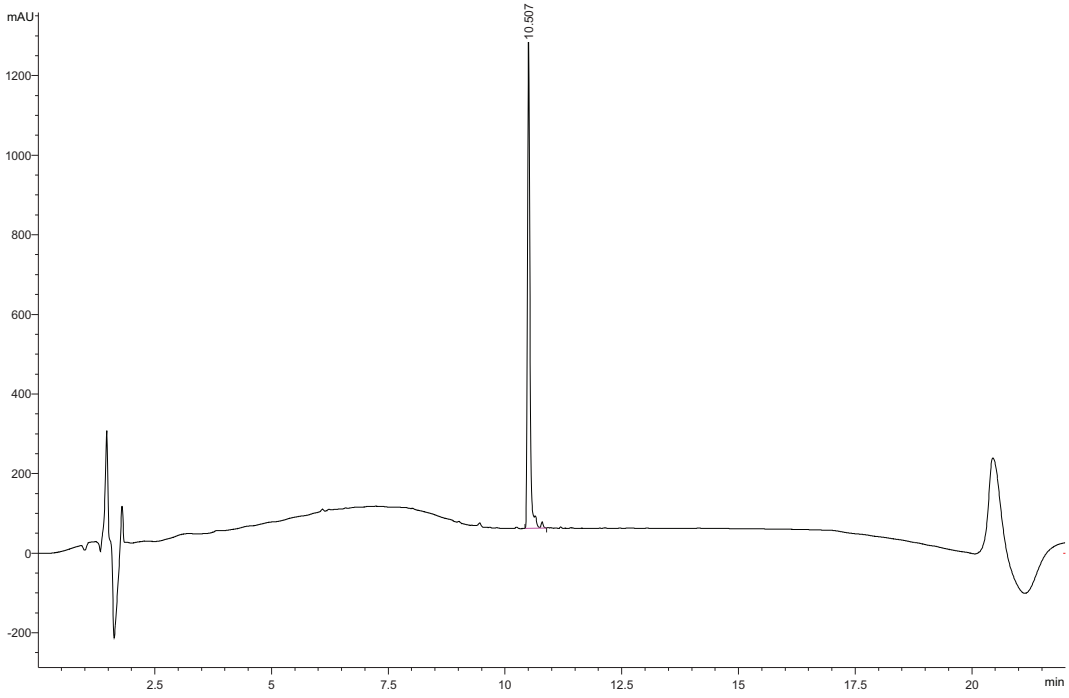

Figure S2.2. Analytical RP-HPLC trace showing the of the complete conversion of Arg_{10}-teixobactin prodrug A after 24 h in 50 mM sodium phosphate buffer at pH 7.4. HPLC was run on a C18 column with a gradient of 5–67% acetonitrile over 15 mins.

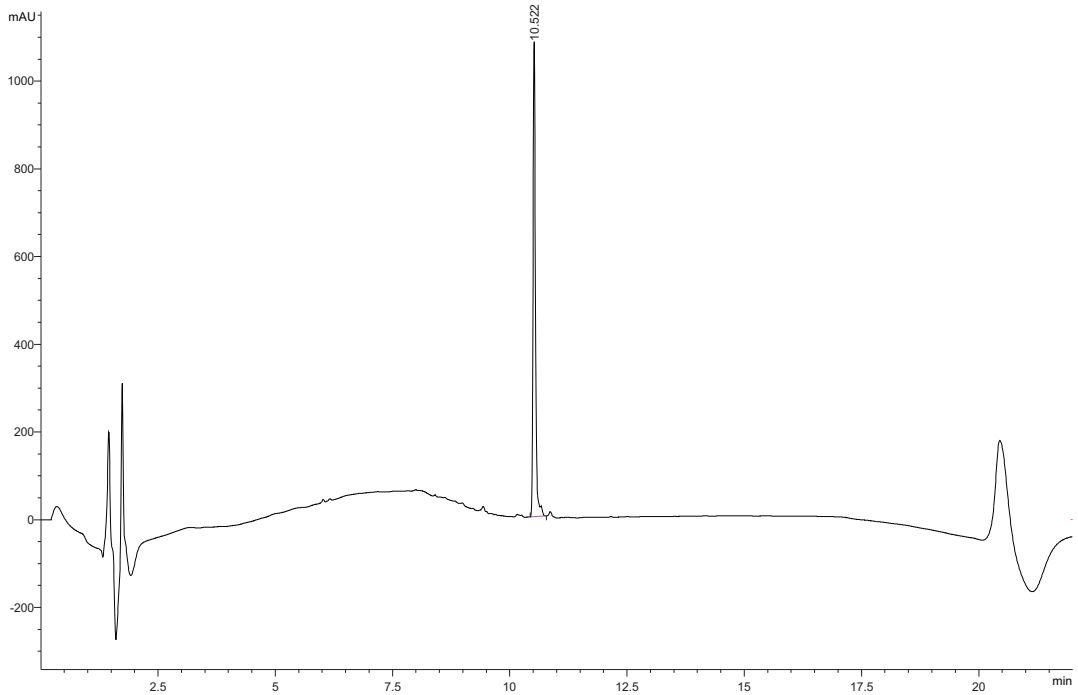

Figure S2.3. Analytical RP-HPLC trace showing the of the complete conversion of Arg_{10}-teixobactin prodrug B after 24 h in 50 mM sodium phosphate buffer at pH 7.4. HPLC was run on a C18 column with a gradient of 5–67% acetonitrile over 15 mins.

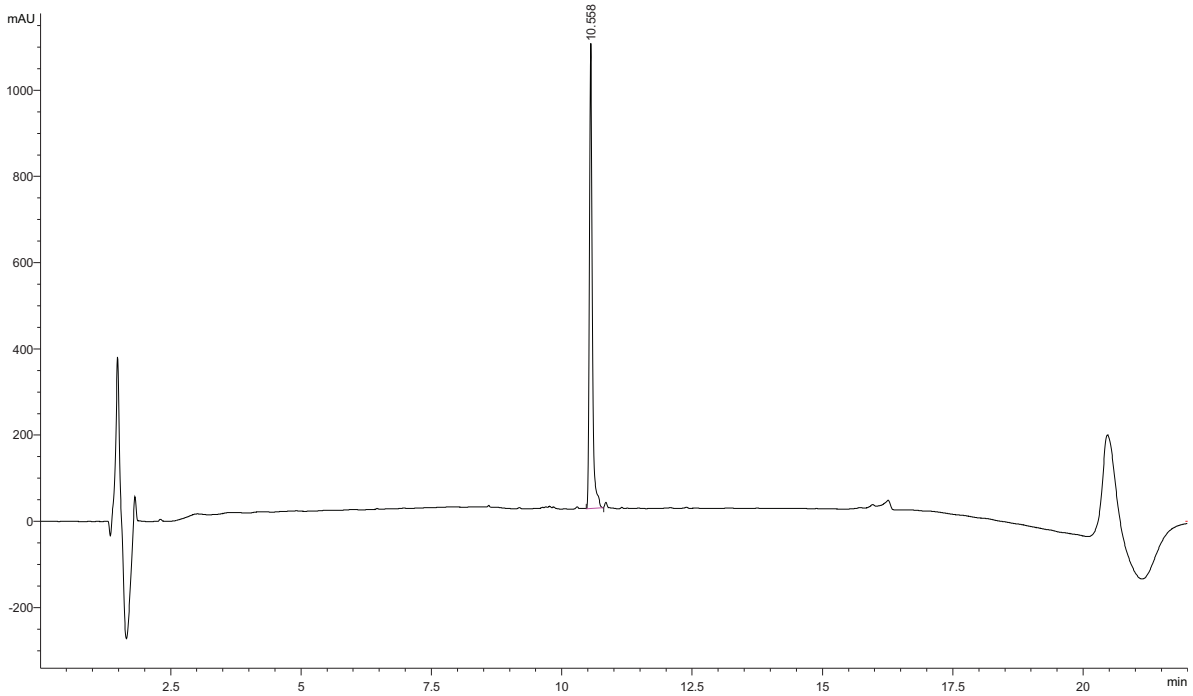

Figure S2.4. Analytical RP-HPLC trace showing the of the complete conversion of Arg_{10}-teixobactin prodrug C after 24 h in 100 mM sodium phosphate buffer at pH 7.4. HPLC was run on a C18 column with a gradient of 5–67% acetonitrile over 15 mins.

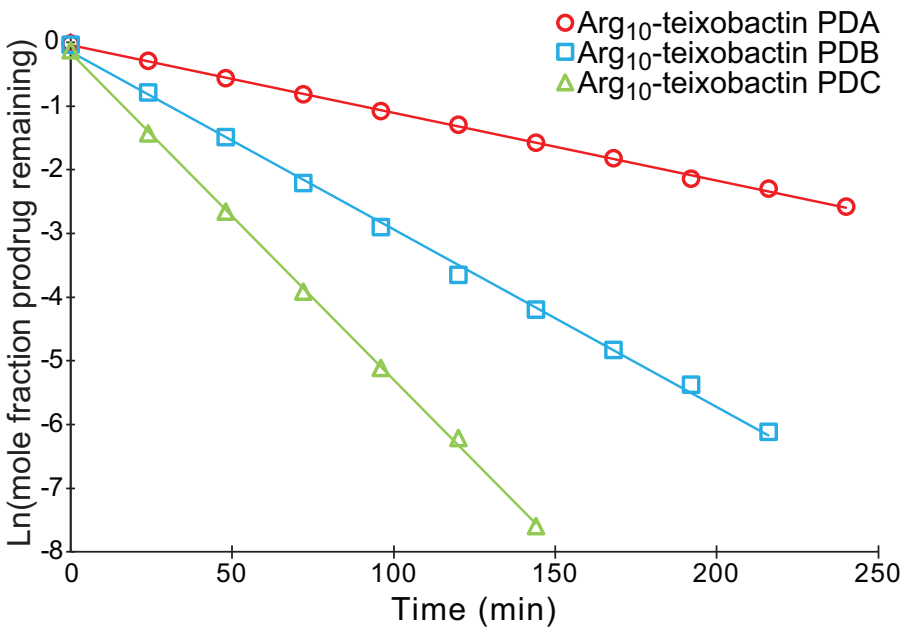

Figure S2.5. Conversion kinetics of Arg_{10}-teixobactin prodrugs A, B, and C, illustrating the disappearance of each prodrug over time. All reactions were run in 50 mM phosphate buffer at pH 7.4 and monitored by HPLC analysis on a C18 column with a gradient of 5–67% acetonitrile over 15 mins. Prodrugs A and B were run at 23 ± 1 °C; prodrug C was run at 25 ± 1 °C.

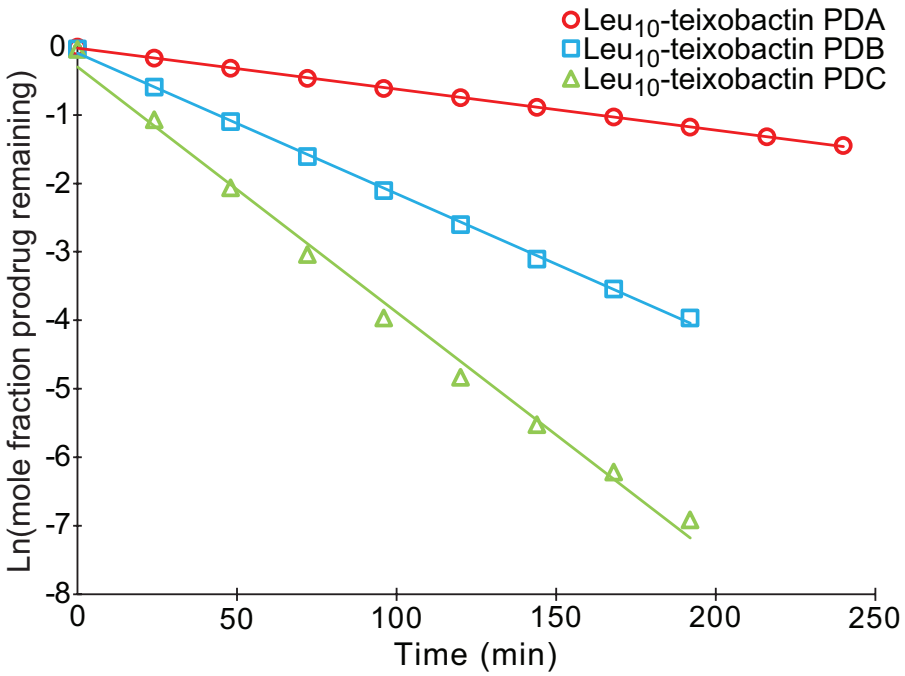

Figure S2.6. Conversion kinetics of Leu_{10}-teixobactin prodrugs A, B, and C, illustrating the disappearance of each prodrug over time. All reactions were run in 50 mM phosphate buffer at pH 7.4 and monitored by HPLC analysis on a C18 column with a gradient of 5–67% acetonitrile over 15 mins. Prodrugs A and B were run at 23 ± 1 °C; prodrug C was run at 25 ± 1 °C.

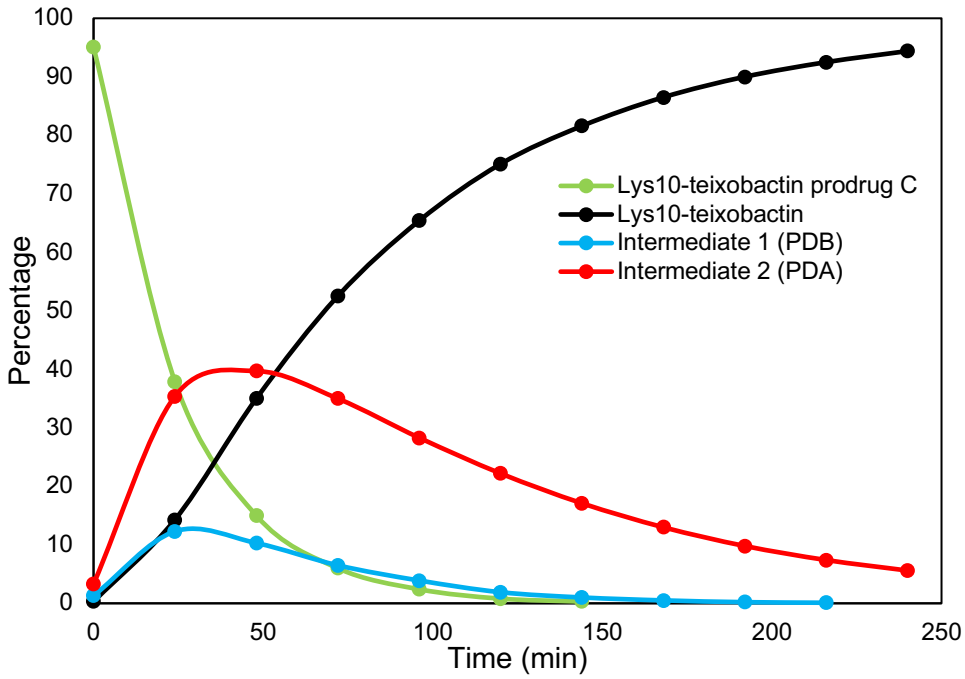

Figure S2.7. Conversion of Lys_{10}-teixobactin prodrug C (green) at 23 ± 2 °C, exhibiting the appearance of Lys_{10}-teixobactin (black) and intermediates corresponding to Lys_{10}-teixobactin prodrugs A (red) and B (blue).

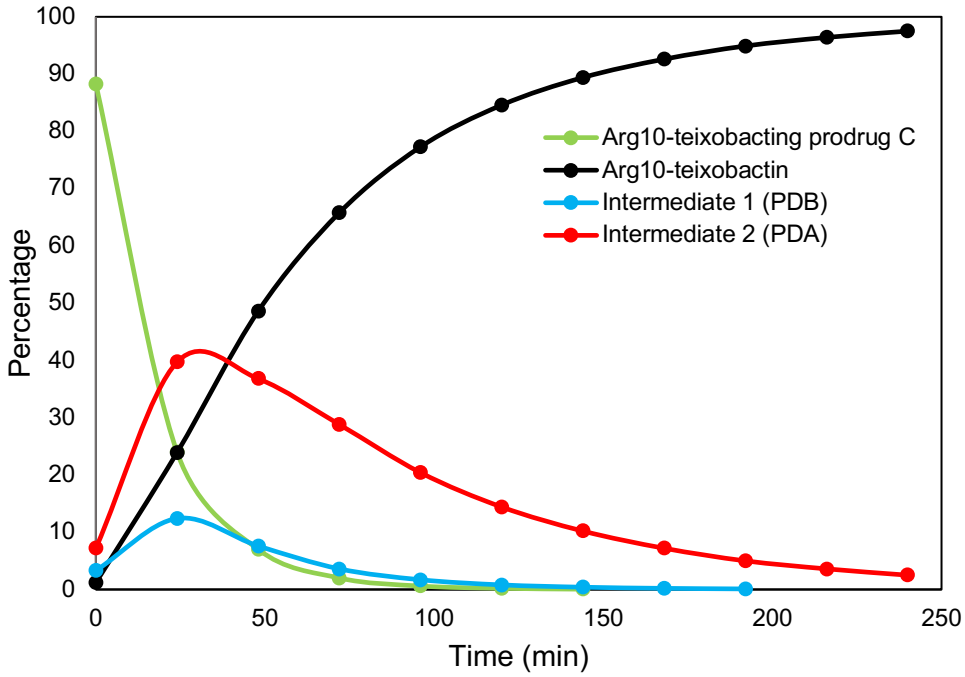

Figure S2.8. Conversion of Arg_{10}-teixobactin prodrug C (green) 25 ± 1 °C, exhibiting the appearance of Arg_{10}-teixobactin (black) and intermediates corresponding to Arg_{10}-teixobactin prodrugs A (red) and B (blue).

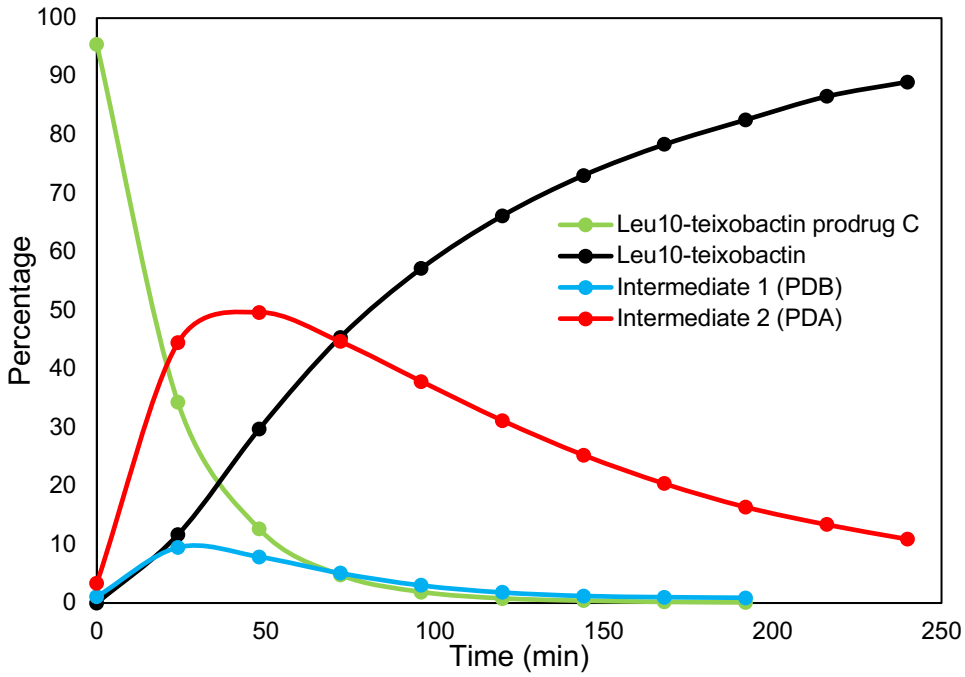

Figure S2.9. Conversion of Leu_{10}-teixobactin prodrug C (green) 25 ± 1 °C, exhibiting the appearance of Leu_{10}-teixobactin (black) and intermediates corresponding to Leu_{10}-teixobactin prodrugs A (red) and B (blue).

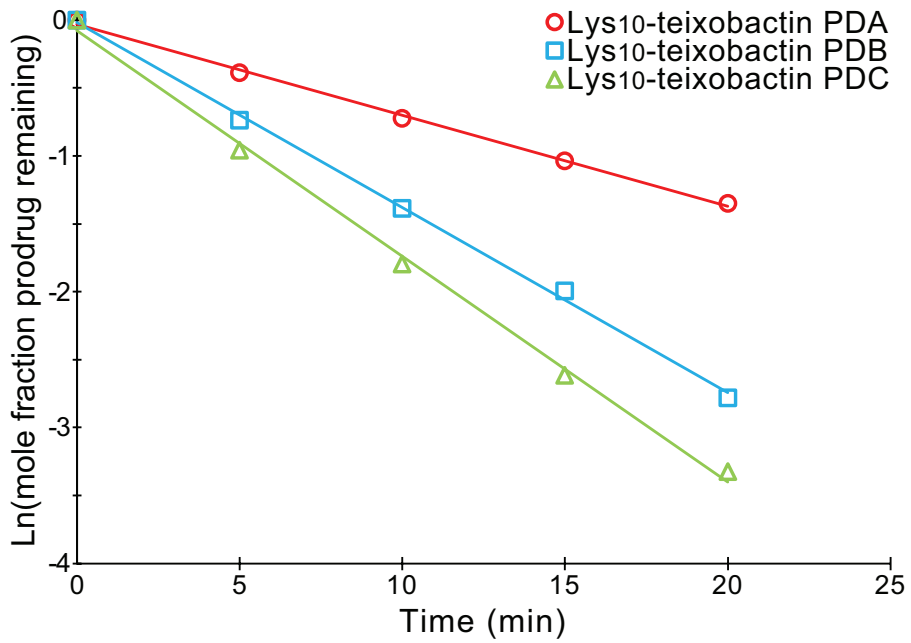

Figure S2.10. Conversion kinetics of Lys_{10}-teixobactin prodrugs A, B, and C, illustrating the disappearance of each prodrug over time at 37 °C. All reactions were run in 100 mM phosphate buffer at pH 7.4 and monitored by HPLC analysis on a C18 column with a gradient of 5–67% acetonitrile over 15 mins.

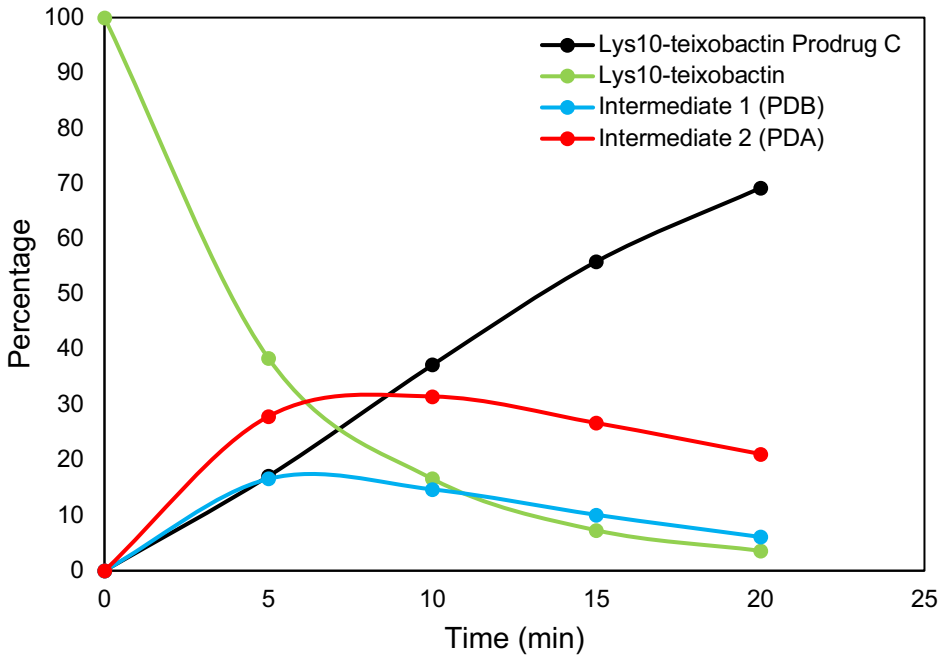

Figure S2.11. Conversion of Lys_{10}-teixobactin prodrug C (green) at 37 °C, exhibiting the appearance of Lys_{10}-teixobactin (black) and intermediates corresponding to Lys_{10}-teixobactin prodrugs A (red) and B (blue).

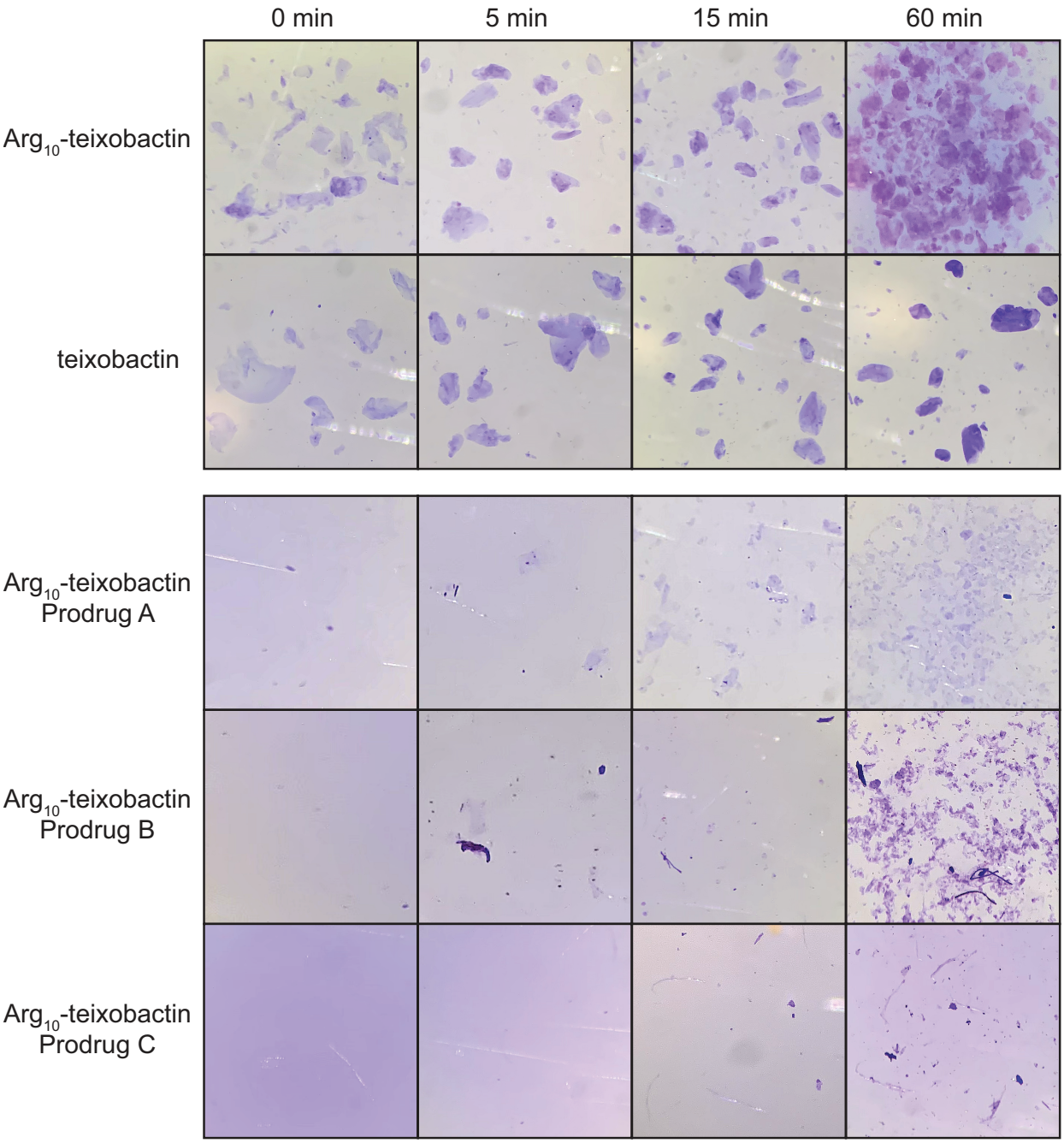

Figure S2.12. Gel formation of Arg_{10}-teixobactin and teixobactin and delayed gel formation of Arg_{10}-teixobactin prodrugs A, B, and C.

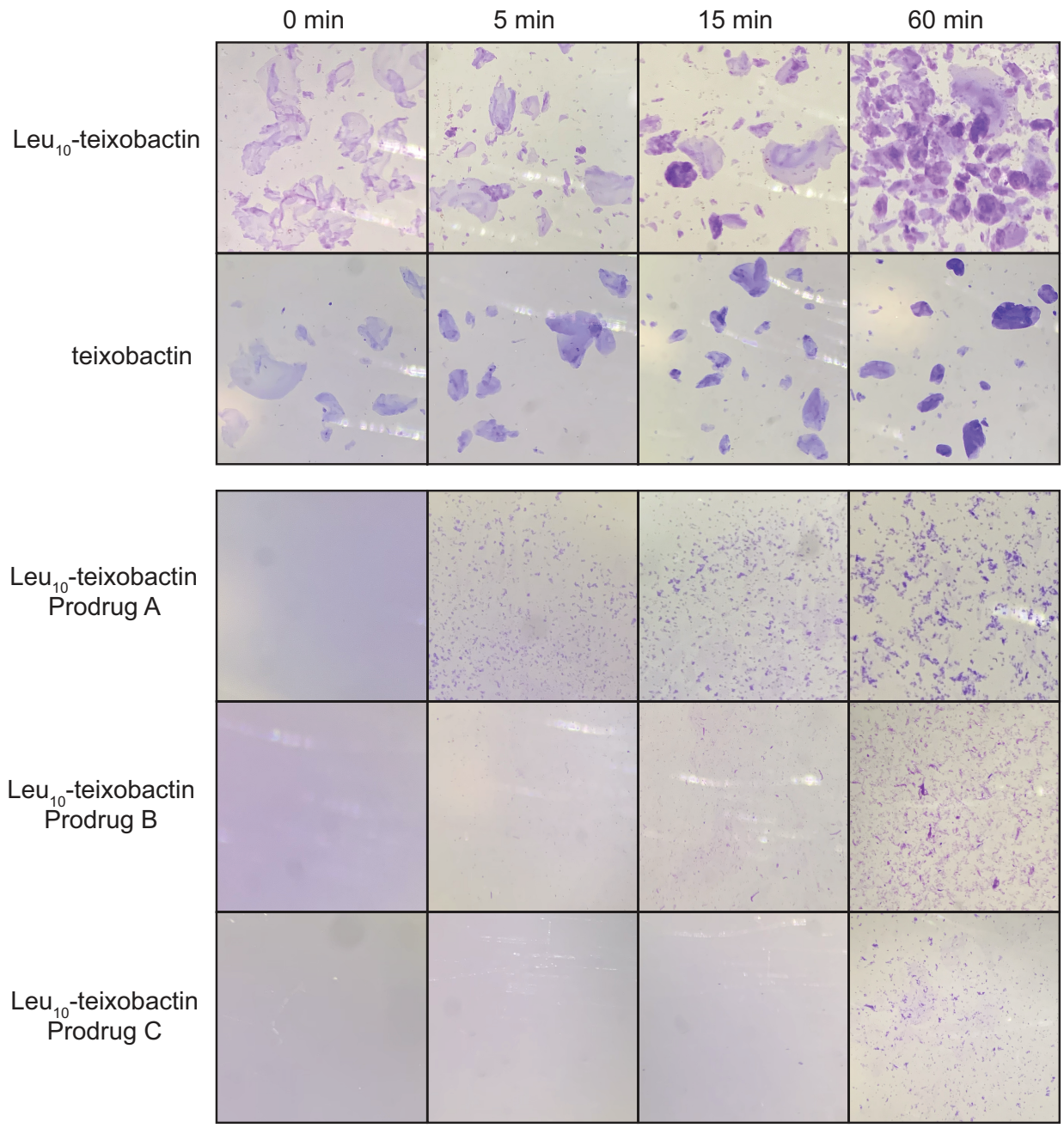

Figure S2.13. Gel formation of Leu_{10}-teixobactin and teixobactin and delayed gel formation of Leu_{10}-teixobactin prodrugs A, B, and C.

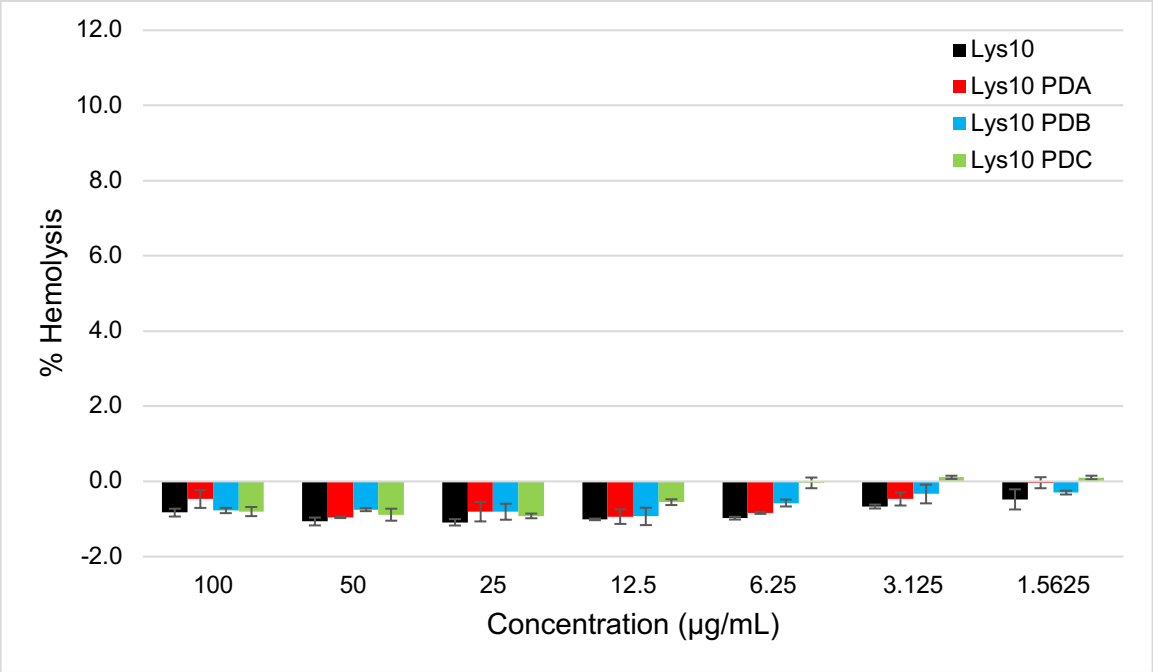

Figure S2.14. Hemolytic assay of Lys_{10}-teixobactin and the Lys_{10}-teixobactin prodrugs without polysorbate 80.

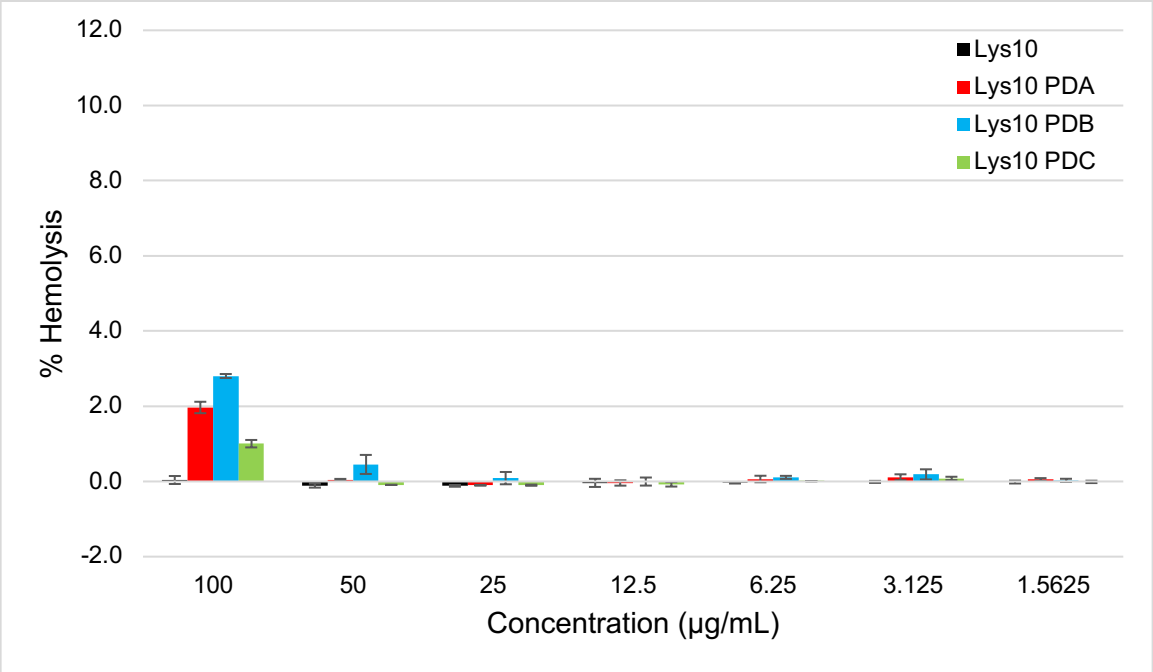

Figure S2.15. Hemolytic assay of Lys_{10}-teixobactin and the Lys_{10}-teixobactin prodrugs with 0.002% polysorbate 80.

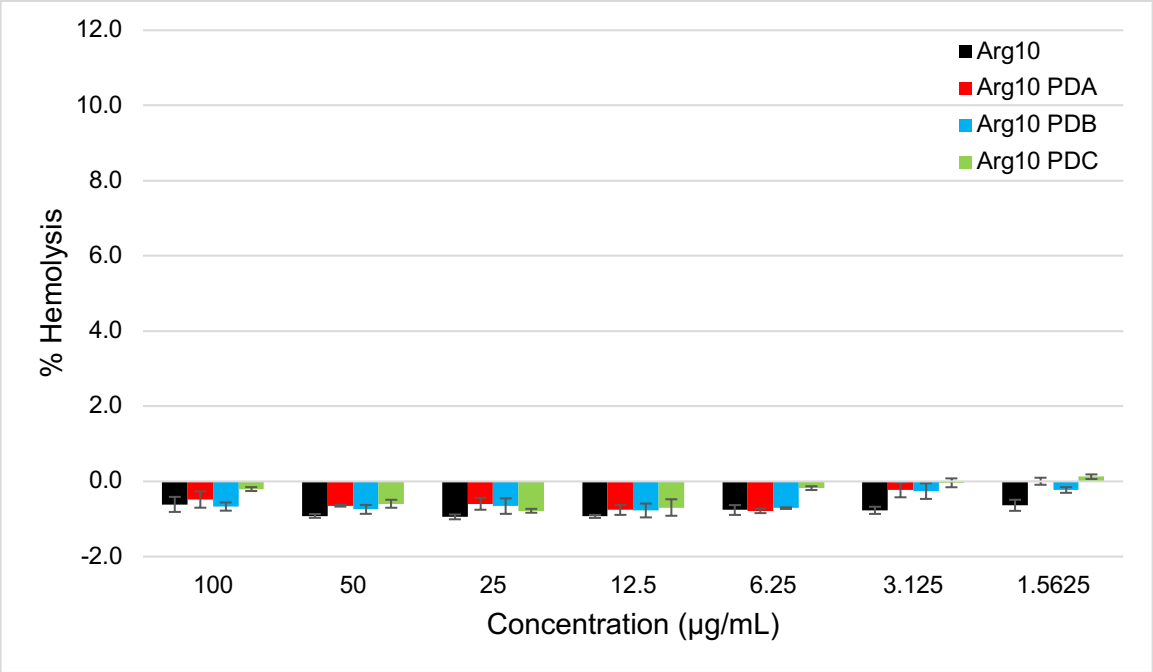

Figure S2.16. Hemolytic assay of Arg_{10}-teixobactin and the Arg_{10}-teixobactin prodrugs without polysorbate 80.

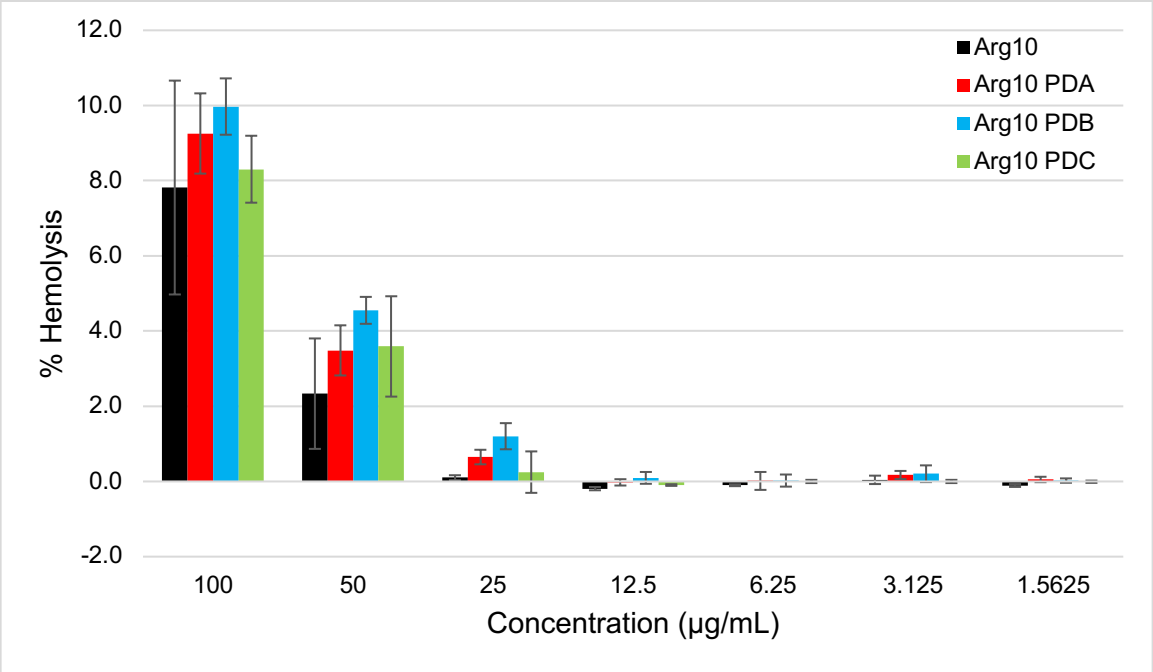

Figure S2.17. Hemolytic assay of Arg_{10}-teixobactin and the Arg_{10}-teixobactin prodrugs with 0.002% polysorbate 80.

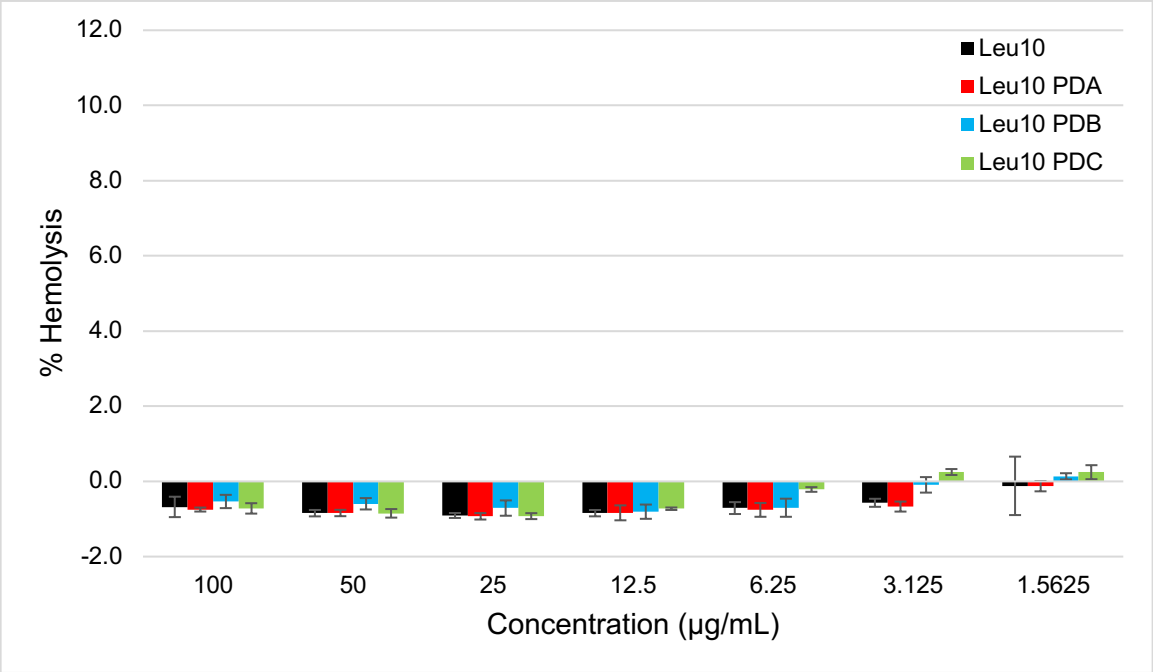

Figure S2.18. Hemolytic assay of Leu_{10}-teixobactin and the Leu_{10}-teixobactin prodrugs without polysorbate 80.

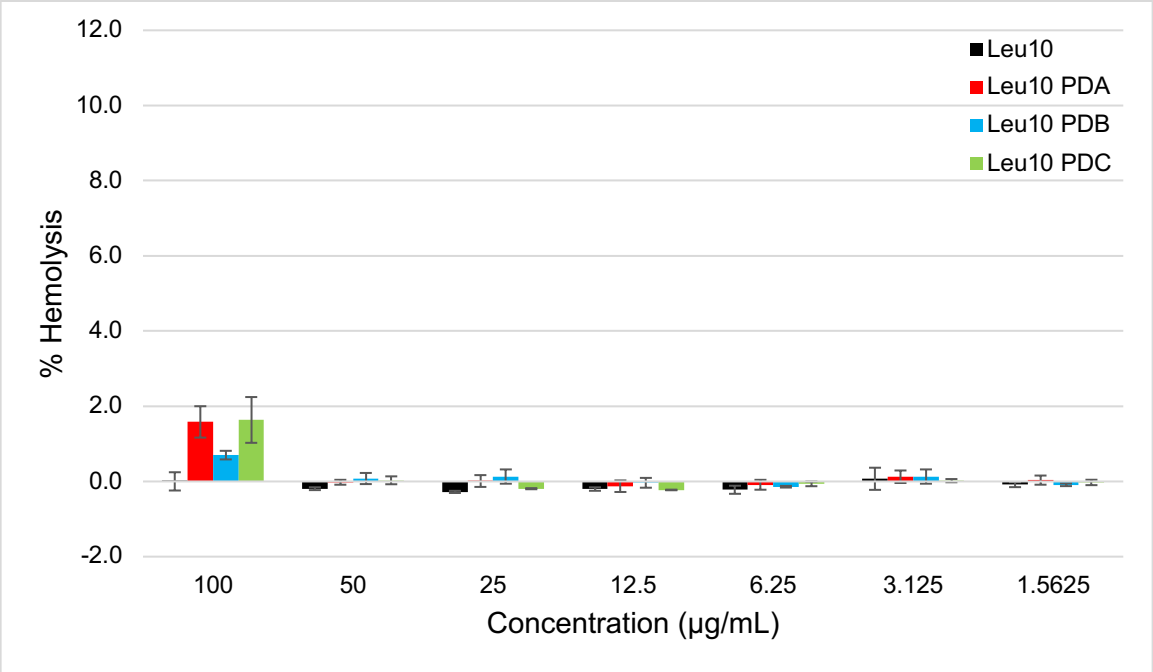

Figure S2.19. Hemolytic assay of Leu_{10}-teixobactin and the Leu_{10}-teixobactin prodrugs with 0.002% polysorbate 80.

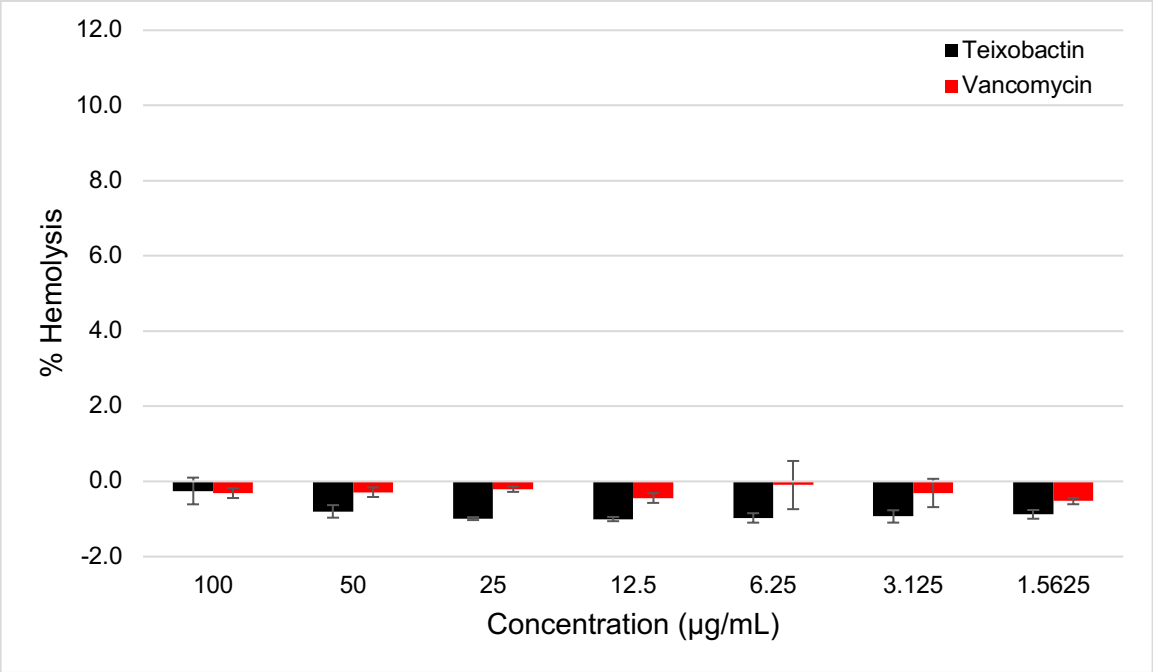

Figure S2.20. Hemolytic assay teixobactin and vancomycin without polysorbate 80.

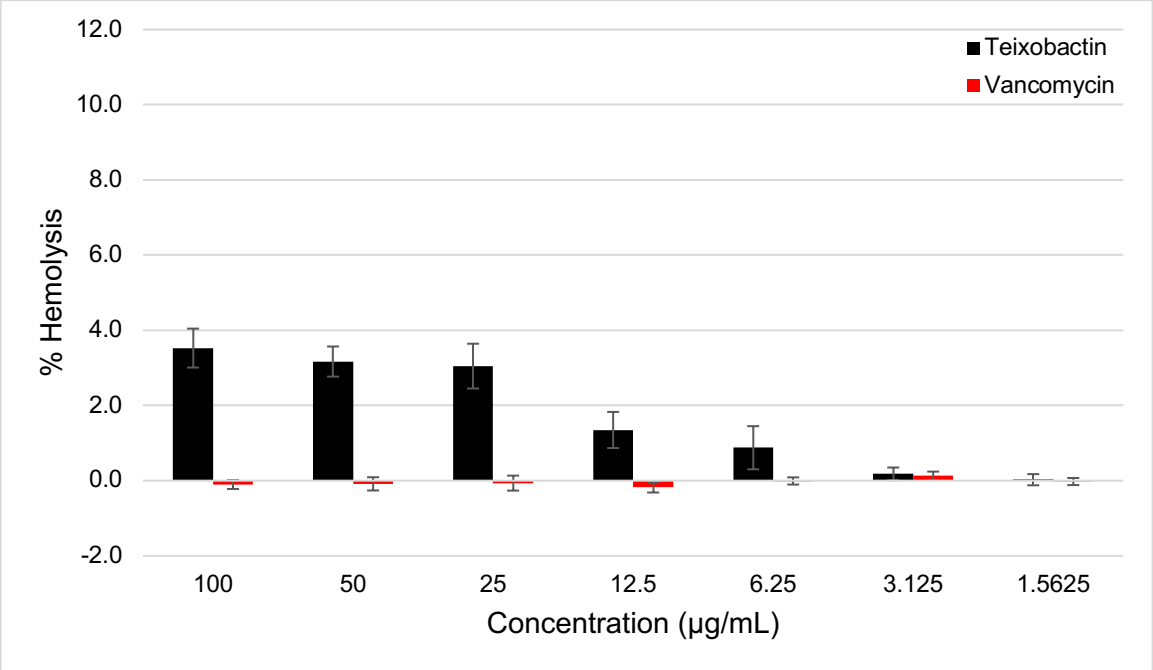

Figure S2.21. Hemolytic assay of teixobactin and vancomycin with 0.002% polysorbate 80.

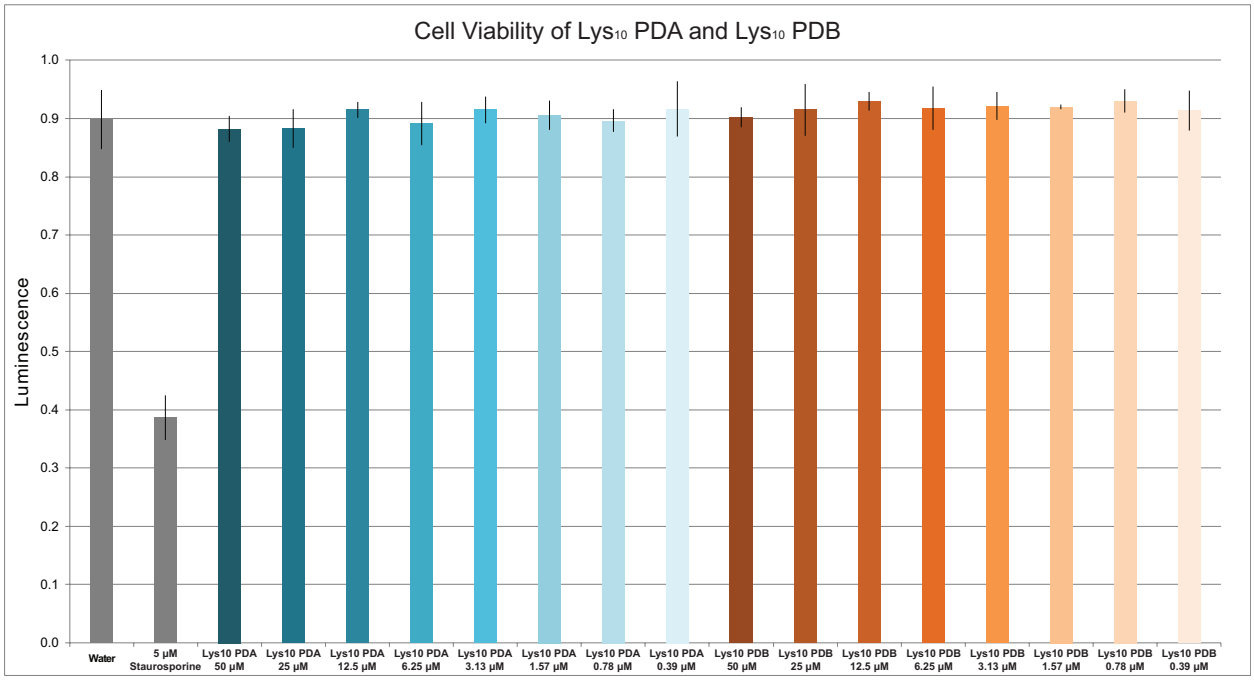

Figure S2.22. Cytotoxicity assay of Lys_{10}-teixobactin prodrug A and prodrug B with HeLa cells.

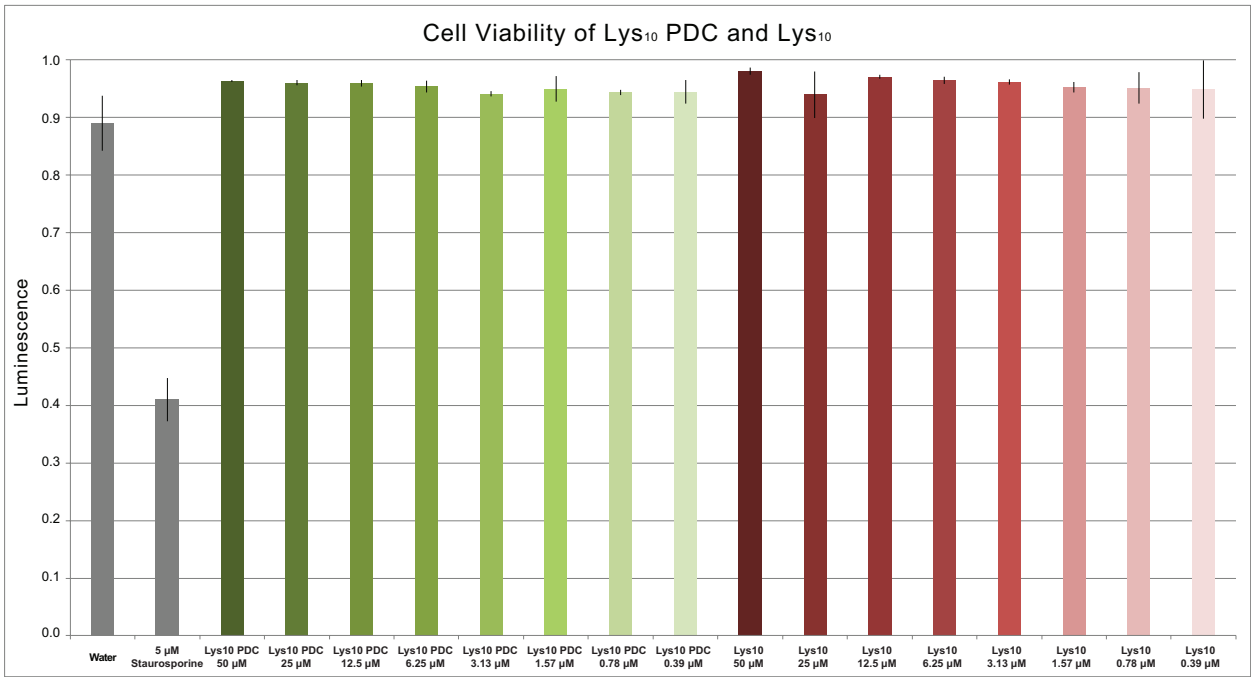

Figure S2.23. Cytotoxicity assay of Lys_{10}-teixobactin prodrug C and Lys_{10}-teixobactin with HeLa cells.

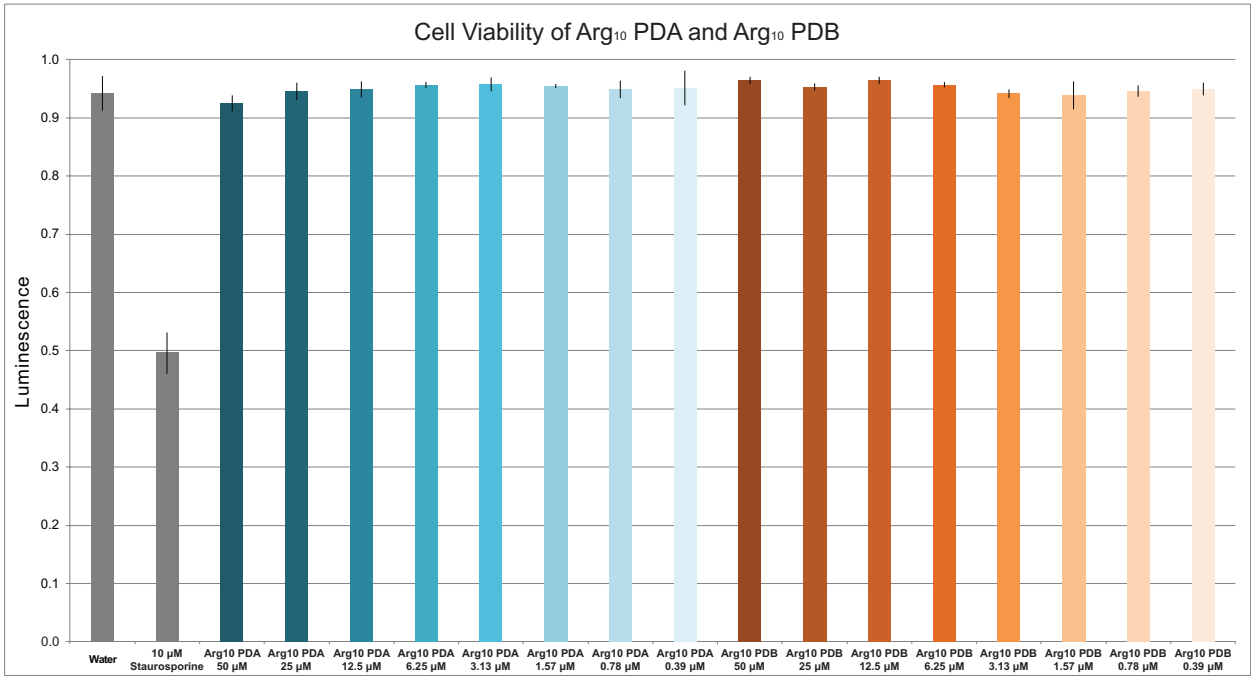

Figure S2.24. Cytotoxicity assay of Arg_{10}-teixobactin prodrug A and prodrug B with HeLa cells.

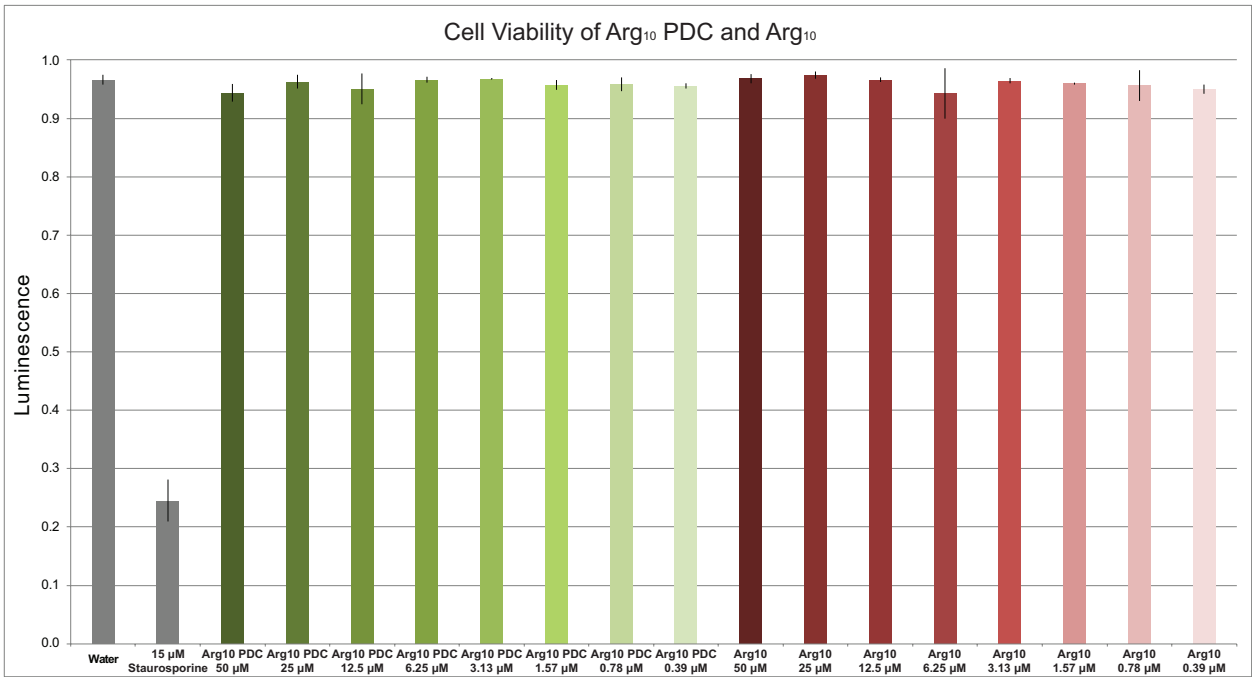

Figure S2.25. Cytotoxicity assay of Arg_{10}-teixobactin prodrug C and Arg_{10}-teixobactin with HeLa cells.

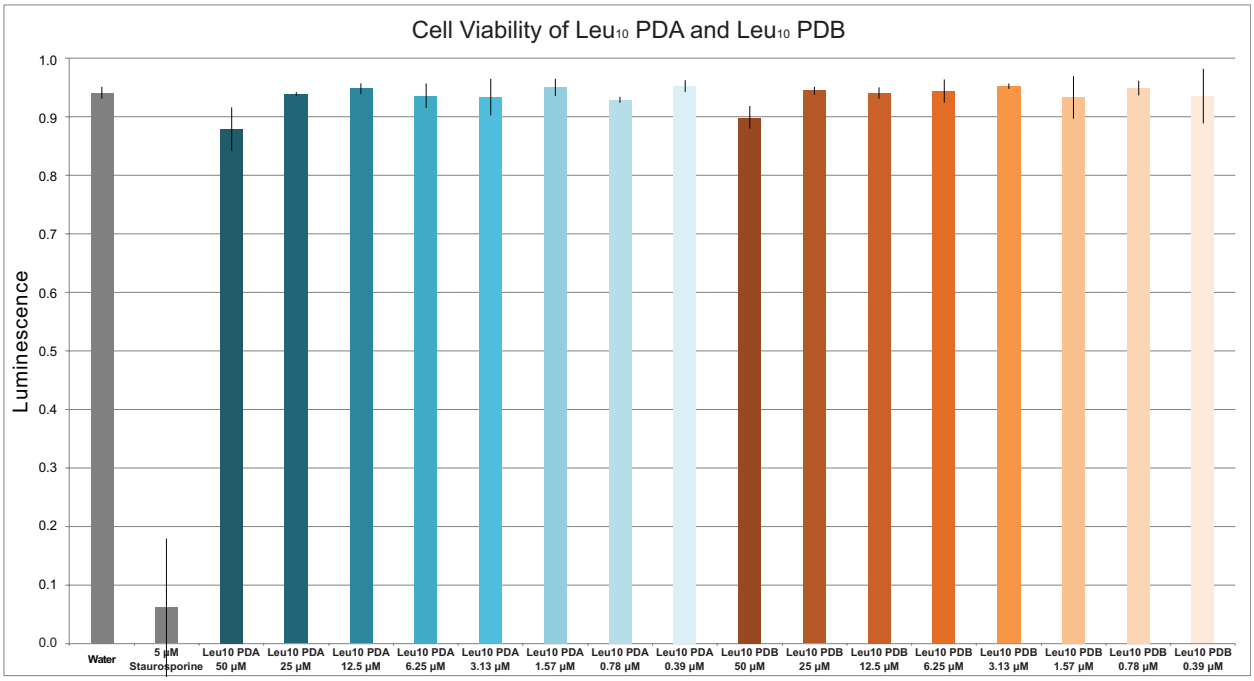

Figure S2.26. Cytotoxicity assay of Leu$_{10}$-teixobactin prodrug A and prodrug B with HeLa cells.

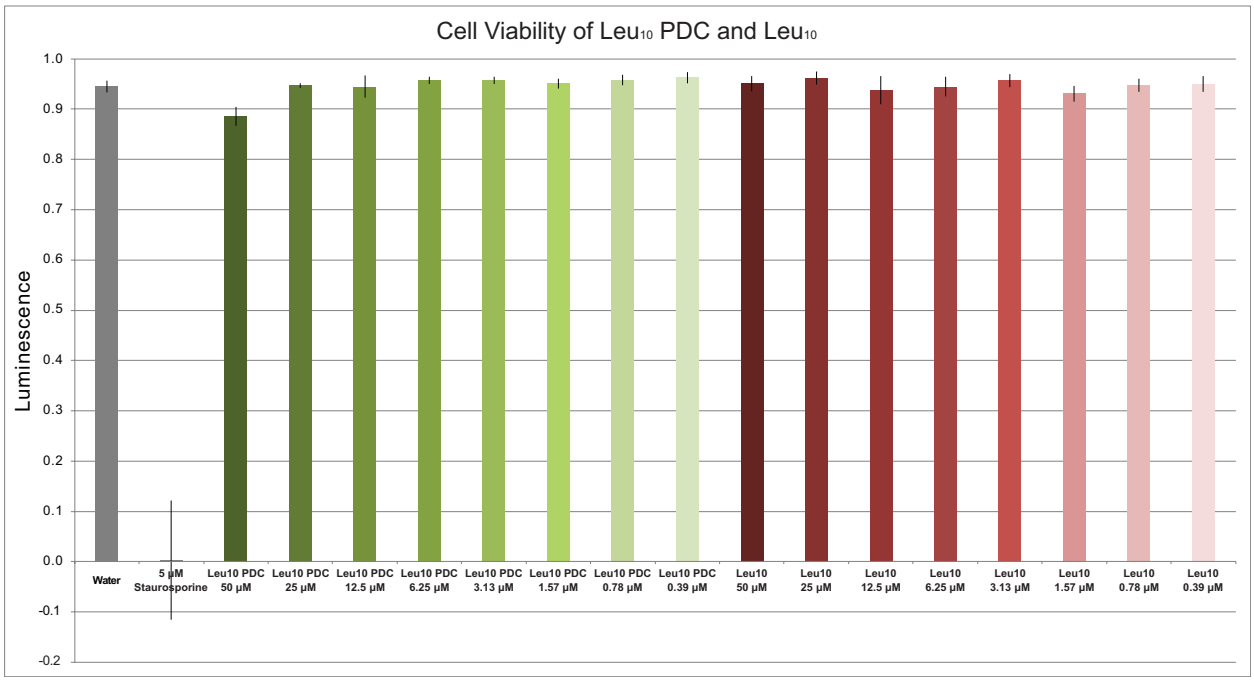

Figure S2.27. Cytotoxicity assay of Leu$_{10}$-teixobactin prodrug C and Leu$_{10}$-teixobactin with HeLa cells.

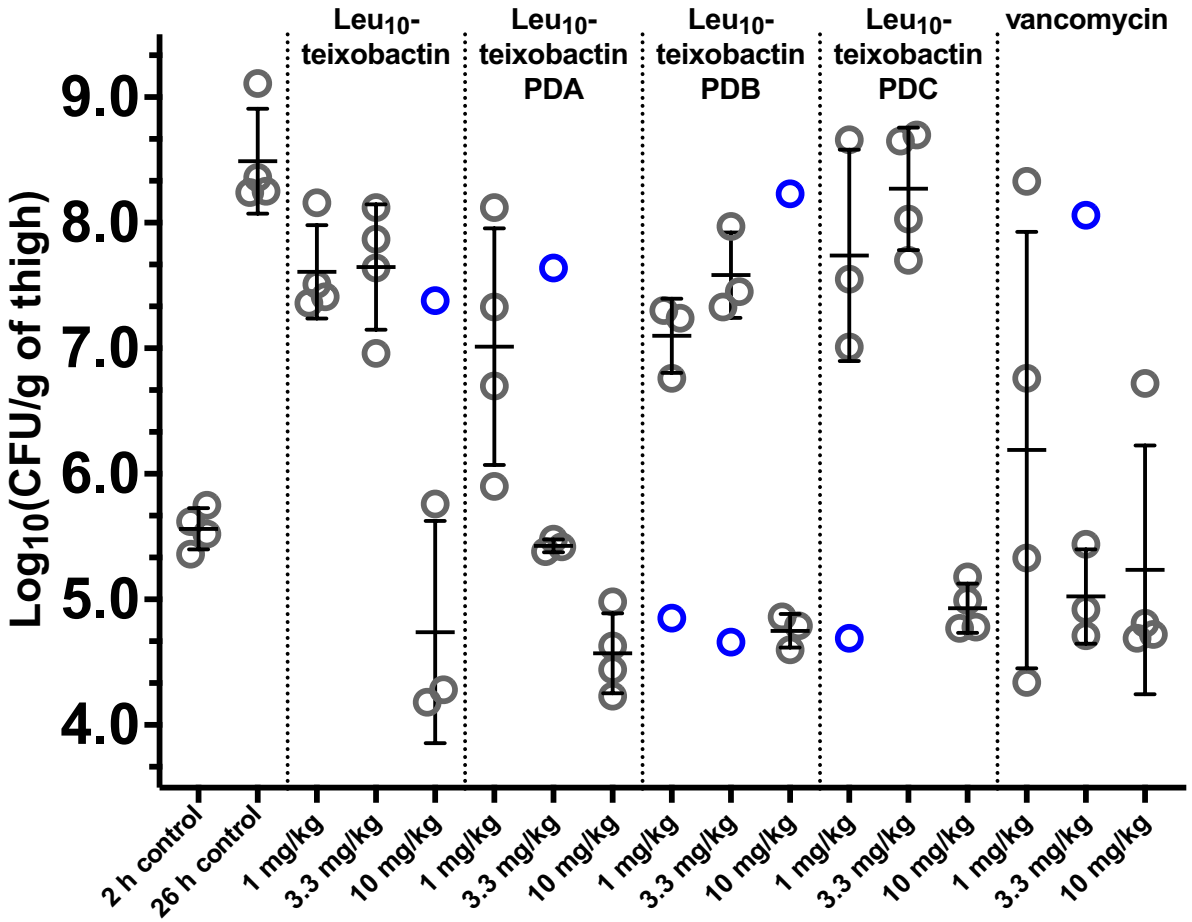

Figure S2.28. Graph of the complete data for the neutropenic mouse thigh infection efficacy model against MRSA (ATCC BAA-1717) of the Leu_{10}-teixobactin prodrugs and Leu_{10}-teixobactin, with vancomycin as a positive control. Data points in blue are the severe outliers that were removed from the data analysis in Figure 2.7 in the main text and not included in the error bar calculations for Figure 2.7 or Figure S2.28.

Materials and Methods[1]

Materials. Amino acids, coupling agents, 2-chlorotrityl chloride resin, DIC, and triisopropylsilane were purchased from Chem-Impex. Boc-Ser(Fmoc-Ile)-OH was purchased from AAPPTec. Vancomycin (hydrochloride salt) was purchased from Sigma-Aldrich. Teixobactin (hydrochloride salt) was provided by NovoBiotic Pharmaceuticals. DMF (amine-free), DIPEA, 2,4,6-collidine, and piperidine were purchased from Alfa-Aesar. DMAP and polysorbate 80 were purchased from Acros Organics. HPLC-grade acetonitrile, and dichloromethane were purchased from Fisher Scientific. TFA and hexafluoroisopropanol were purchased from Oakwood Chemical. Reagent-grade solvents, chemicals, amino acids, and resin were used as received, with the exception of dichloromethane, which was dried through an alumina column under argon, and DMF, which was dried through an alumina column and an amine scavenger resin column under argon.

Methods for Synthesis, Purification, and Analysis of Peptides. Solid-phase peptide synthesis was carried out manually in a solid phase reaction vessel. Analytical reverse-phase HPLC was performed on an Agilent 1260 instrument equipped with an Aeris PEPTIDE 2.6 μm XB-C18 column (Phenomonex). Preparative reverse-phase HPLC was performed on a Rainin Dynamax instrument equipped with a Zorbax SB-C18 column (Agilent) for all teixobactin analogues. All teixobactin prodrug analogues were first purified on a Biotage® Isolera™ One system equipped with a Biotage® Sfär Bio C18 – Duo 300 Å 20 μm column, before repurifying on the Rainin Dynamax instrument. UV detection (214 nm) was used for analytical and preparative HPLC. HPLC grade acetonitrile and 18 MΩ deionized water, each containing 0.1% trifluoroacetic acid, were used for analytical and preparative reverse-phase HPLC. Matrix-assisted laser desorption/ionization time-of-flight (MALDI-TOF) mass spectrometry was performed on an AB

SCIEX TOF/TOF 5800 system and α-cyano-4-hydroxycinnamic acid was used as the sample matrix. All peptides were prepared and used as the trifluoroacetate salts and were assumed to have one trifluoroacetate ion per ammonium group present in each peptide.

Synthesis of teixobactin *O*-acyl isopeptide prodrug analogues and their corresponding teixobactin analogues. Lys_{10}-teixobactin, Arg_{10}-teixobactin, Leu_{10}-teixobactin, and all *O*-acyl isopeptide prodrug analogues were prepared as the trifluoroacetate salts by solid-phase peptide synthesis followed by solution phase cyclization, as previously described.[1,2] In the original procedure, HBTU and HOBt are used in the solution-phase cyclization step, but in the synthesis of these peptides, HATU and HOAt were used instead. For all *O*-acyl isopeptide prodrug analogues, Boc-Ser(Fmoc-Ile)-OH was coupled in place of the desired Ile and Ser residues. Syntheses on a 0.1–0.2 mmol scale afforded 5–39 mg (1.6-21%) of Lys_{10}-teixobactin, Arg_{10}-teixobactin, Leu_{10}-teixobactin and the *O*-acyl isopeptide prodrug analogues.

Representative synthesis of Lys_{10}-teixobactin prodrug A. *Resin Loading.* 2-chlorotrityl chloride resin (300 mg, 1.6 mmol/g) was added to a 10-mL Bio-Rad Poly-Prep chromatography column. The resin was suspended in dry DCM (8 mL) and allowed to swell for 10 mins. The DCM was drained and a solution of Fmoc-Lys(Boc)-OH (150 mg, 0.32 mmol, 1.8 equiv) and 2,4,6-collidine (300 μL) in dry DCM (7 mL) was added. The suspension was gently agitated for 5 h. The solution was drained, and the resin was washed with dry DCM (3X). After washing, a solution of DCM/MeOH/DIPEA (17:2:1, 8 mL) was added to the resin and agitated for 1 h to cap any unreacted 2-chlorotrityl chloride sites. The solution was drained, and the resin was washed with

DCM (3X) and dried with a flow of nitrogen. The resin loading was determined to be 0.18 mmol (0.60 mmol/g, 57% loading) based on UV analysis (290 nm) of the Fmoc cleavage product.

Solid-phase amino acid couplings. The loaded resin was suspended in dry DMF and transferred to a solid-phase peptide synthesis reaction vessel for manual peptide synthesis. Fmoc-Ala-OH, Fmoc-D-Thr-OH, Boc-Ser(Fmoc-Ile)-OH, Fmoc-D-*allo*-Ile-OH, Fmoc-D-Gln(Trt)-OH, Fmoc-Ser(t-Bu)-OH, Fmoc-Ile-OH, and Boc-*N*-methyl-D-Phe-OH were coupled through the following cycles: (1) Fmoc deprotection with 20% (v/v) piperidine in dry DMF (5 mL) for 5 min (2X), (2) resin washing with dry DMF (7X), (3) coupling of amino acid (0.72 mmol, 4.0 equiv) with HCTU (0.72 mmol, 4.0 equiv) in 20% (v/v) collidine in dry DMF (5 mL) for 30 min, and (4) resin washing with dry DMF (7X). After completing the linear synthesis, the resin was transferred to a 10-mL Bio-Rad Poly-Prep chromatography column and washed with dry DMF (3X) and DCM (3X).

Esterification. In a test tube, Fmoc-Ile-OH (630 mg, 1.8 mmol, 9.9 equiv) and diisopropylcarbodiimide (280 µL, 1.8 mmol, 10 equiv) were dissolved in dry DCM (5 mL). The solution was filtered through a 0.20-µm nylon filter into a test tube containing 4-dimethylaminopyridine (21.8 mg, 0.18 mmol, 1.00 equiv). The filtrate was transferred to the resin and gently agitated for 1 h. The solution was drained, and the resin washed with dry DCM (3X) and DMF (3X).

Fmoc deprotection of Ile_{11}. The Fmoc protecting group on Ile_{11} was removed with a solution of 20% (v/v) piperidine in DMF (5 mL) for 15 mins. The solution was drained, and the resin was washed with dry DMF (3X) and DCM (3X).

Cleavage of the linear peptide from the resin. The linear peptide was cleaved from resin by subjecting the resin to a cleavage solution of 20% (v/v) HFIP in dry DCM (7.5 mL) and

agitating for 1 h. The filtrate was collected in a 250-mL round-bottom flask. The HFIP treatment was repeated for 30 mins and the filtrate was added to the first in the round-bottom flask. The resin was washed with dry DCM (3X). The combined filtrates and DCM washes were concentrated under reduced pressure to afford a colorless oil.

Solution-phase cyclization. The oil was dissolved in DMF (125 mL) in the same 250 round-bottom flask as the previous step. HATU (410 mg, 1.1 mmol, 6.0 equiv) and HOAt (150 mg, 1.1 mmol, 6.1 equiv) were added to the solution. The reaction mixture was then stirred under nitrogen for 10 mins. DIPEA (100 μL, 0.6 mmol, 3.2 equiv) was added dropwise to the solution and the mixture was stirred under nitrogen at room temperature for 12 h. The reaction mixture was concentrated under reduced pressure to afford the cyclized peptide as a yellow solid. The solid was placed under vacuum (≤60 mTorr) to remove any residual solvents.

Global Deprotection and Ether Precipitation. The crude protected peptide was dissolved in a mixture of TFA/TIPS/H_2O (90:5:5, 10 mL), and the solution was stirred for 1.5 h. The deprotection mixture was transferred to two 50-mL conical tubes, each containing 35 mL ice-cold diethyl ether, with a precipitate forming immediately. The 50-mL conical tubes were centrifuged (2500 x g) for 10 min to pellet the crude peptide. The diethyl ether supernatant was decanted into a 125-mL Erlenmeyer flask. This process was repeated 2X, adding additional ice-cold ether followed by centrifugation and decantation. The pellet was then dried under nitrogen.

Purifications. The dried peptide pellet was dissolved in 10% (v/v) MeCN in H_2O (10 mL) and purified on a Biotage® Isolera™ One system equipped with a Biotage® Sfär Bio C18 – Duo 300 Å 20 μm column using a H_2O/MeCN (10%-55%) gradient. The fractions were analyzed by MALDI-TOF and analytical HPLC. Fractions containing the desired peptide were combined and lyophilized for repurification. The lyophilized material from the first purification were dissolved

in 20% (v/v) MeCN in H_2O (4 mL) and purified by reverse-phase HPLC with H_2O/MeCN (gradient elution of 20-40% with 0.1% TFA over 120 min) on a C18 column. Fractions were analyzed by MALDI-TOF and analytical HPLC. The pure fractions were combined and lyophilized to give 39 mg (14% yield based on resin loading) of Lys_{10}-teixobactin prodrug A trifluoroacetate (TFA) salt as a white powder.

Table S2.1. Yields of purified teixobactin *O*-acyl isopeptide prodrug analogues and their corresponding teixobactin analogues.

Teixobactin Analogue	Yield (mg)	% Yield	Calculated MW as TFA salt
Lys_{10}-teixobactin	7	2.1%	1443.7 (•2 TFA)
Lys_{10}-teixobactin Prodrug A	39	14%	1557.7 (•3 TFA)
Lys_{10}-teixobactin Prodrug B	9	5.4%	1557.7 (•3 TFA)
Lys_{10}-teixobactin Prodrug C	7	3.2%	1671.7 (•4 TFA)
Arg_{10}-teixobactin	7	2.6%	1471.7 (•2 TFA)
Arg_{10}-teixobactin Prodrug A	20	15%	1585.7 (•3 TFA)
Arg_{10}-teixobactin Prodrug B	9	6.6%	1585.7 (•3 TFA)
Arg_{10}-teixobactin Prodrug C	21	21%	1699.7 (•4 TFA)
Leu_{10}-teixobactin	8	4.1%	1314.7 (•1 TFA)
Leu_{10}-teixobactin Prodrug A	18	10%	1428.7 (•2 TFA)
Leu_{10}-teixobactin Prodrug B	5	1.6%	1428.7 (•2 TFA)
Leu_{10}-teixobactin Prodrug C	10	6.0%	1542.7 (•3 TFA)

Conversion kinetics studies of teixobactin *O*-acyl isopeptide prodrug analogues at room temperature and 37 °C. A 1 mL analytical HPLC vial was charged with 300 µL of 50 mM phosphate buffer followed by 300 µL of a 1 mg/mL stock solution of the peptide in H_2O. An aliquot was then immediately injected onto an Agilent 1260 instrument equipped with an Aeris PEPTIDE 2.6 µm XB-C18 column (Phenomonex). Additional aliquots were injected every 24 minutes for 4 h. Each sample was run on a gradient of 5–67% acetonitrile over 15 min, with monitoring of absorbance at 214 nm. The temperature in the HPLC sample chamber was recorded. Conversion kinetics of all reactions were run at 23–25 ± 1 °C. Peaks corresponding to the prodrug analogue, intermediates (prodrugs C only), and the teixobactin analogue product were integrated using the Agilent software, and the relative areas were recorded for kinetic analysis.

A 1 mL analytical HPLC vial was charged with 400 µL of 100 mM sodium phosphate buffer at pH 7.4. To a second analytical HPLC vial, 400 µL of a 1 mg/mL stock solution of the peptide in H_2O was added. Both vials were placed in a water bath set to 37 °C and allowed to preheat for ca. 15 min. To an additional vial in the 37 °C water bath, 300 µL of the sodium phosphate buffer and 300 µL of the 1 mg/mL stock solution of peptide were added. Aliquots of 100 µL were removed every 5 minutes (5, 10, 15, and 20) into a low-volume analytical HPLC vials and placed immediately on dry ice. After all aliquots were taken, the aliquots were analyzed on the same HPLC instrument, using the same gradient and wavelength as the conversion studies at room temperature (described above). Each sample was thawed immediately before injection but kept at a low enough temperature to minimize further conversion of the prodrug analogues. Peaks corresponding to the prodrug analogue, intermediates (prodrugs C only), and the teixobactin analogue product were integrated using the Agilent software, and the relative areas were recorded for kinetic analysis.

MIC assays of teixobactin *O*-acyl isopeptide prodrug analogues and their corresponding teixobactin analogues. *Bacillus subtilis* (ATCC 6051), *Staphylococcus epidermidis* (ATCC 14990), *Staphylococcus aureus* (ATCC 29213), and *Escherichia coli* (ATCC 10798) were cultured from glycerol stocks in Mueller-Hinton broth overnight in a shaking incubator at 37 °C. *Staphylococcus aureus* (ATCC 700698) was cultured from a glycerol stock in brain heart infusion broth overnight in a shaking incubator at 37 °C. An aliquot of a 1 mg/mL antibiotic stock solution in DMSO was diluted with appropriate culture media to make a 64 µg/mL solution. A 200-µL aliquot of the 64 µg/mL solution was transferred to a sterile, untreated 96-well plate. Two-fold serial dilutions were made with media across a 96-well plate to achieve a final volume of 100 µL in each well. These solutions had the following concentrations: 64, 32, 16, 8, 4,

2, 1, 0.5, 0.25, 0.125, and 0.0625 µg/mL. The overnight cultures of each bacterium were diluted with Mueller-Hinton broth to an OD_{600} of 0.075 as measured for 200 µL in a 96-well plate. The diluted mixture was further diluted to a 1×10^6 CFU/mL with Mueller-Hinton media. A 100-µL aliquot of the 1×10^6 CFU/mL bacterial solution was added to each well in the 96-well plates, resulting in final bacteria concentrations of 5×10^5 CFU/mL in each well. As 100-µL of bacteria were added to each well, the teixobactin analogues and teixobactin prodrug analogues were also diluted to the following concentrations: 32, 16, 8, 4, 2, 1, 0.5, 0.25, 0.125, 0.0625, and 0.03125 µg/mL. The plate was covered with a lid and incubated at 37 °C for 16 h. The OD_{600} were measured using a 96-well UV/vis plate reader (MultiSkan GO, Thermo Scientific). The MIC values were taken as the lowest concentration that had no bacteria growth. Each MIC assay was run in quadruplicate (technical replicates). MIC assays were performed in test media without polysorbate 80 or containing 0.002% polysorbate 80. For MIC assays performed with 0.002% polysorbate 80, the antibiotic stock solution was diluted with appropriate culture media to make a 16 µg/mL solution. Several of the MIC assays were repeated to ensure reproducibility.

Figure S2.29. MIC assay plate layout.[9]

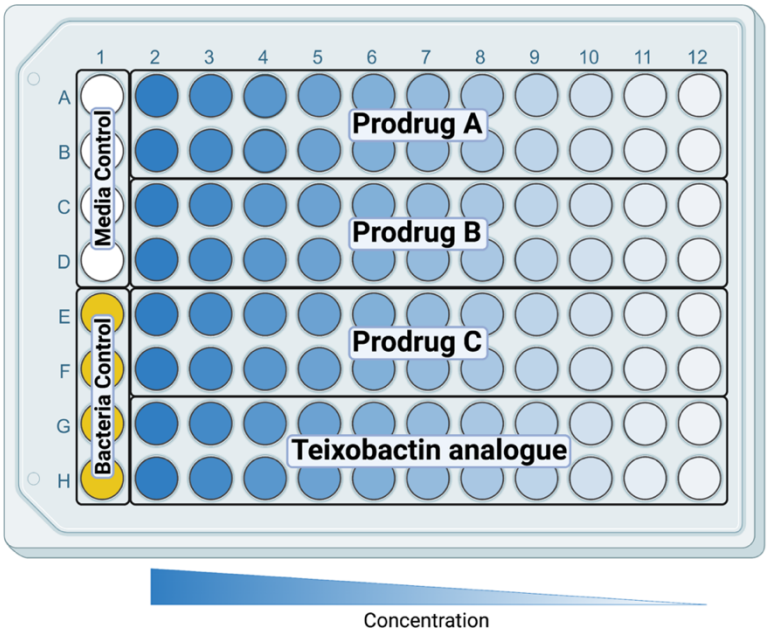

Gel formation studies of teixobactin *O*-acyl isopeptide prodrug analogues and their corresponding teixobactin analogues.[3] A small amount of crystal violet was added to 1X PBS buffer at pH 7.4. The buffer was centrifuged to pellet any undissolved crystal violet. A 20 µL drop of the PBS buffer was placed onto a glass depression well microscope slide. A 1-µL aliquot of the 10 mg/mL peptide stock solution in DMSO was added to the drop of PBS buffer. The mixture was stirred with the pipet tip to form a homogenous solution. A low magnification stereoscopic microscope was used to visually observe the drop. Gel formation was observed and photographed over the course of 60 minutes with stirring of the drop every 10–15 mins.

Hemolytic assay of teixobactin *O*-acyl isopeptide prodrug analogues and their corresponding teixobactin analogues.[4,5] *Preparation of Phosphate-Buffered Saline (PBS) Buffers.* A 10X PBS buffer was prepared by dissolving 8.9 g of Na_2HPO_4, 1.2 g KH_2PO_4, 40 g NaCl, and 1 g KCl in 500 mL of 18 MΩ deionized water. The solution was stirred until the buffer salts were completely dissolved. The pH of the 10X PBS buffer was adjusted to 7.4 using either 1 M HCl or 1 M NaOH and was subsequently sterile filtered. To create a 1X PBS buffer, the 10X PBS buffer was diluted 10-fold using 18 MΩ deionized water. Another 1X PBS buffer was made, supplemented with 0.002% polysorbate 80.

Preparation of human red blood cells. Whole human blood was stored in a 4 °C in K2 EDTA to prevent coagulation. On the day of cell treatment, the blood was centrifuged at 800 x g for 5 min at 4 °C to isolate red blood cells (RBCs). The plasma layer was then removed and discarded. Approximately 3 mL of 150 mM NaCl solution was added to the RBCs and mixed gently by inversion. The RBCs were centrifuged at 800 x g for 8 min at 4 °C and the supernatant was discarded. An additional wash with 150 mM NaCl was performed, centrifuged at 800 x g for 8 min at 4 °C and the supernatant was discarded. 2 mL of whole RBCs were transferred to a 15-

mL conical tube. Approximately 4 mL of 1X PBS was added to the RBCs and inverted gently to mix. The RBCs were centrifuged at 800 x g for 8 min at 4 °C. The supernatant was discarded, and the cells were washed 2–3 more times to ensure that the supernatant was visibly transparent and free of any color from pre-existing lysed RBCs. After the PBS washes, a 5% v/v RBC suspension was prepared by adding 500 µL of the RBCs to 9.5 mL of the desired 1X PBS.

Hemolytic assay procedure. Experiments were performed in triplicate (three technical replicates) in untreated V-bottom 96-well plates. An aliquot of a 1 mg/mL antibiotic stock solution in H_2O was diluted with the proper 1X PBS to make a 200 µg/mL solution. A 100-µL aliquot of the 200 µg/mL solution was transferred to a V-bottom 96-well plate. Two-fold serial dilutions were made with the desired 1X PBS down the V-bottom 96-well plate to achieve a final volume of 50 µL in each well. These solutions had the following concentrations: 200, 100, 50, 25, 12.5, 6.25, 3.125 µg/mL. The final row was used for controls, with each well receiving a 50-µL aliquot of the appropriate control. Four wells were used for a positive control with 4% Triton X-100 solution in 1X PBS. Four wells were used for a peptidic positive control with a 2.5 µM melittin solution in 1X PBS. Four wells were used for a vehicle control with 0.98X PBS (1X PBS diluted with 2% 18 MΩ deionized water). A 50-µL aliquot of the 5% RBC suspension was added to each well in the V-bottom 96-well plates. After addition of the RBCs to each well, the concentrations of the peptides were: 100, 50, 25, 12.5, 6.25, 3.125, and 1.5625 µg/mL, and the concentrations of the controls were 2% Triton X-100 and 1.25 µM melittin. The plates were sealed with a Axygen AxySeal Sealing Film and incubated at 37 °C for 1 h.

Hemolytic assay readout. A replica plate was prepared by adding a 50-µL aliquot of 1X PBS to all wells of a flat-bottomed 96-well plate. After the 1 h incubation period, the V-bottom 96-well plate was centrifuged at 1000 x g for 10 min at 4 °C to pellet the RBCs. A 50-µL aliquot

of the supernatant from each well was transferred to the replica plate. The transfer was performed quickly, but very carefully to not disturb the RBC pellet. [If any RBCs were disturbed, the V-bottom 96-well plate should be centrifuged again to re-pellet the RBCs.] The final volume of each well in the flat-bottom 96-well plate was 100 µL. The OD_{540} of each well was measured using a 96-well UV/vis plate reader (MultiSkan GO, Thermo Scientific). The data were processed by comparing those values to the Triton X-100 controls and vehicle controls:

$$\% \text{ hemolytic activity} = [(A_{540})_{compound} - (A_{540})_{vehicle}] / [(A_{540})_{triton} - (A_{540})_{vehicle}] \times 100$$

Figure S2.30. Hemolytic assay plate layout.[9]

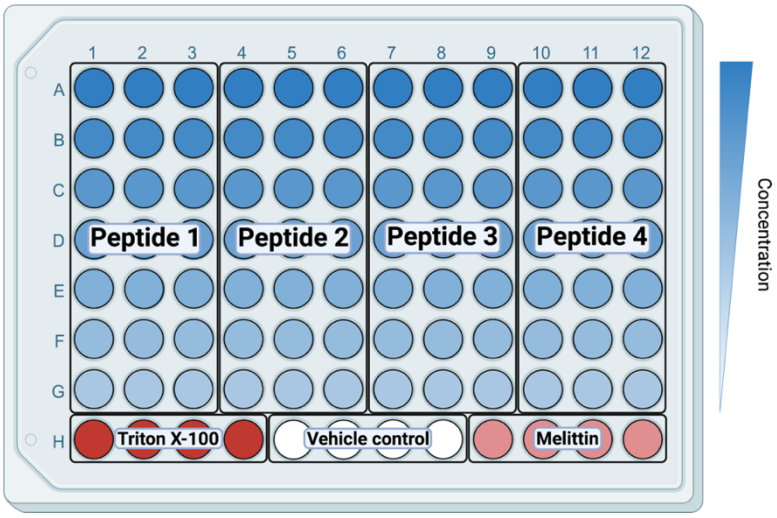

Cell culture and cytotoxicity assays of teixobactin *O*-acyl isopeptide prodrug analogues and their corresponding teixobactin analogues. *Cell culture.* HeLa cell cultures were maintained in complete media of Eagle's Minimum Essential Medium (EMEM) supplemented with 10% heat-inactivated fetal bovine serum (FBS), 100 µg/mL penicillin, and 100 µg/mL streptomycin at pH 7.4 in a humidified 5% CO_2 atmosphere at 37 °C using a Fischer Scientific Forma Series 3 Water Jacketed CO_2 Incubator. All experiments were performed in triplicate in sterile half-area 96-well plates that were cell-culture treated.

Plating cells. HeLa cells were seeded at 2,500 cells per well in the inner 60 wells of half-area 96-well plates to a total volume of 50 µL using complete media. The outer wells of the plate were filled with 100 µL of EMEM without any cells. The plates were incubated in a 5% CO_2 atmosphere at 37 °C for 24 h after plating. Prior to treatment with peptide, the media was removed by pipet from the cells.

Treatment of cells with peptide. An aliquot of a 1 mg/mL antibiotic stock solution in H_2O was diluted with EMEM to make a 50 µM solution. A 100-µL aliquot of the 50 µM solution was transferred to the sterile, half-area 96-well plate. Two-fold serial dilutions were made with EMEM across a 96-well plate to achieve a final volume of 50 µL in each well. Each treatment was run in triplicate (technical replicates). An additional six wells were used as controls. Three wells received 50 µL of a 7% solution of 18 MΩ deionized water in EMEM (vehicle control) and the other three wells received 50 µL of either a 5, 10, or 15 µM staurosporine in EMEM solution (positive control). The plates were then incubated in a 5% CO_2 atmosphere at 37 °C for 48 h.

Cytotoxicity assay plate readout. The CytoTox-Glo Assay (CytoTox-Glo™ Cytotoxicity Assay, Promega) was performed according to manufacturer's instructions. Luminescence was measured using a microplate reader (GloMax(R) Discover System, Promega).

Figure S2.31. Cytotoxicity assay plate layout. All outer wells are filled with media.[9]

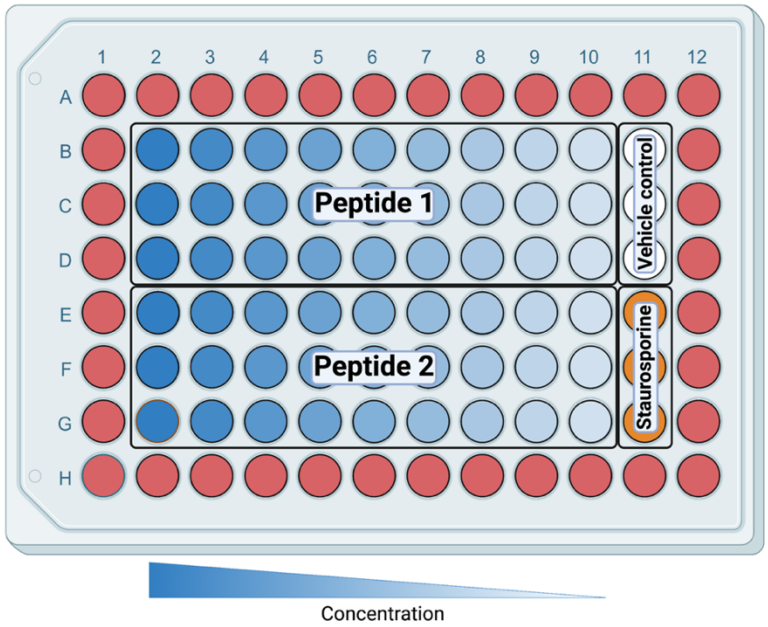

Conversion of the peptide TFA salts to HCl salts.[6] Leu_{10}-teixobactin and Leu_{10}-teixobactin prodrugs A, B, and C were converted from the trifluoroacetate (TFA) salts to the hydrochloride (HCl) salts for use in *in vivo* studies by lyophilization three times in 100 mM aqueous HCl in 18 MΩ deionized water. The lyophilized peptides (ca. 15 mg) as the TFA salts were dissolved in a 100 mM aqueous HCl (ca. 10 mL) and allowed to incubate for 5 min. The solutions were then frozen in liquid nitrogen and lyophilized. The treatment with 100 mM aqueous HCl and lyophilization was repeated two additional times. Finally, the peptides were lyophilized from 18 MΩ deionized water to remove excess HCl.

Neutropenic mouse thigh infection efficacy study against MRSA.[7,8] All *in vivo* efficacy experiments were performed at NeoSome Life Sciences, LLC. NeoSome maintains both OLAW assurance and USDA certification. NeoSome follows all regulatory guidelines and conforms to established NIH animal research guidelines. All animal research is reviewed by the NeoSome IACUC committee.

Female CD-1 mice were rendered neutropenic by cyclophosphamide on days -4 and -1 with 150 mg/kg and 100 mg/kg, delivered IP, respectively. *S. aureus* strain ATCC BAA-1717 was prepared for infection from an overnight plate culture. A portion of the plate was resuspended in sterile saline and adjusted to an OD of 0.10 at 625 nm. The adjusted bacterial suspension was further diluted to the predetermined infection inoculum of $1.0x10^5$ CFU/mouse thigh. Plate counts of the inoculum were performed to confirm inoculum concentration, the actual inoculum size was $1.05x10^5$ CFU/mouse thigh. Mice were infected with 100 µL of the prepared bacterial inoculum into the right thigh muscle. A total of 68 mice were infected (four mice per group). At 2 and 14 h post-infection, mice received treatment with Leu_{10}-teixobactin or the Leu_{10}-teixobactin prodrugs (as the HCl salts) at 1, 3.3, or 10 mg/kg in D5W (5% dextrose in water) administered via IV tail vein injection in volumes of 10 mL/kg. Another group of four mice received treatment with vancomycin following the same dosing strategy.

At 2 and 26 h post-infection groups of 4 mice were euthanized. The right thighs from each animal were aseptically explanted, weighed, and homogenized to a uniform consistency. Homogenized samples were serially diluted and plated on bacterial growth media for CFU determination. CFUs were enumerated after overnight incubation at 37 °C. The CFUs were adjusted for dilution and tissue weight for each thigh with averages and standard deviation calculated for each group. Severe outliers were excluded from the data analysis.

References for Supporting Information

1. Taken verbatim or adapted from: M. A. Morris, M. Malek, M. H. Hashemian, B. T. Nguyen, S. Manuse, K. Lewis and J. S. Nowick, *ACS Chem. Biol.*, 2020, **15**, 1222–1231.

2. H. Yang, K. H. Chen, and J. S. Nowick, *ACS Chem. Biol.*, 2016, **11**, 1823–1826.

3. Taken verbatim or adapted from: K. H. Chen, S. P. Le, X. Han, J. M. Frias, and J. S. Nowick, *Chem. Commun.*, 2017, **53**, 11357–11359.

4. Adapted from: B. C. Evans, C. E. Nelson, S. S. Yu, K. R. Beavers, A. J. Kim, H. Li, H. M. Nelson, T. D. Giorgio and C. L. Duvall, *J. Vis. Exp.*, 2013, 50166.

5. Adapted from: A. Oddo and P. R. Hansen, in *Antimicrobial Peptides: Methods and Protocols*, ed. P. R. Hansen, Springer, New York, NY, 2017, pp. 427–435.

6. Taken verbatim or adapted from: K. Sikora, D. Neubauer, M. Jaśkiewicz and W. Kamysz, *Int. J. Pept. Res. Ther.*, 2018, **24**, 265–270.

7. Taken verbatim or adapted from: L. L. Ling, T. Schneider, A. J. Peoples, A. L. Spoering, I. Engels, B. P. Conlon, A. Mueller, T. F. Schäberle, D. E. Hughes, S. Epstein, M. Jones, L. Lazarides, V. A. Steadman, D. R. Cohen, C. R. Felix, K. A. Fetterman, W. P. Millett, A. G. Nitti, A. M. Zullo, C. Chen and K. Lewis, *Nature*, 2015, **517**, 455–459.

8. Taken verbatim or adapted from procedure provided by NeoSome Life Sciences, LLC.

9. All plate layout figures were created using BioRender.com.

Characterization data

Lys_{10}-teixobactin Analytical HPLC Trace and MALDI-TOF

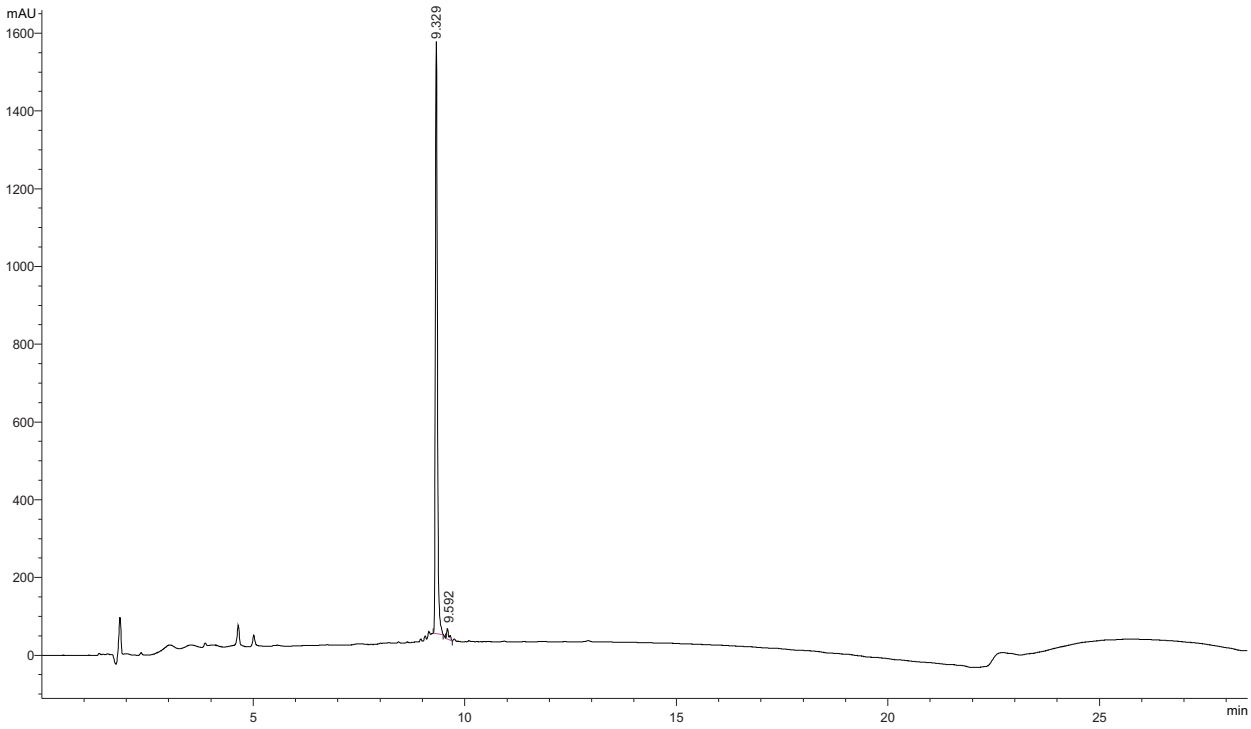

Peak #	RetTime [min]	Type	Width [min]	Area [mAU*s]	Height [mAU]	Area %
1	9.329	MM	0.0555	5090.91113	1529.24243	98.0622
2	9.592	MM	0.0627	100.60265	26.76234	1.9378
Totals :				5191.51379	1556.00477	

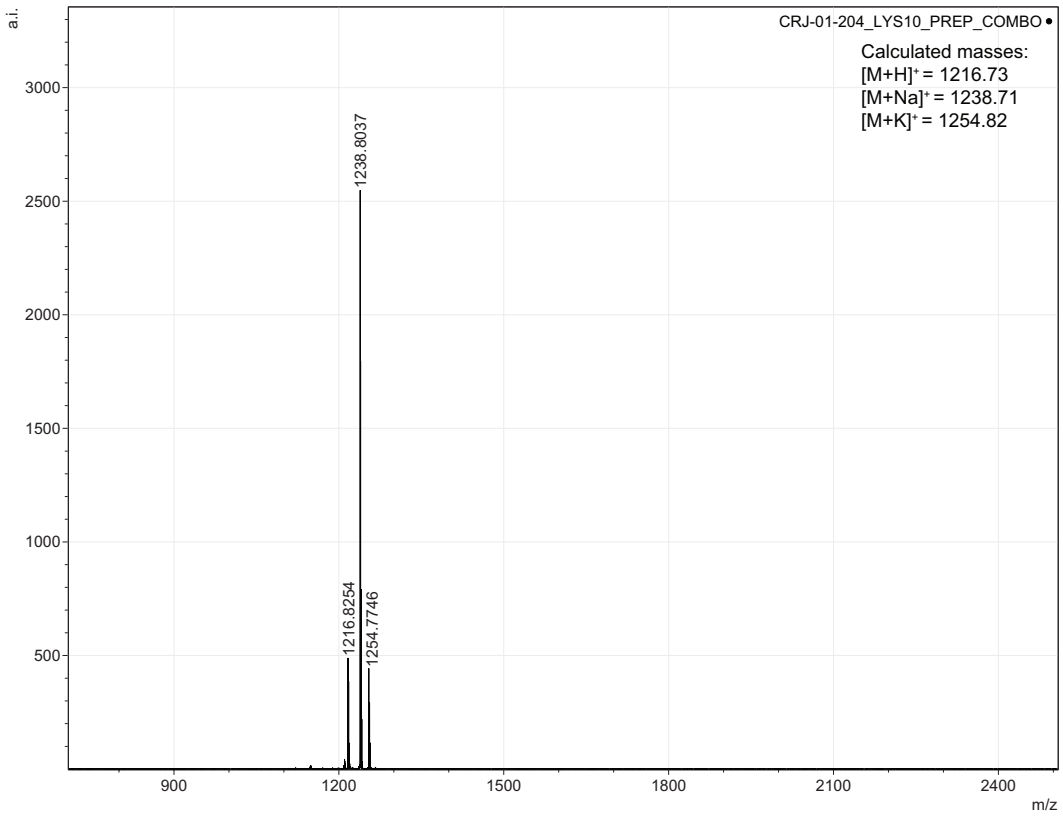
CRJ-01-204_LYS10_PREP_COMBO
Calculated masses:
[M+H]+ = 1216.73
[M+Na]+ = 1238.71
[M+K]+ = 1254.82
1238.8037
1216.8254
1254.7746
a.i.
m/z

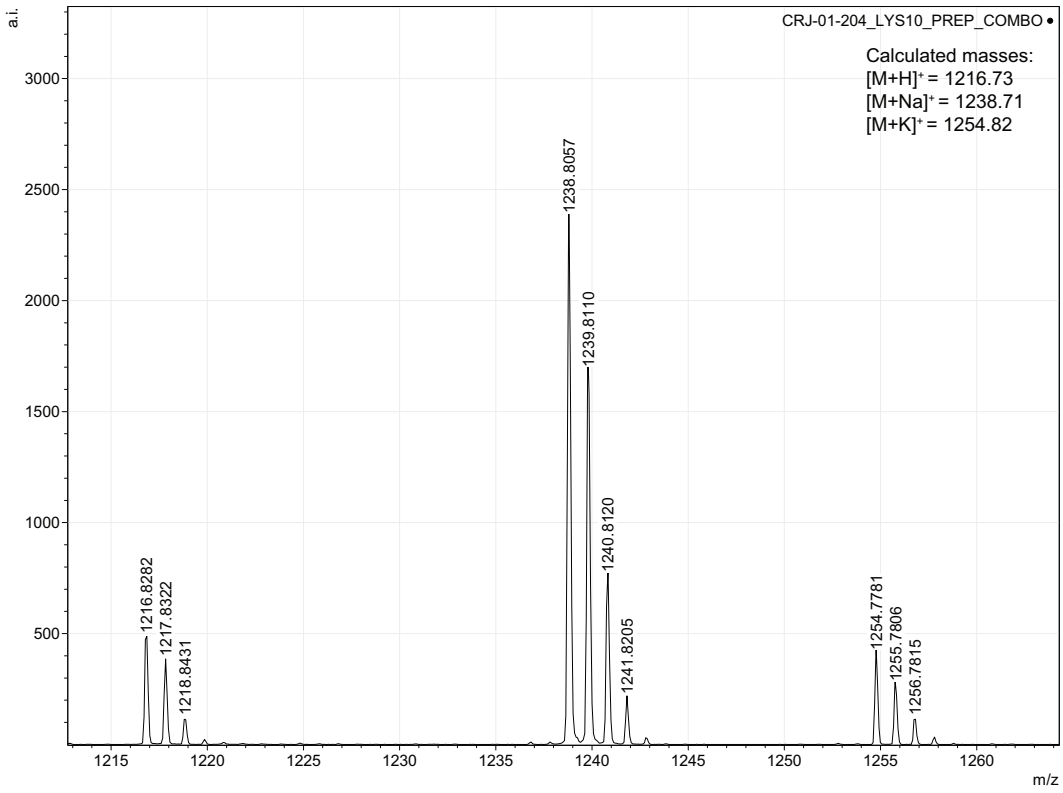
CRJ-01-204_LYS10_PREP_COMBO
Calculated masses:
[M+H]+ = 1216.73
[M+Na]+ = 1238.71
[M+K]+ = 1254.82
1238.8057
1239.8110
1240.8120
1241.8205
1216.8282
1217.8322
1218.8431
1254.7781
1255.7806
1256.7815
a.i.
m/z

Lys$_{10}$-teixobactin Prodrug A Analytical HPLC Trace and MALDI-TOF

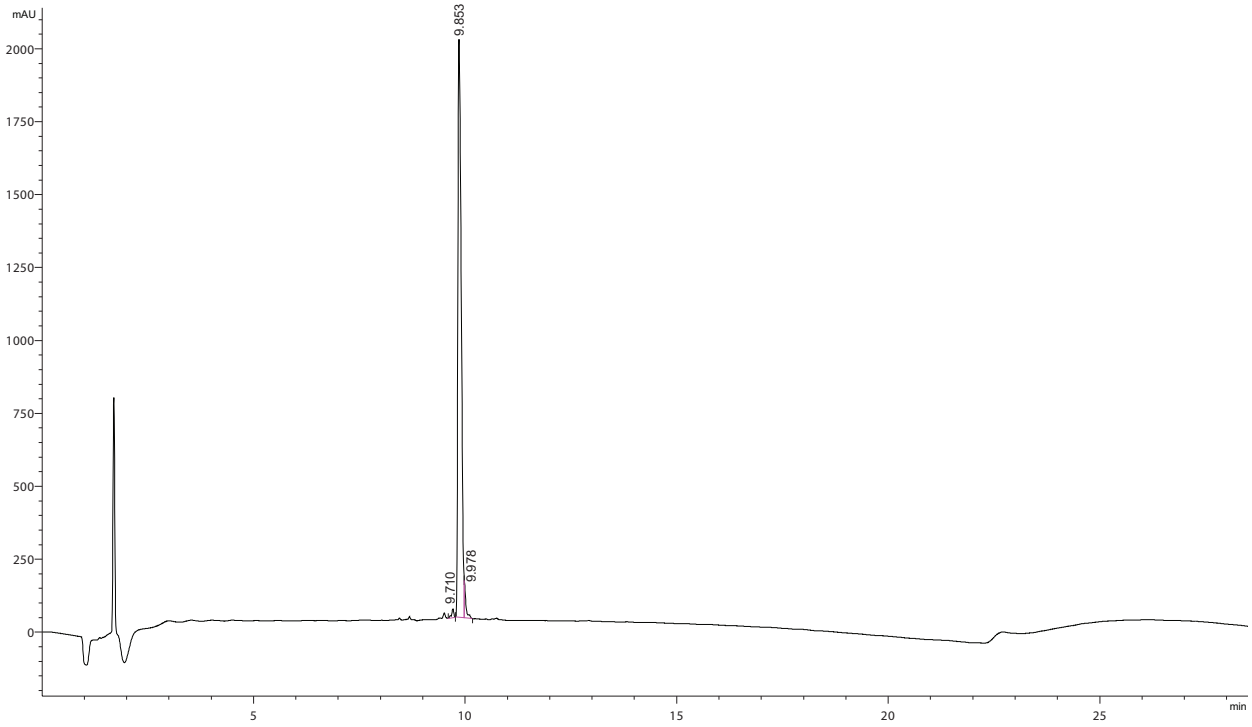

Peak #	RetTime [min]	Type	Width [min]	Area [mAU*s]	Height [mAU]	Area %
1	9.710	MM	0.0603	107.60345	29.74174	0.9415
2	9.853	MF	0.0924	1.10231e4	1988.32227	96.4500
3	9.978	FM	0.0382	298.12329	130.14198	2.6085
Totals :				1.14288e4	2148.20599	

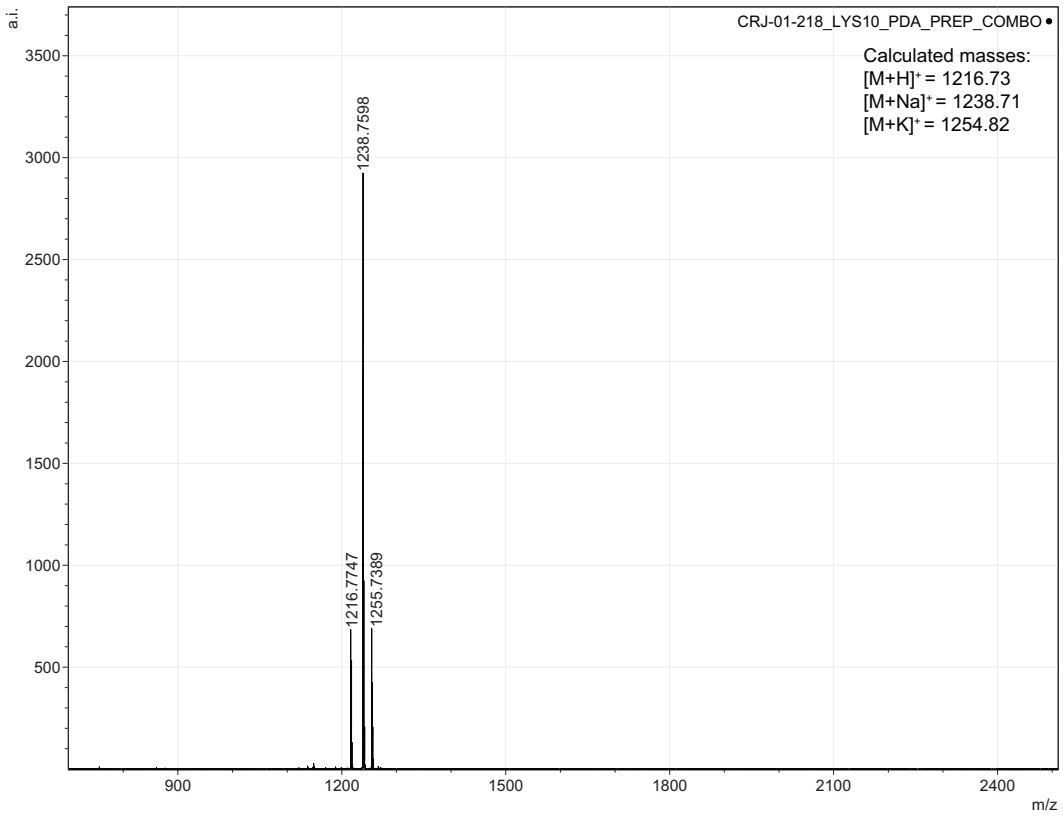
CRJ-01-218_LYS10_PDA_PREP_COMBO
Calculated masses:
[M+H]+ = 1216.73
[M+Na]+ = 1238.71
[M+K]+ = 1254.82
1238.7598
1216.7747
1255.7389
a.i.
m/z

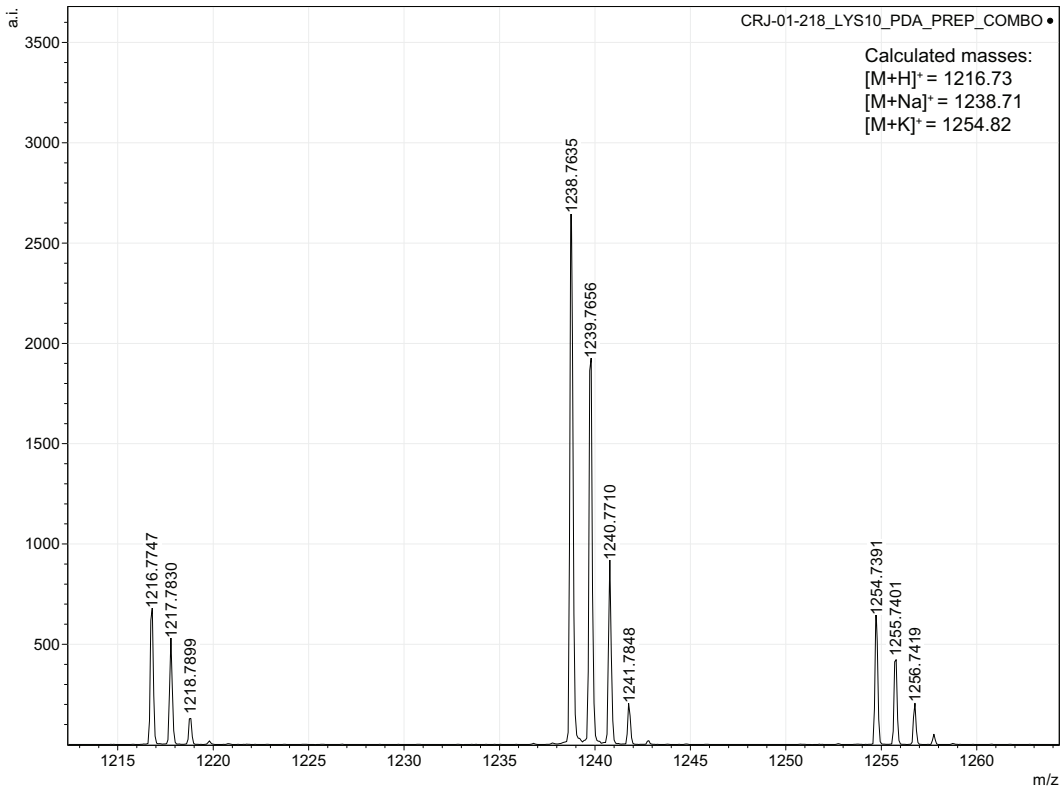
CRJ-01-218_LYS10_PDA_PREP_COMBO
Calculated masses:
[M+H]+ = 1216.73
[M+Na]+ = 1238.71
[M+K]+ = 1254.82
1238.7635
1239.7656
1240.7710
1241.7848
1216.7747
1217.7830
1218.7899
1254.7391
1255.7401
1256.7419
a.i.
m/z

Lys$_{10}$-teixobactin Prodrug B Analytical HPLC Trace and MALDI-TOF

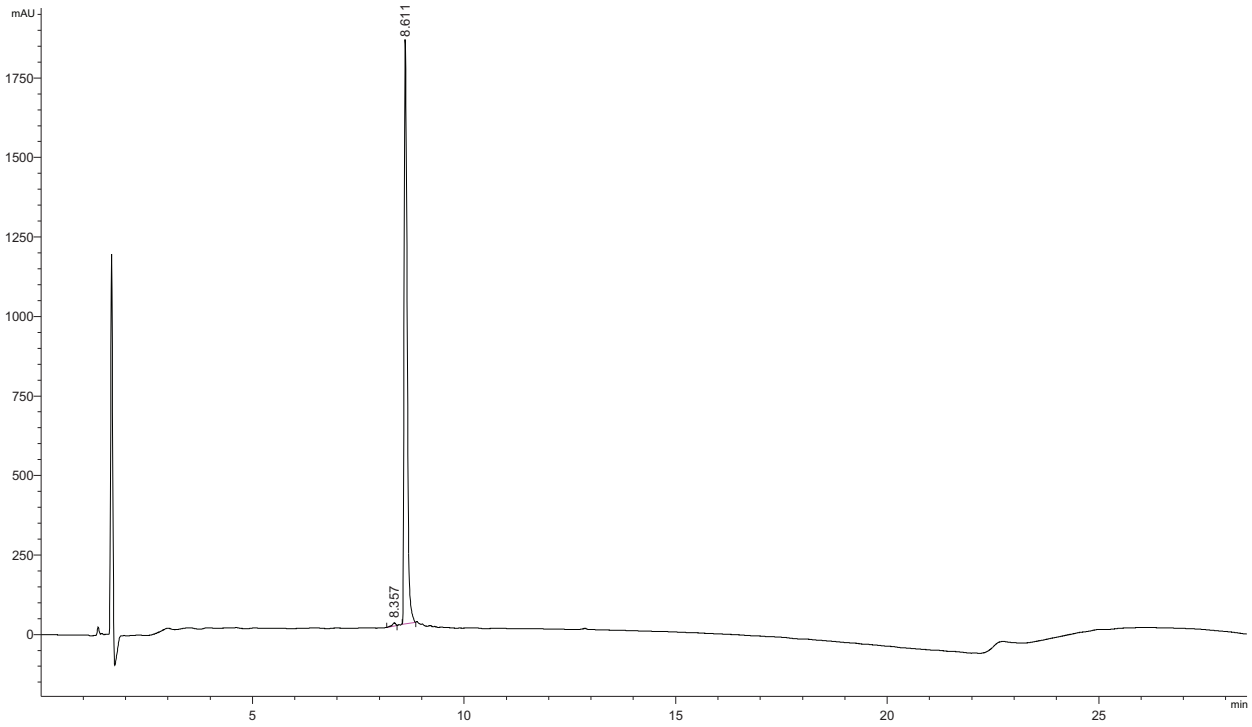

Peak #	RetTime [min]	Type	Width [min]	Area [mAU*s]	Height [mAU]	Area %
1	8.357	MM	0.1002	62.18367	10.33866	0.6828
2	8.611	MM	0.0815	9045.53809	1848.98840	99.3172
Totals :				9107.72176	1859.32707	

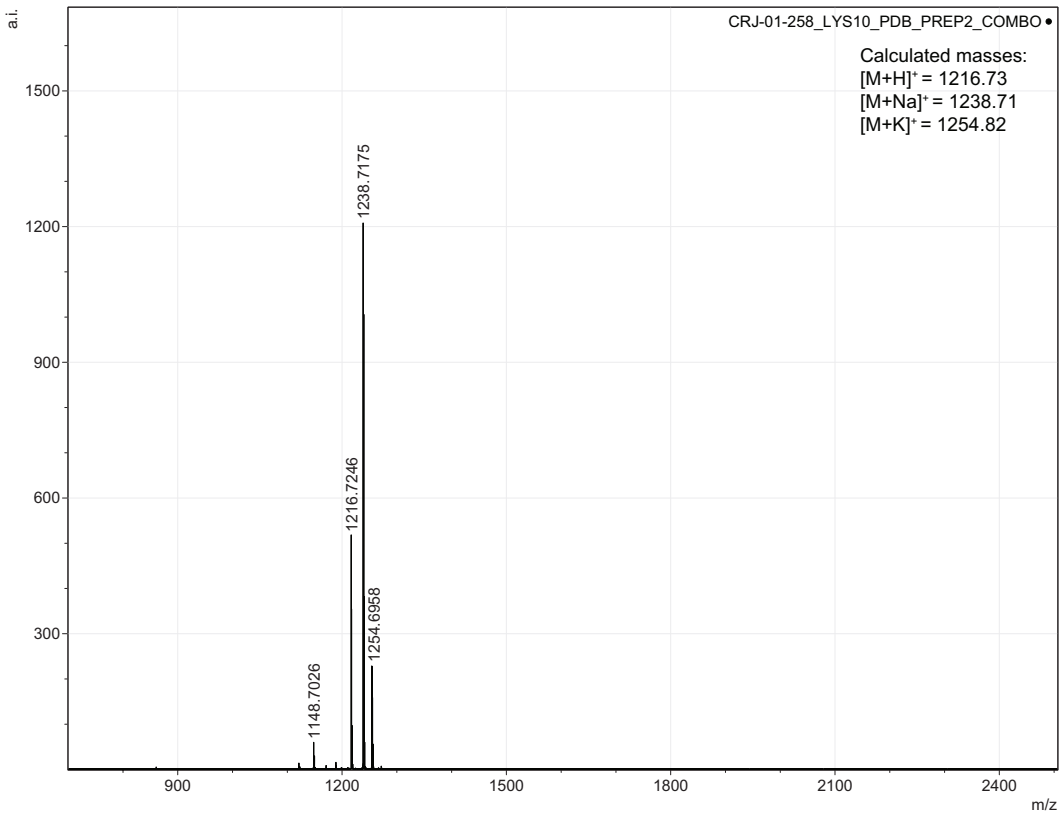
CRJ-01-258_LYS10_PDB_PREP2_COMBO
Calculated masses:
[M+H]+ = 1216.73
[M+Na]+ = 1238.71
[M+K]+ = 1254.82
a.i.
1500
1200
900
600
300
1238.7175
1216.7246
1254.6958
1148.7026
900
1200
1500
1800
2100
2400
m/z

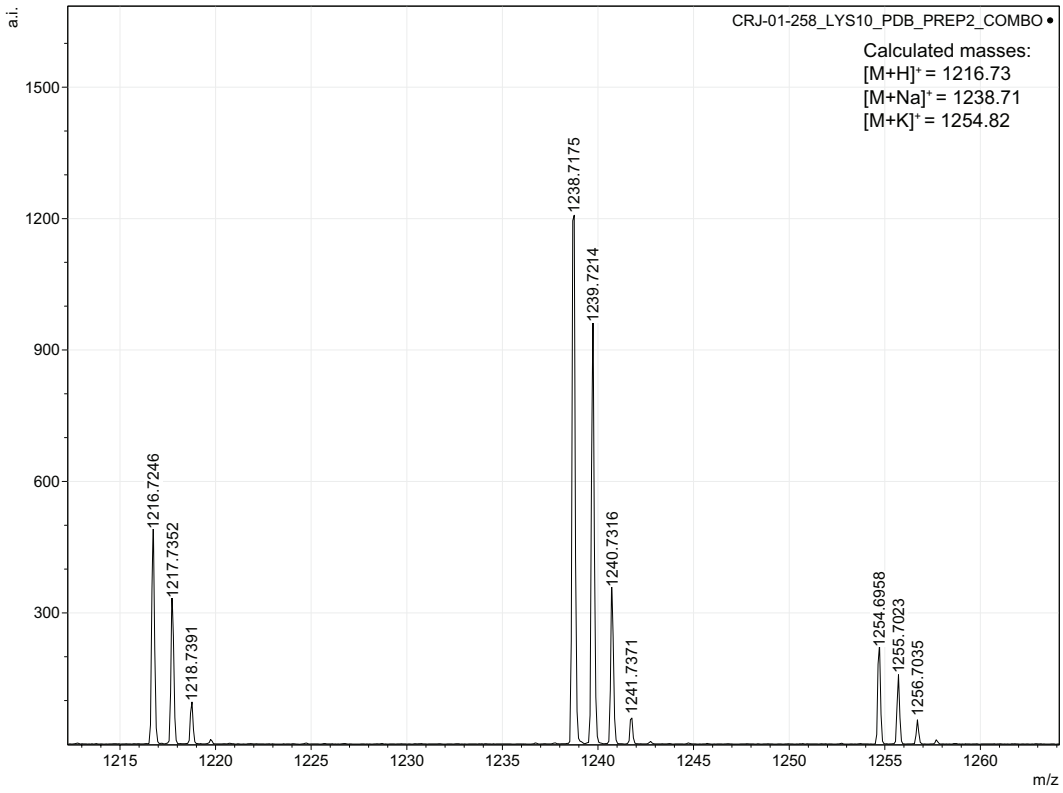
CRJ-01-258_LYS10_PDB_PREP2_COMBO
Calculated masses:
[M+H]+ = 1216.73
[M+Na]+ = 1238.71
[M+K]+ = 1254.82
a.i.
1500
1200
900
600
300
1238.7175
1239.7214
1216.7246
1217.7352
1240.7316
1218.7391
1241.7371
1254.6958
1255.7023
1256.7035
1215
1220
1225
1230
1235
1240
1245
1250
1255
1260
m/z

Lys$_{10}$-teixobactin Prodrug C Analytical HPLC Trace and MALDI-TOF

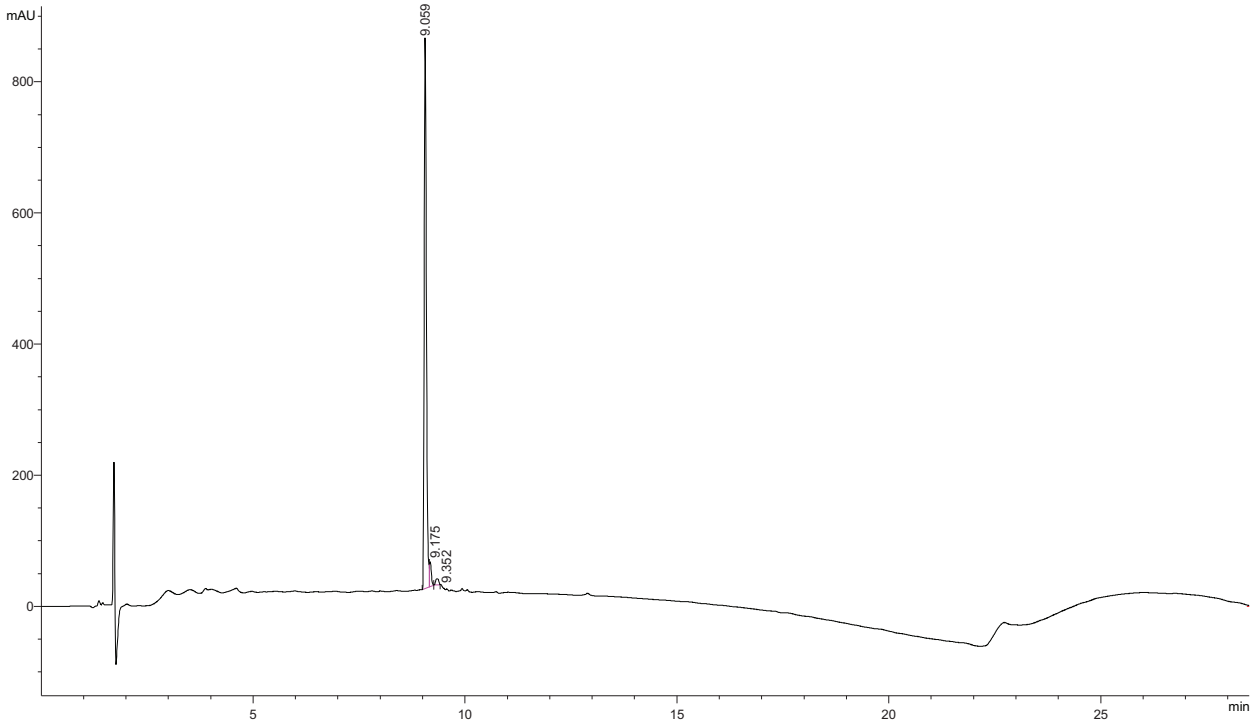

Peak #	RetTime [min]	Type	Width [min]	Area [mAU*s]	Height [mAU]	Area %
1	9.059	MF	0.0602	3045.64526	843.11633	95.0579
2	9.175	FM	0.0479	108.82409	37.82890	3.3965
3	9.352	MM	0.0870	49.51868	9.48839	1.5455
Totals :				3203.98803	890.43363	

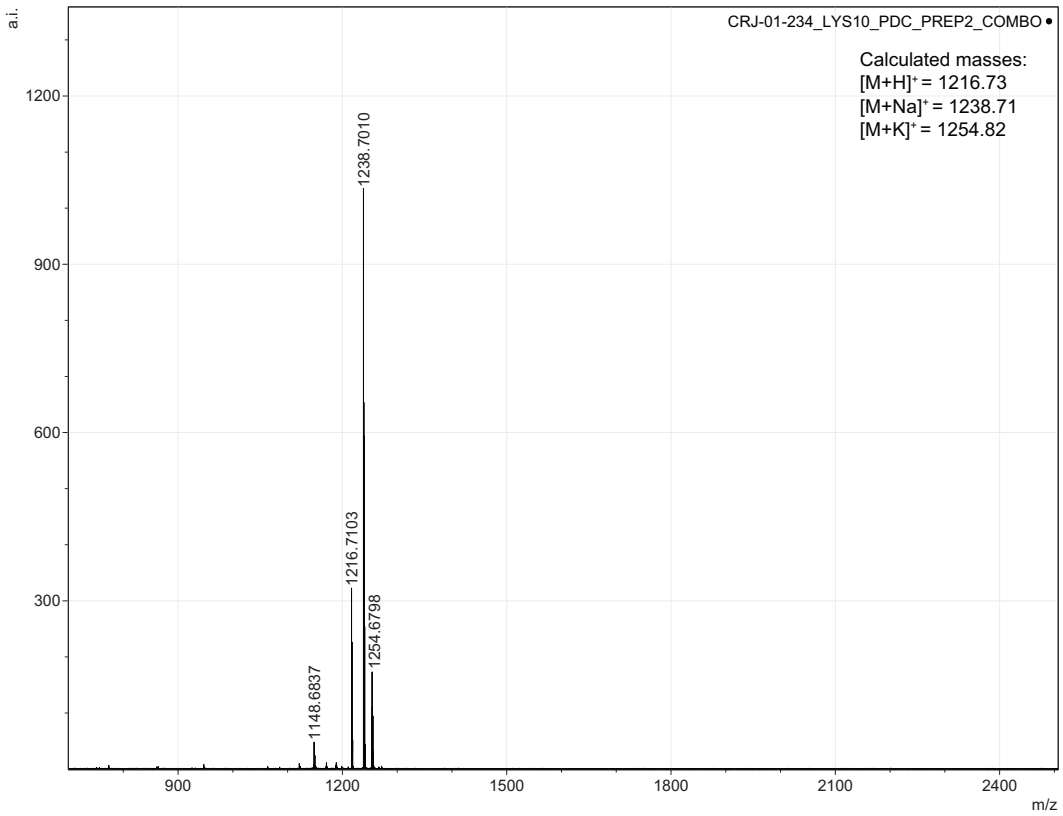
CRJ-01-234_LYS10_PDC_PREP2_COMBO
Calculated masses:
[M+H]+ = 1216.73
[M+Na]+ = 1238.71
[M+K]+ = 1254.82
a.i.
1200
900
600
300
1238.7010
1216.7103
1254.6798
1148.6837
900
1200
1500
1800
2100
2400
m/z

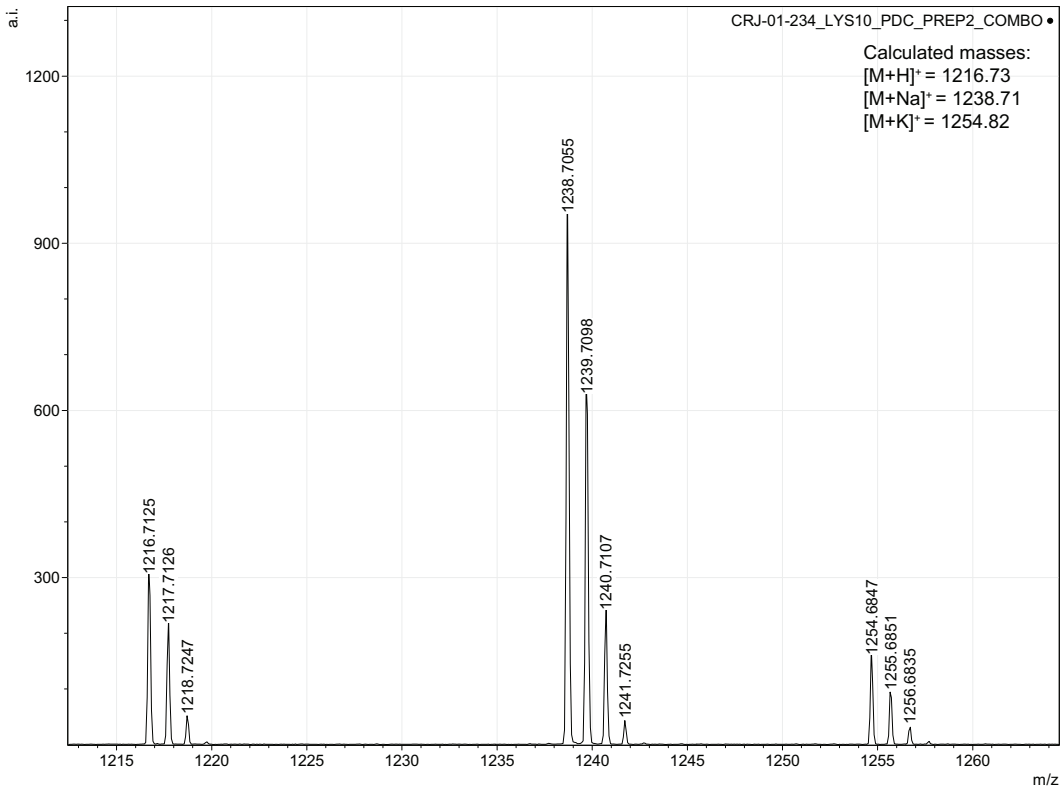
CRJ-01-234_LYS10_PDC_PREP2_COMBO
Calculated masses:
[M+H]+ = 1216.73
[M+Na]+ = 1238.71
[M+K]+ = 1254.82
a.i.
1200
900
600
300
1238.7055
1239.7098
1216.7125
1217.7126
1240.7107
1218.7247
1241.7255
1254.6847
1255.6851
1256.6835
1215
1220
1225
1230
1235
1240
1245
1250
1255
1260
m/z

Arg$_{10}$-teixobactin Analytical HPLC Trace and MALDI-TOF

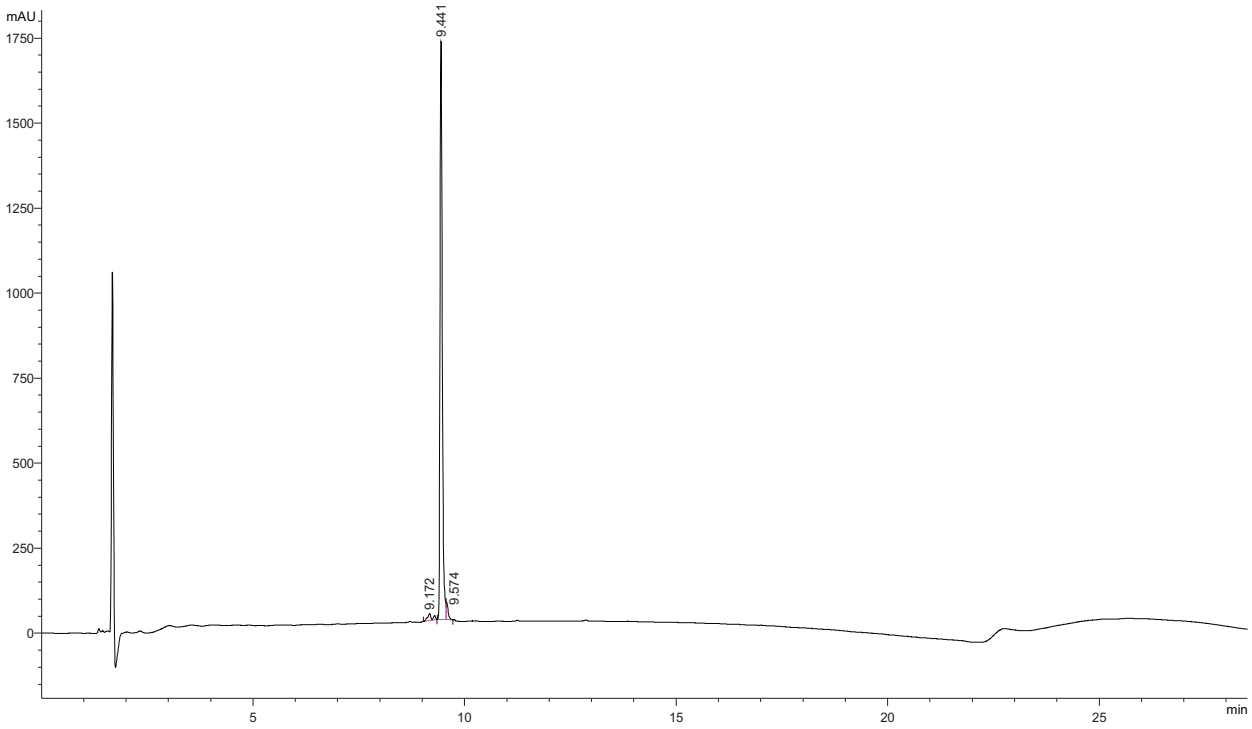

Peak #	RetTime [min]	Type	Width [min]	Area [mAU*s]	Height [mAU]	Area %
1	9.172	MM	0.1281	162.81050	21.17930	2.4426
2	9.441	MF	0.0614	6344.79980	1722.18896	95.1874
3	9.574	FM	0.0517	157.97453	50.89952	2.3700
Totals :				6665.58484	1794.26778	

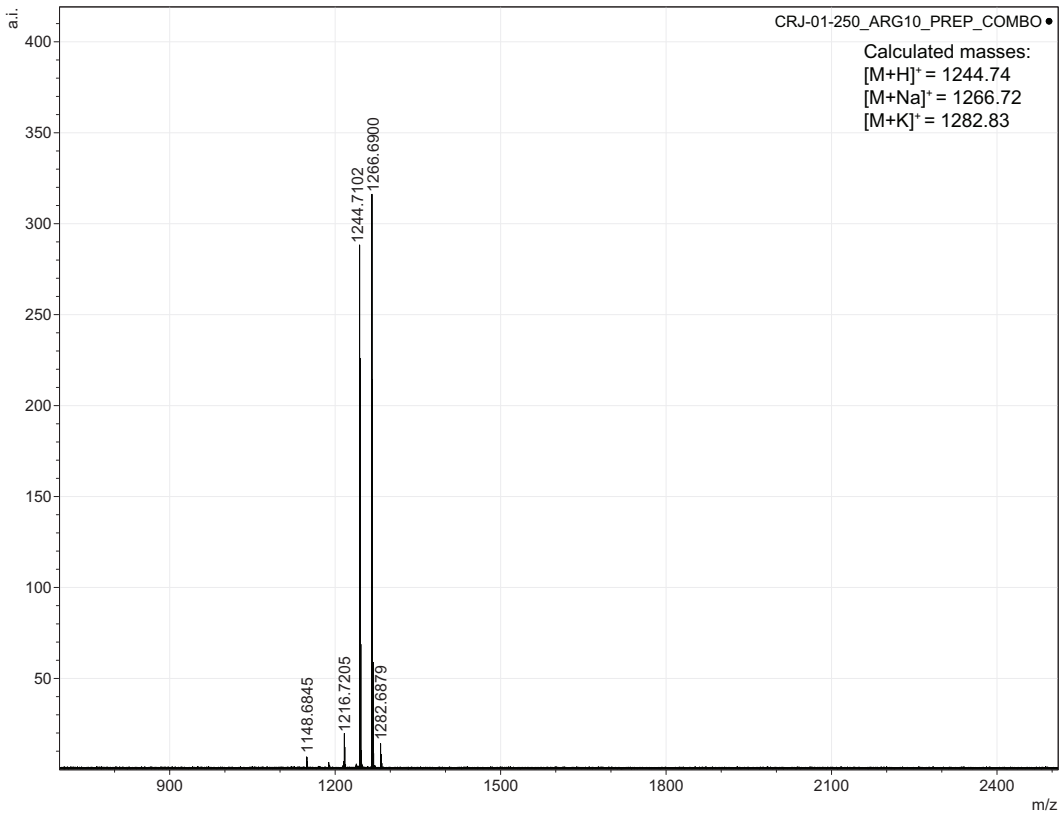
CRJ-01-250_ARG10_PREP_COMBO
Calculated masses:
[M+H]+ = 1244.74
[M+Na]+ = 1266.72
[M+K]+ = 1282.83
a.i.
m/z
1148.6845
1216.7205
1244.7102
1266.6900
1282.6879

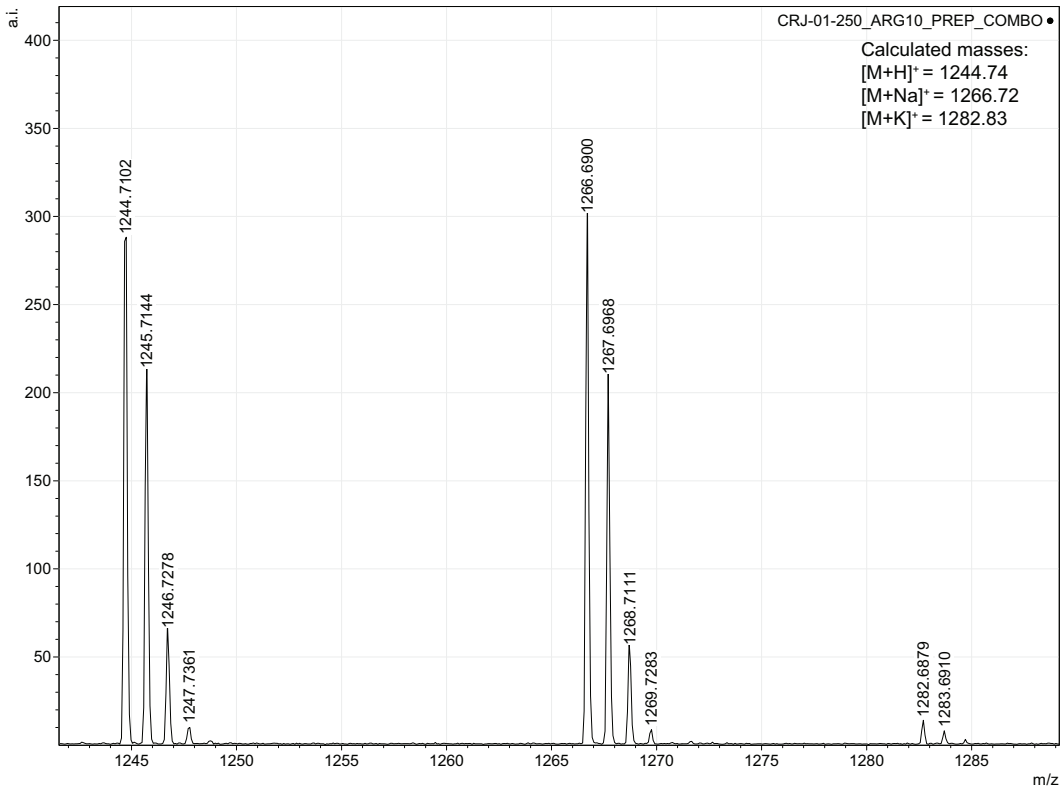
CRJ-01-250_ARG10_PREP_COMBO
Calculated masses:
[M+H]+ = 1244.74
[M+Na]+ = 1266.72
[M+K]+ = 1282.83
a.i.
m/z
1244.7102
1245.7144
1246.7278
1247.7361
1266.6900
1267.6968
1268.7111
1269.7283
1282.6879
1283.6910

Arg_{10}-teixobactin Prodrug A Analytical HPLC Trace and MALDI-TOF

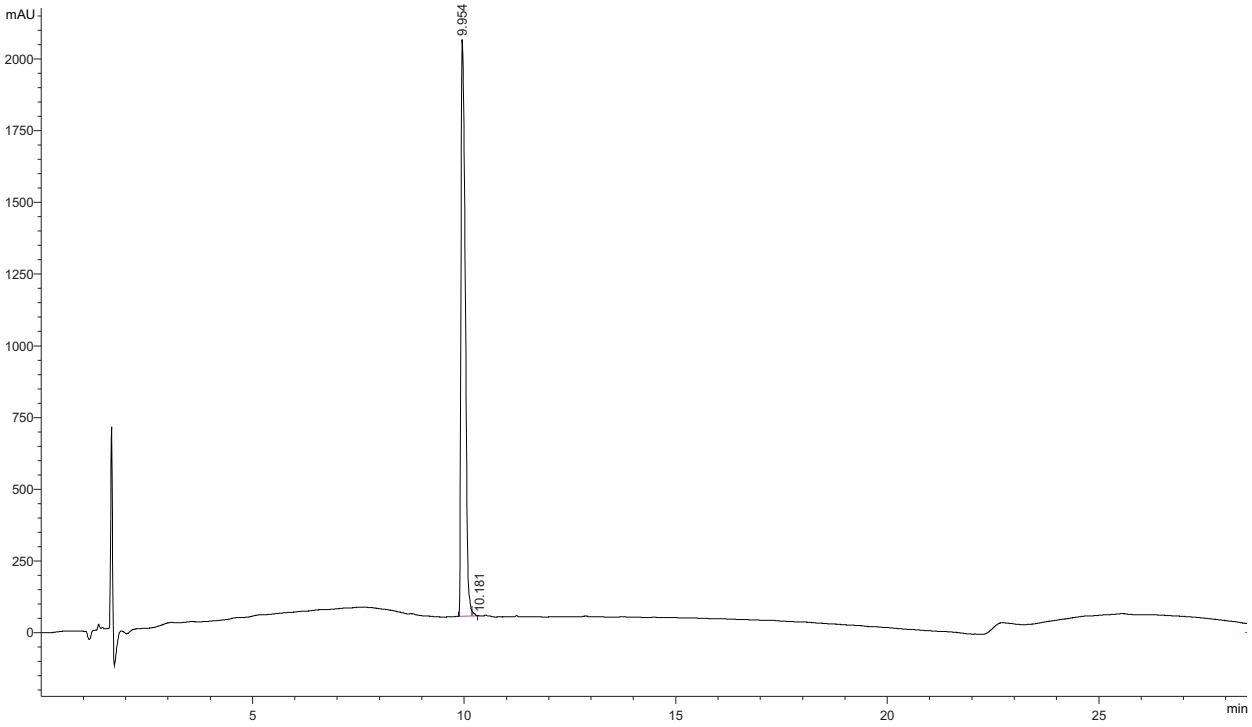

Peak #	RetTime [min]	Type	Width [min]	Area [mAU*s]	Height [mAU]	Area %
1	9.954	MF	0.1167	1.41014e4	2013.23596	99.6042
2	10.181	FM	0.0521	56.02947	17.92281	0.3958
Totals :				1.41574e4	2031.15877	

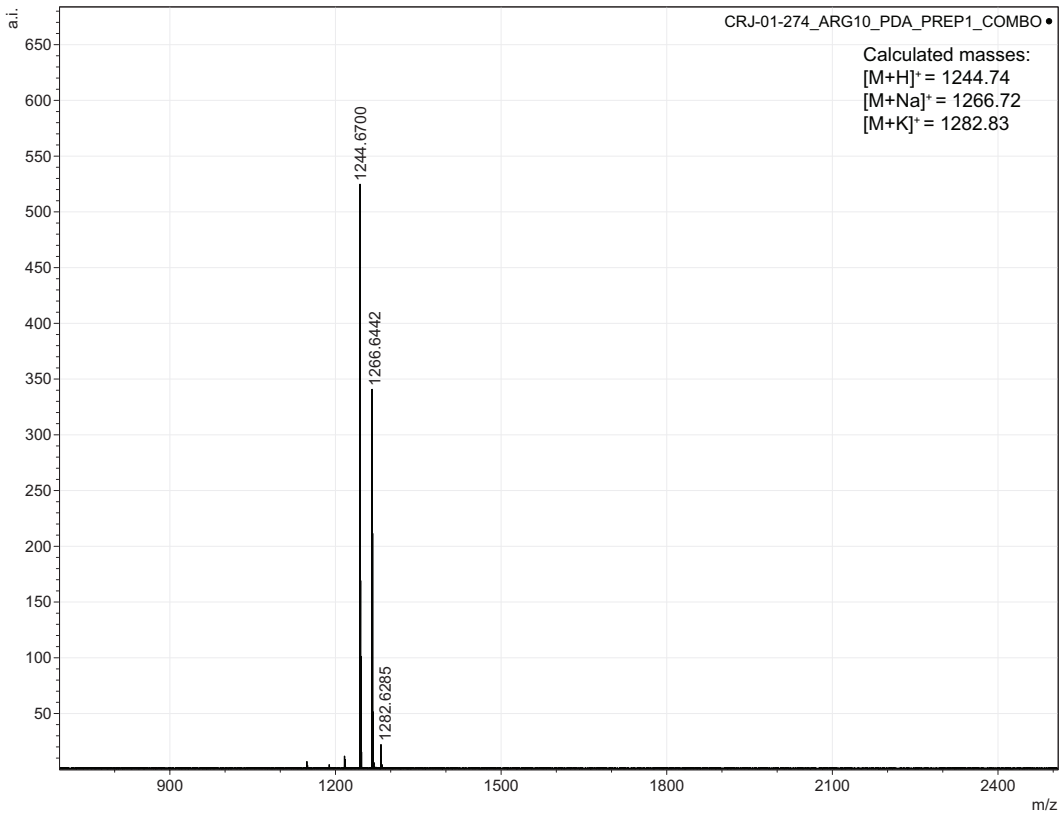
CRJ-01-274_ARG10_PDA_PREP1_COMBO
Calculated masses:
[M+H]+ = 1244.74
[M+Na]+ = 1266.72
[M+K]+ = 1282.83
1244.6700
1266.6442
1282.6285
a.i.
m/z

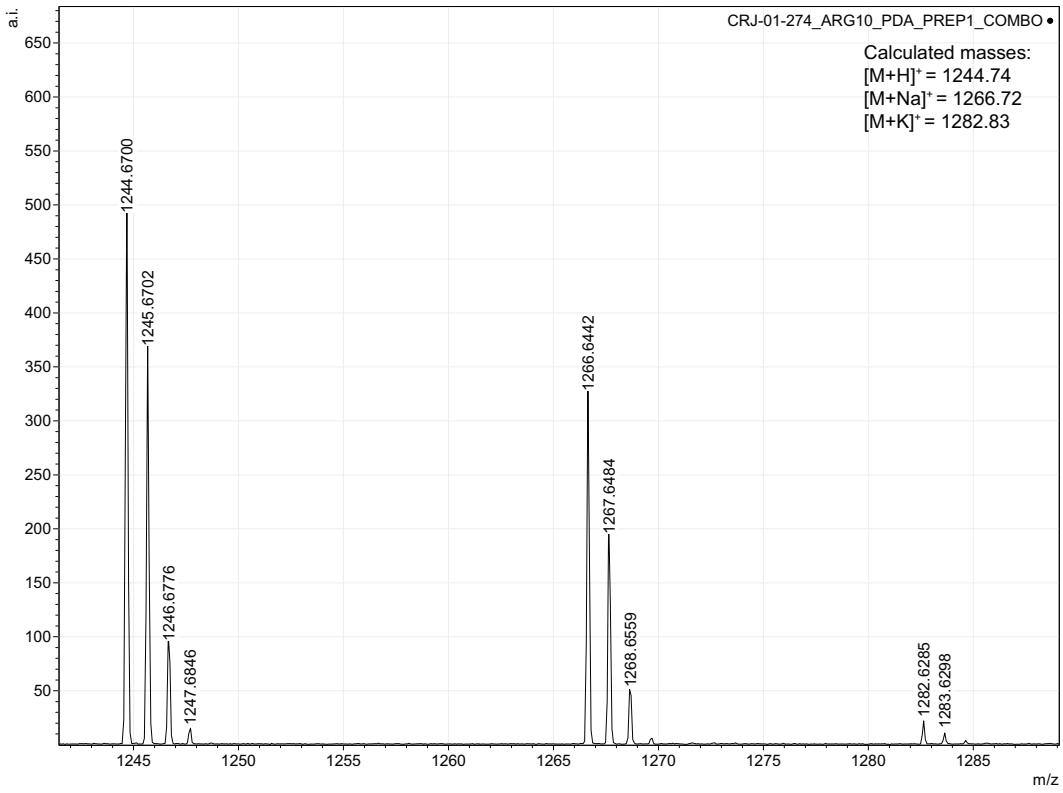
CRJ-01-274_ARG10_PDA_PREP1_COMBO
Calculated masses:
[M+H]+ = 1244.74
[M+Na]+ = 1266.72
[M+K]+ = 1282.83
1244.6700
1245.6702
1246.6776
1247.6846
1266.6442
1267.6484
1268.6559
1282.6285
1283.6298
a.i.
m/z

Arg$_{10}$-teixobactin Prodrug B Analytical HPLC Trace and MALDI-TOF

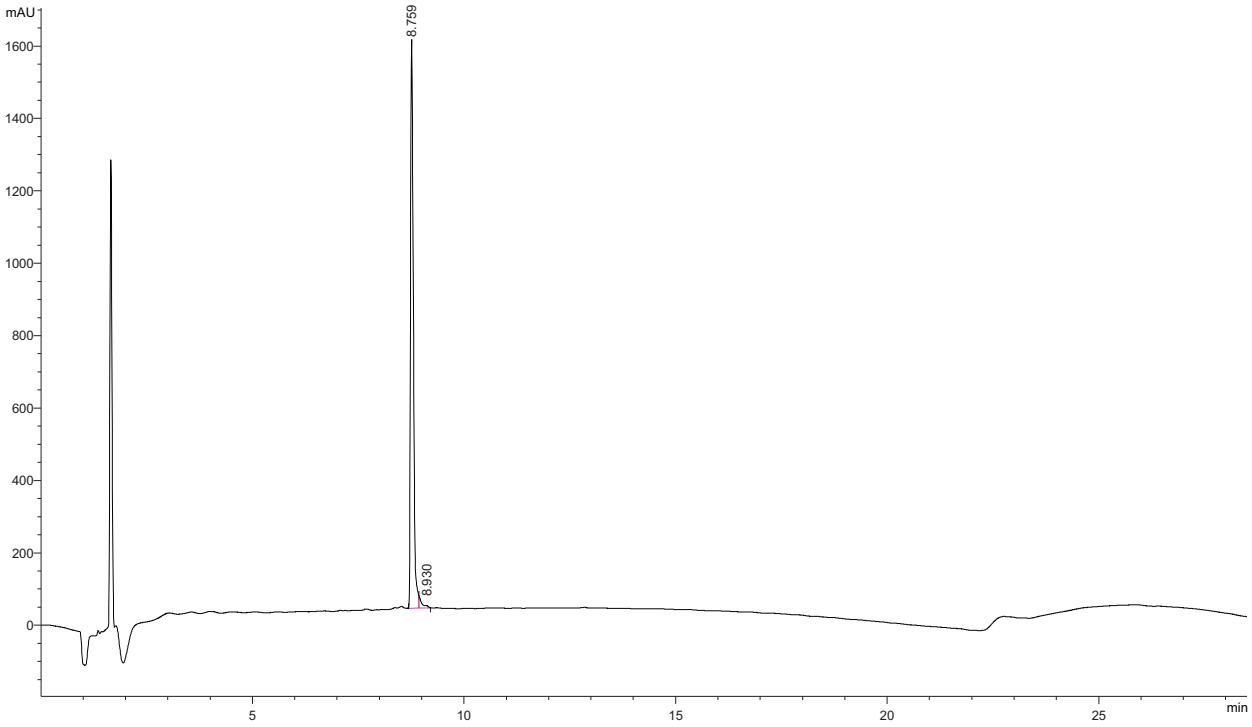

Peak #	RetTime [min]	Type	Width [min]	Area [mAU*s]	Height [mAU]	Area %
1	8.759	MF	0.0775	7334.88721	1576.97510	97.7861
2	8.930	FM	0.0803	166.06308	34.45243	2.2139
Totals :				7500.95029	1611.42752	

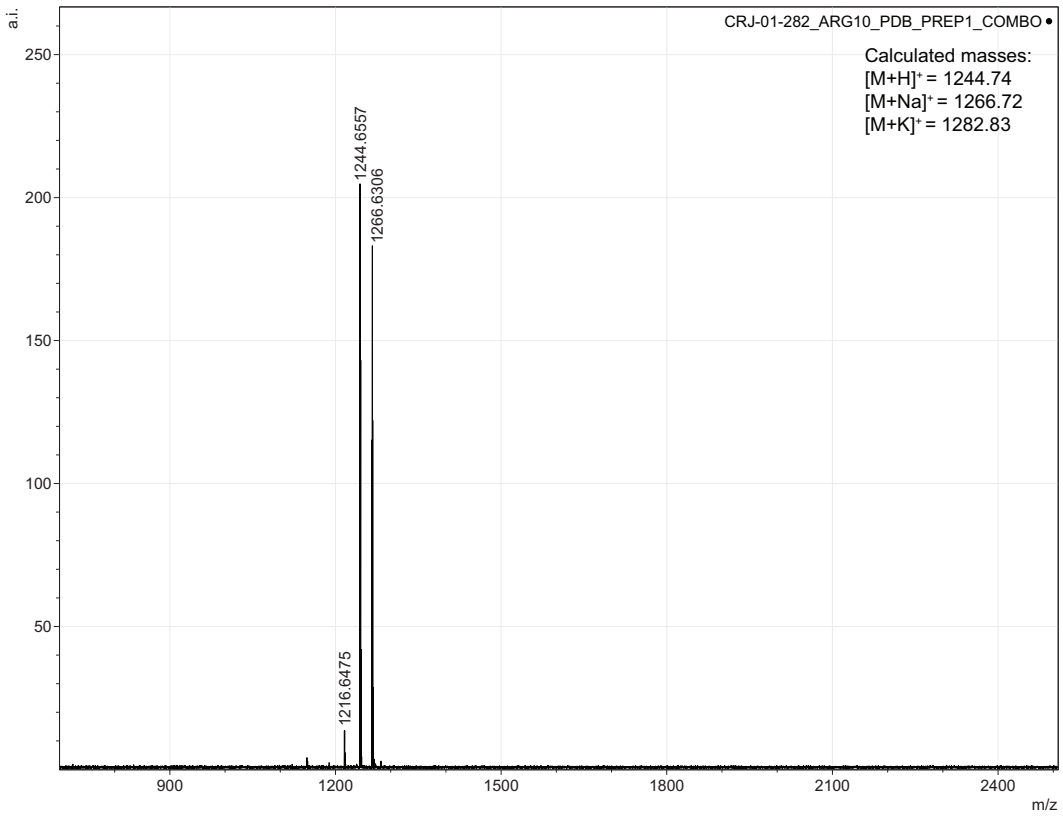
CRJ-01-282_ARG10_PDB_PREP1_COMBO
Calculated masses:
[M+H]+ = 1244.74
[M+Na]+ = 1266.72
[M+K]+ = 1282.83
1244.6557
1266.6306
1216.6475
a.i.
m/z

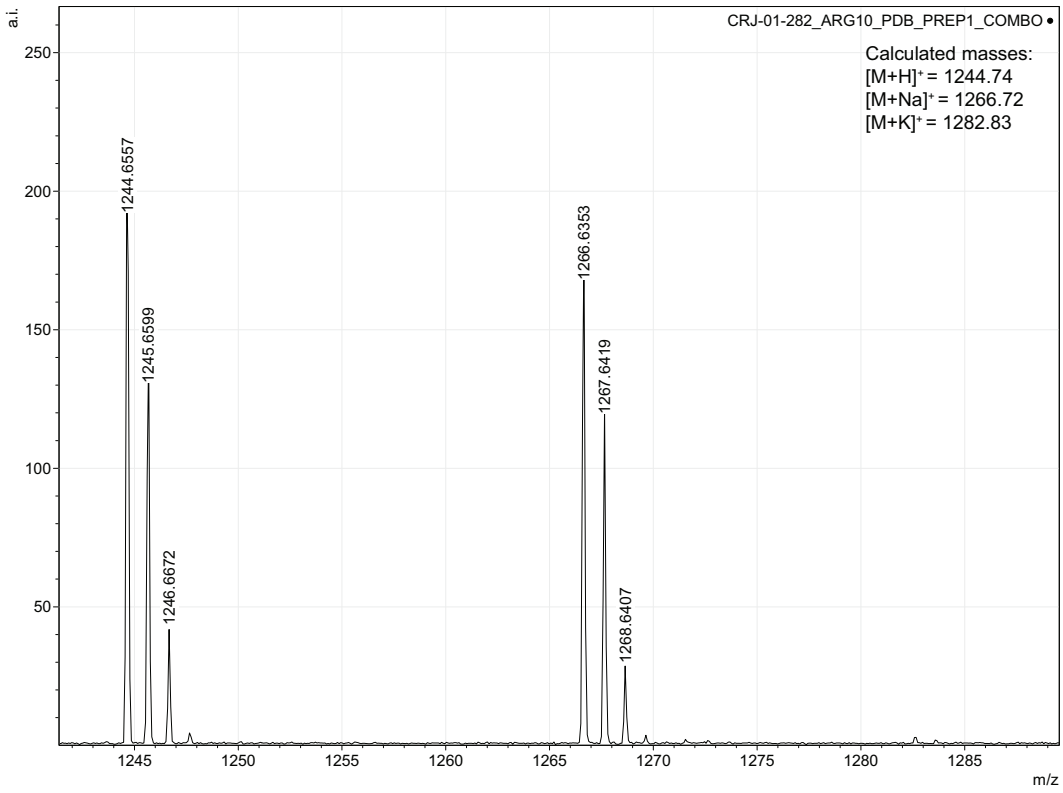
CRJ-01-282_ARG10_PDB_PREP1_COMBO
Calculated masses:
[M+H]+ = 1244.74
[M+Na]+ = 1266.72
[M+K]+ = 1282.83
1244.6557
1245.6599
1246.6672
1266.6353
1267.6419
1268.6407
a.i.
m/z

Arg_{10}-teixobactin Prodrug C Analytical HPLC Trace and MALDI-TOF

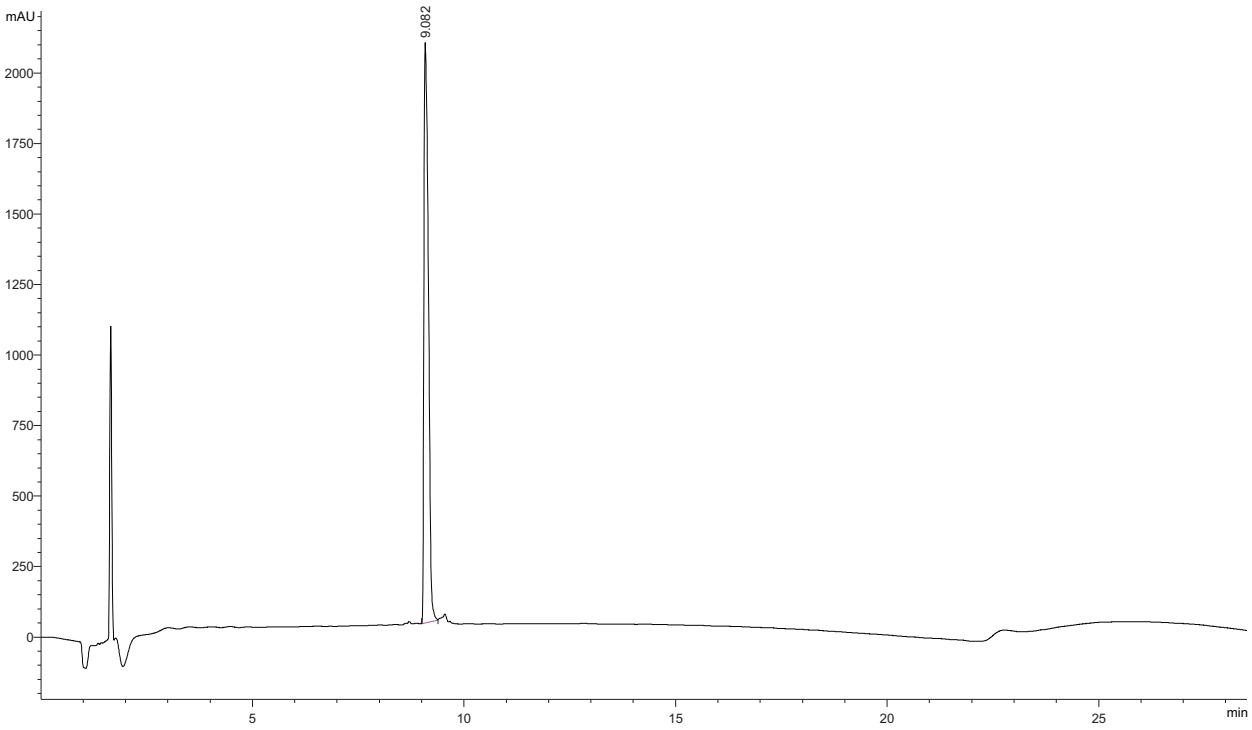

Peak #	RetTime [min]	Type	Width [min]	Area [mAU*s]	Height [mAU]	Area %
1	9.082	MM	0.1211	1.49948e4	2064.42993	100.0000
Totals :				1.49948e4	2064.42993	

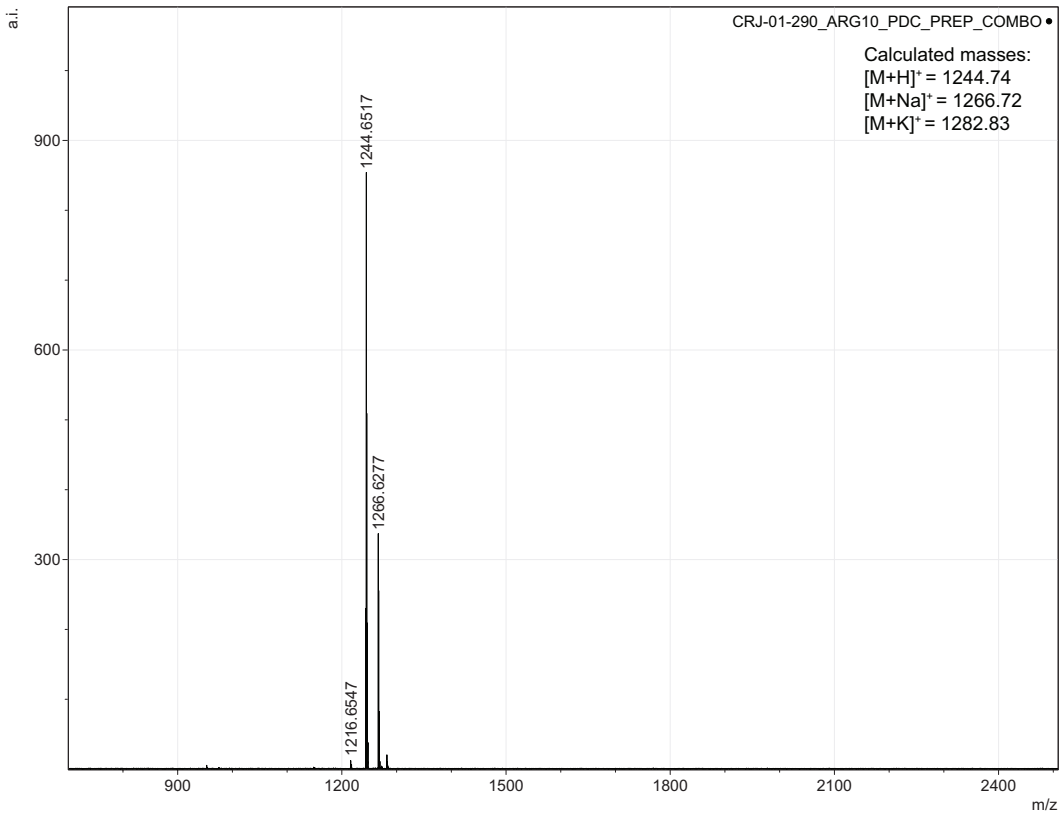
a.i.
CRJ-01-290_ARG10_PDC_PREP_COMBO
Calculated masses:
[M+H]+ = 1244.74
[M+Na]+ = 1266.72
[M+K]+ = 1282.83
1244.6517
1266.6277
1216.6547
900
600
300
900
1200
1500
1800
2100
2400
m/z

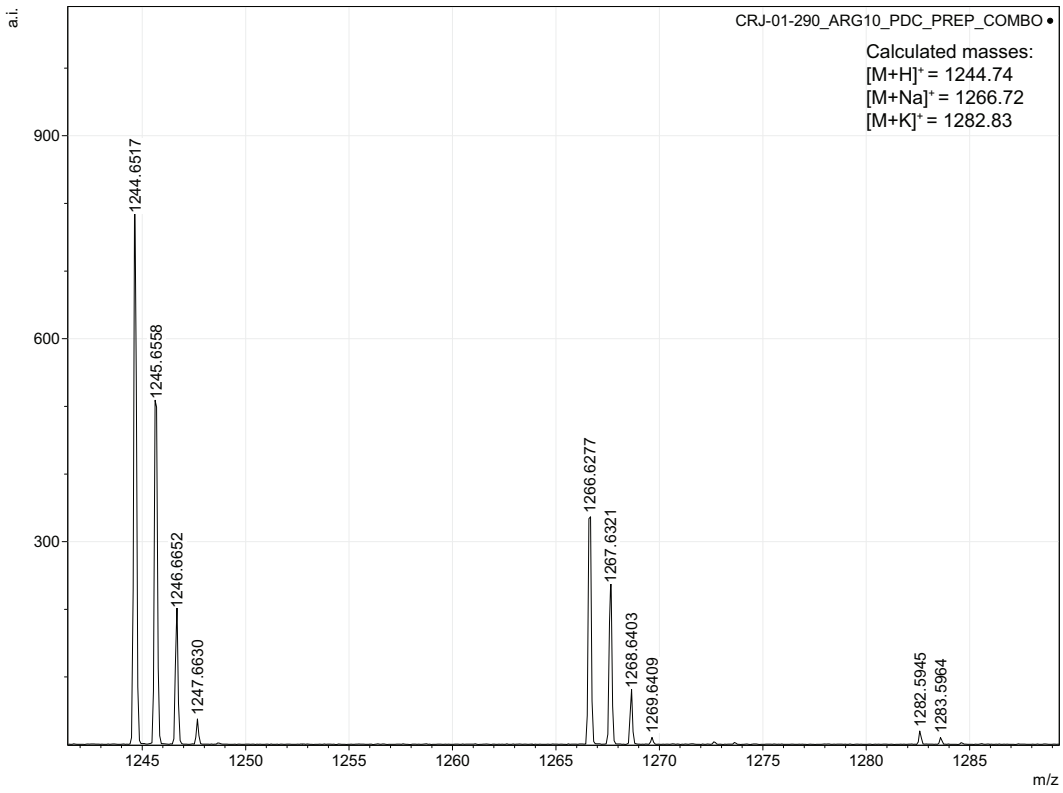
a.i.
CRJ-01-290_ARG10_PDC_PREP_COMBO
Calculated masses:
[M+H]+ = 1244.74
[M+Na]+ = 1266.72
[M+K]+ = 1282.83
1244.6517
1245.6558
1246.6652
1247.6630
1266.6277
1267.6321
1268.6403
1269.6409
1282.5945
1283.5964
900
600
300
1245
1250
1255
1260
1265
1270
1275
1280
1285
m/z

Leu$_{10}$-teixobactin Analytical HPLC Trace and MALDI-TOF

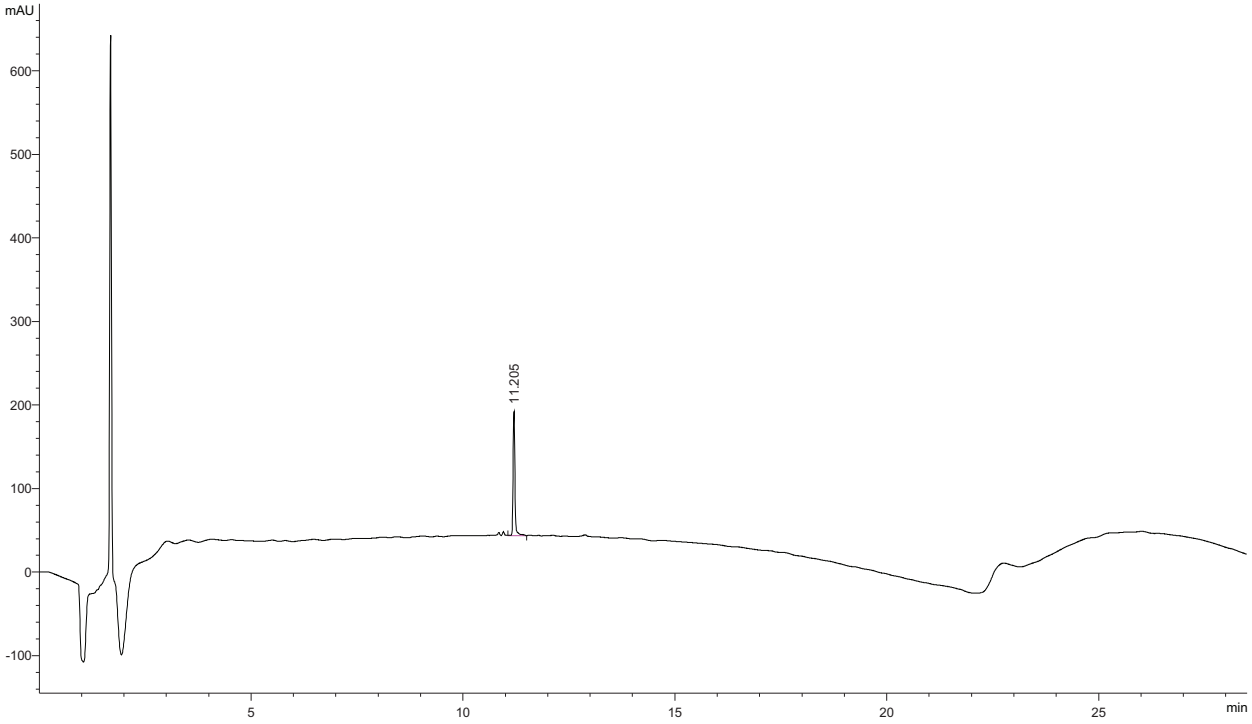

Peak #	RetTime [min]	Type	Width [min]	Area [mAU*s]	Height [mAU]	Area %
1	11.205	VV R	0.0475	456.96954	150.00790	100.0000
Totals :				456.96954	150.00790	

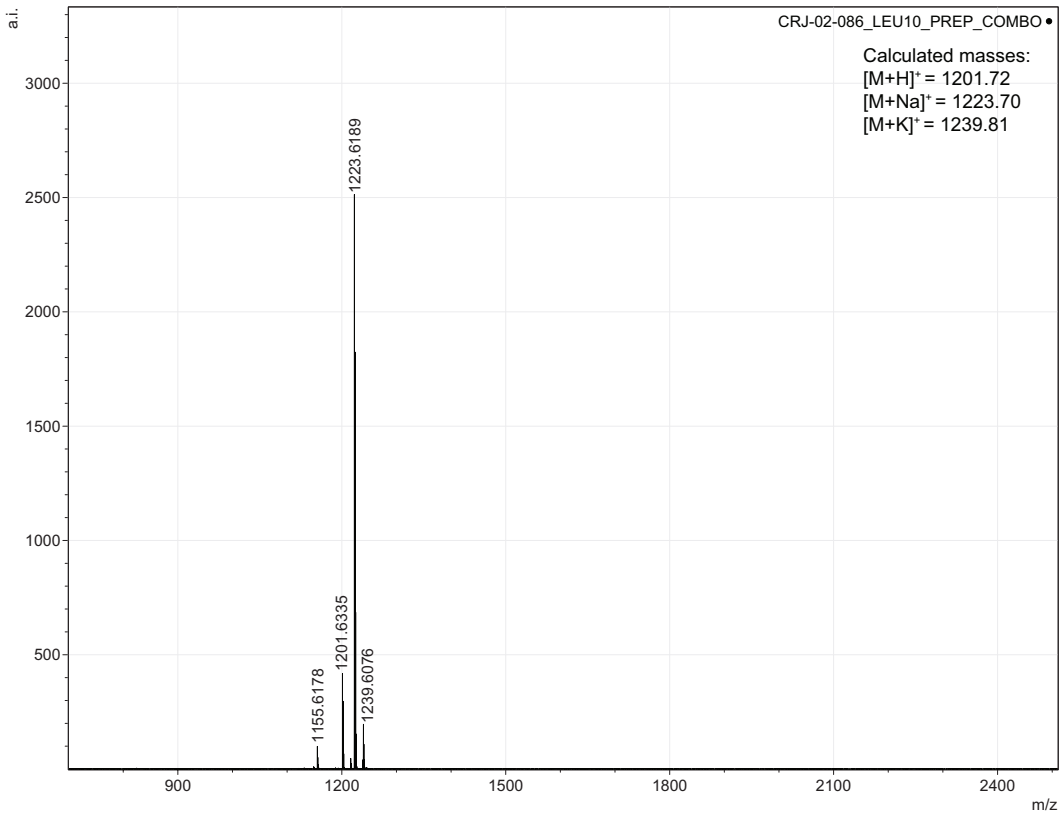
CRJ-02-086_LEU10_PREP_COMBO
Calculated masses:
[M+H]+ = 1201.72
[M+Na]+ = 1223.70
[M+K]+ = 1239.81
a.i.
m/z
1223.6189
1201.6335
1155.6178
1239.6076

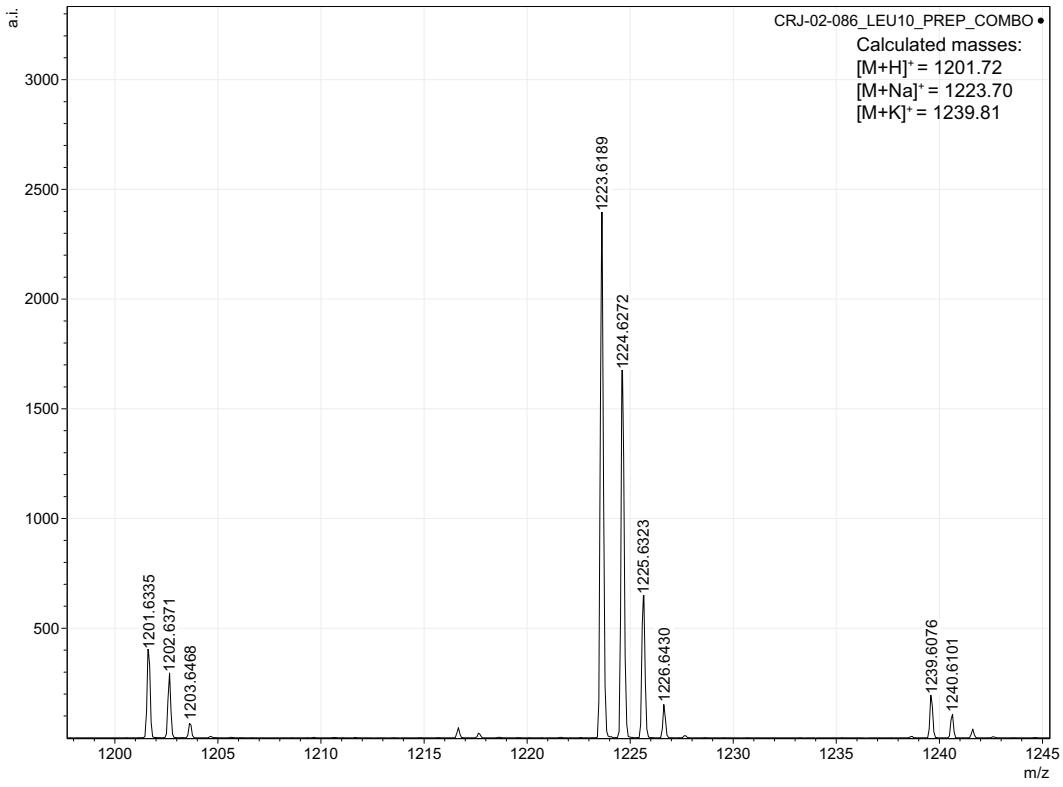
CRJ-02-086_LEU10_PREP_COMBO
Calculated masses:
[M+H]+ = 1201.72
[M+Na]+ = 1223.70
[M+K]+ = 1239.81
a.i.
m/z
1223.6189
1224.6272
1225.6323
1201.6335
1202.6371
1203.6468
1226.6430
1239.6076
1240.6101

Leu$_{10}$-teixobactin Prodrug A Analytical HPLC Trace and MALDI-TOF

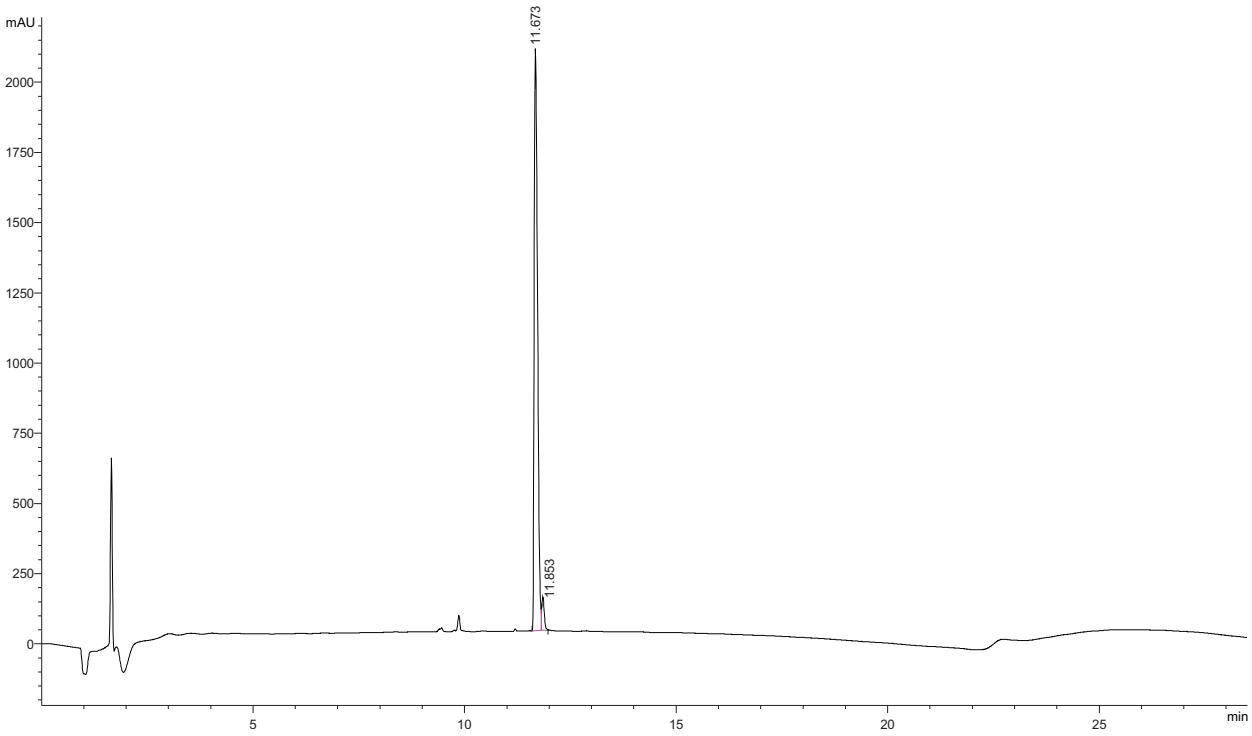

Peak #	RetTime [min]	Type	Width [min]	Area [mAU*s]	Height [mAU]	Area %
1	11.673	MF	0.0931	1.15965e4	2076.78662	96.1550
2	11.853	FM	0.0652	463.71695	118.46477	3.8450
Totals :				1.20603e4	2195.25139	

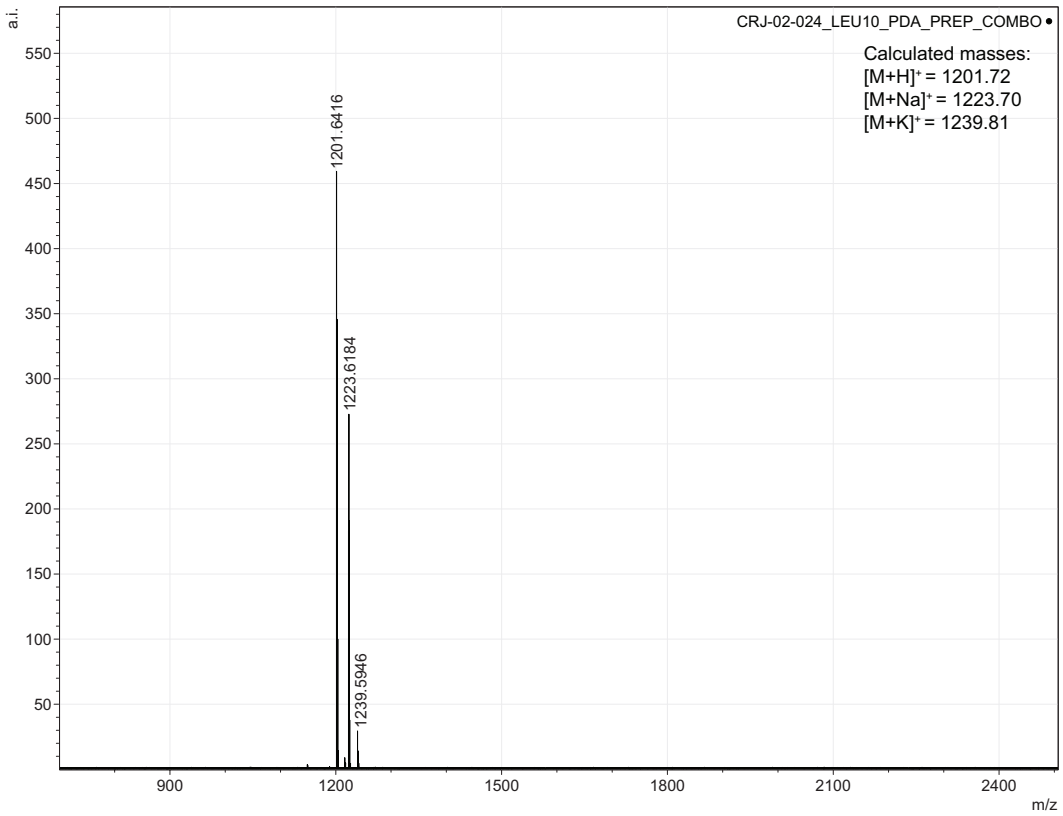
CRJ-02-024_LEU10_PDA_PREP_COMBO
Calculated masses:
[M+H]+ = 1201.72
[M+Na]+ = 1223.70
[M+K]+ = 1239.81
1201.6416
1223.6184
1239.5946
a.i.
m/z

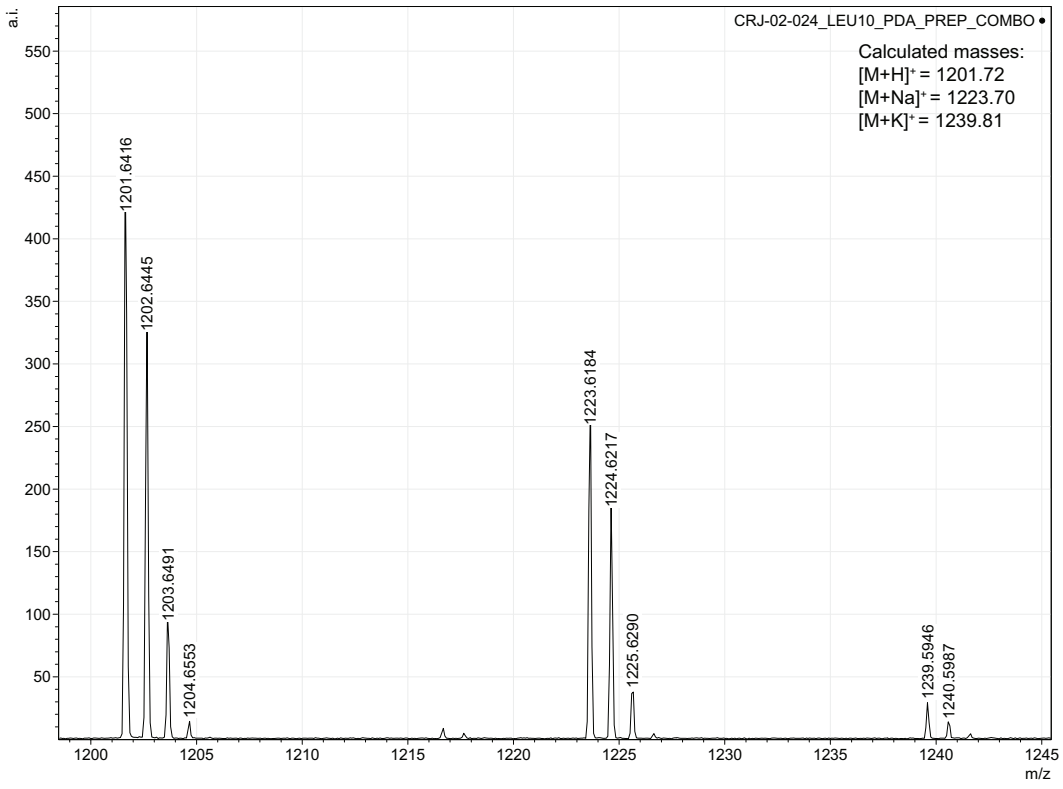
CRJ-02-024_LEU10_PDA_PREP_COMBO
Calculated masses:
[M+H]+ = 1201.72
[M+Na]+ = 1223.70
[M+K]+ = 1239.81
1201.6416
1202.6445
1203.6491
1204.6553
1223.6184
1224.6217
1225.6290
1239.5946
1240.5987
a.i.
m/z

Leu$_{10}$-teixobactin Prodrug B Analytical HPLC Trace and MALDI-TOF

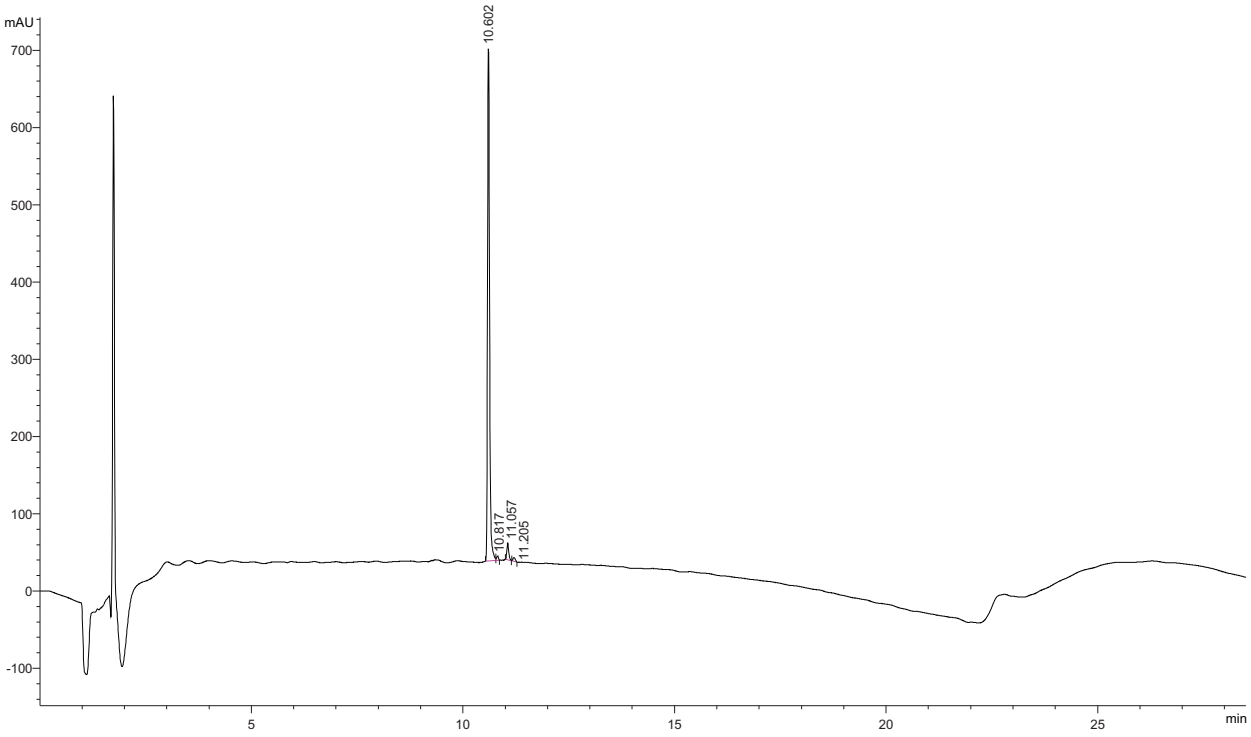

Peak #	RetTime [min]	Type	Width [min]	Area [mAU*s]	Height [mAU]	Area %
1	10.602	MF	0.0548	2208.07813	671.77911	95.6761
2	10.817	FM	0.0498	16.49998	5.52031	0.7149
3	11.057	MM	0.0499	65.42590	21.83677	2.8349
4	11.205	MM	0.0614	17.86347	4.85005	0.7740
Totals :				2307.86747	703.98624	

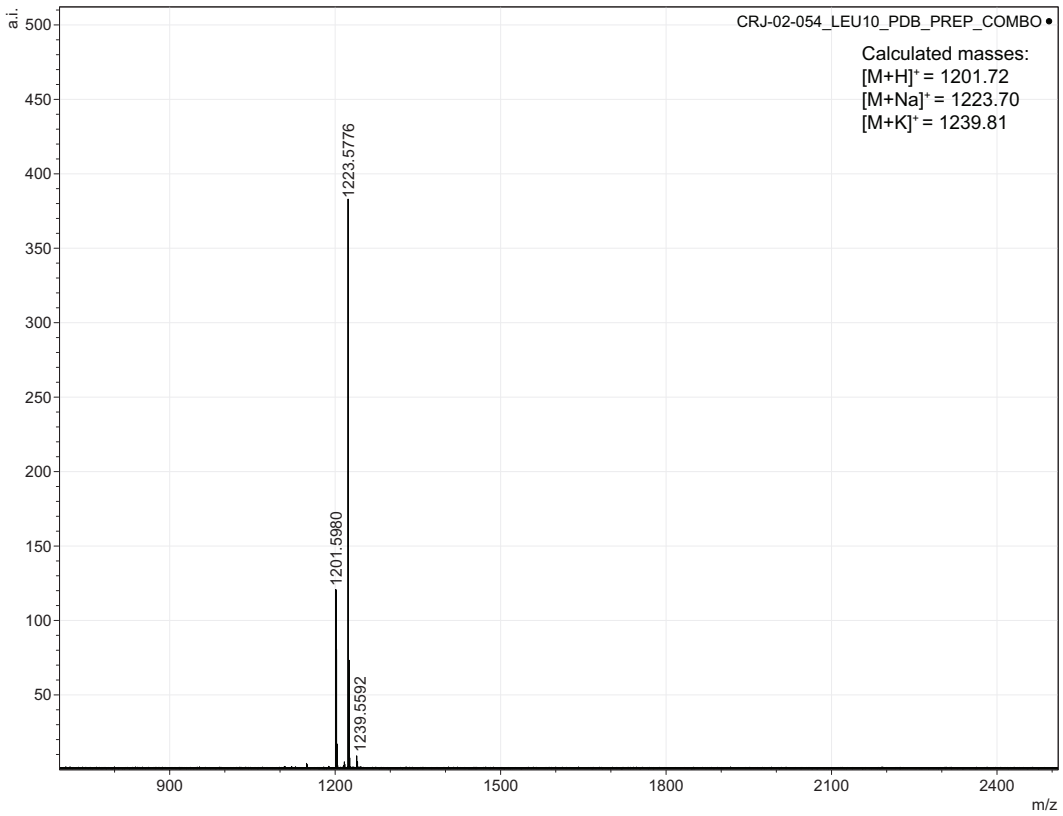
CRJ-02-054_LEU10_PDB_PREP_COMBO
Calculated masses:
[M+H]+ = 1201.72
[M+Na]+ = 1223.70
[M+K]+ = 1239.81
1223.5776
1201.5980
1239.5592
a.i.
m/z

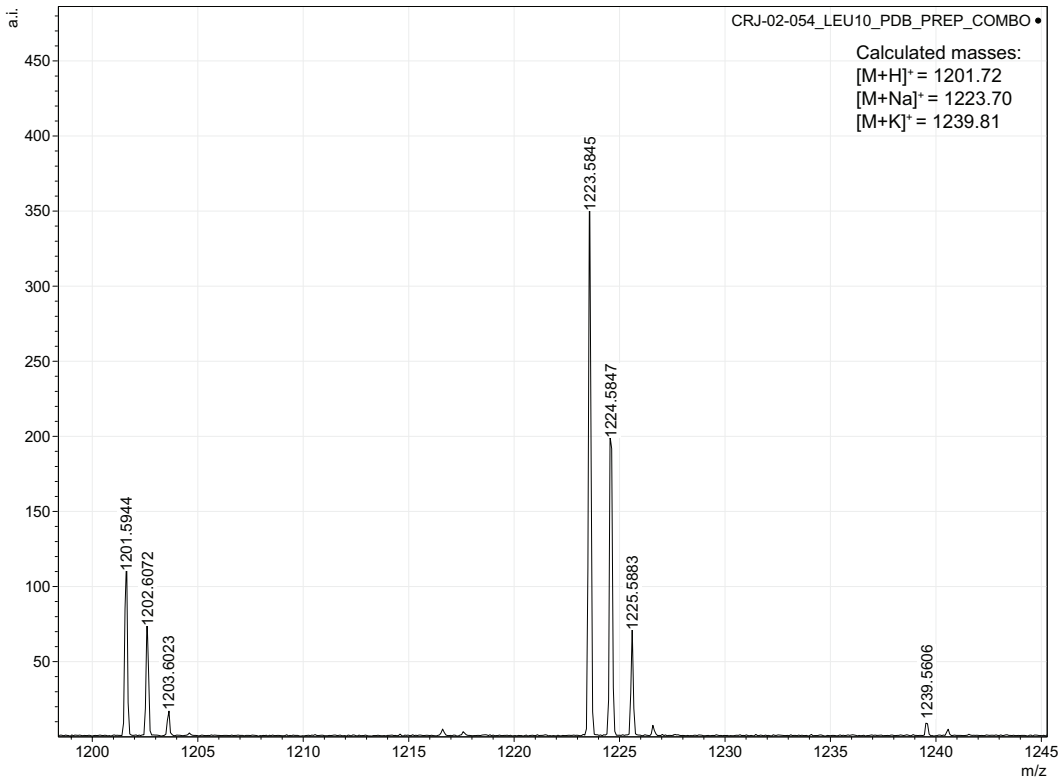
CRJ-02-054_LEU10_PDB_PREP_COMBO
Calculated masses:
[M+H]+ = 1201.72
[M+Na]+ = 1223.70
[M+K]+ = 1239.81
1223.5845
1224.5847
1201.5944
1202.6072
1203.6023
1225.5883
1239.5606
a.i.
m/z

Leu$_{10}$-teixobactin Prodrug C Analytical HPLC Trace and MALDI-TOF

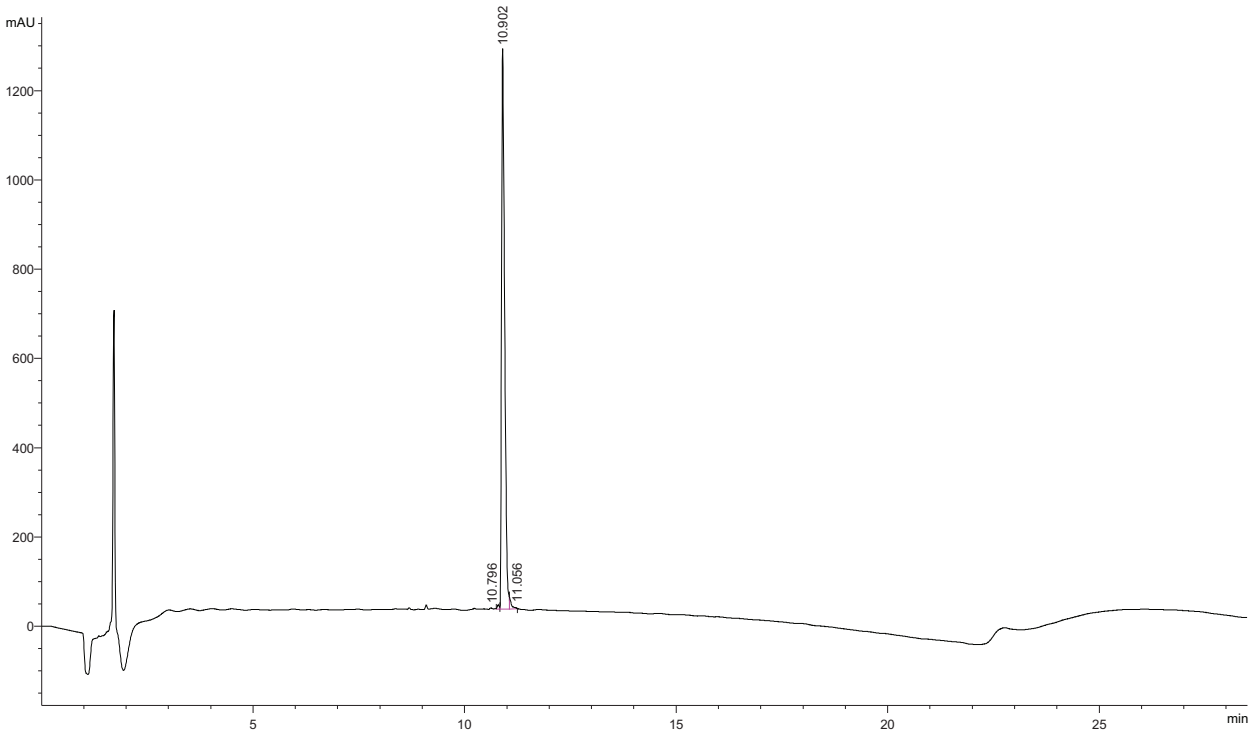

Peak #	RetTime [min]	Type	Width [min]	Area [mAU*s]	Height [mAU]	Area %
1	10.796	MF	0.0560	33.51337	9.98297	0.5203
2	10.902	MF	0.0836	6319.58105	1259.25037	98.1043
3	11.056	FM	0.0524	88.60129	28.16475	1.3754
Totals :				6441.69571	1297.39809	

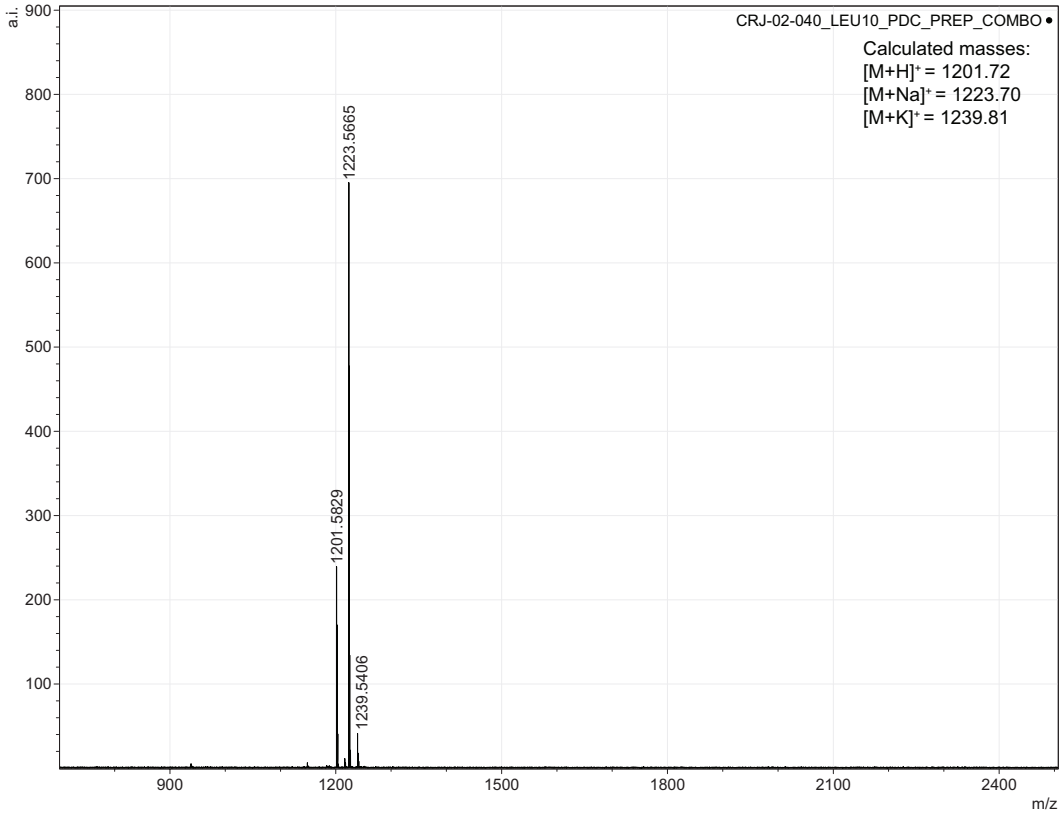
CRJ-02-040_LEU10_PDC_PREP_COMBO
Calculated masses:
[M+H]+ = 1201.72
[M+Na]+ = 1223.70
[M+K]+ = 1239.81
1223.5665
1201.5829
1239.5406
a.i.
m/z

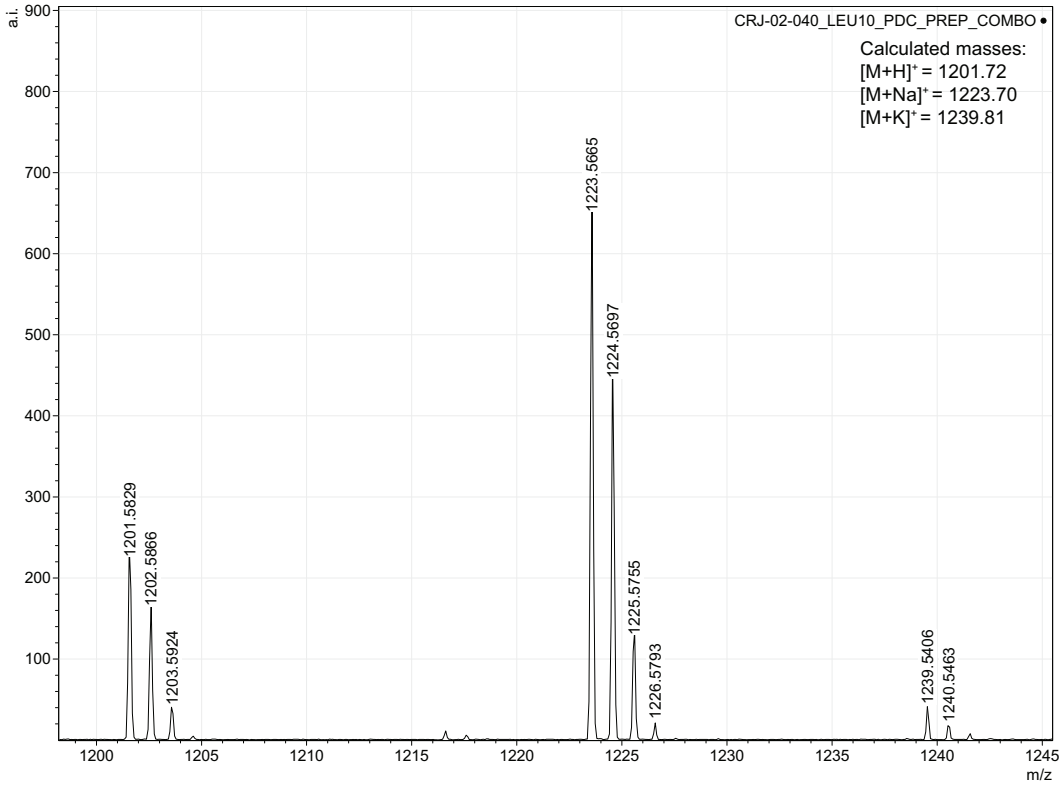
CRJ-02-040_LEU10_PDC_PREP_COMBO
Calculated masses:
[M+H]+ = 1201.72
[M+Na]+ = 1223.70
[M+K]+ = 1239.81
1223.5665
1224.5697
1201.5829
1202.5866
1203.5924
1225.5755
1226.5793
1239.5406
1240.5463
a.i.
m/z

Chapter 3[b]

Investigation of Additional Isobactin Analogues of Teixobactin

Prologue to Chapter 3

Chapter 3 has been taken verbatim or adapted from a manuscript that has been submitted for publication focused on the investigation of additional isobactin analogues of teixobactin. This project aimed to further improve upon the isobactin analogues and consists of almost the same experiments to evaluate the isobactin analogues seen in chapter 2. In this work, I designed the isobactin analogues following previously published teixobactin analogues. All peptides were synthesized by Grant Lai, Sophie Padilla, and I, with all purifications and characterizations of the peptides completed by me. The MIC assays were also performed by Grant Lai, Sophie Padilla, and I. Grant Lai and I performed conversion kinetic studies. The gelation, hemolytic, and cytotoxicity experiments were all performed by me.

In the initial report of isobactin analogues describe in chapter 2, all MIC assays were run in the absence and presence of 0.002% polysorbate 80 as this is believed to prevent teixobactin and teixobactin analogues from adhering to the polystyrene plates. Our laboratory has found that the addition of polysorbate 80 to the assay is important in obtaining accurate results. Therefore, the MIC assays performed in this chapter were only run in the presence of 0.002% polysorbate 80. Hemolytic assays were still performed in the absence and presence of 0.002% polysorbate 80 as there is less knowledge on the effect the polysorbate 80 has on these experiments. With the assistance of Grant Lai and Sophie Padilla, I was able to further investigate isobactin analogues.

[b]Chapter 3 is taken verbatim from or adapted from a manuscript that has been submitted for publication.

INTRODUCTION

Teixobactin is a non-ribosomal depsipeptide with potent antibiotic activity against Gram-positive bacteria, including drug-resistant strains such as MRSA and VRE.[1] This promising antibiotic candidate has limited solubility in serum or buffer and aggregates to form gels in the physiological conditions needed for intravenous administration.[2–5] The limited solubility and propensity to form gels has the potential to jeopardize its promise as a clinically useful intravenous antibiotic against drug-resistant Gram-positive pathogens by limiting dosing to low concentrations that do not form gels or aggregates.

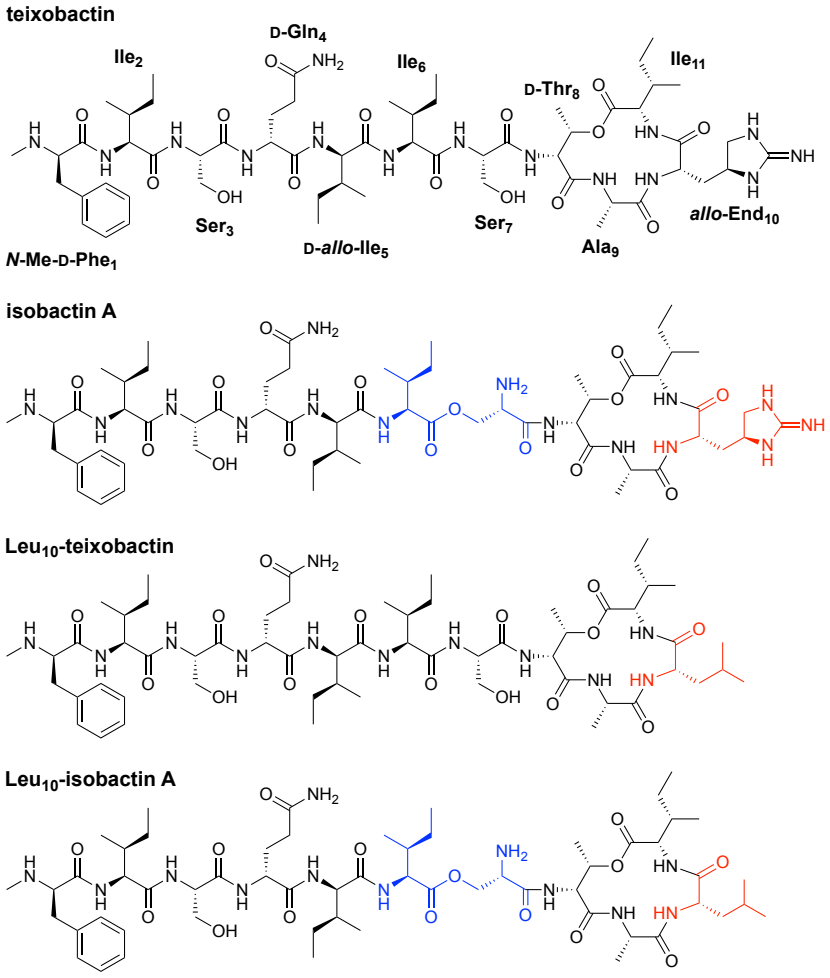

Figure 3.1. Structures of teixobactin, isobactin A, Leu$_{10}$-teixobactin, and Leu$_{10}$-isobactin A. Leu$_{10}$-teixobactin and Leu$_{10}$-isobactins A, B, and C were previously reported by Jones *et al.*[6]

Our laboratory recently introduced *O*-acyl isopeptide prodrug analogues of teixobactin, termed isobactins, that are stable and non-gelating in acidic solution but convert to the corresponding active teixobactin analogue at neutral pH (Figure 3.1).[6] We studied analogues with arginine, lysine, and leucine at position 10, because the native *allo*-enduracididine is not commercially available. The isobactin analogues exhibited improved solubility in aqueous conditions and delayed gel formation over the corresponding peptides. These isobactin analogues exhibit comparable if not slightly improved antibiotic activity compared to their corresponding teixobactin analogues. Leu_{10}-isobactin A, for example, exhibits *in vitro* activity against MRSA at 0.5 μg/mL and *in vivo* activity in a neutropenic mouse thigh infection assay at 3–10 mg/Kg. It is stable as the trifluoroacetate or hydrochloride salt but converts to Leu_{10}-teixobactin at neutral pH (Figure 3.2).

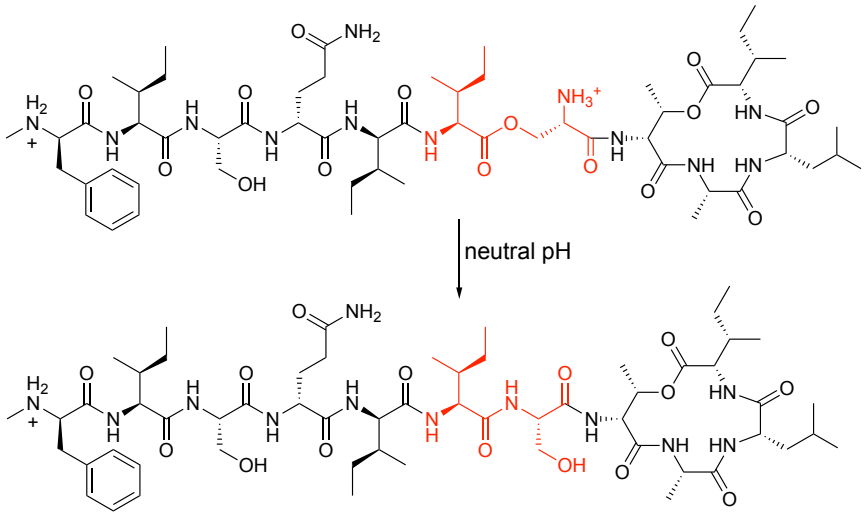

Figure 3.2. Conversion of Leu_{10}-isobactin A to Leu_{10}-teixobactin at neutral pH.

Leu_{10}-teixobactin and the corresponding Leu_{10}-isobactins are not as active as teixobactin itself, because the *allo*-enduracididine (*allo*-End) residue at position 10 makes critical contacts with the MurNAc residue in lipid II and related cell-wall precursors.[7,8] Singh and coworkers have

reported that teixobactin analogues with cyclohexylgylcine (Chg) at position 10 exhibit good antibiotic activity and have suggested that the Chg group can better interact with the MurNAc residue of lipid II.[9–11] The increased hydrophobicity and lack of charge of Chg greatly limits the solubility of Chg_{10}-teixobactin. For this reason, Singh and coworkers have further pursued analogues in which D-Gln_4 is replaced with D-Arg_4 to offset the loss of the charge provided by *allo*-End_{10}. The commercial availability of Chg and D-Arg building blocks render these teixobactin analogues potential alternatives to teixobactin that can easily be prepared by chemical synthesis.

In spite of the charge provided by the D-Arg residue, D-Arg_4,Chg_{10}-teixobactin has only modest solubility and forms gels, both of which may limit its utility as an intravenous antibiotic. In the current paper, we set out to prepare isobactin prodrugs of Chg_{10}-teixobactin, D-Arg_4,Chg_{10}-teixobactin, and D-Arg_4,Leu_{10}-teixobactin and compare their solubility and antibiotic activity to Chg_{10}-teixobactin, D-Arg_4,Chg_{10}-teixobactin, and D-Arg_4,Leu_{10}-teixobactin. Our working hypothesis was that the corresponding isobactin prodrugs would have enhanced solubility and diminished propensity to form gels, while exhibiting comparable or improved antibiotic activity.

RESULTS AND DISCUSSION

We have introduced three different *O*-acyl isopeptide linkages, resulting in isobactins A, B, and C.[6,12–14] These isobactin prodrugs vary in the position at which the *O*-acyl isopeptide linkage is present — between Ile_6 and Ser_7, between Ile_2 and Ser_3, or between both Ile_6 and Ser_7 and Ile_2 and Ser_3. We synthesized the isobactin prodrug analogues as the trifluoroacetate (TFA) salts using our previously reported synthesis that uses Fmoc-based solid-phase peptide synthesis (SPPS) and the commercially available Boc-Ser(Fmoc-Ile)-OH *O*-acyl isodipeptide building block (Figure 3.3). Yields for all the new isobactin analogues prepared in this study are reported in Table S3.2.

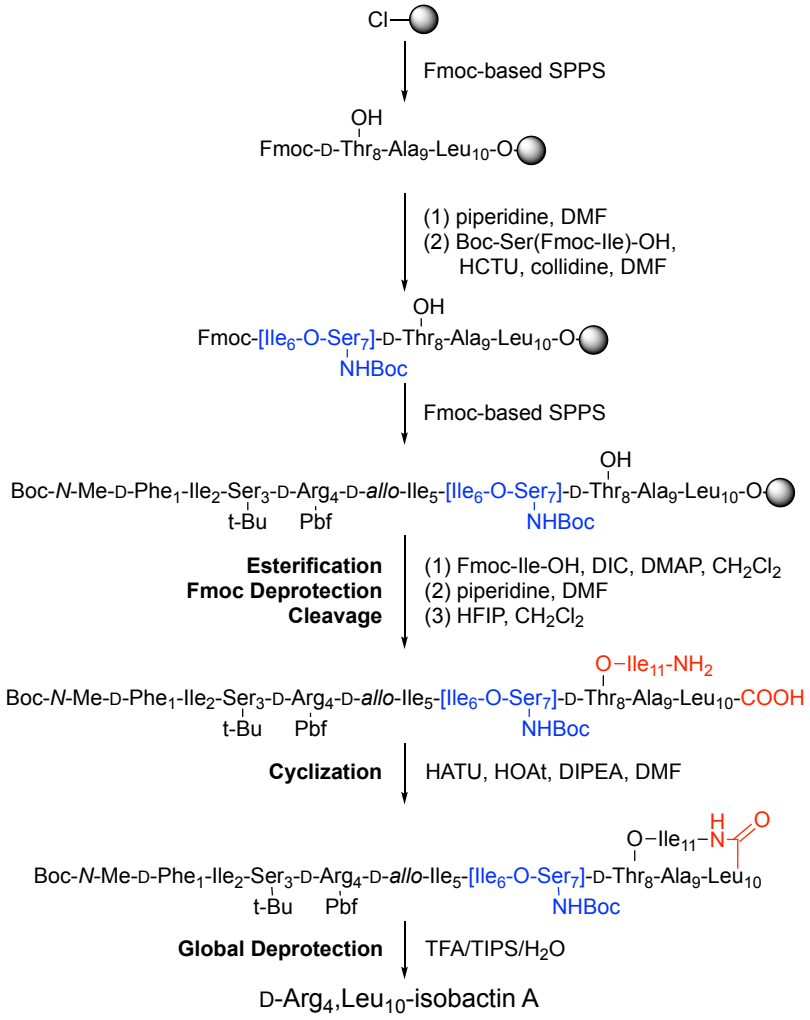

Figure 3.3. Synthesis of D-Arg$_4$,Leu$_{10}$-isobactin A.

Using this approach, we synthesized isobactin prodrugs of Chg$_{10}$-teixobactin, D-Arg$_4$,Chg$_{10}$-teixobactin, and D-Arg$_4$,Leu$_{10}$-teixobactin (Figure 3.4A). The Chg$_{10}$-isobactins replace the native *allo*-End with the commercially available cyclic hydrophobic residue cyclohexylglycine (Figure 3.4B). The D-Arg$_4$,Chg$_{10}$-isobactins again replace the native *allo*-End with cyclohexylglycine and also replace the native D-Gln$_4$ with D-Arg to restore the charge lost by the substitution at position 10 (Figure 3.4B). The D-Arg$_4$,Leu$_{10}$-isobactins replace the native *allo*-End with an uncharged residue and also replace the native D-Gln$_4$ with D-Arg to restore the natural charge of teixobactin (Figure 3.4B).

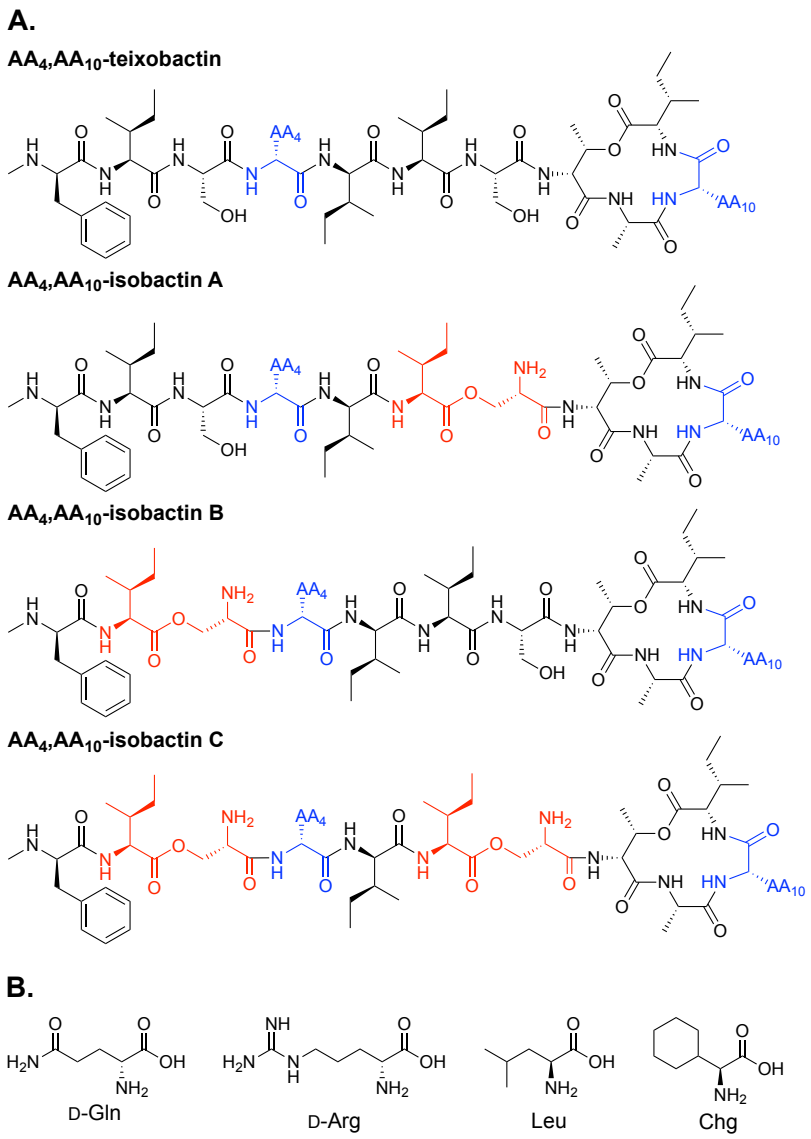

Figure 3.4. (A) Structures of teixobactin analogues and isobactins A, B, and C. AA_4 is D-Gln or D-Arg; AA_{10} is Leu or Chg. (B) Structures of D-Gln, D-Arg, Leu, and Chg.

Antibiotic Activity

We evaluated the antibiotic activity of the isobactin analogues using minimum inhibitory concentration (MIC) assays with five Gram-positive bacteria and compared the MIC values to those of the parent teixobactin analogues. We also used *E.* coli as a Gram-negative control. We compared the activities of the teixobactin analogues and prodrugs to those of teixobactin and

vancomycin. We performed these MIC assays in the presence of 0.002% polysorbate 80, as this additive is thought to prevent teixobactin and its derivatives from being adsorbed by 96-well polystyrene plates and has been shown to significantly affect MIC results.[1,15–17]

Each of the teixobactin analogues proved active against the Gram-positive bacteria, and the corresponding isobactin analogues exhibited comparable or slightly better antibiotic activity than the teixobactin analogues (Table 3.1). The D-Arg$_4$,Leu$_{10}$-isobactins showed equal or slightly improved activity to D-Arg$_4$,Leu$_{10}$-teixobactin. Thus, the D-Arg$_4$,Leu$_{10}$-isobactins exhibited MICs of 0.0078–1 μg/mL, while D-Arg$_4$,Leu$_{10}$-teixobactin exhibited MICs of 0.0078–2 μg/mL. D-Arg$_4$,Leu$_{10}$-teixobactin, for example, exhibited an MIC of 1 μg/mL against MRSA, while the D-Arg$_4$,Leu$_{10}$-isobactins A, B, and C exhibited MICs of 1, 0.5–1, and 1 μg/mL, respectively. The D-Arg$_4$,Leu$_{10}$-isobactins also exhibited similar activities to those that we had previously observed for the Leu$_{10}$-isobactins.[6]

The Chg$_{10}$-isobactins showed equal or slightly improved activity to Chg$_{10}$-teixobactin. Thus, the Chg$_{10}$-isobactins exhibited MICs of 0.0625–1 μg/mL and Chg$_{10}$-teixobactin exhibited MICs of 0.125–1 μg/mL. Chg$_{10}$-teixobactin, for example, exhibited an MIC of 1 μg/mL against MRSA, while the Chg$_{10}$-isobactins A, B, and C exhibited MICs of 0.5, 0.5, and 1 μg/mL, respectively. The D-Arg$_4$,Chg$_{10}$-isobactins exhibited similar activities to D-Arg$_4$,Chg$_{10}$-teixobactin, with MICs of 0.125–2 μg/mL. The D-Arg$_4$,Chg$_{10}$-isobactins were generally slightly less active than the corresponding Chg$_{10}$-isobactins.

Table 3.1. MIC values of isobactin analogues, teixobactin analogues, teixobactin, and vancomycin in μg/mL with 0.002% polysorbate 80.

	Bacillus subtilis ATCC 6051	*Staphylococcus epidermidis* ATCC 14990	*Staphylococcus aureus (MSSA)* ATCC 29213	*Staphylococcus aureus (MRSA)* ATCC 700698	*Enterococcus faecalis (VRE)* ATCC 51299	*Escherichia coli* ATCC 10798
Chg_{10}-teixobactin	0.125	0.5	1	1	1	>8
Chg_{10}-isobactin A	0.0625	0.25	0.5	0.5	0.5	>8
Chg_{10}-isobactin B	0.0625	0.25	0.25	0.5	0.5	>8
Chg_{10}-isobactin C	0.125	0.5	0.5	1	1	>8
D-Arg_4,Chg_{10}-teixobactin	0.125	0.125	2	0.5	1	>8
D-Arg_4,Chg_{10}-isobactin A	0.125	0.25	1	1	1	>8
D-Arg_4,Chg_{10}-isobactin B	0.125	0.25	2	1	1	>8
D-Arg_4,Chg_{10}-isobactin C	0.125	0.125	1	1	1	>8
D-Arg_4,Leu_{10}-teixobactin	≤0.0078	0.0625	0.25–0.5	1	2	>8
D-Arg_4,Leu_{10}-isobactin A	≤0.0078	0.0156–0.03125	0.125–0.25	1	1	>8
D-Arg_4,Leu_{10}-isobactin B	0.0078–0.0156	0.03125–0.0625	0.125	0.5–1	1	>8
D-Arg_4,Leu_{10}-isobactin C	0.0156–0.03125	0.0625	0.25	1	1–2	>8
Teixobactin	0.0078	0.0078	0.5	0.25	0.25	>8
Vancomycin	0.5	2	1	2	>8	>8

Conversion Kinetics of the Isobactin Analogues to Teixobactin Analogues

The isobactin analogues convert cleanly to the corresponding teixobactin analogues under physiological conditions, with pH being the trigger that allows deprotonation of the α-amino group

of serine and rearrangement of the ester linkage to an amide linkage. Thus, D-Arg$_4$,Leu$_{10}$-isobactins A and B convert to D-Arg$_4$,Leu$_{10}$-teixobactin with half-lives of 41 and 27 minutes respectively at pH 7.4 and ambient temperature, and half-lives of 16 and 9 minutes at 37 °C. D-Arg$_4$,Leu$_{10}$-isobactin C converts to D-Arg$_4$,Leu$_{10}$-teixobactin via D-Arg$_4$,Leu$_{10}$-isobactins A and B, and the overall conversion is 93.5% complete at 60 minutes at 37°C. The Chg$_{10}$-isobactins and D-Arg$_4$,Chg$_{10}$-isobactins also undergo clean conversion to the corresponding teixobactin analogues. The rates of conversion are similar to those of the D-Arg$_4$,Leu$_{10}$-isobactins, however precise measurement of the rates of conversion was impeded by precipitation of the Chg$_{10}$-teixobactin and D-Arg$_4$,Chg$_{10}$-teixobactin products, which are poorly soluble at 0.5 mg/mL in the phosphate buffer used for the conversion assay.

Gel Formation and Solubility

The isobactin analogues are more soluble and have a diminished propensity to form gels, making them attractive alternatives to the corresponding teixobactin analogues. We evaluated gel formation of isobactin analogues and the corresponding teixobactin analogues by adding DMSO solutions of the peptide TFA salts to phosphate buffered saline (PBS) at pH 7.4 and observing gel formation over time.[6] When D-Arg$_4$,Leu$_{10}$-teixobactin is added to PBS, moderate sized gelatinous aggregates form immediately (Figure 3.5). In contrast, when the D-Arg$_4$,Leu$_{10}$-isobactins are added, no immediate gel formation occurs. After 5 minutes, almost no gelatinous aggregates are observed. After 15 minutes, the number of aggregates increases but the size of the aggregates does not. By 60 minutes, gel formation increases but only small gelatinous aggregates are observed. Although we had previously observed delayed gel formation in the Leu$_{10}$-isobactins, the reduction in gel formation is even more pronounced in the D-Arg$_4$,Leu$_{10}$-isobactins. Thus, it appears that the

additional positive charge associated with the replacement of D-Gln$_4$ with D-Arg is responsible for further diminishing gel formation.

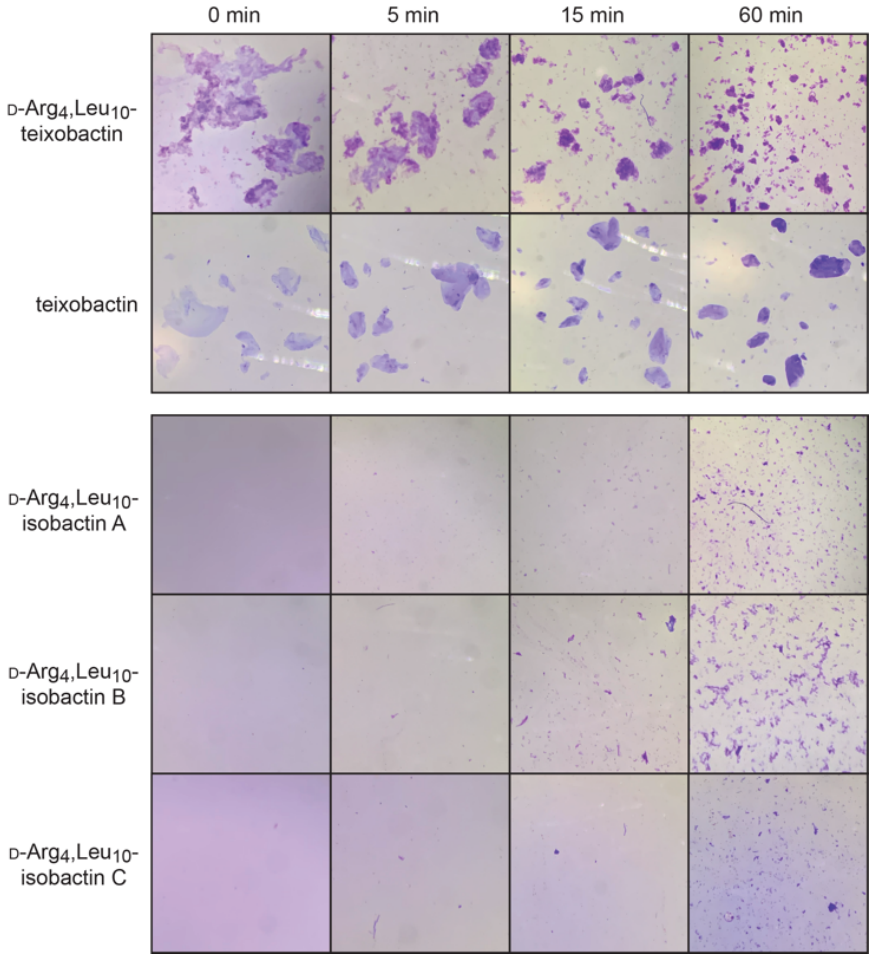

Figure 3.5. Gel formation of D-Arg$_4$,Leu$_{10}$-teixobactin and teixobactin and delayed gel formation of D-Arg$_4$,Leu$_{10}$-isobactin A, B, and C.

The Chg$_{10}$-isobactins exhibit greater gel formation than the Leu$_{10}$-isobactins but still exhibit substantially less gel formation than Chg$_{10}$-teixobactin, Leu$_{10}$-teixobactin, or teixobactin itself. Chg$_{10}$-teixobactin forms large gelatinous aggregates immediately upon addition to PBS. When the Chg$_{10}$-isobactins are added to PBS, a few small aggregates form immediately, and the quantity of gelatinous aggregates increases over time, with moderate levels of aggregates being visible at 60 minutes (Figure S3.2). Fewer aggregates are observed for Chg$_{10}$-isobactin C than for

Chg_{10}-isobactins A and B at each time point of comparison (0, 5, 15, and 60 minutes). D-Arg_4,Chg_{10}-teixobactin also forms large gelatinous aggregates immediately upon addition to PBS. The D-Arg_4,Chg_{10}-isobactins exhibit delayed gel formation and less gel formation over 60 minutes than the corresponding Chg_{10}-isobactins (Figure S3.3).

Collectively, these observations indicate that the isobactin analogues exhibit substantially less gel formation than teixobactin or the corresponding teixobactin analogues. Furthermore, the observations suggest that isobactin and teixobactin analogues with greater hydrophobicity or less net positive charge exhibit more gel formation than those with less hydrophobicity or greater net positive charge. The D-Arg_4,Leu_{10}-isobactins emerge from these comparisons as having the best balance of activity and delayed gel formation. Although the Chg_{10}-isobactins exhibit somewhat greater activity against MRSA and VRE, we believe the greater gel formation of these compounds make them less attractive to pursue for drug development than the D-Arg_4,Leu_{10}-isobactins.

In synthesizing and purifying these isobactin and teixobactin analogues, we have observed similar differences in solubility. We prepare all of these peptides as the TFA salts and purify them by reverse-phase HPLC in acetonitrile-water mixtures. The D-Arg_4,Leu_{10}-isobactins exhibit good solubilities in 20% acetonitrile in water, which is the solvent we typically use for injecting samples onto the preparative HPLC column. For D-Arg_4,Leu_{10}-teixobactin, a higher concentration of acetonitrile is required, typically 35%. The D-Arg_4,Chg_{10}-isobactins and Chg_{10}-isobactins typically require 30% acetonitrile. Even higher concentrations of acetonitrile are required to dissolve D-Arg_4,Chg_{10}-teixobactin and Chg_{10}-teixobactin for HPLC injection, typically 40%.

Cytotoxicity and Hemolytic Assays

We evaluated the cytotoxicity of the isobactin analogues and their corresponding teixobactin analogues in HeLa cells using a Promega Cytotox-Glo assay (Figures S3.4–S3.9). In

these experiments, all the isobactin analogues tested exhibited no cytotoxicity at concentrations up to 25 μM (36–43 μg/mL) and slight cytotoxicity at 50 μM (73–86 μg/mL), with the D-Arg_4,Chg_{10}-isobactins exhibiting the most cytotoxicity at 50 μM. The parent teixobactin analogues generally exhibited no significant cytotoxicity at concentrations as high as 50 μM. Thus, it appears that the extra ammonium group associated with the isobactins imparts slightly enhanced cytotoxicity to the isobactins, perhaps by promoting interaction with cell membranes.

We further evaluated the isobactin analogues and the corresponding teixobactin analogues in hemolytic assays with human red blood cells in the absence and presence of 0.002% polysorbate 80 (Figures S3.10–S3.15). We used Triton X-100 and water (vehicle) as positive (100% lysis) and negative (0% lysis) controls in the hemolysis assays.[3,6,18,19] We used 1.25 μM (3.6 μg/mL) melittin as an additional positive control. In the absence of polysorbate 80, all the isobactin analogues exhibited no hemolytic activity at concentrations as high as 25 μg/mL and mild hemolytic activity at higher concentrations, with values between 2–5% at 100 μg/mL. In the presence of polysorbate 80, all the isobactin analogues exhibited even lower hemolytic activity with hemolysis between 0–2% at 100 μg/mL. We observed 20–50% hemolysis with 1.25 μM melittin in the absence and presence of polysorbate 80. These studies suggest that the isobactin analogues are suitable for intravenous administration at concentrations well above the MIC values.

CONCLUSIONS

In conclusion, the isobactin prodrug analogues have good antibiotic activity against Gram-positive pathogens while overcoming the problems of poor solubility and gel formation of teixobactin and teixobactin analogues that are likely to limit their preclinical development. The isoacyl peptide linkage of these prodrugs enhances solubility and delays gel formation, allowing the prodrugs to disperse before undergoing rearrangement to the active peptide drugs. Although

the isobactin prodrugs described herein do not contain the natural *allo*-End residue at position 10, they still exhibit excellent antibiotic activity against the pathogens MSSA, MRSA, and VRE and are generally more active than vancomycin. Incorporation of the hydrophobic residues Leu or Chg at position 10 in place of the synthetically challenging *allo*-End allows for potent analogues for preclinical development that are readily accessible through chemical synthesis. Replacement of D-Gln with D-Arg at position 4 further enhances solubility and compensates for the increased hydrophobicity associated with the loss of the charged residue *allo*-End at position 10.

The isobactin prodrugs are stable at acidic pH but undergo clean conversion to the active drugs at physiological pH. They exhibit little to no hemolysis or cytotoxicity. The D-Arg_4,Leu_{10}-isobactins exhibit the best balance of delayed gel formation and antibiotic activity, making them superior candidates for intravenous administration. The Chg_{10}-isobactins and D-Arg_4,Chg_{10}-isobactins also exhibit good antibiotic activity, but have limited solubility when compared to the D-Arg_4,Leu_{10}-isobactins. The D-Arg_4,Leu_{10}-isobactins are more soluble and less prone to gel formation than the Leu_{10}-isobactins and may thus be superior candidates for preclinical development.

REFERENCES AND NOTES

1. Ling, L. L.; Schneider, T.; Peoples, A. J.; Spoering, A. L.; Engels, I.; Conlon, B. P.; Mueller, A.; Schäberle, T. F.; Hughes, D. E.; Epstein, S.; Jones, M.; Lazarides, L.; Steadman, V. A.; Cohen, D. R.; Felix, C. R.; Fetterman, K. A.; Millett, W. P.; Nitti, A. G.; Zullo, A. M.; Chen, C.; Lewis, K. A New Antibiotic Kills Pathogens without Detectable Resistance. *Nature* **2015**, *517*, 455–459.

2. Yang, H.; Wierzbicki, M.; Du Bois, D. R.; Nowick, J. S. X-Ray Crystallographic Structure of a Teixobactin Derivative Reveals Amyloid-like Assembly. *J. Am. Chem. Soc.* **2018**, *140*, 14028–14032.

3. Chen, K. H.; Le, S. P.; Han, X.; Frias, J. M.; Nowick, J. S. Alanine Scan Reveals Modifiable Residues in Teixobactin. *Chem. Commun.* **2017**, *53*, 11357–11359.

4. Yang, H.; Pishenko, A. V.; Li, X.; Nowick, J. S. Design, Synthesis, and Study of Lactam and Ring-Expanded Analogues of Teixobactin. *J. Org. Chem.* **2020**, *85*, 1331–1339.

5. Öster, C.; Walkowiak, G. P.; Hughes, D. E.; Spoering, A. L.; Peoples, A. J.; Catherwood, A. C.; Tod, J. A.; Lloyd, A. J.; Herrmann, T.; Lewis, K.; Dowson, C. G.; Lewandowski, J. R. Structural Studies Suggest Aggregation as One of the Modes of Action for Teixobactin. *Chem. Sci.* **2018**, *9*, 8850–8859.

6. Jones, C. R.; Guaglianone, G.; Lai, G. H.; Nowick, J. S. Isobactins: O-Acyl Isopeptide Prodrugs of Teixobactin and Teixobactin Derivatives. *Chem. Sci.* **2022**, *13*, 13110–13116.

7. Shukla, R.; Lavore, F.; Maity, S.; Derks, M. G. N.; Jones, C. R.; Vermeulen, B. J. A.; Melcrová, A.; Morris, M. A.; Becker, L. M.; Wang, X.; Kumar, R.; Medeiros-Silva, J.; van Beekveld, R. A. M.; Bonvin, A. M. J. J.; Lorent, J. H.; Lelli, M.; Nowick, J. S.; MacGillavry, H. D.; Peoples, A. J.; Spoering, A. L.; Ling, L. L.; Hughes, D. E.; Roos, W. H.; Breukink, E.; Lewis, K.; Weingarth, M. Teixobactin Kills Bacteria by a Two-Pronged Attack on the Cell Envelope. *Nature* **2022**, *608*, 390–396.

8. Shukla, R.; Medeiros-Silva, J.; Parmar, A.; Vermeulen, B. J. A.; Das, S.; Paioni, A. L.; Jekhmane, S.; Lorent, J.; Bonvin, A. M. J. J.; Baldus, M.; Lelli, M.; Veldhuizen, E. J. A.; Breukink, E.; Singh, I.; Weingarth, M. Mode of Action of Teixobactins in Cellular Membranes. *Nat Commun* **2020**, *11*, 2848.

9. Parmar, A.; Lakshminarayanan, R.; Iyer, A.; Goh, E. T. L.; To, T. Y.; Yam, J. K. H.; Yang, L.; Newire, E.; Robertson, M. C.; Prior, S. H.; Breukink, E.; Madder, A.; Singh, I. Development of Teixobactin Analogues Containing Hydrophobic, Non-Proteogenic Amino Acids That Are Highly Potent against Multidrug-Resistant Bacteria and Biofilms. *European Journal of Medicinal Chemistry* **2023**, *261*, 115853.

10. Parmar, A.; Lakshminarayanan, R.; Iyer, A.; Mayandi, V.; Leng Goh, E. T.; Lloyd, D. G.; Chalasani, M. L. S.; Verma, N. K.; Prior, S. H.; Beuerman, R. W.; Madder, A.; Taylor, E. J.; Singh, I. Design and Syntheses of Highly Potent Teixobactin Analogues against

Staphylococcus Aureus, Methicillin-Resistant Staphylococcus Aureus (MRSA), and Vancomycin-Resistant Enterococci (VRE) in Vitro and in Vivo. *J. Med. Chem.* **2018**, *61*, 2009–2017.

11. Jin, K.; Po, K. H. L.; Kong, W. Y.; Lo, C. H.; Lo, C. W.; Lam, H. Y.; Sirinimal, A.; Reuven, J. A.; Chen, S.; Li, X. Synthesis and Antibacterial Studies of Teixobactin Analogues with Non-Isostere Substitution of Enduracididine. *Bioorganic & Medicinal Chemistry* **2018**, *26*, 1062–1068.

12. Mailig, M.; Liu, F. The Application of Isoacyl Structural Motifs in Prodrug Design and Peptide Chemistry. *ChemBioChem* **2019**, *20*, 2017–2031.

13. Yoshiya, T.; Taniguchi, A.; Sohma, Y.; Fukao, F.; Nakamura, S.; Abe, N.; Ito, N.; Skwarczynski, M.; Kimura, T.; Hayashi, Y.; Kiso, Y. "O-Acyl Isopeptide Method" for Peptide Synthesis: Synthesis of Forty Kinds of "O-Acyl Isodipeptide Unit" Boc-Ser/Thr(Fmoc-Xaa)-OH. *Org. Biomol. Chem.* **2007**, *5*, 1720–1730.

14. Mroz, P. A.; Perez-Tilve, D.; Liu, F.; Mayer, J. P.; DiMarchi, R. D. Native Design of Soluble, Aggregation-Resistant Bioactive Peptides: Chemical Evolution of Human Glucagon. *ACS Chem. Biol.* **2016**, *11*, 3412–3420.

15. Yang, H.; Chen, K. H.; Nowick, J. S. Elucidation of the Teixobactin Pharmacophore. *ACS Chem. Biol.* **2016**, *11*, 1823–1826.

16. Arhin, F. F.; Sarmiento, I.; Belley, A.; McKay, G. A.; Draghi, D. C.; Grover, P.; Sahm, D. F.; Parr, T. R.; Moeck, G. Effect of Polysorbate 80 on Oritavancin Binding to Plastic Surfaces: Implications for Susceptibility Testing. *Antimicrob Agents Chemother* **2008**, *52*, 1597–1603.

17. Kavanagh, A.; Ramu, S.; Gong, Y.; Cooper, M. A.; Blaskovich, M. A. T. Effects of Microplate Type and Broth Additives on Microdilution MIC Susceptibility Assays. *Antimicrobial Agents and Chemotherapy* **2018**, *63*, e01760-18.

18. Evans, B. C.; Nelson, C. E.; Yu, S. S.; Beavers, K. R.; Kim, A. J.; Li, H.; Nelson, H. M.; Giorgio, T. D.; Duvall, C. L. Ex Vivo Red Blood Cell Hemolysis Assay for the Evaluation of pH-Responsive Endosomolytic Agents for Cytosolic Delivery of Biomacromolecular Drugs. *JoVE* **2013**, No. 73, 50166.

19. Oddo, A.; Hansen, P. R. Hemolytic Activity of Antimicrobial Peptides. In *Antimicrobial Peptides: Methods and Protocols*; Hansen, P. R., Ed.; Methods in Molecular Biology; Springer: New York, NY, 2017; pp 427–435.

Supporting Information for Chapter 3:

Investigation of Additional Isobactin Analogues of Teixobactin

Table of Contents

Supplementary figures

Supplementary figures.

Table S3.1. Half-lives of the isobactin analogues at room temperature

	Half-life (min)
Chg_{10}-isobactin A	ND[a]
Chg_{10}-isobactin B	30
Chg_{10}-isobactin C	10
D-Arg_4,Chg_{10}-isobactin A	44
D-Arg_4,Chg_{10}-isobactin B	ND[a]
D-Arg_4,Chg_{10}-isobactin C	ND[b]
D-Arg_4,Leu_{10}-isobactin A	41
D-Arg_4,Leu_{10}-isobactin B	27
D-Arg_4,Leu_{10}-isobactin C	ND[b]

[a]Unable to determine half-life due to insolubility. [b]Unable to determine half-life as the isobactin B and isobactin C of the same series has the same retention time.

Table S3.1. Half-lives of the isobactin analogues at room temperature.

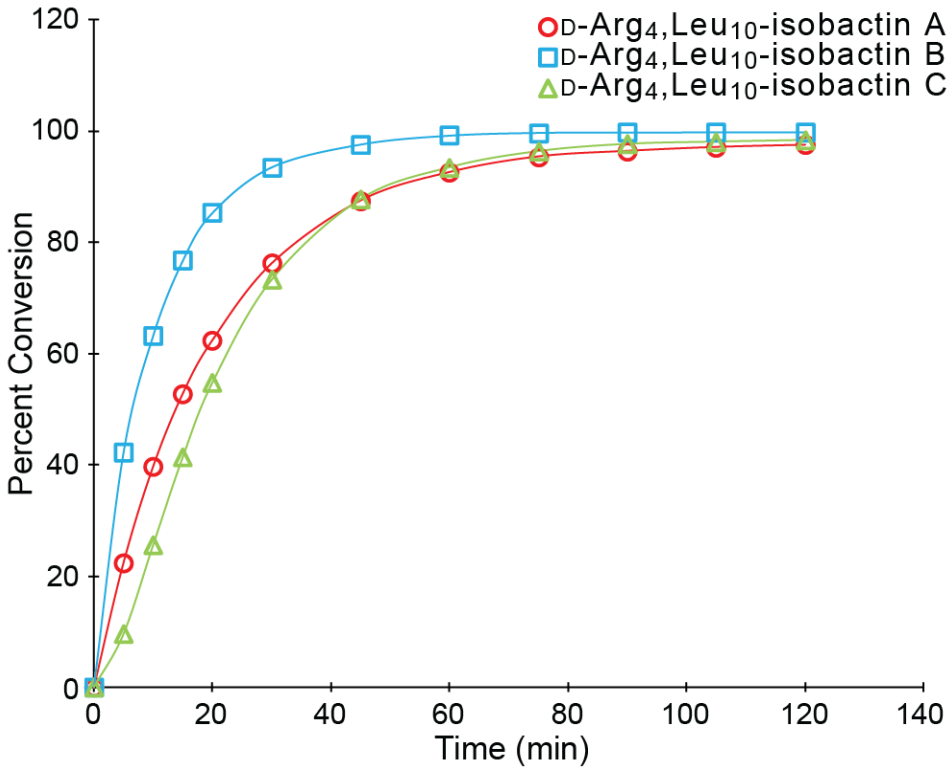

Figure S3.1. Percent conversion of the D-Arg_4,Leu_{10}-isobactins at 37 °C.

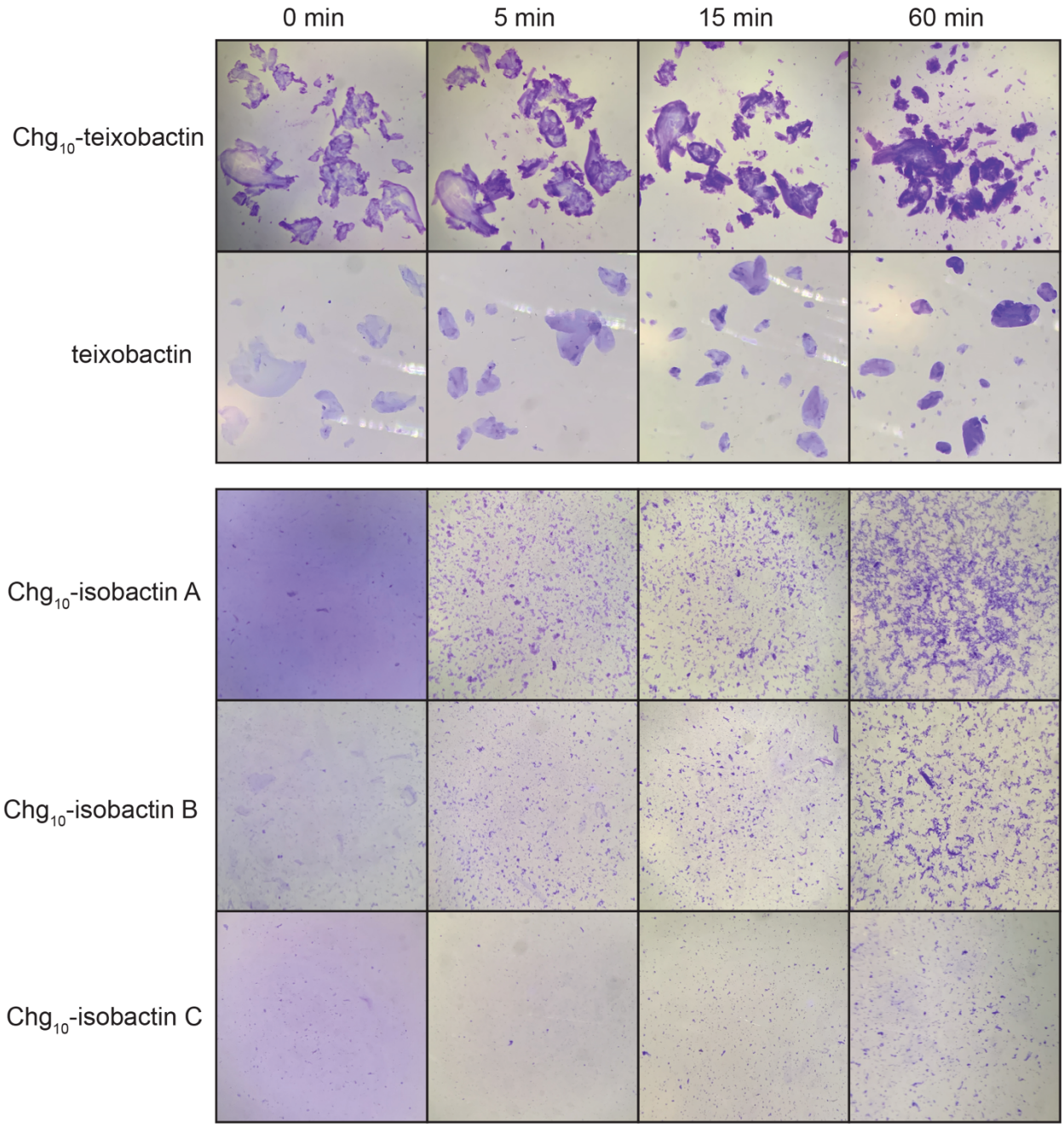

Figure S3.2. Gel formation of Chg_{10}-teixobactin and teixobactin and delayed gel formation of Chg_{10}-isobactins A, B, and C.

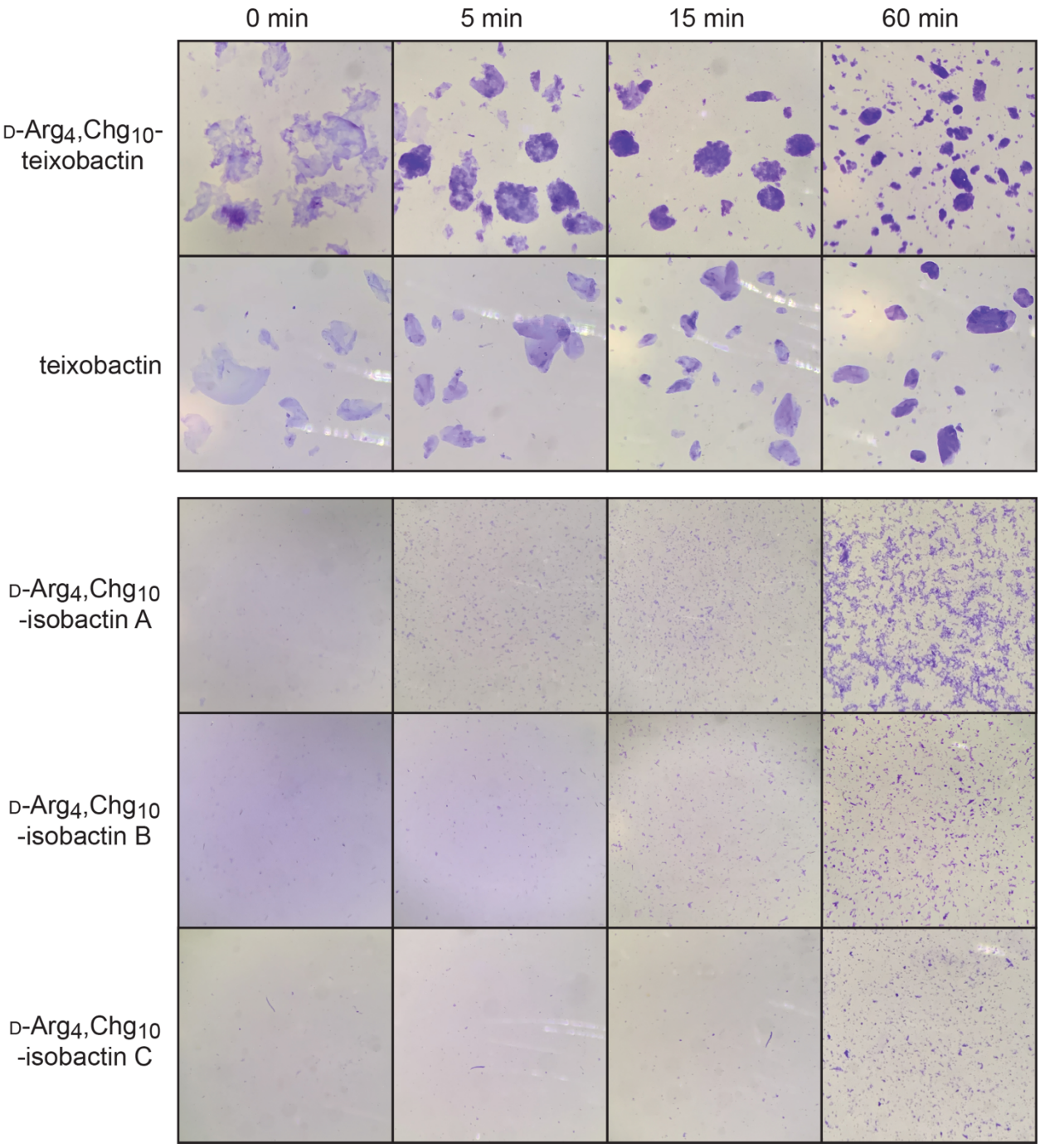

Figure S3.3. Gel formation of D-Arg_4,Chg_{10}-teixobactin and teixobactin and delayed gel formation of D-Arg_4,Chg_{10}-isobactins A, B, and C.

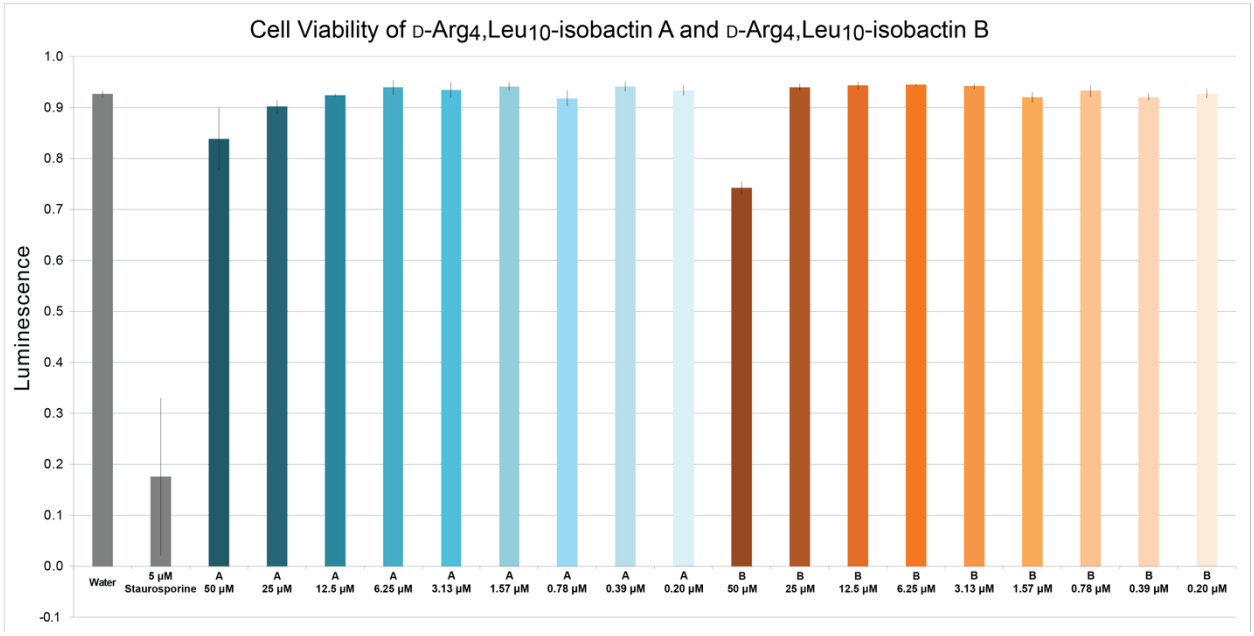

Figure S3.4. Cytotoxicity assay of D-Arg$_4$,Leu$_{10}$-isobactin A and B with HeLa cells.

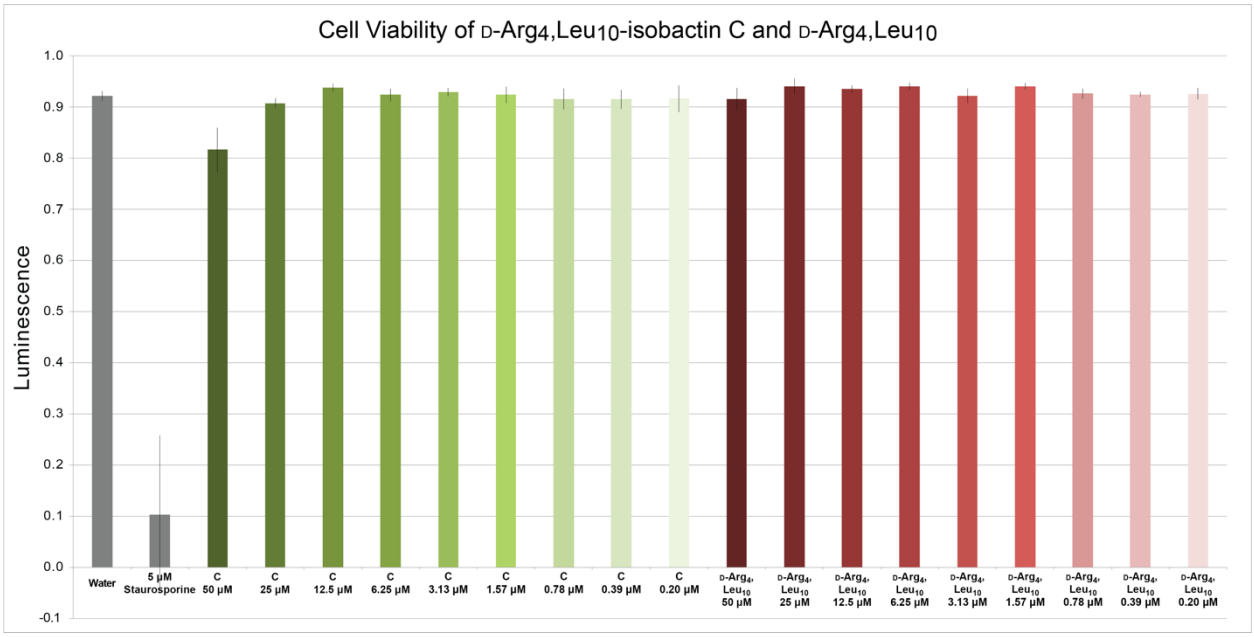

Figure S3.5. Cytotoxicity assay of D-Arg$_4$,Leu$_{10}$-isobactin C and D-Arg$_4$,Leu$_{10}$-teixobactin with HeLa cells.

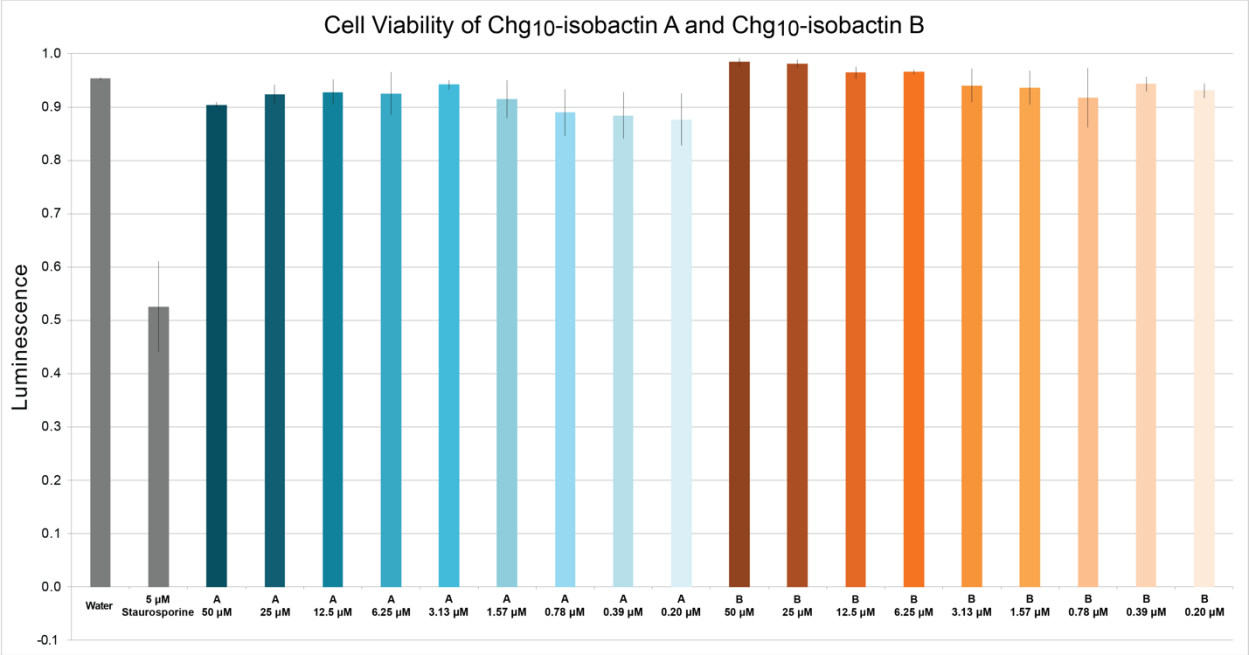

Figure S3.6. Cytotoxicity assay of Chg$_{10}$-isobactin A and B with HeLa cells.

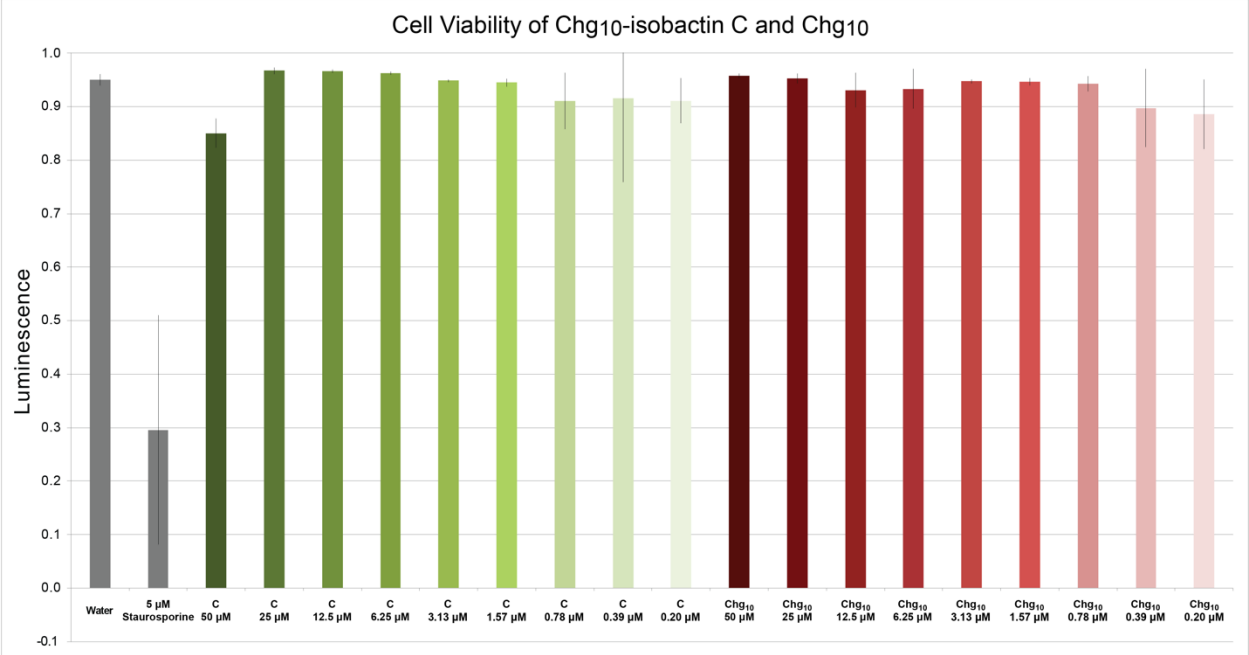

Figure S3.7. Cytotoxicity assay of Chg$_{10}$-isobactin C and Chg$_{10}$-teixobactin with HeLa cells.

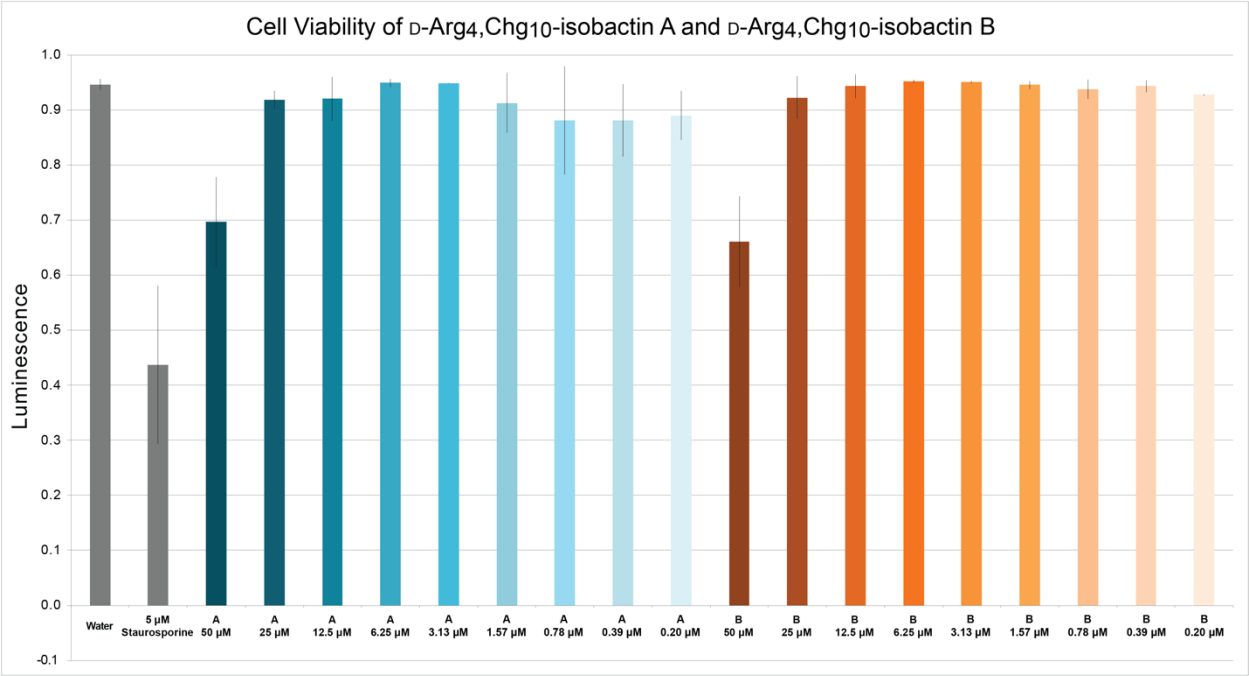

Figure S3.8. Cytotoxicity assay of D-Arg$_4$,Chg$_{10}$-isobactin A and B with HeLa cells.

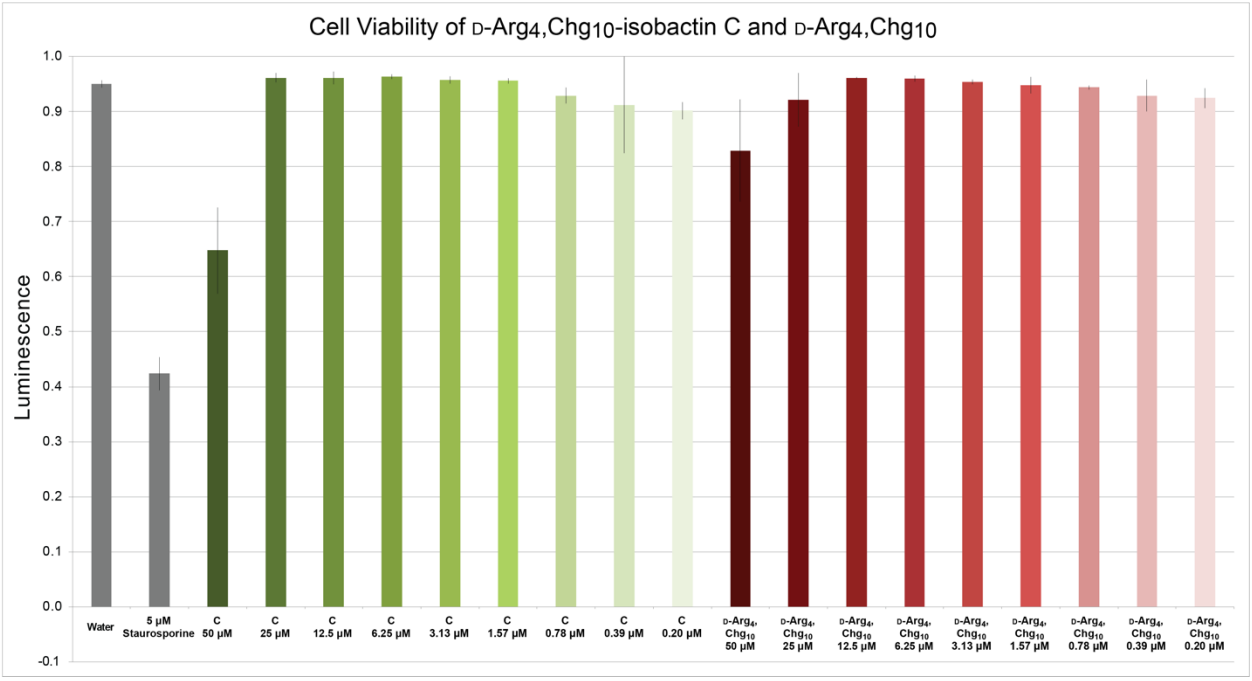

Figure S3.9. Cytotoxicity assay of D-Arg$_4$,Chg$_{10}$-isobactin C and D-Arg$_4$,Chg$_{10}$-teixobactin with HeLa cells.

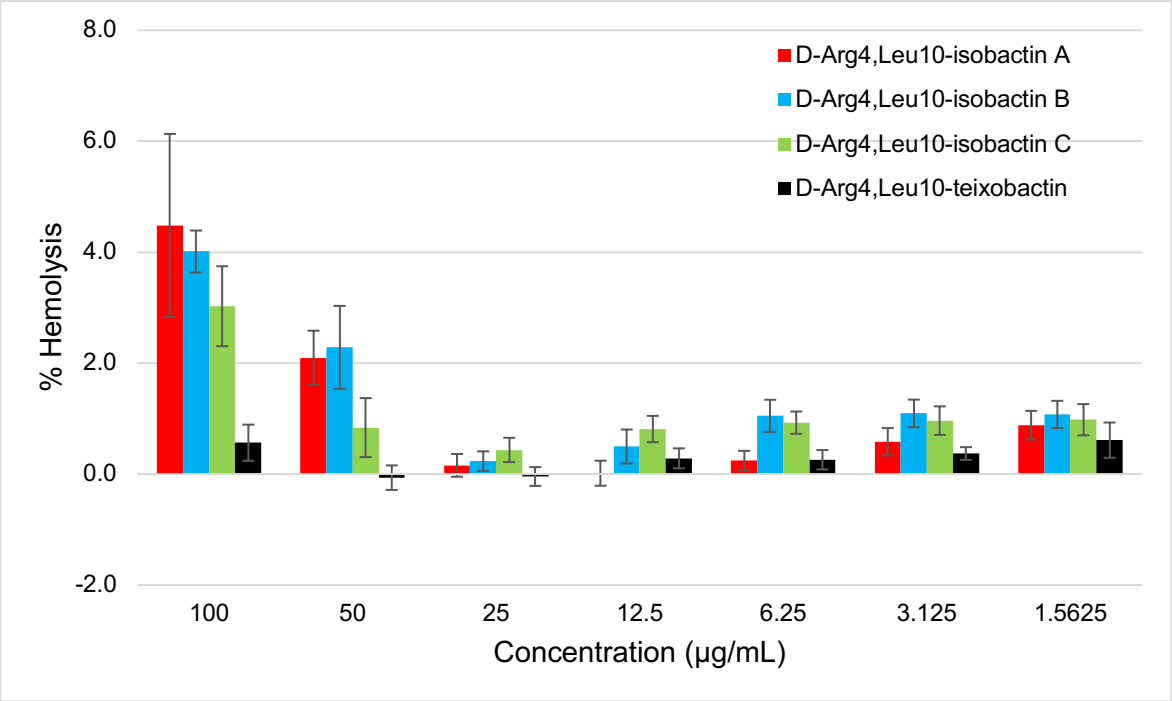

Figure S3.10. Hemolytic assay of D-Arg$_4$,Leu$_{10}$-teixobactin and the D-Arg$_4$,Leu$_{10}$-isobactins without polysorbate 80.

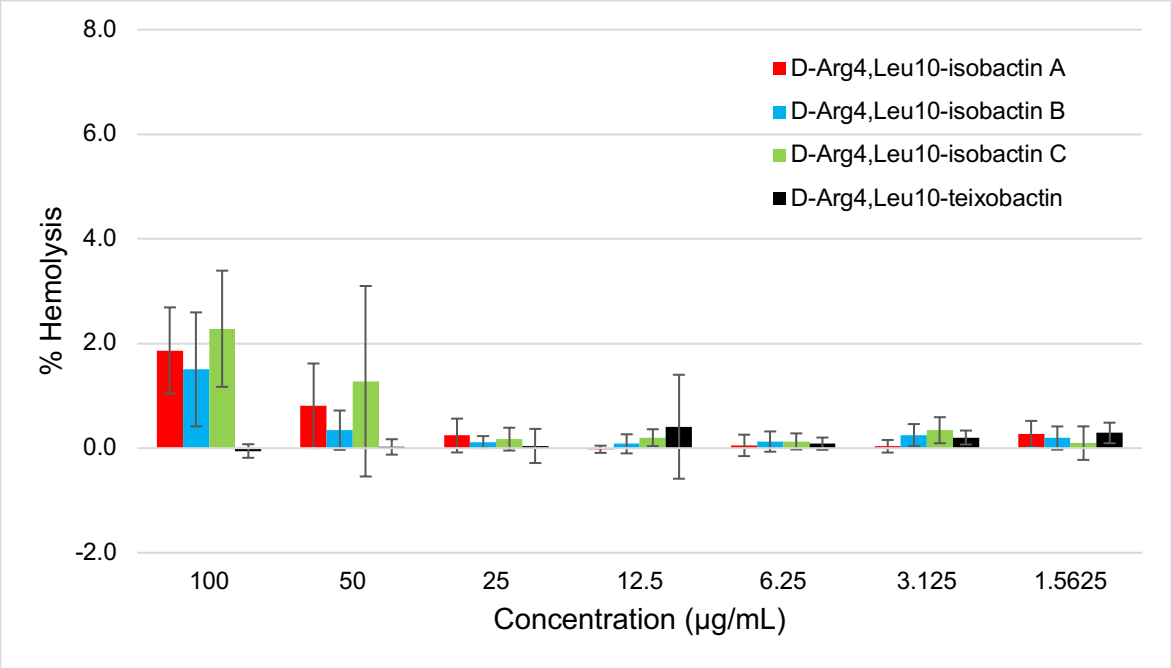

Figure S3.11. Hemolytic assay of D-Arg$_4$,Leu$_{10}$-teixobactin and the D-Arg$_4$,Leu$_{10}$-isobactins with 0.002% polysorbate 80.

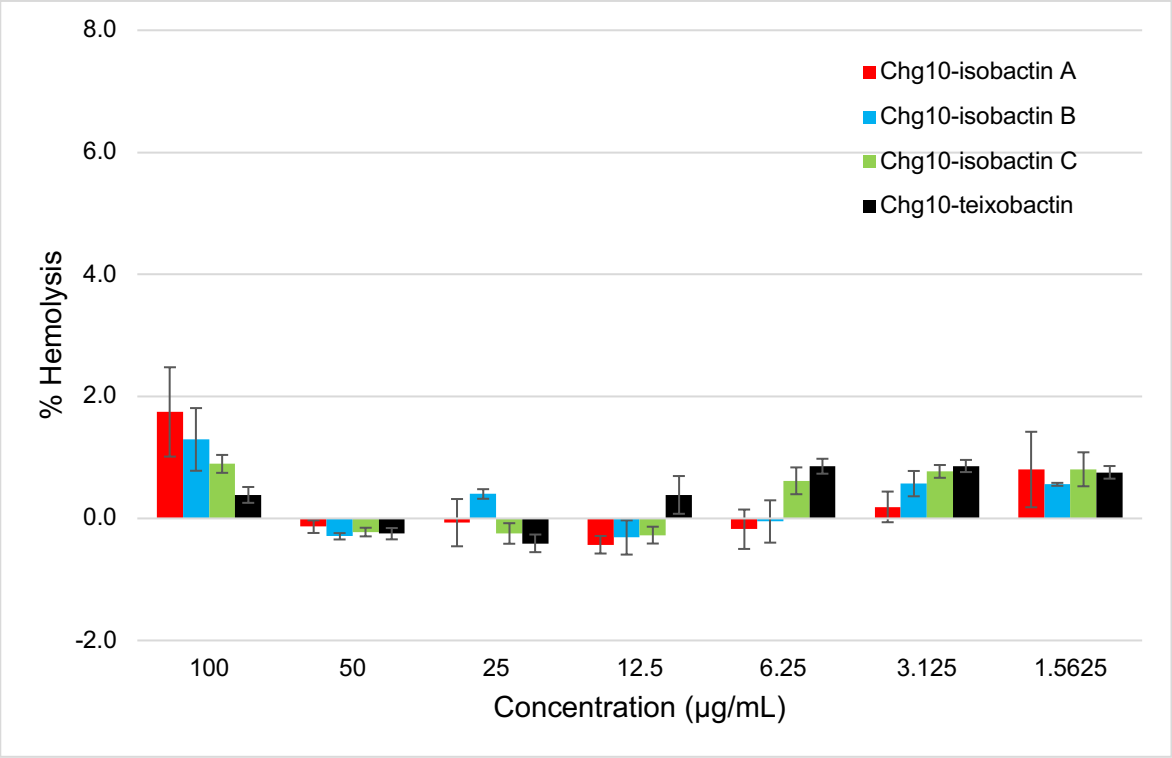

Figure S3.12. Hemolytic assay of Chg_{10}-teixobactin and the Chg_{10}-isobactins without polysorbate 80.

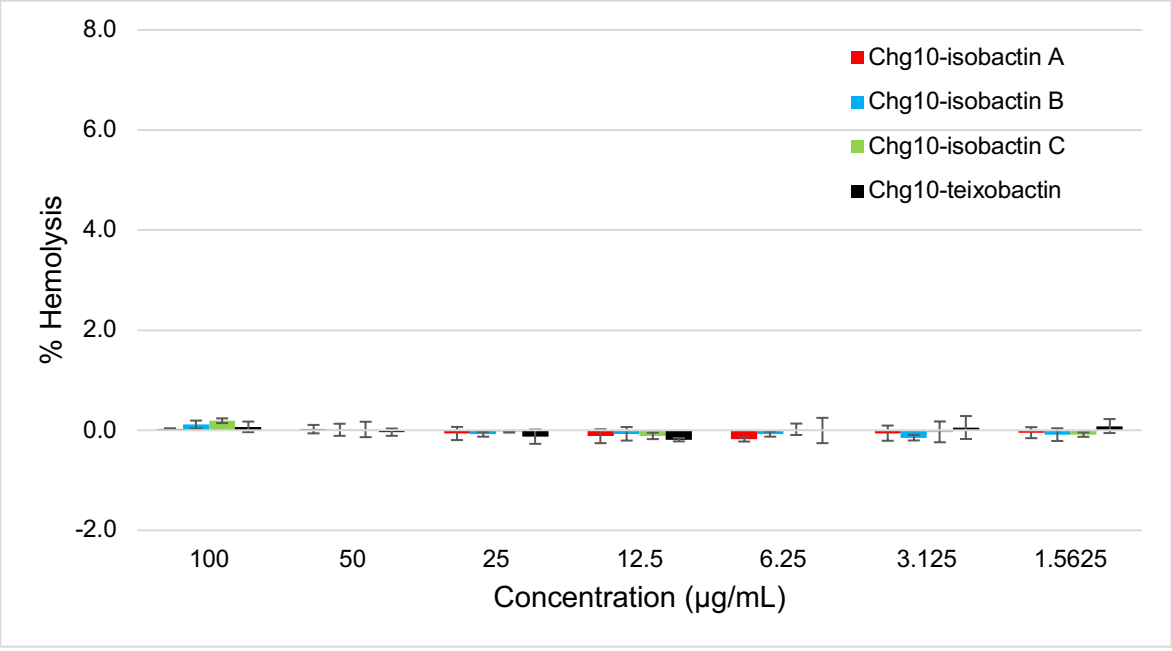

Figure S3.13. Hemolytic assay of Chg_{10}-teixobactin and the Chg_{10}-isobactins with 0.002% polysorbate 80.

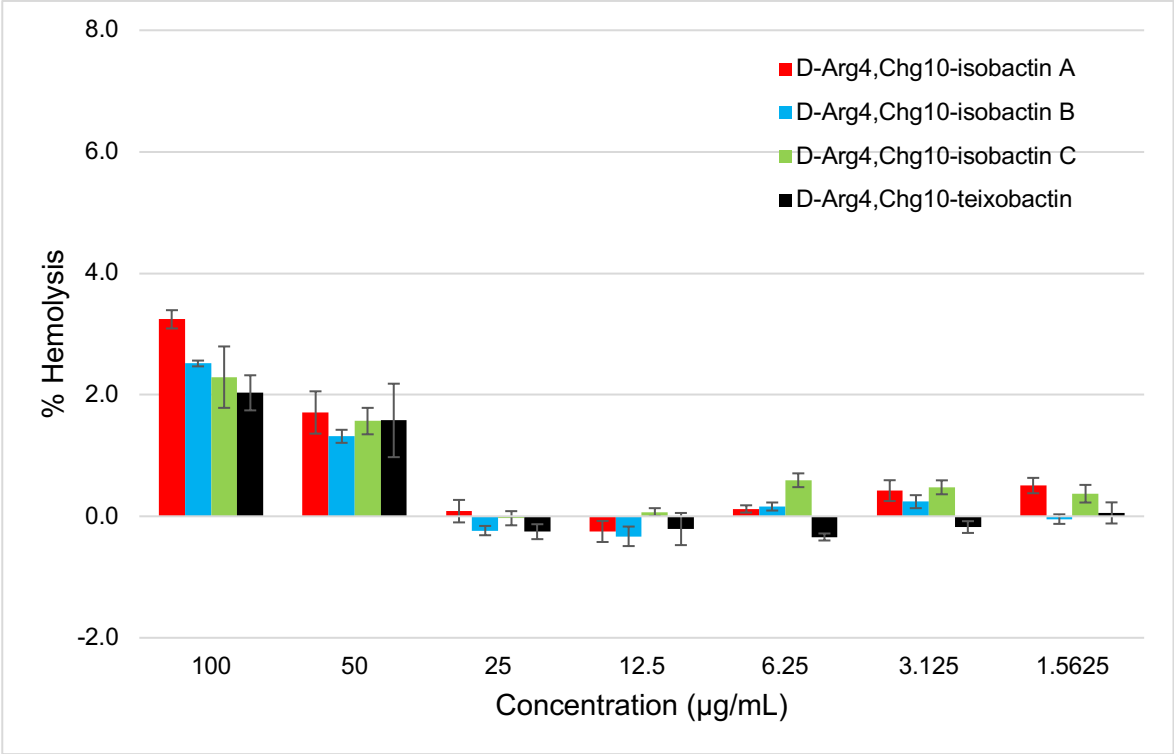

Figure S3.14. Hemolytic assay of D-Arg$_4$,Chg$_{10}$-teixobactin and the D-Arg$_4$,Chg$_{10}$-isobactins without polysorbate 80.

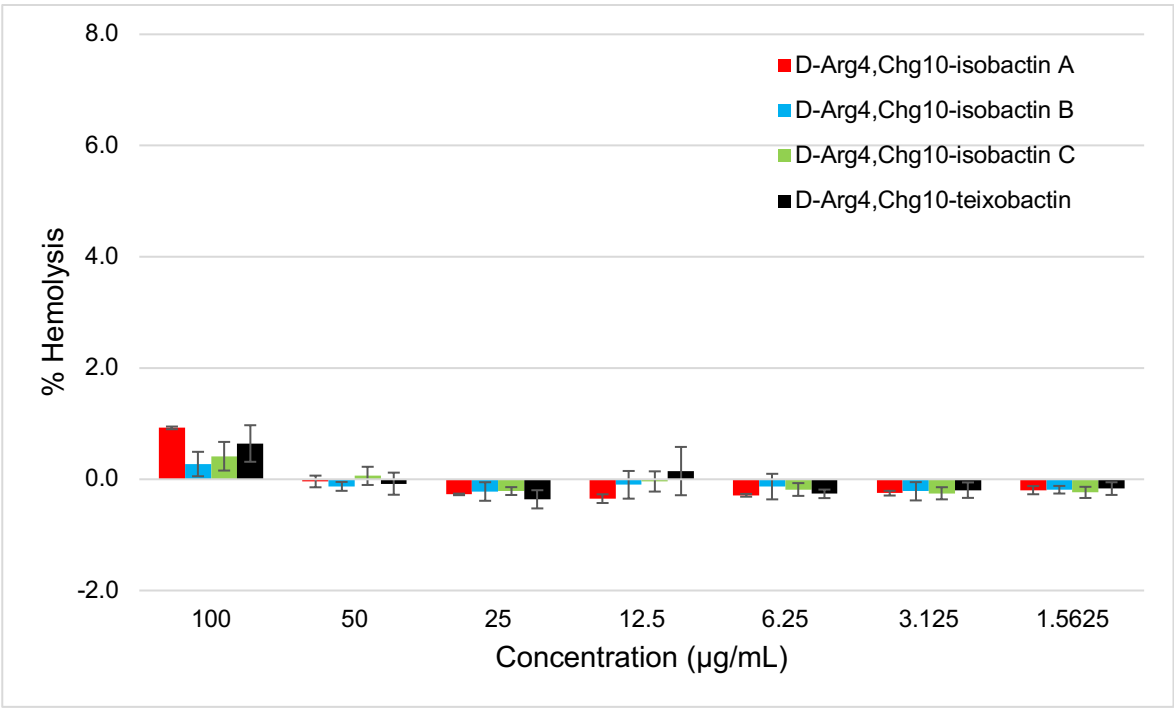

Figure S3.15. Hemolytic assay of D-Arg$_4$,Chg$_{10}$-teixobactin and the D-Arg$_4$,Chg$_{10}$-isobactins with 0.002% polysorbate 80.

Table S2. Yields, molecular formulas, calculated MW as TFA salt, expected mass, and mass found of purified isobactin analogues and their corresponding teixobactin analogues.

Teixobactin Analogue	Molecular formula	Yield (mg)	Yield (%)	Calculated MW as TFA salt	Expected mass	Mass found $[M+H]^+$
D-Arg_4,Leu_{10}-teixobactin	$C_{59}H_{100}N_{14}O_{14}$	28	13%	1457.6 (•2 TFA)	1229.76	1229.59
D-Arg_4,Leu_{10}-isobactin A	$C_{59}H_{100}N_{14}O_{14}$	64	33%	1571.6 (•3 TFA)	1229.76	1229.54
D-Arg_4,Leu_{10}-isobactin B	$C_{59}H_{100}N_{14}O_{14}$	19	9%	1571.6 (•3 TFA)	1229.76	1229.50
D-Arg_4,Leu_{10}-isobactin C	$C_{59}H_{100}N_{14}O_{14}$	74	45%	1685.6 (•4 TFA)	1229.76	1229.48
Chg_{10}-teixobactin	$C_{60}H_{98}N_{12}O_{15}$	22	8%	1341.5 (•1 TFA)	1227.74	1227.49
Chg_{10}-isobactin A	$C_{60}H_{98}N_{12}O_{15}$	95	34%	1455.6 (•2 TFA)	1227.74	1227.47
Chg_{10}-isobactin B	$C_{60}H_{98}N_{12}O_{15}$	17	12%	1455.6 (•2 TFA)	1227.74	1227.51
Chg_{10}-isobactin C	$C_{60}H_{98}N_{12}O_{15}$	37	24%	1569.6 (•3 TFA)	1227.74	1227.51
D-Arg_4,Chg_{10}-teixobactin	$C_{61}H_{102}N_{14}O_{14}$	17	9%	1483.6 (•2 TFA)	1255.78	1255.60
D-Arg_4,Chg_{10}-isobactin A	$C_{61}H_{102}N_{14}O_{14}$	101	52%	1597.6 (•3 TFA)	1255.78	1255.56
D-Arg_4,Chg_{10}-isobactin B	$C_{61}H_{102}N_{14}O_{14}$	8	6%	1597.6 (•3 TFA)	1255.78	1255.55
D-Arg_4,Chg_{10}-isobactin C	$C_{61}H_{102}N_{14}O_{14}$	22	13%	1711.7 (•4 TFA)	1255.78	1255.54

Experimental Section[c]

Materials and Methods. Materials and methods for the synthesis, purification, and analysis of the isobactin analogues and teixobactin analogues are the same as previously described.

Synthesis of the isobactin analogues and their corresponding teixobactin analogues. All isobactin analogues and teixobactin analogues were prepared as the trifluoroacetate salts by solid-phase peptide synthesis followed by solution phase cyclization, as previously described. For all isobactin prodrug analogues, Boc-Ser(Fmoc-Ile)-OH was coupled in place of the desired Ile and Ser residues. Syntheses on a 0.1–0.2 mmol scale afforded 8–101 mg (6–52%) of the isobactins and corresponding teixobactin analogues. The A-series prodrugs typically afforded the highest yields (33–52%). All isobactins and teixobactin analogues prepared were >95% pure by HPLC.

Conversion kinetics studies of the isobactin analogues at room temperature and 37 °C. Conversion kinetics studies at room temperature and 37 °C were performed as previously described.

MIC assays of the isobactin analogues and their corresponding teixobactin analogues. All bacterial cultures and MIC assays were performed in media containing 0.002% polysorbate 80. *Bacillus subtilis* (ATCC 6051), *Staphylococcus epidermidis* (ATCC 14990), *Staphylococcus aureus* (ATCC 29213), and *Escherichia coli* (ATCC 10798) were cultured from glycerol stocks in Mueller-Hinton broth overnight in a shaking incubator at 37 °C. *Staphylococcus aureus* (ATCC 700698) was cultured from a glycerol stock in brain heart infusion broth overnight in a shaking incubator at 37 °C. *Enterococcus faecalis* (ATCC 51299) was cultured from a glycerol stock in

[c]All experiments in this section were performed or adapted from as those described in the supporting information for Chapter 2 of this dissertation. Chapter 2 and the supporting information for Chapter 2 is taken verbatim from Jones, C. R.; Guaglianone, G.; Lai, G. H.; Nowick, J. S. Isobactins: *O*-Acyl Isopeptide Prodrugs of Teixobactin and Teixobactin Derivatives. *Chem. Sci.*, **2022**, *13*, 13110–13116.

brain heart infusion broth containing 4 μg/mL of vancomycin overnight in a shaking incubator at 37 °C.

An aliquot of a 1 mg/mL antibiotic stock solution in DMSO was diluted with appropriate culture medium to make a 16 μg/mL solution. A 200-μL aliquot of the 16 μg/mL solution was transferred to a sterile, polystyrene 96-well plate. Two-fold serial dilutions were made with media across a 96-well plate to achieve a final volume of 100 μL in each well. These solutions had the following concentrations: 16, 8, 4, 2, 1, 0.5, 0.25, 0.125, 0.0625, 0.0313, and 0.0156 μg/mL.

An OD_{600} value was obtained for the overnight cultures of each bacterium as measured for 200 μL in a 96-well plate. The background absorbance of each culture medium was then subtracted from the OD_{600} obtained for each bacterium using its corresponding culture medium. An appropriate volume of each overnight cultures was then diluted in the correct medium to create a 1 mL stock solution with an OD_{600} of 0.075. Each diluted stock was then further diluted (to approximately 1×10^6 CFU/mL) by adding 130 μL to 15.4 mL of the correct culture medium. A 100-μL aliquot of the diluted bacterial solution was added to each well in the 96-well plates, resulting in final bacteria concentrations of approximately 5×10^5 CFU/mL in each well. With the addition of 100-μL of bacteria in broth to each well, the teixobactin analogues and isobactin analogues were thus diluted to the following concentrations: 8, 4, 2, 1, 0.5, 0.25, 0.125, 0.0625, 0.0313, 0.0156, and 0.0078 μg/mL.

The plate was covered with a lid and incubated at 37 °C for 16 h. The OD_{600} were measured using a 96-well UV/vis plate reader. The MIC values were taken as the lowest concentration that had no bacterial growth. Each MIC assay was run in quadruplicate (technical replicates). Several of the MIC assays were repeated to ensure reproducibility.

Gel formation studies of the isobactin analogues and their corresponding teixobactin analogues. Gel formation studies were performed as previously described.

Hemolytic assay of the isobactin analogues and their corresponding teixobactin analogues. Hemolytic assays of the isobactin analogues and their corresponding teixobactin analogues were performed as previously described.

Cell culture and cytotoxicity assays of the isobactin analogues and their corresponding teixobactin analogues. Cell culture and cytotoxicity assays of the isobactin analogues and their corresponding teixobactin analogues were performed as previously described.

Characterization data

D-Arg$_4$,Leu$_{10}$-teixobactin Analytical HPLC Trace and MALDI-TOF

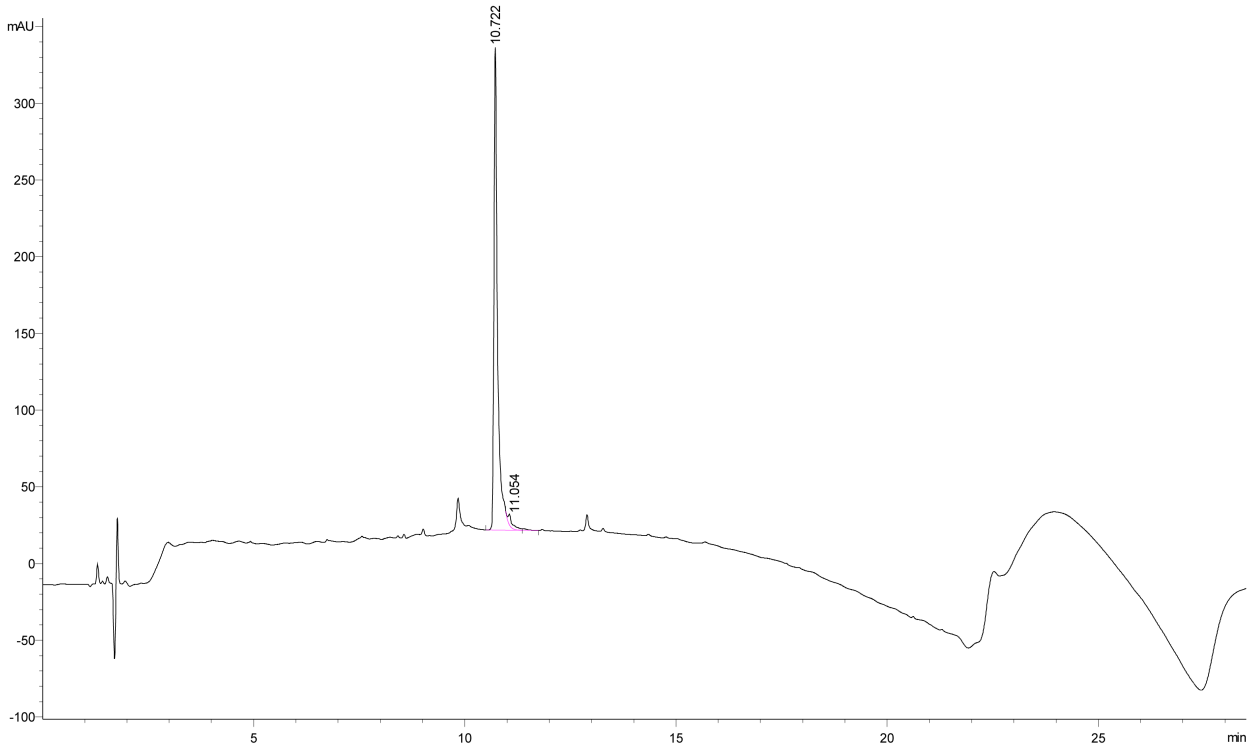

Peak #	RetTime [min]	Type	Width [min]	Area [mAU*s]	Height [mAU]	Area %
1	11.054	BV E	0.0662	10.37853	2.41307	0.9909
2	11.311	VV R	0.0707	1037.05627	213.29471	99.0091
Totals :				1047.43481	215.70778	

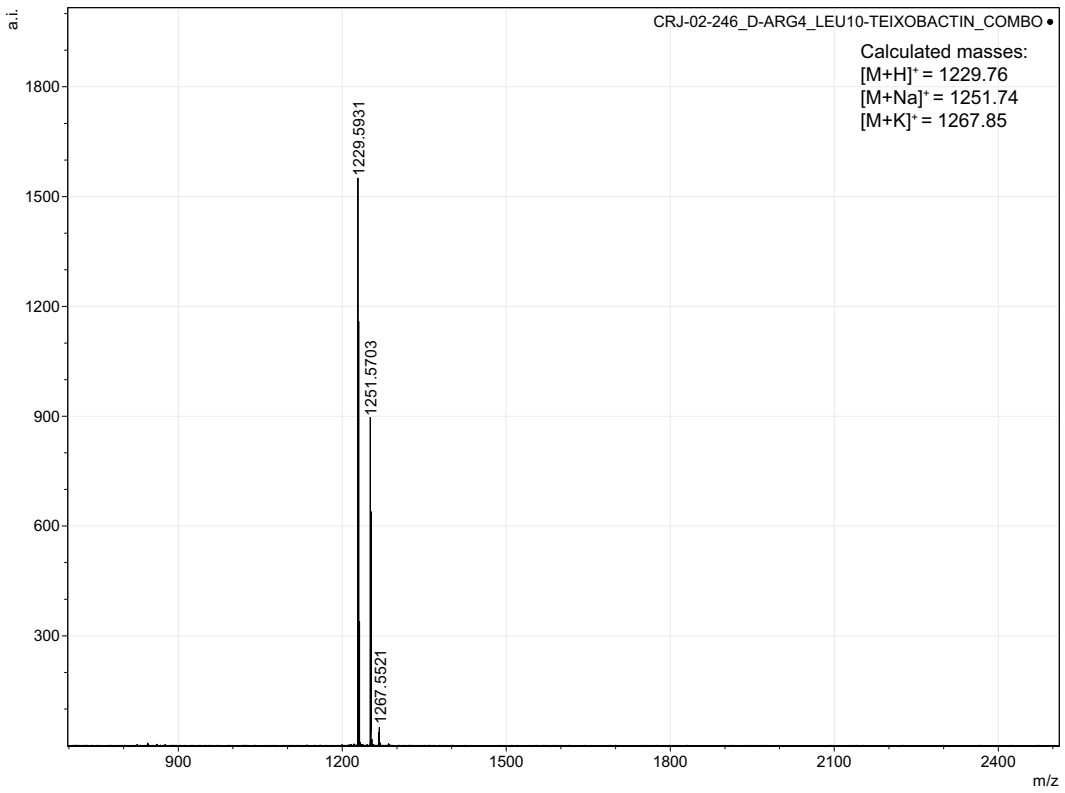
CRJ-02-246_D-ARG4_LEU10-TEIXOBACTIN_COMBO
Calculated masses:
[M+H]+ = 1229.76
[M+Na]+ = 1251.74
[M+K]+ = 1267.85
1229.5931
1251.5703
1267.5521
a.i.
m/z

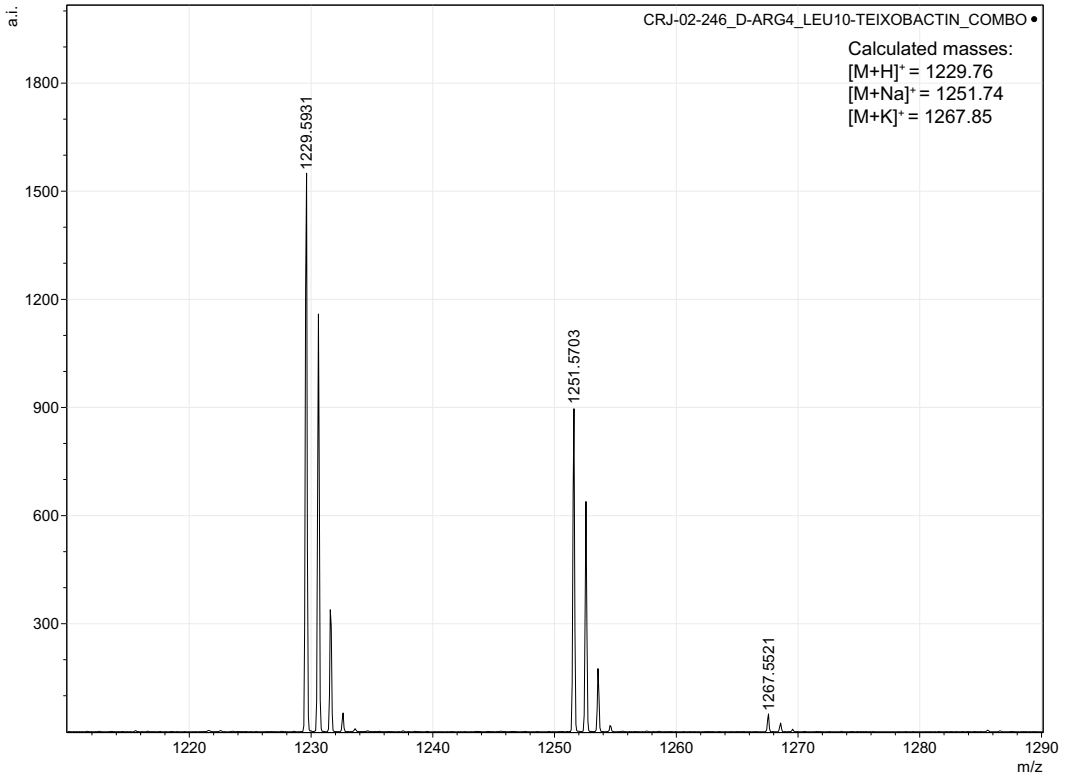
CRJ-02-246_D-ARG4_LEU10-TEIXOBACTIN_COMBO
Calculated masses:
[M+H]+ = 1229.76
[M+Na]+ = 1251.74
[M+K]+ = 1267.85
1229.5931
1251.5703
1267.5521
a.i.
m/z

D-Arg$_4$,Leu$_{10}$-isobactin A Analytical HPLC Trace and MALDI-TOF

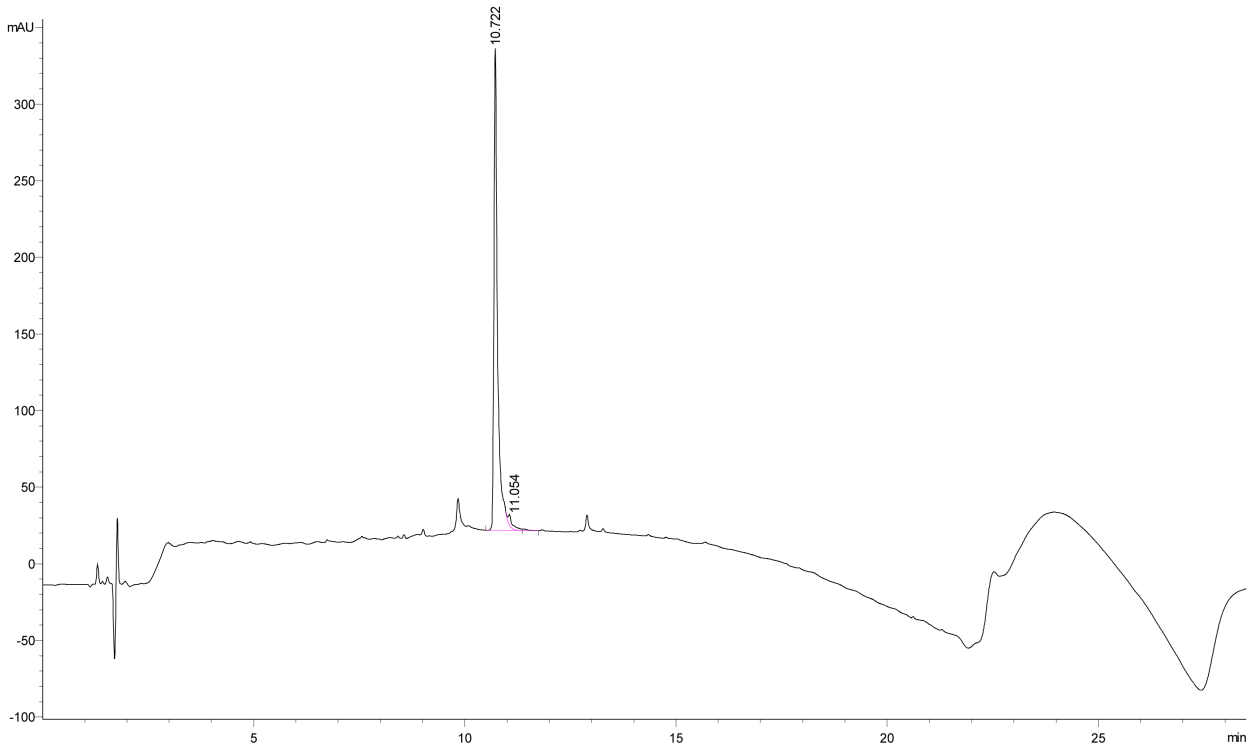

Peak #	RetTime [min]	Type	Width [min]	Area [mAU*s]	Height [mAU]	Area %
1	11.055	BB	0.0595	14.78912	3.96282	0.3913
2	11.444	VV R	0.1054	3764.27979	491.16724	99.6087
Totals :				3779.06891	495.13006	

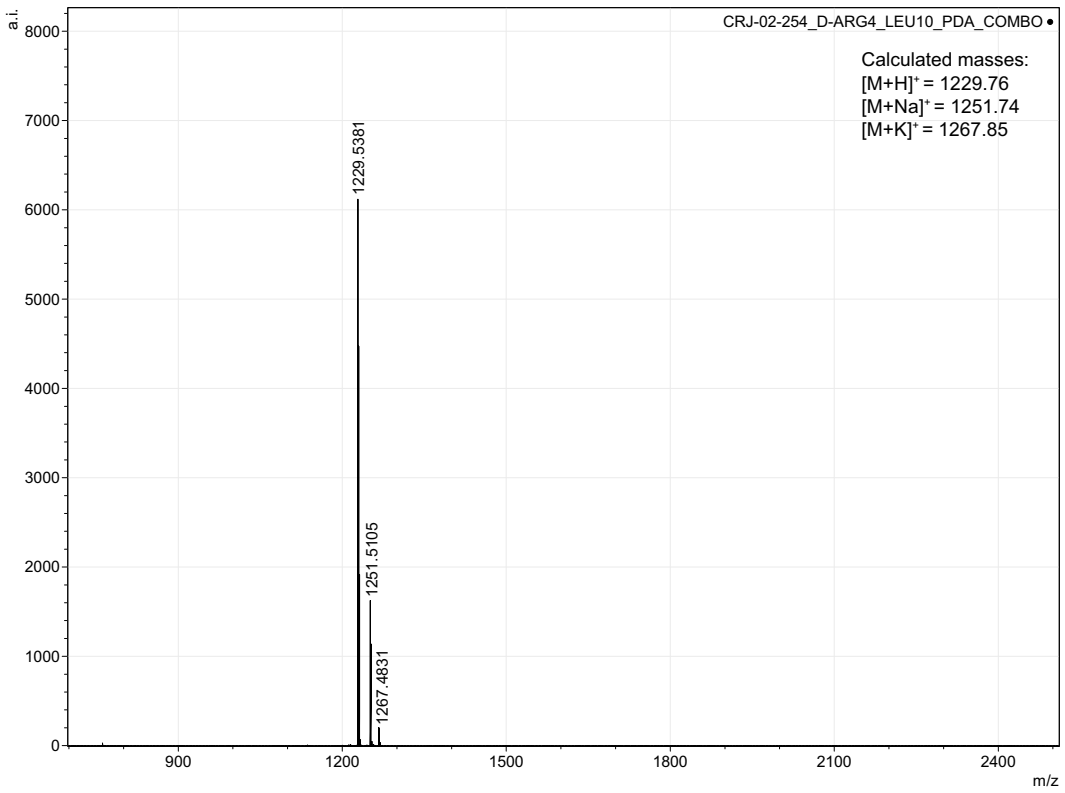
CRJ-02-254_D-ARG4_LEU10_PDA_COMBO
Calculated masses:
[M+H]+ = 1229.76
[M+Na]+ = 1251.74
[M+K]+ = 1267.85
1229.5381
1251.5105
1267.4831
a.i.
m/z

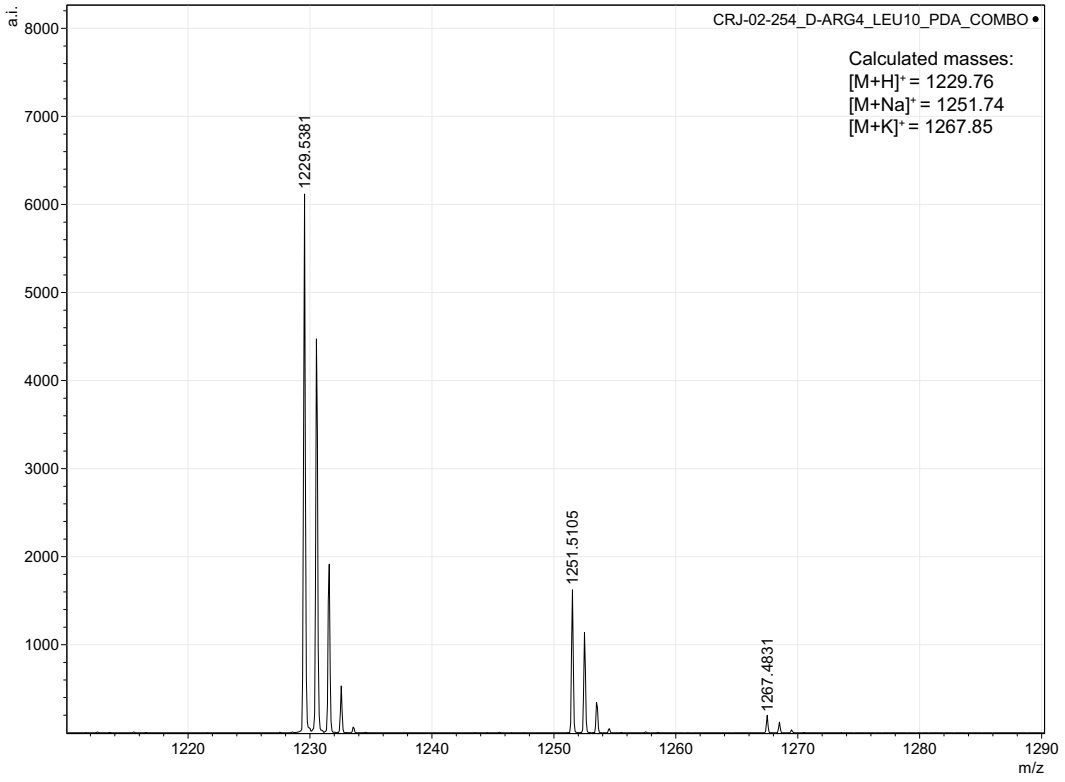
CRJ-02-254_D-ARG4_LEU10_PDA_COMBO
Calculated masses:
[M+H]+ = 1229.76
[M+Na]+ = 1251.74
[M+K]+ = 1267.85
1229.5381
1251.5105
1267.4831
a.i.
m/z

D-Arg$_4$,Leu$_{10}$-isobactin B Analytical HPLC Trace and MALDI-TOF

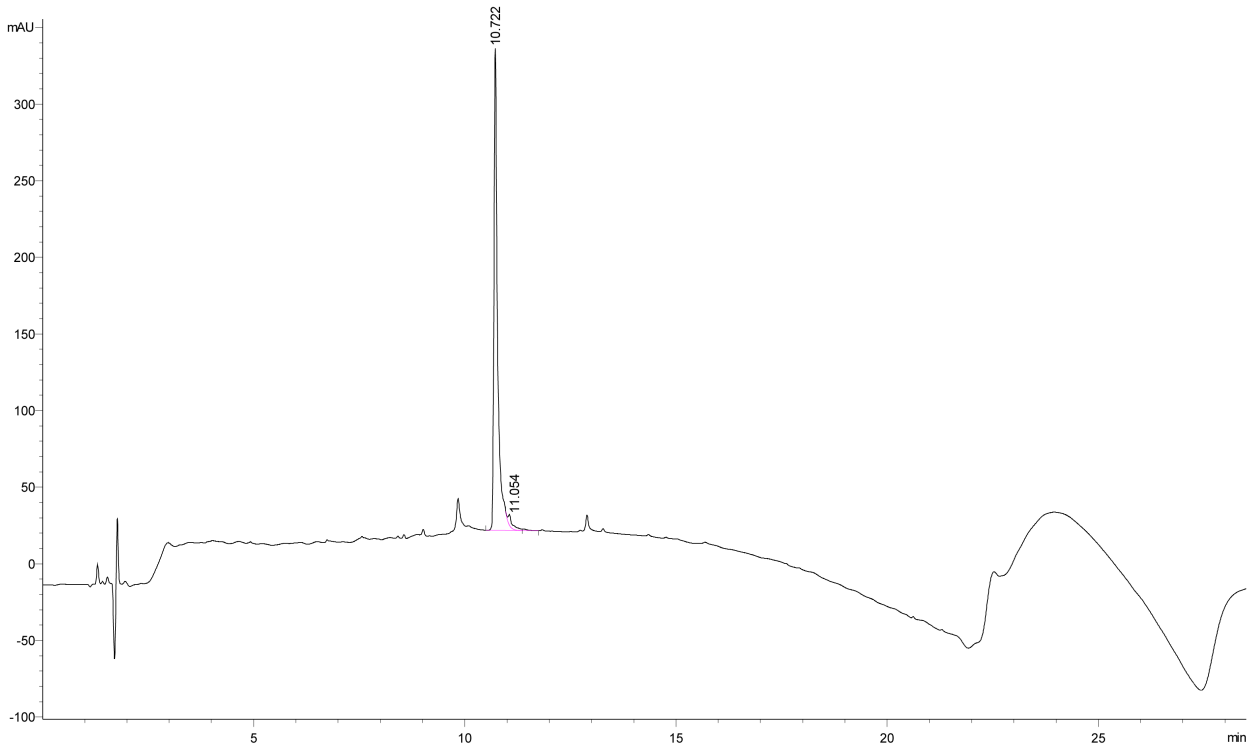

Peak #	RetTime [min]	Type	Width [min]	Area [mAU*s]	Height [mAU]	Area %
1	10.722	BV R	0.0871	1728.03259	283.69421	97.0997
2	11.054	VV E	0.1116	51.61475	6.16774	2.9003
Totals :				1779.64735	289.86196	

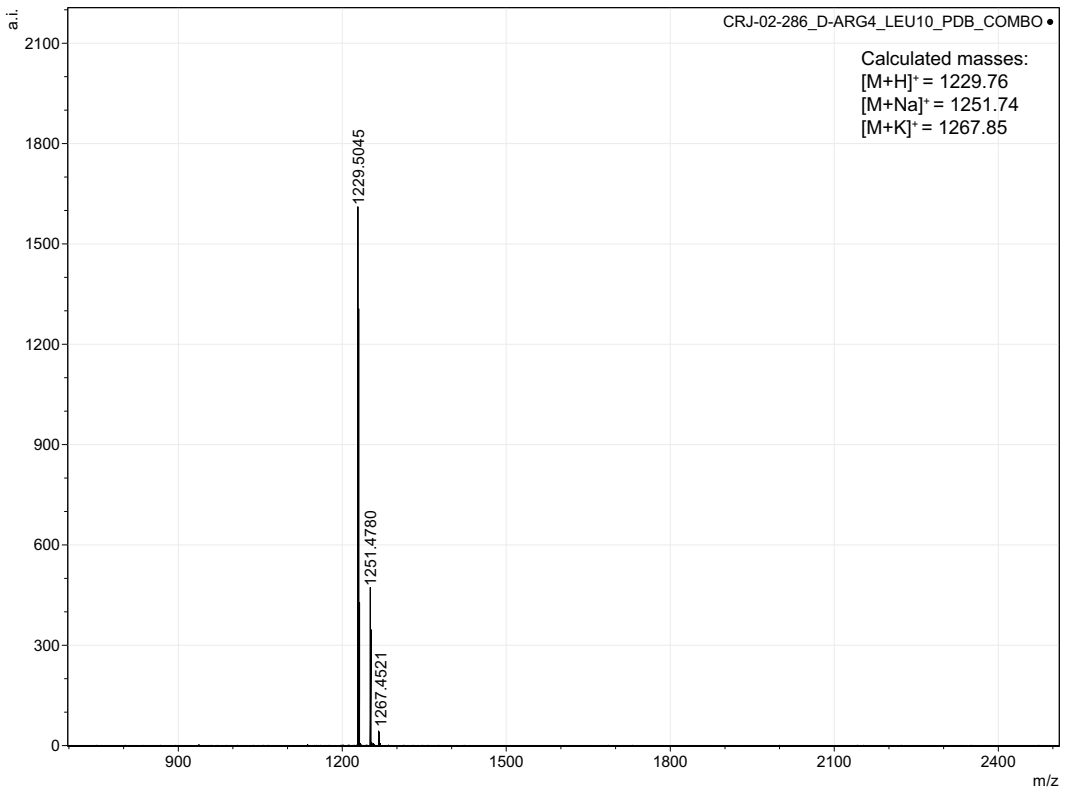
CRJ-02-286_D-ARG4_LEU10_PDB_COMBO
Calculated masses:
[M+H]+ = 1229.76
[M+Na]+ = 1251.74
[M+K]+ = 1267.85
1229.5045
1251.4780
1267.4521
a.i.
m/z

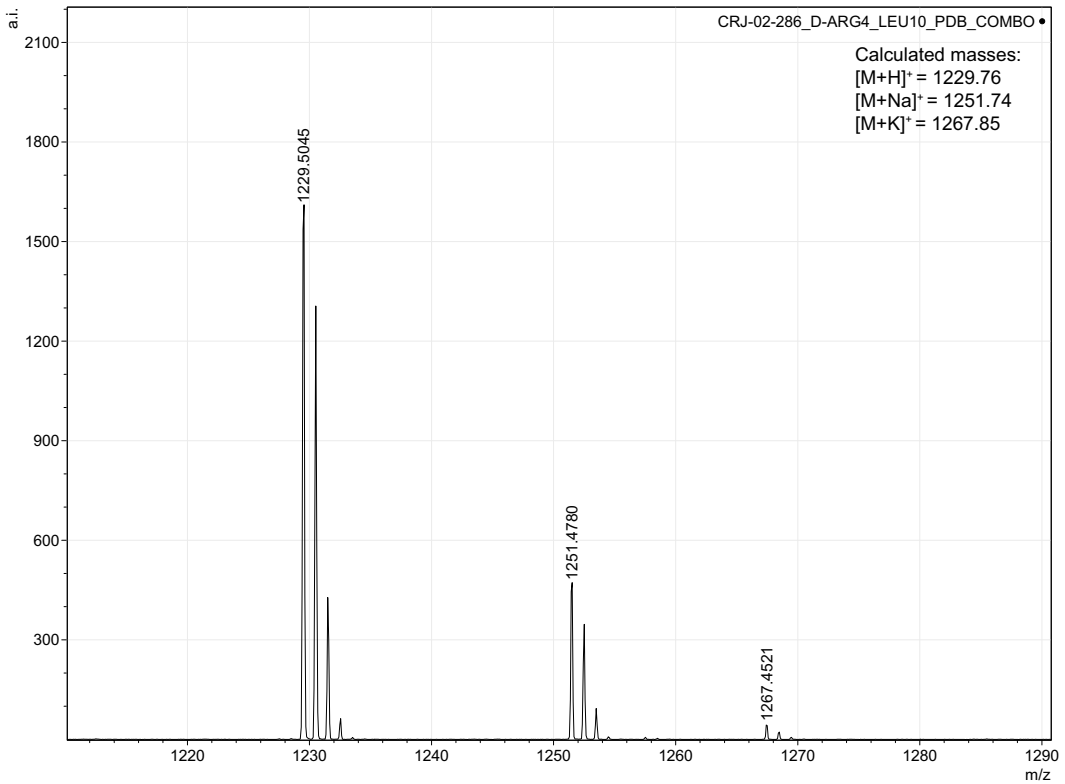
CRJ-02-286_D-ARG4_LEU10_PDB_COMBO
Calculated masses:
[M+H]+ = 1229.76
[M+Na]+ = 1251.74
[M+K]+ = 1267.85
1229.5045
1251.4780
1267.4521
a.i.
m/z

D-Arg$_4$,Leu$_{10}$-isobactin C Analytical HPLC Trace and MALDI-TOF

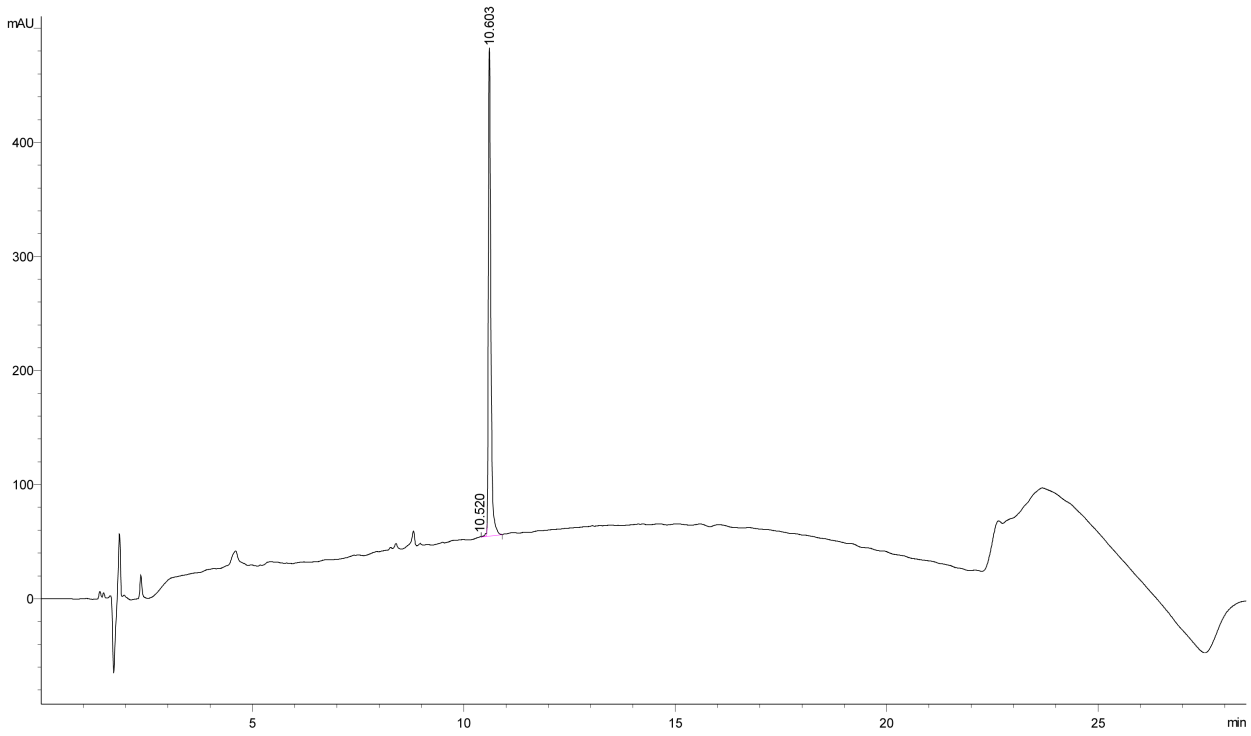

Peak #	RetTime [min]	Type	Width [min]	Area [mAU*s]	Height [mAU]	Area %
1	10.520	BV E	0.0492	8.91377	2.62514	0.5140
2	10.603	VB R	0.0608	1725.37646	430.06204	99.4860
Totals :				1734.29023	432.68718	

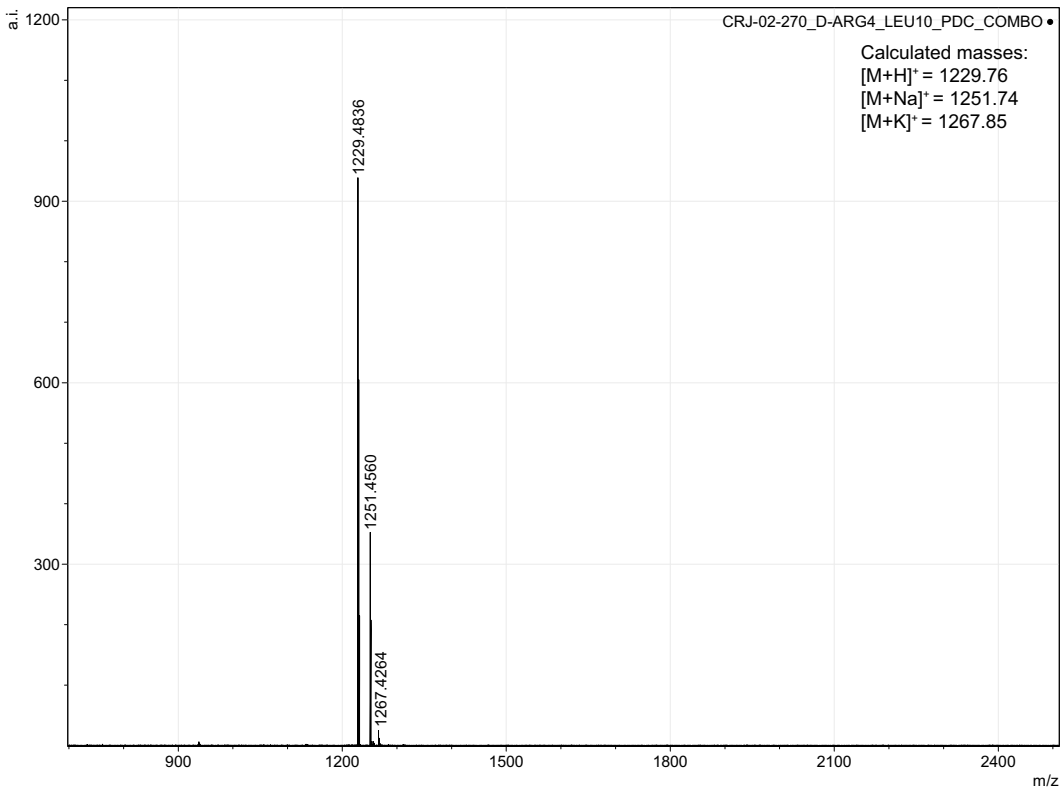
a.i.
1200
900
600
300
CRJ-02-270_D-ARG4_LEU10_PDC_COMBO
Calculated masses:
[M+H]+ = 1229.76
[M+Na]+ = 1251.74
[M+K]+ = 1267.85
1229.4836
1251.4560
1267.4264
900
1200
1500
1800
2100
2400
m/z

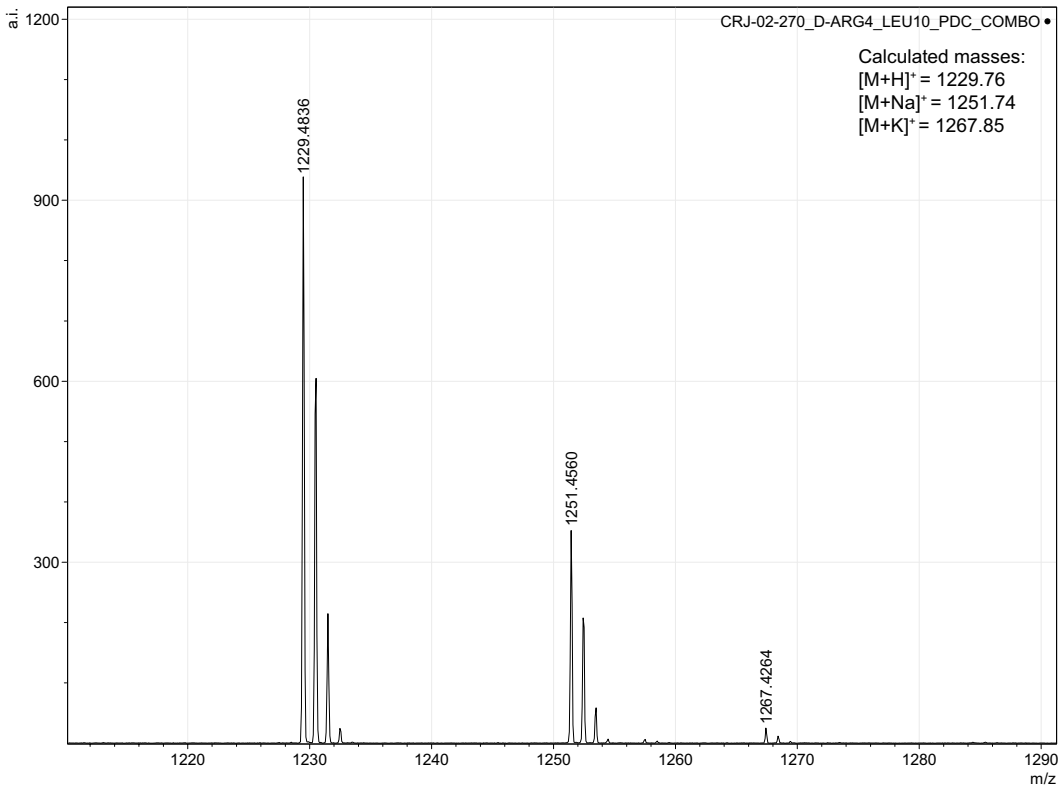
a.i.
1200
900
600
300
CRJ-02-270_D-ARG4_LEU10_PDC_COMBO
Calculated masses:
[M+H]+ = 1229.76
[M+Na]+ = 1251.74
[M+K]+ = 1267.85
1229.4836
1251.4560
1267.4264
1220
1230
1240
1250
1260
1270
1280
1290
m/z

Chg$_{10}$-teixobactin Analytical HPLC Trace and MALDI-TOF

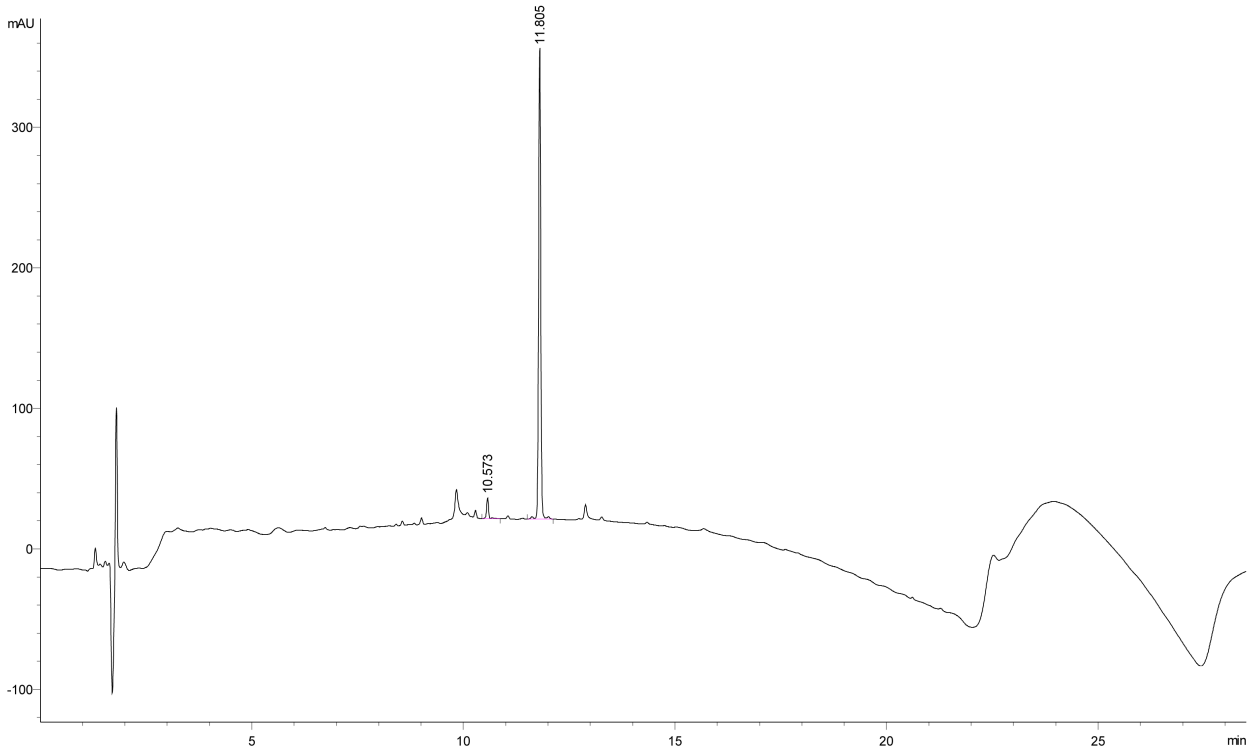

Peak #	RetTime [min]	Type	Width [min]	Area [mAU*s]	Height [mAU]	Area %
1	10.573	BV R	0.0539	45.86185	13.41298	4.1413
2	11.805	VV R	0.0547	1061.56128	304.35638	95.8587
Totals :				1107.42313	317.76936	

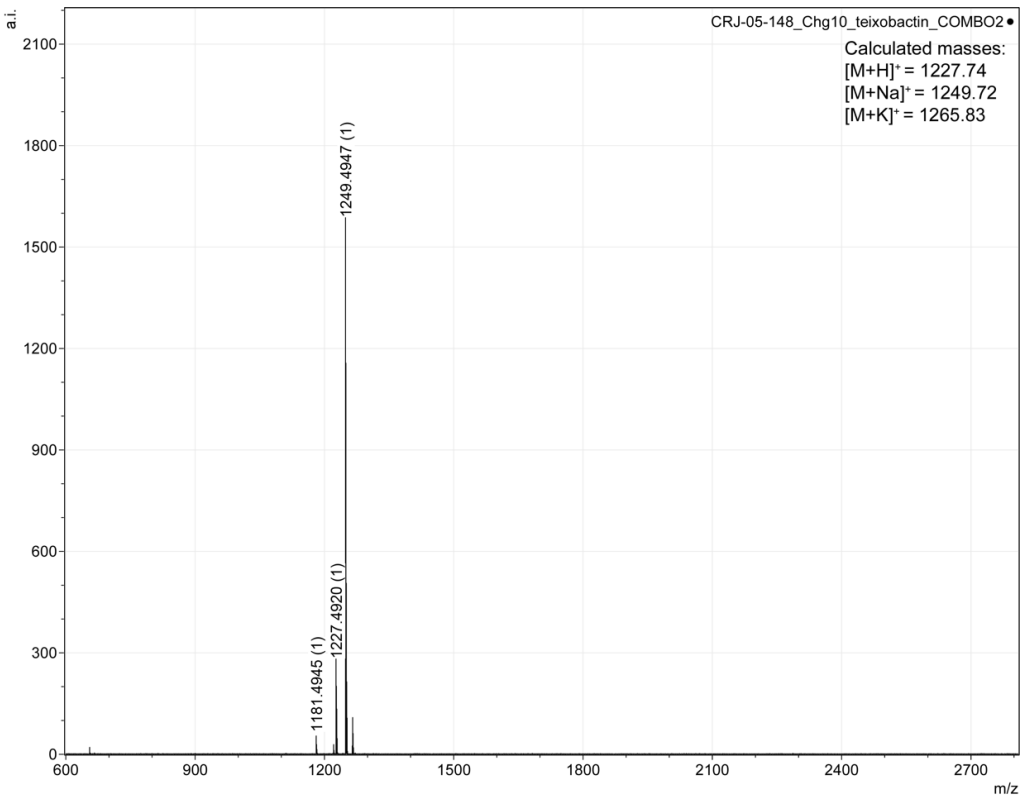
CRJ-05-148_Chg10_teixobactin_COMBO2
Calculated masses:
[M+H]+ = 1227.74
[M+Na]+ = 1249.72
[M+K]+ = 1265.83
1249.4947 (1)
1227.4920 (1)
1181.4945 (1)
a.i.
m/z

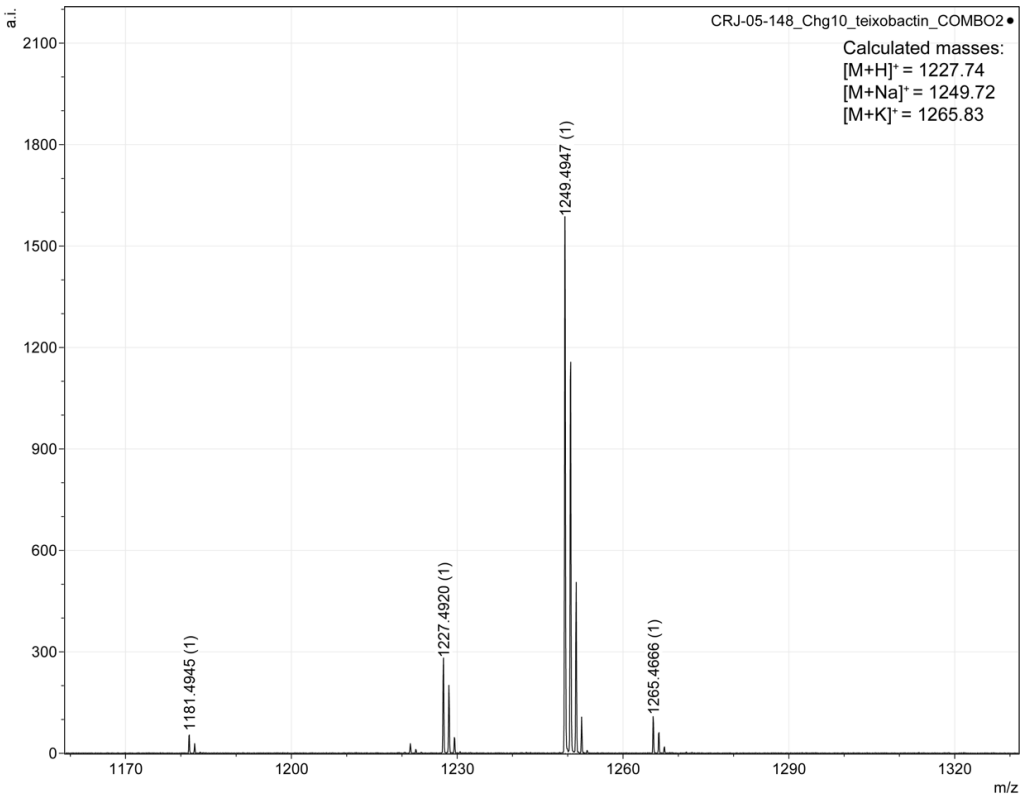
CRJ-05-148_Chg10_teixobactin_COMBO2
Calculated masses:
[M+H]+ = 1227.74
[M+Na]+ = 1249.72
[M+K]+ = 1265.83
1249.4947 (1)
1227.4920 (1)
1265.4666 (1)
1181.4945 (1)
a.i.
m/z

Chg$_{10}$-isobactin A Analytical HPLC Trace and MALDI-TOF

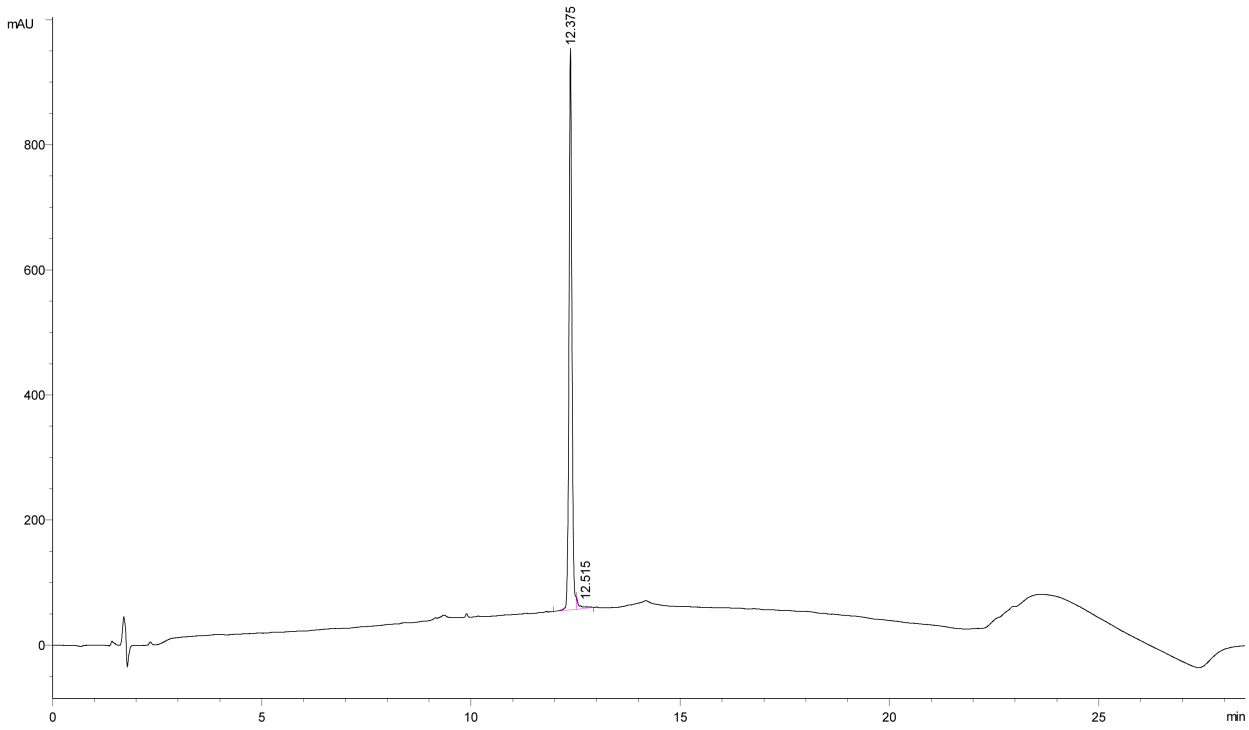

Peak #	RetTime [min]	Type	Width [min]	Area mAU *s	Height [mAU]	Area %
1	12.375	MF	0.0793	4279.87988	899.86743	97.9889
2	12.515	FM	0.0745	87.83923	19.66221	2.0111
Totals :				4367.71911	919.52965	

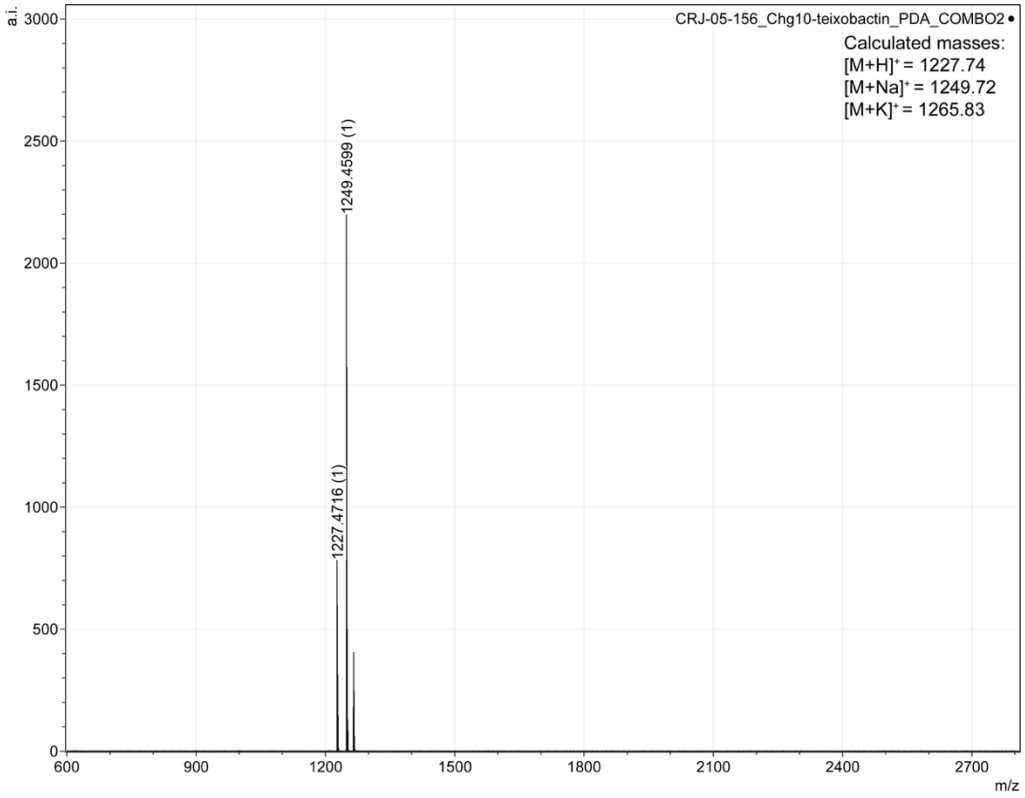
CRJ-05-156_Chg10-teixobactin_PDA_COMBO2
Calculated masses:
[M+H]+ = 1227.74
[M+Na]+ = 1249.72
[M+K]+ = 1265.83
1249.4599 (1)
1227.4716 (1)
a.i.
m/z

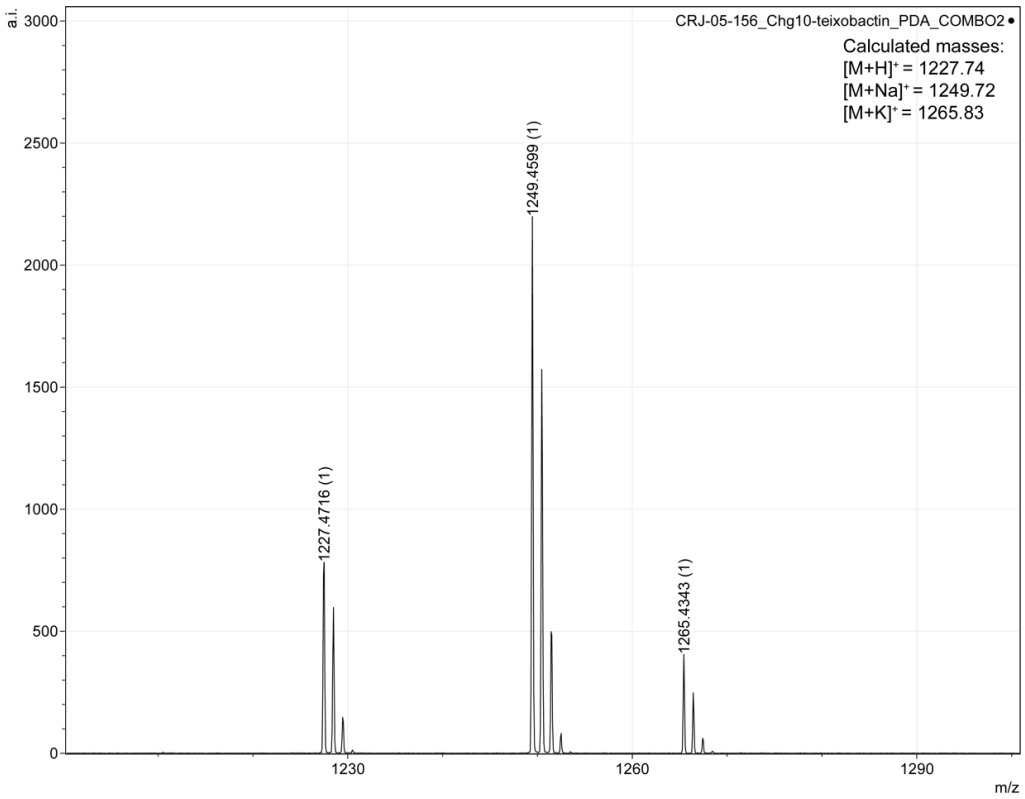
CRJ-05-156_Chg10-teixobactin_PDA_COMBO2
Calculated masses:
[M+H]+ = 1227.74
[M+Na]+ = 1249.72
[M+K]+ = 1265.83
1249.4599 (1)
1227.4716 (1)
1265.4343 (1)
a.i.
m/z

Chg$_{10}$-isobactin B Analytical HPLC Trace and MALDI-TOF

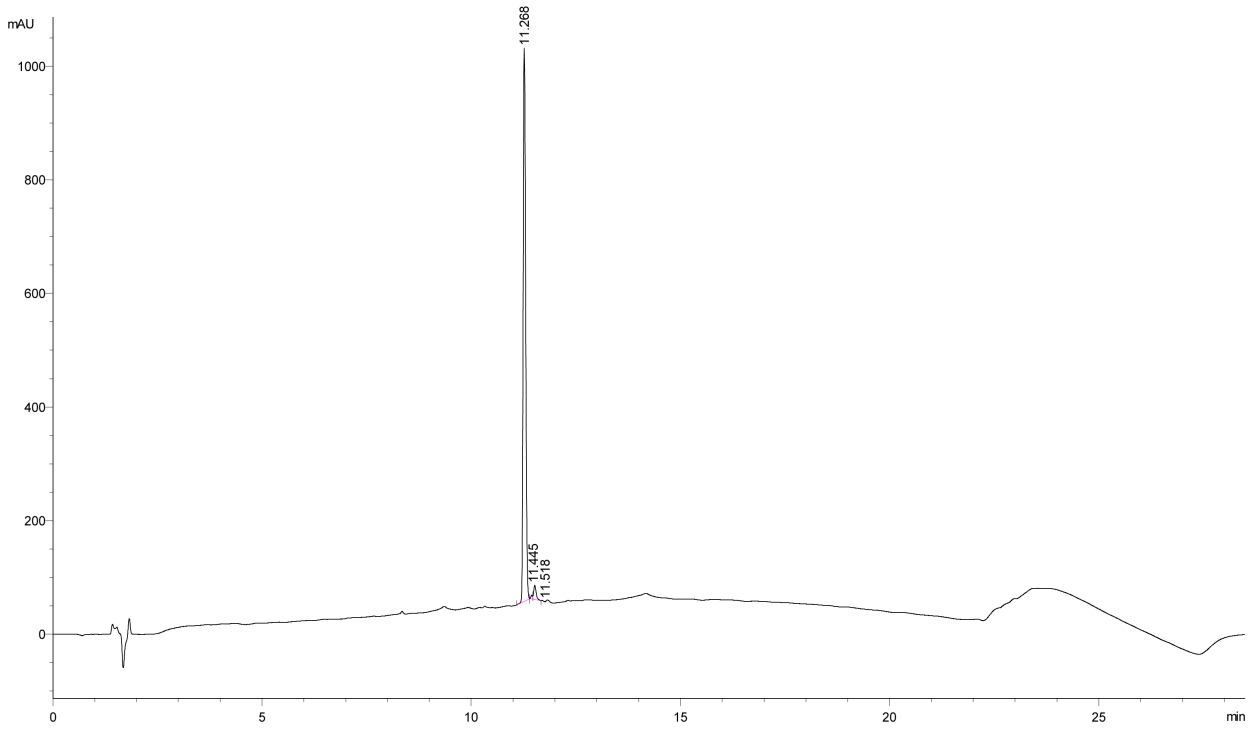

Peak #	RetTime [min]	Type	Width [min]	Area mAU *s	Height [mAU]	Area %
1	11.268	BB	0.0624	3882.94067	975.85962	96.8879
2	11.445	BV	0.0399	17.78160	6.99371	0.4437
3	11.518	VB	0.0637	106.93921	25.39650	2.6684
Totals :				4007.66149	1008.24983	

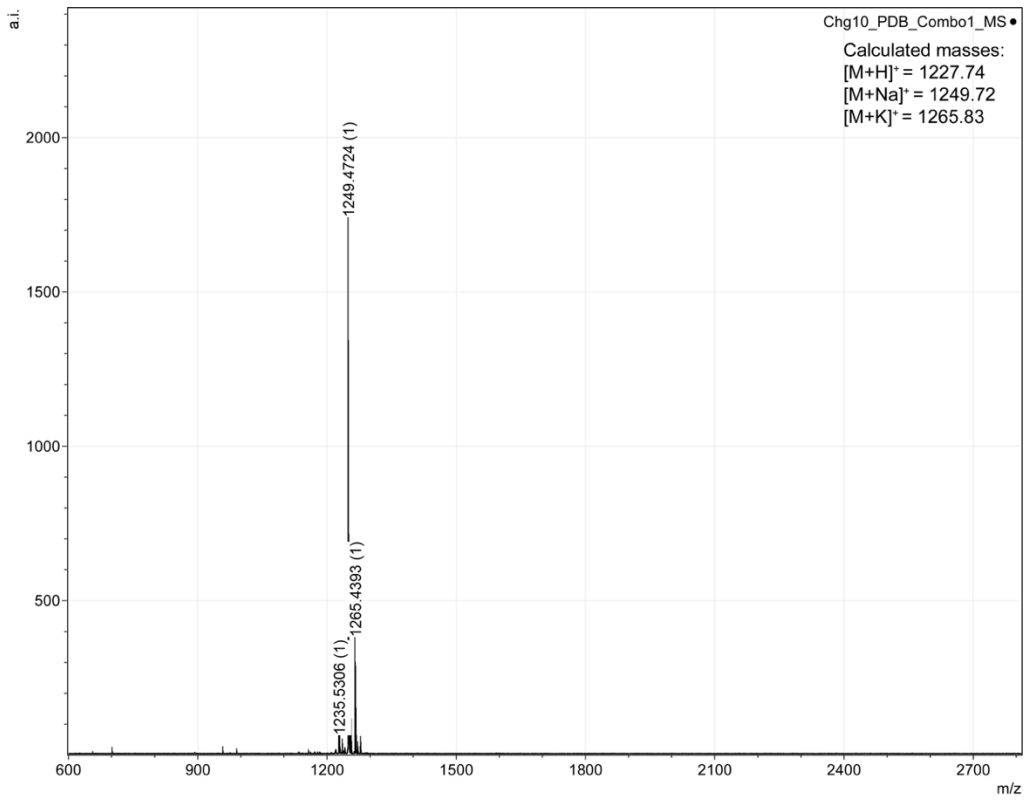
a.i.
Chg10_PDB_Combo1_MS
Calculated masses:
[M+H]+ = 1227.74
[M+Na]+ = 1249.72
[M+K]+ = 1265.83
1249.4724 (1)
1265.4393 (1)
1235.5306 (1)
2000
1500
1000
500
600
900
1200
1500
1800
2100
2400
2700
m/z

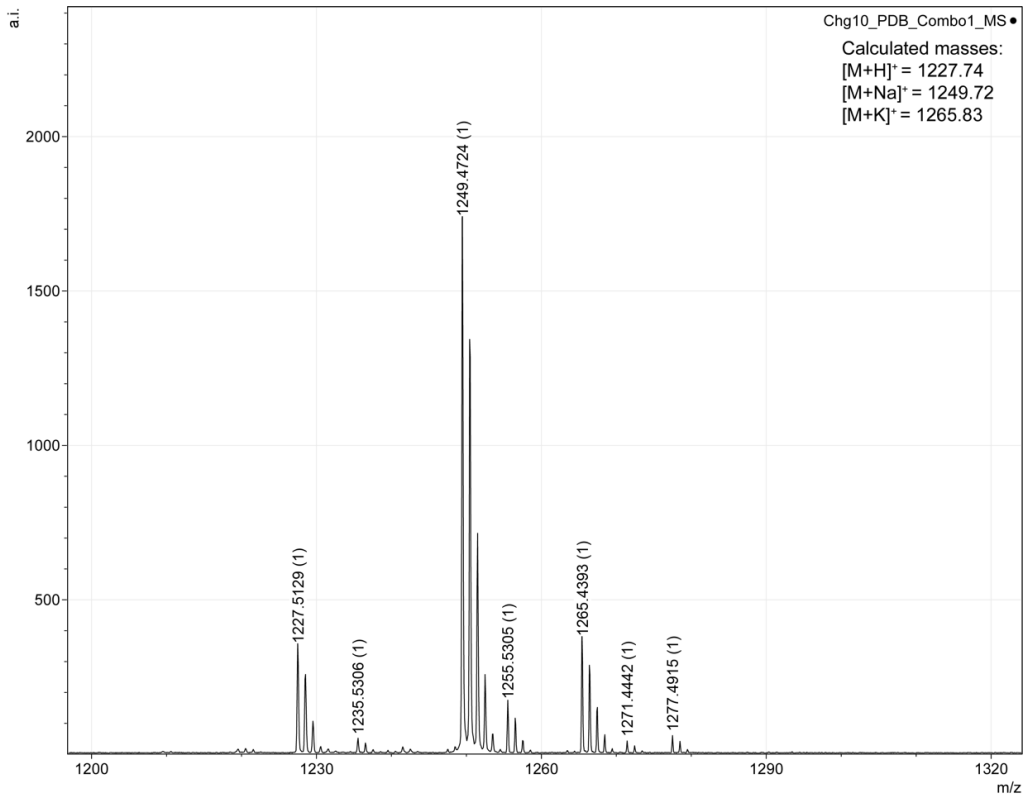
a.i.
Chg10_PDB_Combo1_MS
Calculated masses:
[M+H]+ = 1227.74
[M+Na]+ = 1249.72
[M+K]+ = 1265.83
1249.4724 (1)
1227.5129 (1)
1265.4393 (1)
1235.5306 (1)
1255.5305 (1)
1271.4442 (1)
1277.4915 (1)
2000
1500
1000
500
1200
1230
1260
1290
1320
m/z

Chg_{10}-isobactin C Analytical HPLC Trace and MALDI-TOF

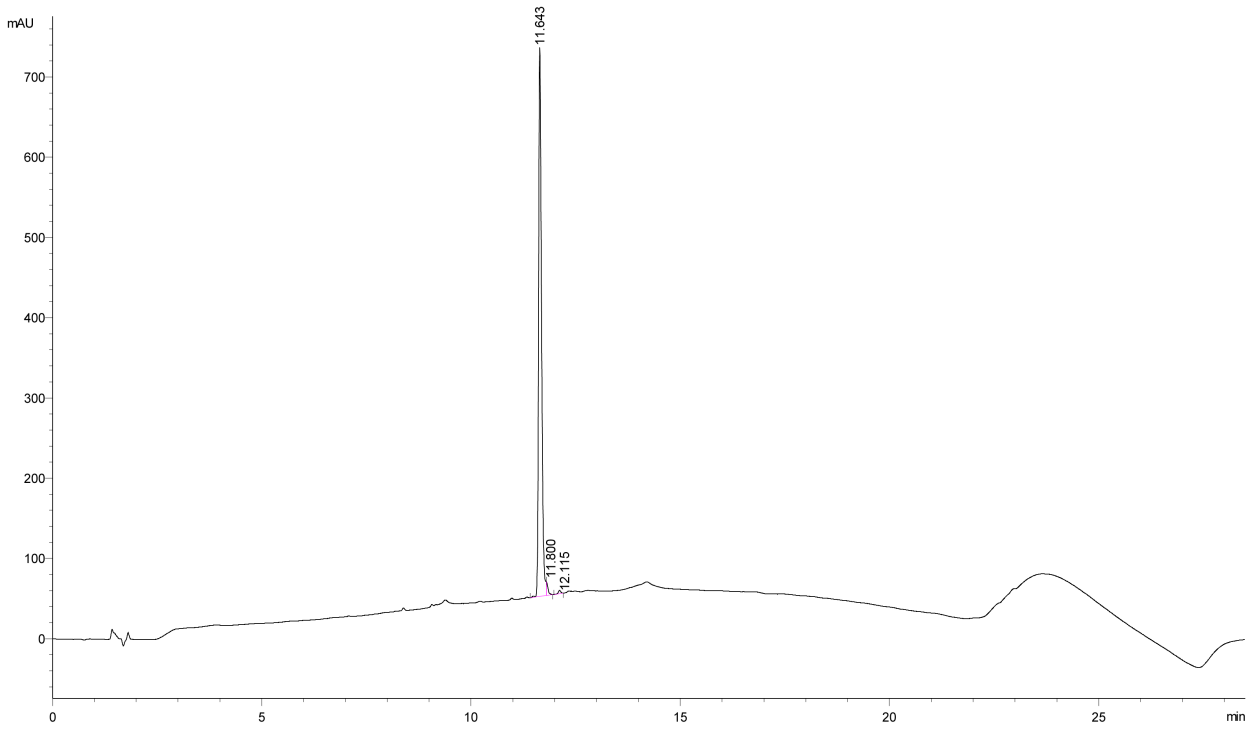

Peak #	RetTime [min]	Type	Width [min]	Area mAU *s	Height [mAU]	Area %
1	11.643	MF	0.0824	3385.51660	685.01074	98.1946
2	11.800	FM	0.0436	44.90172	17.15775	1.3023
3	12.115	BB	0.0595	17.34487	4.36299	0.5031
Totals :				3447.76319	706.53148	

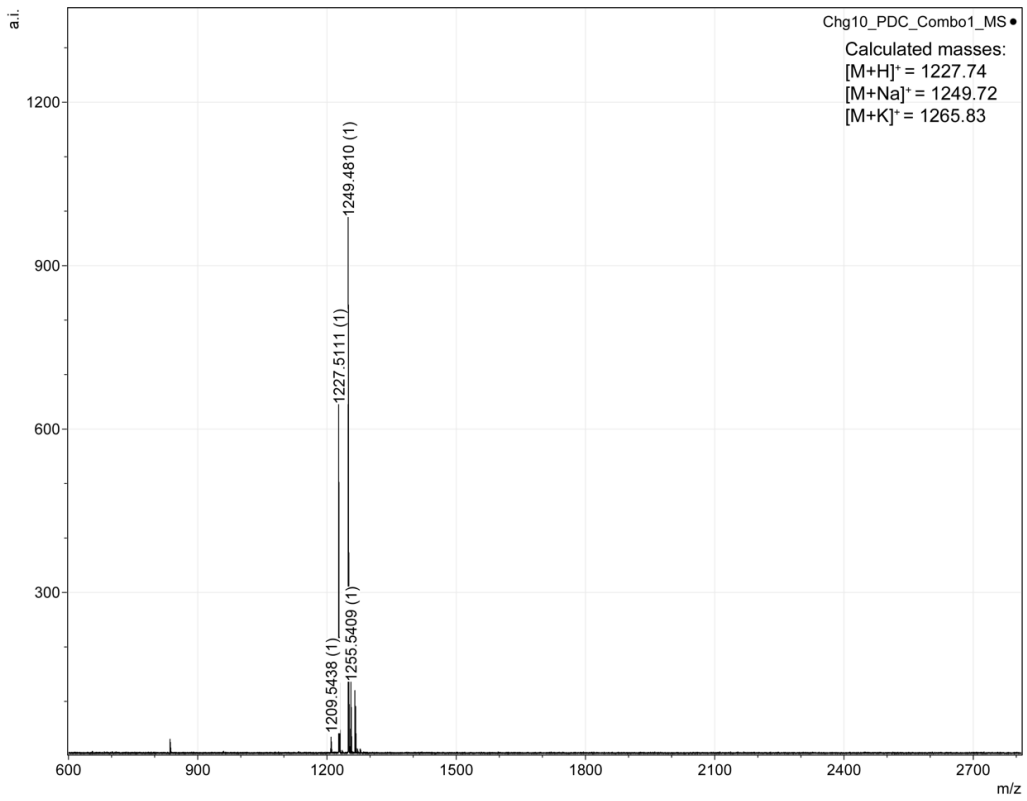
a.i.
Chg10_PDC_Combo1_MS
Calculated masses:
[M+H]+ = 1227.74
[M+Na]+ = 1249.72
[M+K]+ = 1265.83
1249.4810 (1)
1227.5111 (1)
1209.5438 (1)
1255.5409 (1)
1200
900
600
300
600
900
1200
1500
1800
2100
2400
2700
m/z

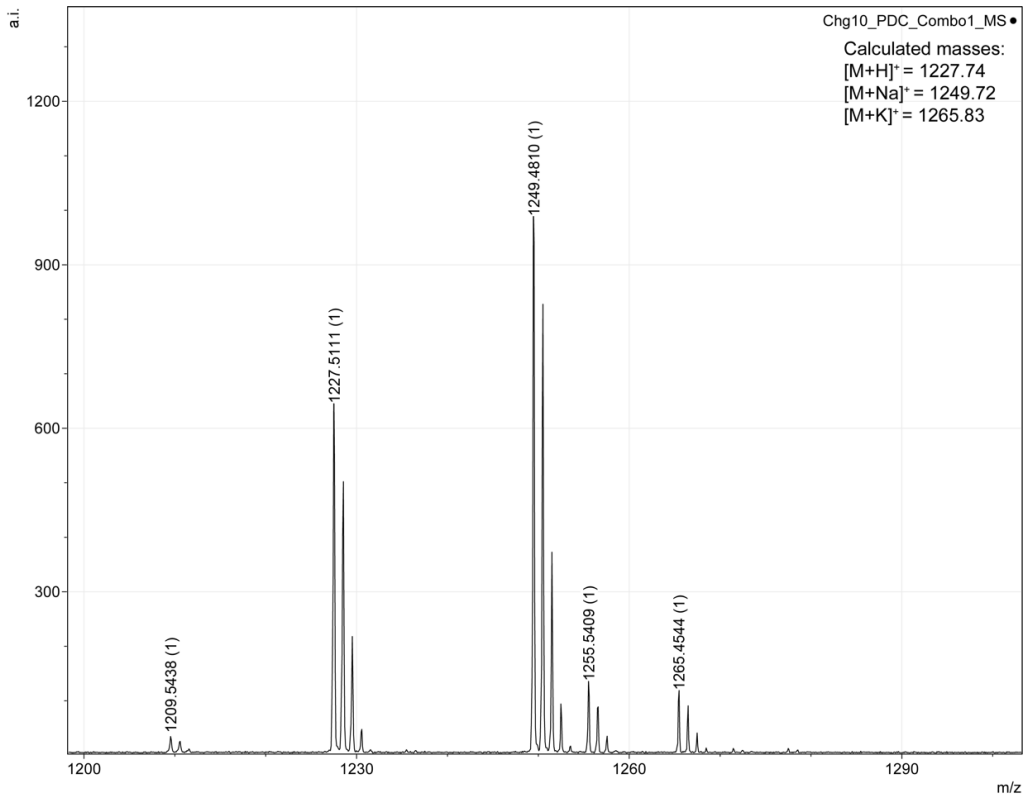
a.i.
Chg10_PDC_Combo1_MS
Calculated masses:
[M+H]+ = 1227.74
[M+Na]+ = 1249.72
[M+K]+ = 1265.83
1249.4810 (1)
1227.5111 (1)
1209.5438 (1)
1255.5409 (1)
1265.4544 (1)
1200
900
600
300
1200
1230
1260
1290
m/z

D-Arg$_4$,Chg$_{10}$-teixobactin Analytical HPLC Trace and MALDI-TOF

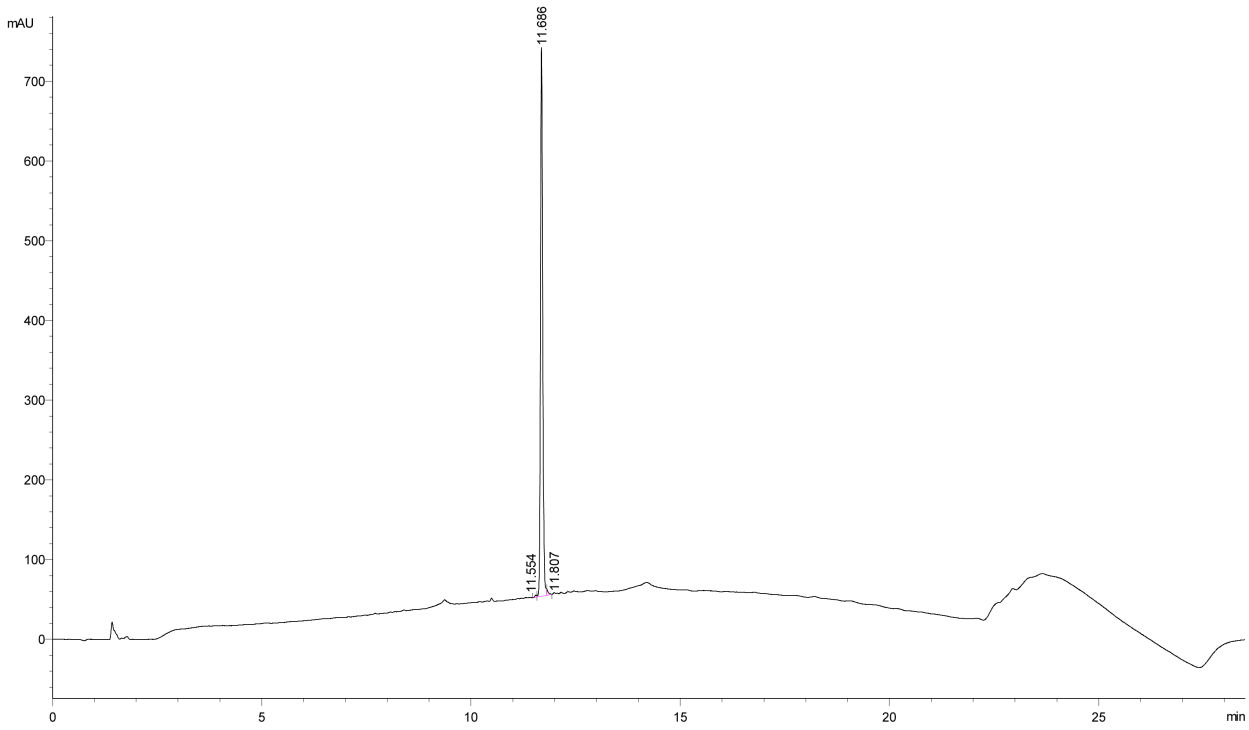

Peak #	RetTime [min]	Type	Width [min]	Area mAU *s	Height [mAU]	Area %
1	11.554	MF	0.0520	7.52254	2.40915	0.2921
2	11.686	MF	0.0616	2548.50732	689.98853	98.9709
3	11.807	FM	0.0398	18.97640	7.95189	0.7369
Totals :				2575.00626	700.34956	

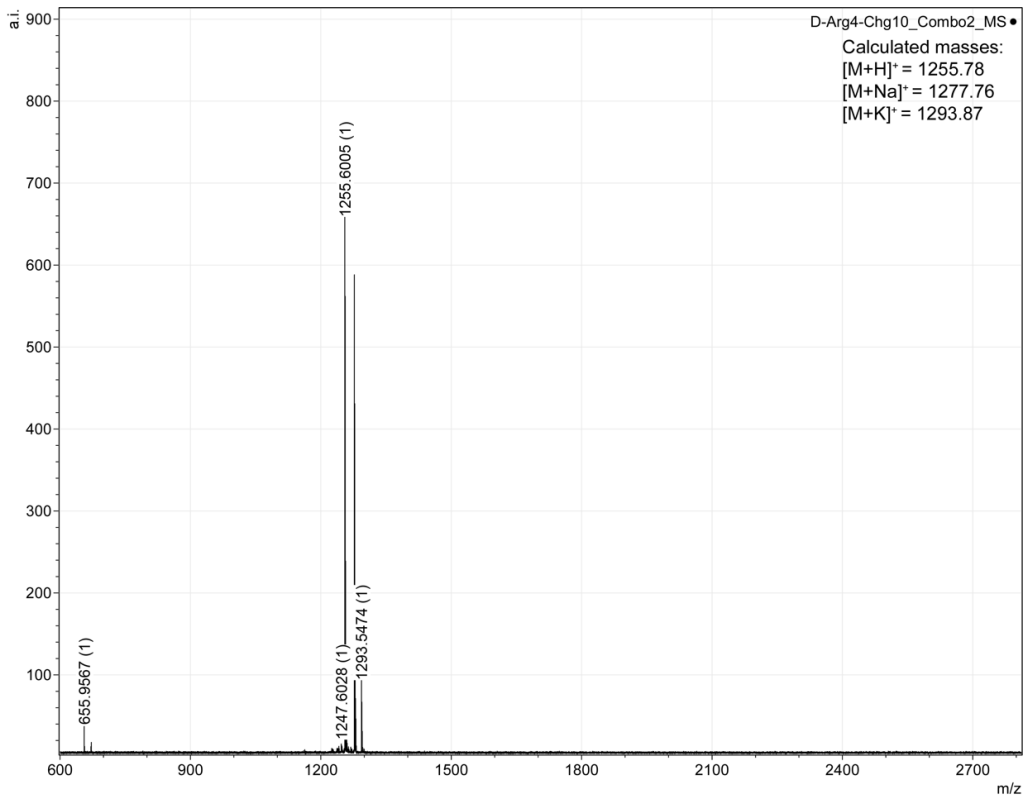
a.i.
D-Arg4-Chg10_Combo2_MS
Calculated masses:
[M+H]+ = 1255.78
[M+Na]+ = 1277.76
[M+K]+ = 1293.87
1255.6005 (1)
655.9567 (1)
1247.6028 (1)
1293.5474 (1)
m/z

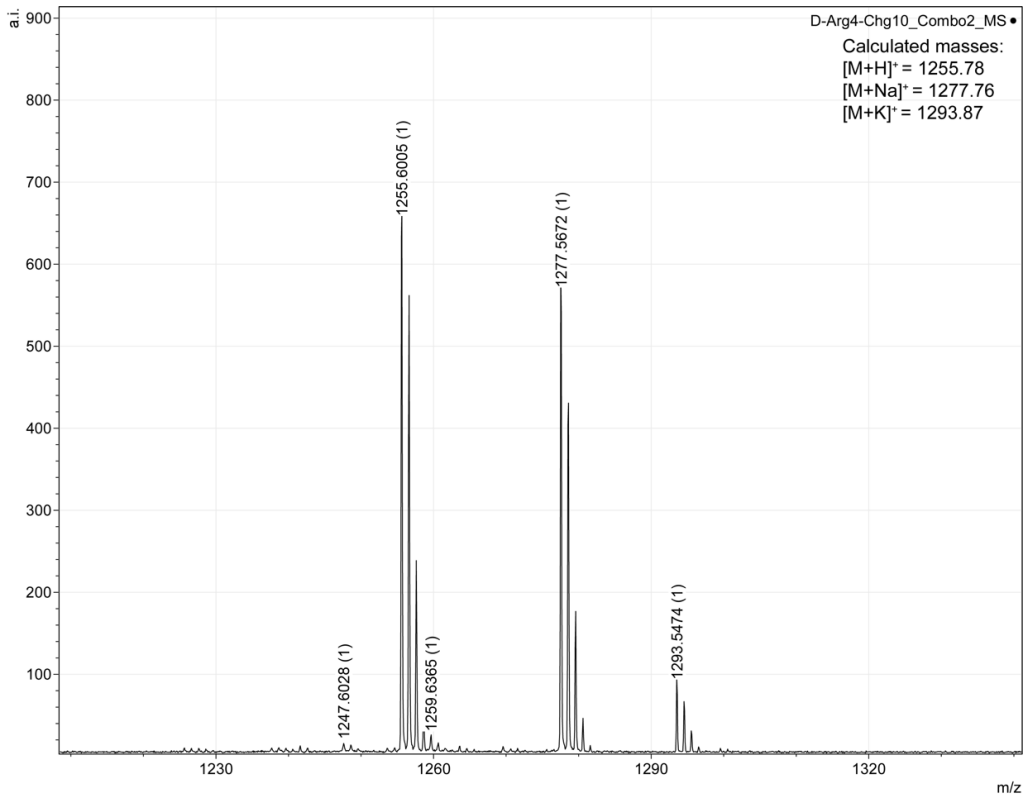
a.i.
D-Arg4-Chg10_Combo2_MS
Calculated masses:
[M+H]+ = 1255.78
[M+Na]+ = 1277.76
[M+K]+ = 1293.87
1255.6005 (1)
1277.5672 (1)
1247.6028 (1)
1259.6365 (1)
1293.5474 (1)
m/z

D-Arg$_4$,Chg$_{10}$-isobactin A Analytical HPLC Trace and MALDI-TOF

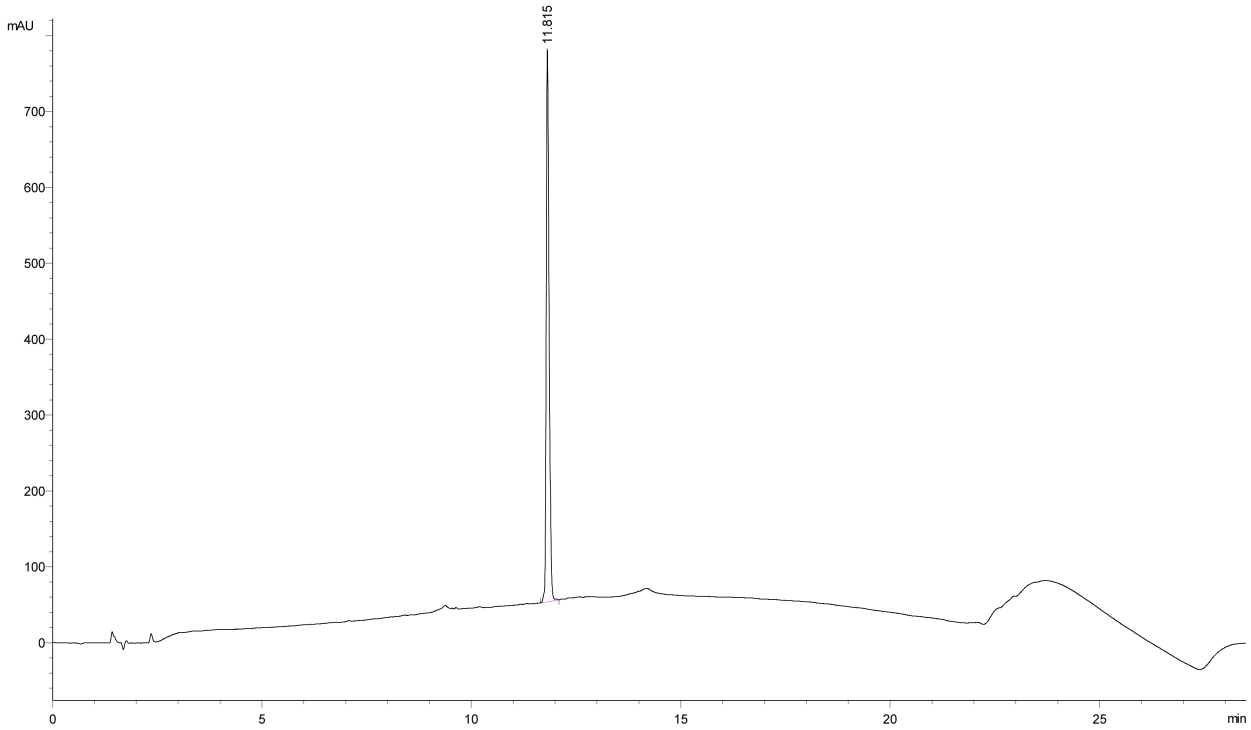

Peak #	RetTime [min]	Type	Width [min]	Area mAU *s	Height [mAU]	Area %
1	11.815	BV R	0.0738	3518.70728	728.92242	100.0000
Totals :				3518.70728	728.92242	

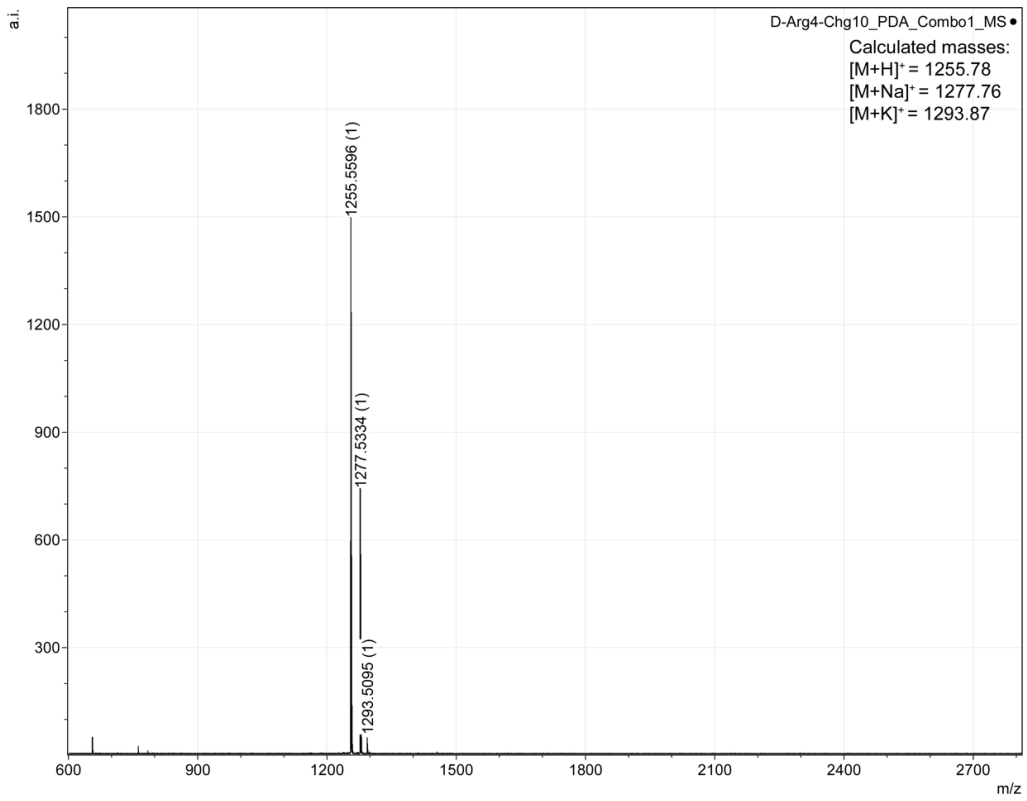
D-Arg4-Chg10_PDA_Combo1_MS
Calculated masses:
[M+H]+ = 1255.78
[M+Na]+ = 1277.76
[M+K]+ = 1293.87
1255.5596 (1)
1277.5334 (1)
1293.5095 (1)
a.i.
m/z

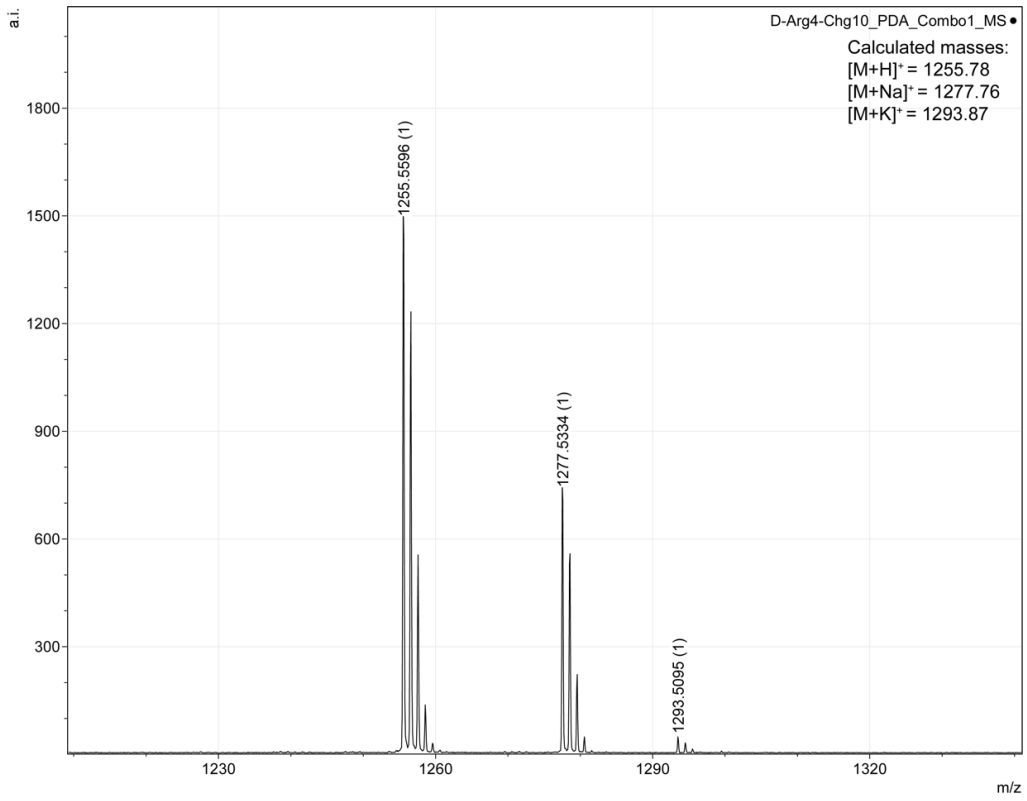
D-Arg4-Chg10_PDA_Combo1_MS
Calculated masses:
[M+H]+ = 1255.78
[M+Na]+ = 1277.76
[M+K]+ = 1293.87
1255.5596 (1)
1277.5334 (1)
1293.5095 (1)
a.i.
m/z

D-Arg$_4$,Chg$_{10}$-isobactin B Analytical HPLC Trace and MALDI-TOF

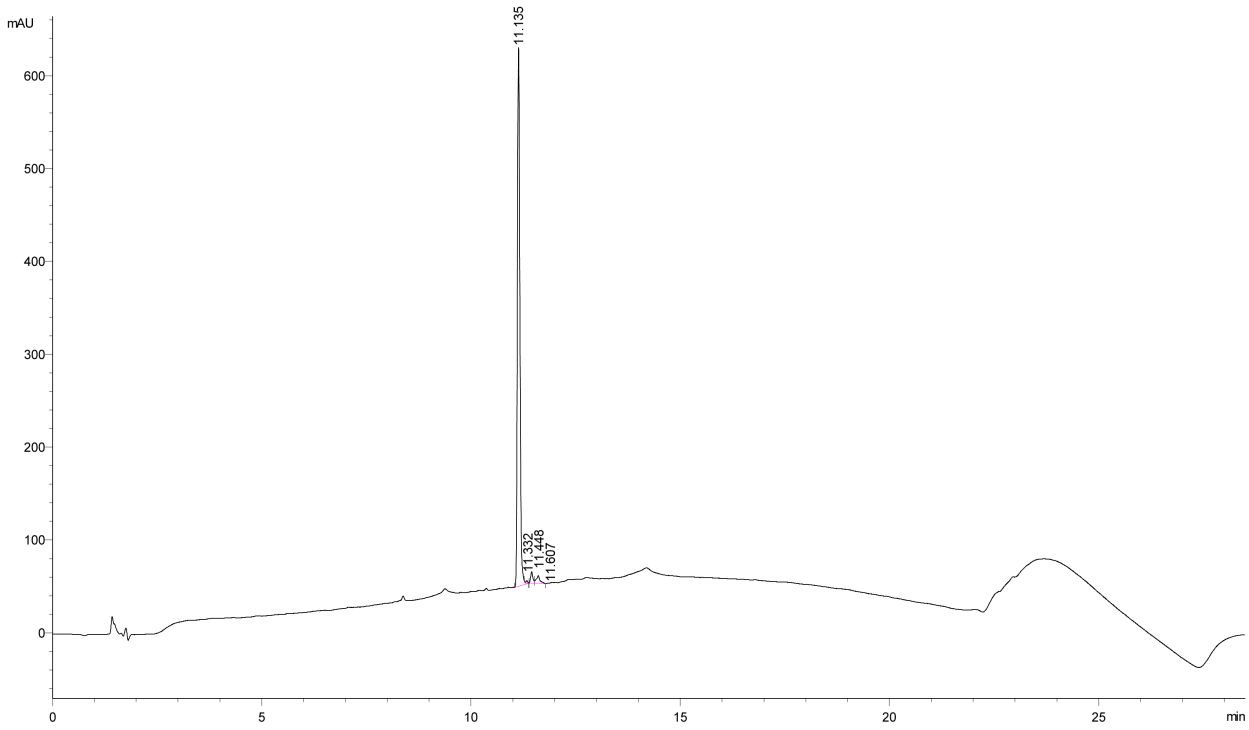

Peak #	RetTime [min]	Type	Width [min]	Area mAU *s	Height [mAU]	Area %
1	11.135	BV R	0.0611	2318.76929	581.44897	95.5992
2	11.332	VB E	0.0468	8.57739	2.84980	0.3536
3	11.448	BV	0.0547	45.39404	12.30303	1.8715
4	11.607	VB	0.0850	52.77007	8.23296	2.1756
Totals :				2425.51079	604.83477	

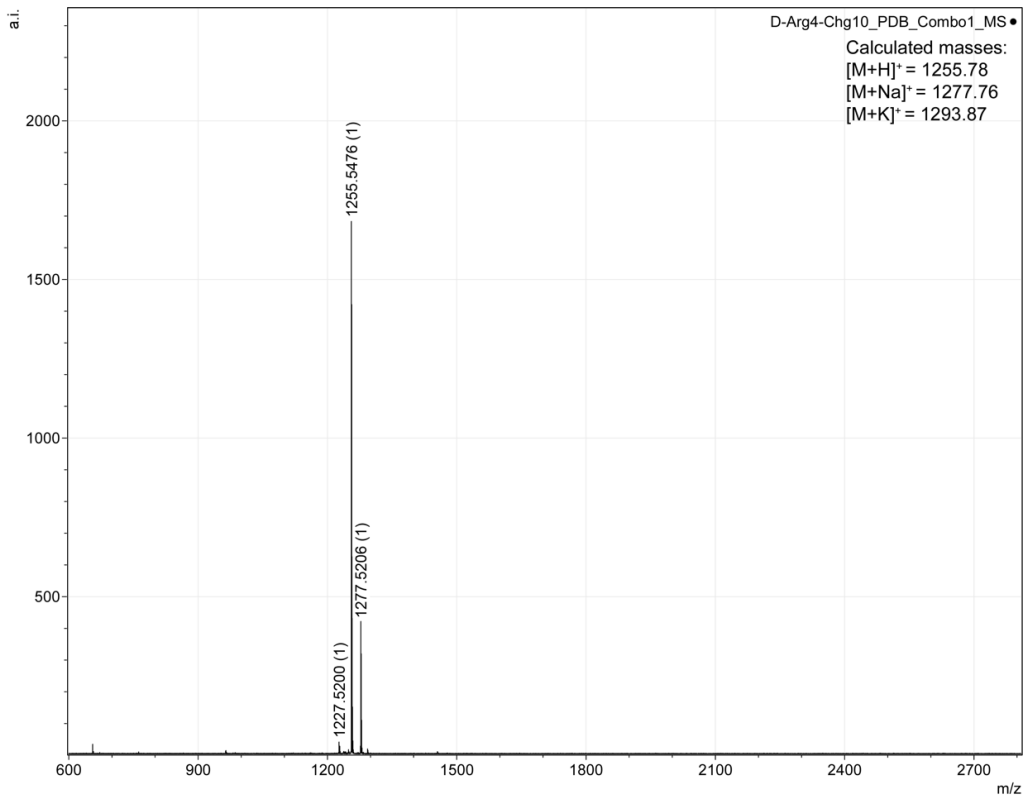
a.i.
D-Arg4-Chg10_PDB_Combo1_MS
Calculated masses:
[M+H]+ = 1255.78
[M+Na]+ = 1277.76
[M+K]+ = 1293.87
1255.5476 (1)
1277.5206 (1)
1227.5200 (1)
2000
1500
1000
500
600
900
1200
1500
1800
2100
2400
2700
m/z

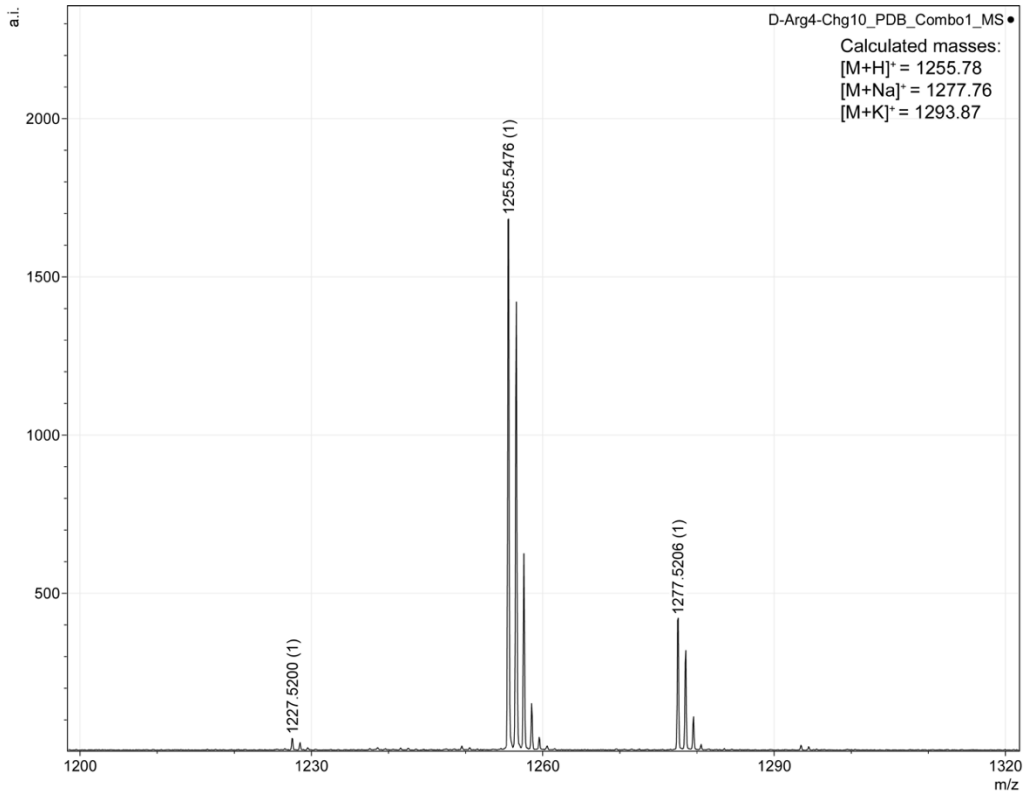
a.i.
D-Arg4-Chg10_PDB_Combo1_MS
Calculated masses:
[M+H]+ = 1255.78
[M+Na]+ = 1277.76
[M+K]+ = 1293.87
1255.5476 (1)
1277.5206 (1)
1227.5200 (1)
2000
1500
1000
500
1200
1230
1260
1290
1320
m/z

D-Arg$_4$,Chg$_{10}$-isobactin C Analytical HPLC Trace and MALDI-TOF

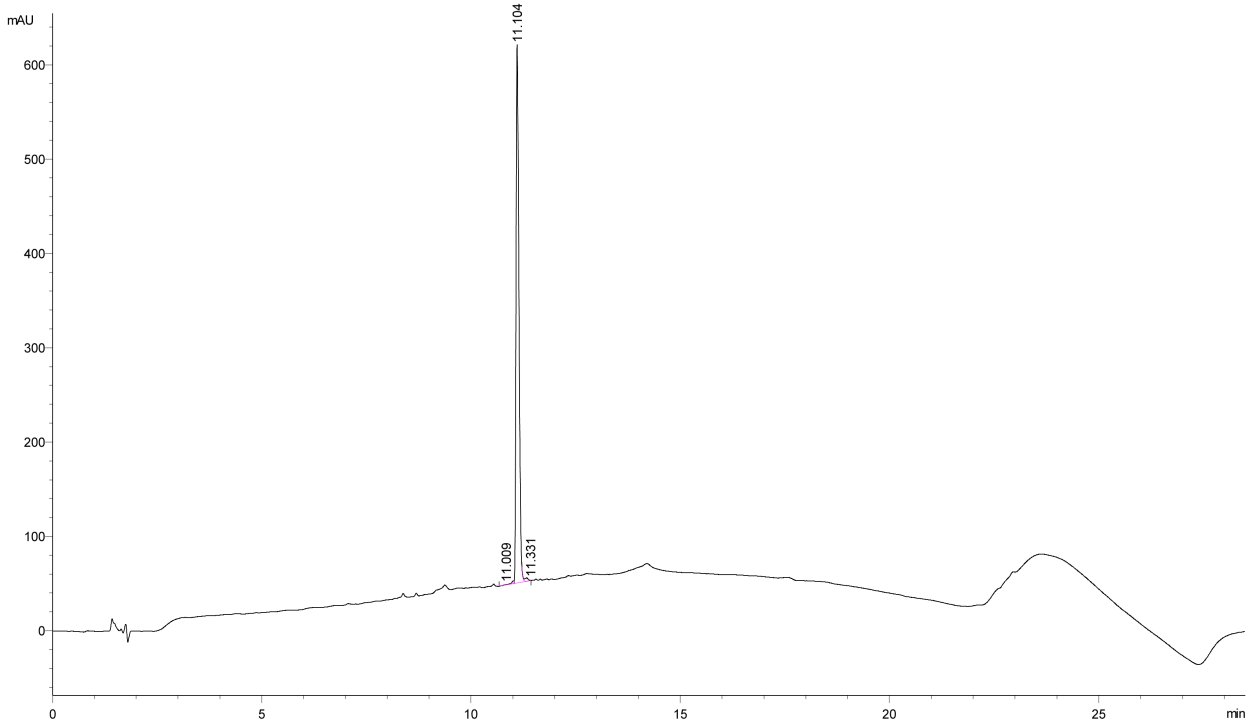

Peak #	RetTime [min]	Type	Width [min]	Area mAU *s	Height [mAU]	Area %
1	11.009	BV E	0.0711	14.43276	2.76251	0.5336
2	11.104	VV R	0.0705	2667.35986	571.05859	98.6239
3	11.331	VB E	0.0919	22.78377	3.50267	0.8424
Totals :				2704.57639	577.32378	

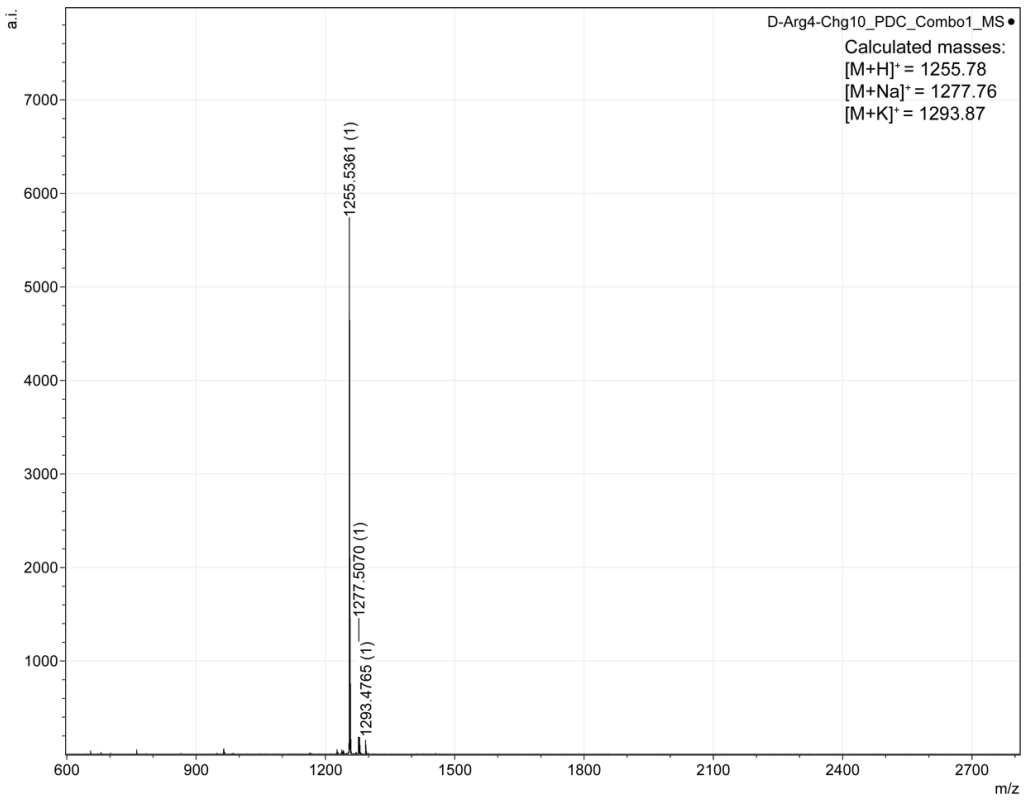
D-Arg4-Chg10_PDC_Combo1_MS
Calculated masses:
[M+H]+ = 1255.78
[M+Na]+ = 1277.76
[M+K]+ = 1293.87
1255.5361 (1)
1277.5070 (1)
1293.4765 (1)
a.i.
m/z

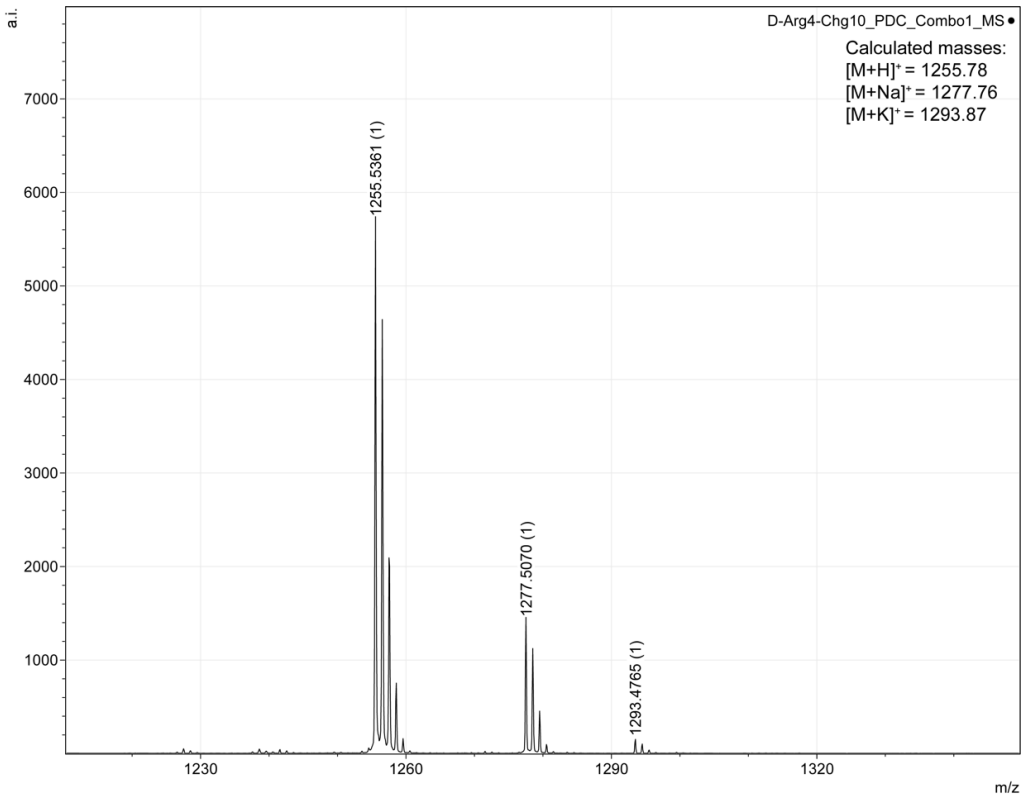
D-Arg4-Chg10_PDC_Combo1_MS
Calculated masses:
[M+H]+ = 1255.78
[M+Na]+ = 1277.76
[M+K]+ = 1293.87
1255.5361 (1)
1277.5070 (1)
1293.4765 (1)
a.i.
m/z

Chapter 4

Efforts Towards the Synthesis of Teixobactin and Isobactins A, B, and C

INTRODUCTION

Natural teixobactin contains the noncanonical amino acid L-*allo*-enduracididine (*allo*-End) at position 10 (Figure 4.1).[1] This noncanonical amino acid is difficult to synthesize and not commercially available. Therefore, many analogues of teixobactin in which the *allo*-End was replaced with commercially available amino acids have been reported.[2] Many potent analogues of teixobactin have been synthesized, with some of the most potent analogues containing cationic or hydrophobic residues at position 10.[2–7] Although these analogues still exhibit good antibiotic activity, they are not as active as teixobactin itself because the *allo*-End makes critical contacts with the MurNAc residue in lipid II and related cell-wall precursors.[8,9]

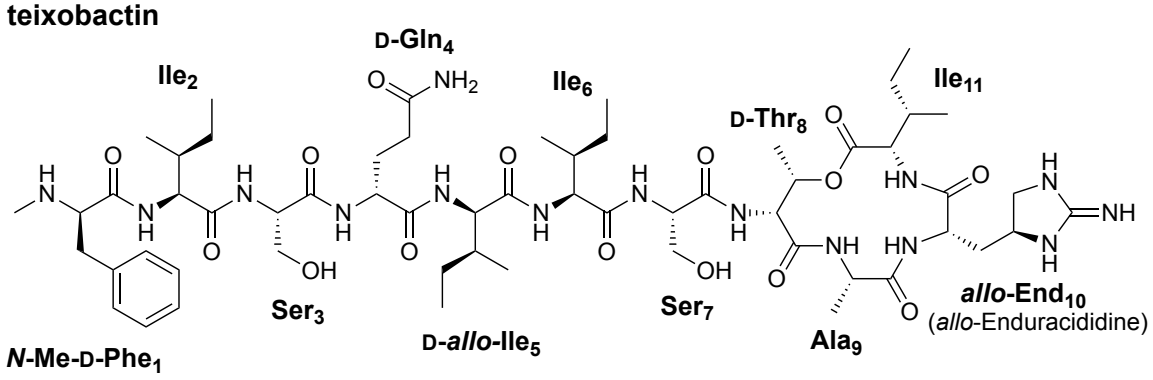

Figure 4.1. Structure of natural teixobactin.

Our goal was to synthesize the *O*-acyl isopeptide prodrugs, isobactins, of teixobactin, by incorporation of the native *allo*-End. To achieve this we first aimed to synthesize Fmoc-L-*allo*-End(Cbz)$_2$-OH which could be easily incorporated into our SPPS protocol developed for the

isobactin analogues. Teixobactin is not the only peptide natural product that contains enduracididine (End) in some form but very few syntheses of *allo*-End exist. Before the discovery of teixobactin, only a couple syntheses of enduracididine were reported, with Shiba *et al*. and Dodd *et al*. reporting the syntheses of End and *allo*-End (Figure 4.2).[10–12] With the discovery of teixobactin came a reinvigoration on the synthesis of enduracididine. The Du Bois lab in 2014 reported a synthesis of End and *allo*-End.[13] The research group that also discovered teixobactin included a synthesis of *allo*-End in their patent of teixobactin.[14] In 2015, Yuan *et al*. reported the synthesis of *allo*-End and in 2016 the Payne group reported their total synthesis of teixobactin which included their synthetic procedure for the synthesis of *allo*-End.[15,16] In 2019, Rao *et al*. published a new synthesis of *allo*-End leading to the gram-scale synthesis of teixobactin.[17] Most recently, Chandrasekhar *et al*. in 2021 reported the synthesis of Boc-End(Cbz)$_2$-OH.[18]

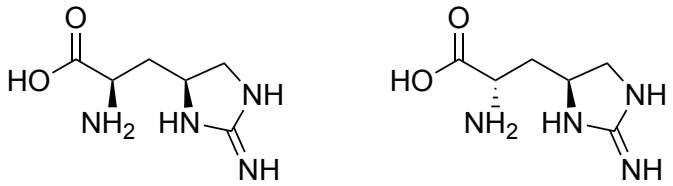

Figure 4.2. Structures of L-enduracididine (End) and L-*allo*-enduracididine (*allo*-End).

Proposed approach to the synthesis of Fmoc-L-*allo*-End(Cbz)$_2$-OH and isobactins A, B, and C

For our work, we decided to synthesis L-*allo*-enduracididine using the route reported by Rao *et al*. in 2019. This convergent synthesis affords the Fmoc-protected methyl ester of L-*allo*-End. We then planned to convert the methyl ester to the suitably protected Fmoc-L-*allo*-End(Cbz)$_2$-

OH. This building block could then be incorporated into our established SPPS protocol described in chapter 2 for the synthesis of teixobactin and isobactins A, B, and C (Figure 4.3).

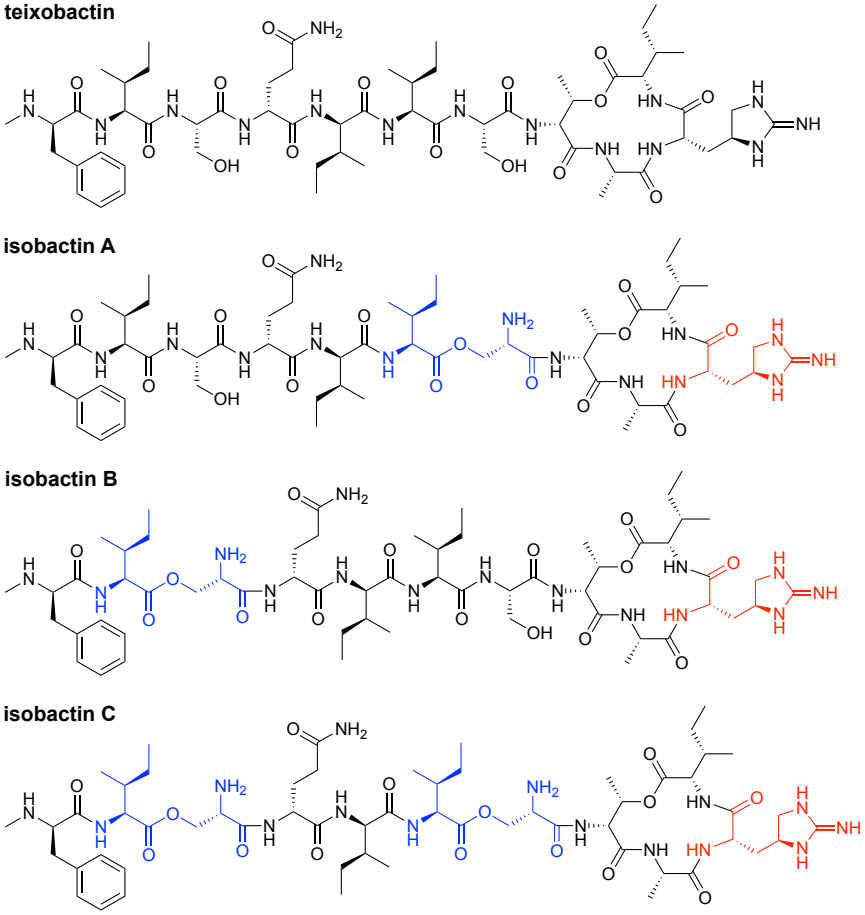

Figure 4.3. Structures of teixobactin and isobactins A, B, and C.

We planned to synthesis the Fmoc-L-*allo*-End(Cbz)$_2$-OH as shown in Scheme 4.1. Guanidine hydrochloride will first be converted to Cbz-guanidine (**1**). L-Allylglycine will be Fmoc protected with Fmoc-OSu and $NaHCO_3$. Coupling of the Cbz-guanidine (**1**) and Fmoc-allylglycine (**2**) in the presence of BOP and NMM will afford acylguanidine **3**. Intramolecular cyclization with iodine and $NaHCO_3$ forms a bicyclic intermediate that can then be converted to the methyl ester **4** through an acid-catalyzed methanolysis and subsequent Cbz protection of the guanidine group.

Rao *et al*. found that treatment with LiOH at 0 °C for four minutes selectively saponifies the methyl ester without significant loss of the Cbz protecting groups. We anticipate that the Fmoc on the α-amino group will be removed in these conditions, and we will thus re-protect the α-amino group with Fmoc-OSu and $NaHCO_3$ to yield Fmoc-L-*allo*-End(Cbz)$_2$-OH.

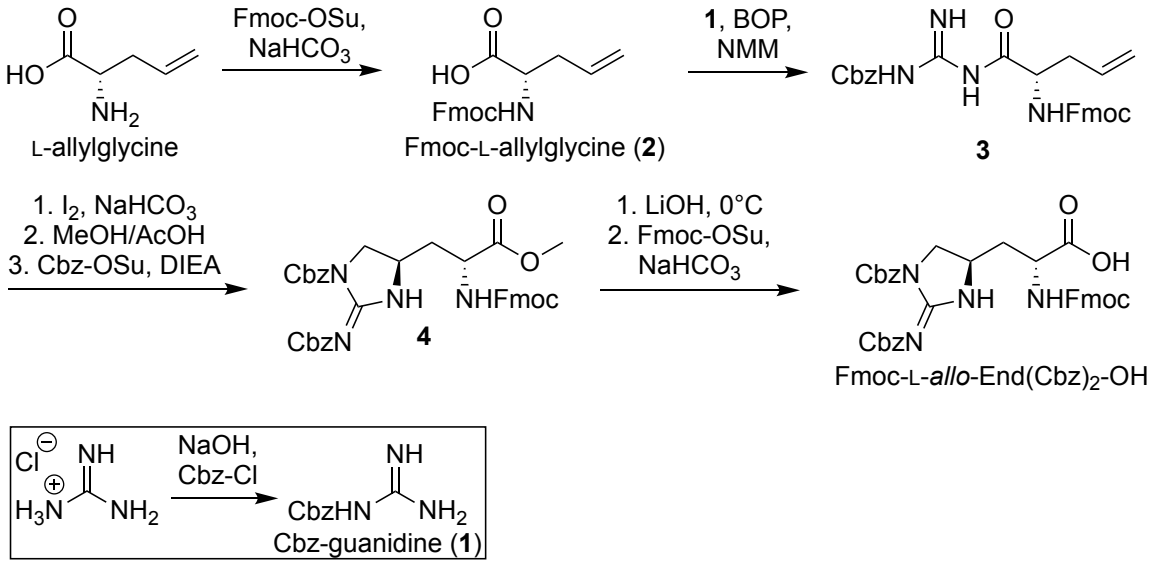

Scheme 4.1. Synthetic route to Fmoc-L-*allo*-End(Cbz)$_2$-OH.

Once we completed the synthesis of Fmoc-L-*allo*-End(Cbz)$_2$-OH, we planned to synthesize isobactins A, B, and C using the same route we have established for the all previously synthesized isobactin analogues with Fmoc-L-*allo*-End(Cbz)$_2$-OH in place of Fmoc-Lys(Boc)-OH described in chapter 2 (Scheme 2.1).[19] To the synthesis, we will include a hydrogenation step in the final deprotection using H_2 and $Pd(OH)_2/C$ in MeOH and formic acid to remove the Cbz groups.[17] This hydrogenation step will be completed before the TFA global deprotection step in our standard SPPS protocol for the synthesis of natural teixobactin and isobactins A, B, and C.

RESULTS AND DISCUSSION

Synthesis of Fmoc-End(Cbz)$_2$-OMe

We began with my undergraduate student, Grant Lai, pursuing the synthesis of Fmoc-L-*allo*-End(Cbz)$_2$-OH following the above described conditions (Scheme 4.1). Grant was able to successfully synthesize the methyl ester **4** with a yield of 298.7 mg. As the synthesis of *allo*-End is complex, we were also able to contract Charnwood Discovery to synthesize Fmoc-End(Cbz)$_2$-OMe, following the Rao *et al*. synthesis published in 2019. With methyl ester **4** in hand, provided by Grant and the roughly 30 g purchased from Charnwood Discovery, we were able to begin pursuing the hydrolysis reaction to afford Fmoc-L-*allo*-End(Cbz)$_2$-OH for the incorporation into our SPPS protocol.

Hydrolysis of methyl ester

As previously stated, Rao *et al*. found that treatment of the methyl ester with LiOH at 0 °C for four minutes selectively hydrolyzed the methyl ester without significant loss of the Cbz protecting groups. In the Rao synthesis, they took Fmoc-L-*allo*-End(Cbz)$_2$-OMe (**4**) and Fmoc deprotected to allow for coupling of the amine to alloc-Ala-OH affording the dipeptide Alloc-Ala-allo-End(Cbz)$_2$-OMe (Scheme 4.2). They then performed hydrolysis of the methyl ester using LiOH to afford Alloc-Ala-*allo*-End(Cbz)$_2$-OH. We believed we could use these conditions on Fmoc-L-*allo*-End(Cbz)$_2$-OMe, but anticipated the Fmoc on the α-amino group would be removed in these conditions. Therefore, we planned to re-protect the α-amino group with Fmoc-OSu and $NaHCO_3$ to yield Fmoc-L-*allo*-End(Cbz)$_2$-OH.

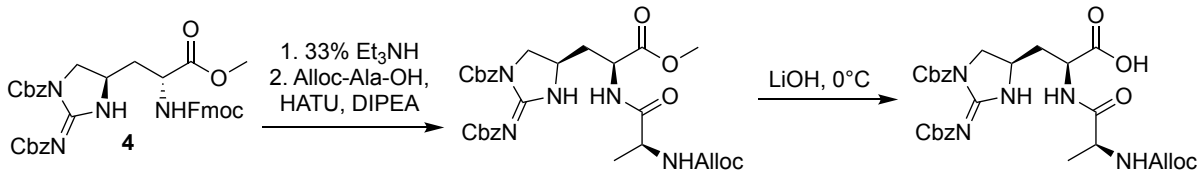

Scheme 4.2. Synthetic procedure performed by Rao *et al*. to obtain their carboxylic acid dipeptide building block, Alloc-Ala-*allo*-End(Cbz)$_2$-OH (**6**).[17]

Initial attempts by Grant using these conditions were unsuccessful at obtaining the desired hydrolyzed product (Figure 4.4, entry 1). Modifications such as reaction time temperature did not prove successful. When setting up a reaction myself to test different bases such as KOH instead of LiOH, I noticed an error in the conditions Grant was using. Based on the Rao synthesis, the hydrolysis reaction was run at a concentration of 304 mM, but Grant was running the reaction at 50 mM. Reattempting the hydrolysis at 25 °C, but at the correct concentration provided some conversion of methyl ester **4** to the expected product **5** (Table 4.1, entries 4 and 5). Further optimization of increasing reaction time to 60 mins and returning to 0 °C gave complete conversion of the starting material **4** to L-*allo*-End(Cbz)$_2$-OH **5** (table 4.1, entry 6).

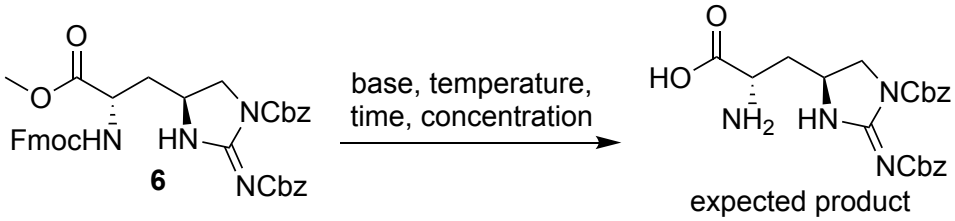

entry	base	temp (°C)	time (mins)	concentration (M)	outcome
1	LiOH	0	4	0.05	No hydrolysis
2	LiOH	0	10	0.05	No hydrolysis
3	LiOH	25	60	0.05	No hydrolysis
4	LiOH	25	10	0.3	Partial hydrolysis + Fmoc deprotection
5	KOH	25	10	0.3	Partial hydrolysis + Fmoc deprotection
6	LiOH	0	60	0.3	Complete hydrolysis + Fmoc deprotection

Figure 4.4 and Table 4.1. Overview of the reaction conditions that were attempted for hydrolysis of methyl ester **4** to the expected product **5**.

With the optimized LiOH hydrolysis conditions in hand, we proceeded to resubject the material to Fmoc protection to afford the desired Fmoc-L-*allo*-End(Cbz)$_2$-OH. We did this by adding equimolar 1 M HCl to the reaction to neutralize the LiOH. Upon addition of the HCl, solids precipitated out of the solution. We believed that the addition of the Fmoc-OSu dissolved in THF would help resolubilize any material as we would bring the reaction back to a 3:1 ratio of THF:H_2O. We proceeded to Fmoc-protect this material by adding Fmoc-OSu in THF and $NaHCO_3$ and allowing to stir overnight. Analysis of the reaction after 24 h showed only the starting material **5** and no desired product, suggesting the Fmoc protection did not occur.

We hypothesized that solubility may by playing a role in the incomplete Fmoc-protection of the α-amino group, as the material obtained from the LiOH hydrolysis was quite insoluble after the addition of the 1 M HCl. We attempted to increase the THF to water ratio to 5:1 instead of 3:1

as well as test a stronger base to see if this would help improve the Fmoc protection reaction. I began the reaction by dissolving starting material **4** in 5:1 THF:H_2O. LiOH was then added to the reaction and allowed to stir for 1 h, before the addition of 1 M HCl to quench the reaction. I carried onto the Fmoc-protection by adding the Et_3N as the base, followed by Fmoc-OSu in THF. The reaction was allowed to stir on ice for 1 h, before stirring for 24 h at room temperature. The reaction was then acidifying on ice to pH 3, concentrated to remove THF, extracted in EtOAc, and the organic layer was isolated as a solid. Analysis of the solid by mass spectrometry (MS) that the material was still the Fmoc-deprotected starting material **5**.

Further analysis of this material led us to believe that the mass we were seeing corresponded to the carbamate intermediate formed during Fmoc deprotection by LiOH, but that the CO_2 was ionizing off upon MS analysis (Figure 4.5). This would suggest that the LiOH was not fully deprotecting the Fmoc group on the α-amino group and stalling at the carbamate. This would further support the reason as to why solids were present during the reaction after hydrolysis and during and after the extraction of the product following the Fmoc-protection reaction. These solids were highly insoluble, further supporting this hypothesis. As we now believed the reaction was stalling at the carbamate, our goal was to find a way to prevent carbamate formation all together by either Fmoc deprotecting the amino acid before hydrolysis or using acidic conditions for the hydrolysis instead of basic conditions.

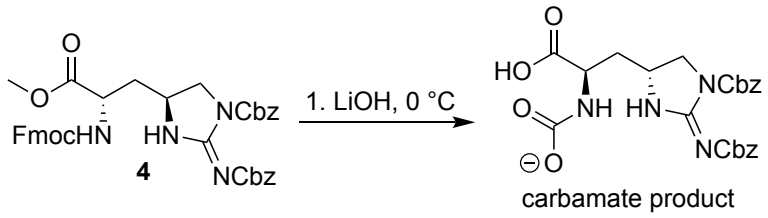

Figure 4.5. Hypothesized carbamate product formed during LiOH hydrolysis of methyl ester **4**.

I first began by testing Fmoc deprotection conditions, in which we would first Fmoc deprotect methyl ester **4**, then saponify using LiOH, before re-protecting the α-amino group to obtain Fmoc-L-*allo*-End(Cbz)$_2$-OH. Conditions tested included 20% piperidine, 5% piperidine, and 33% diethylamine (Figure 4.6, Table 4.2). All attempted Fmoc deprotection reactions resulted in Cbz deprotection and decomposition of product when carried onto the LiOH hydrolysis or Fmoc protection. Any solids obtained from these reactions were also highly insoluble in any organic solvent including MeOH, EtOAc, DCM, and DMF, suggesting the solids were not the desired amino acid product.

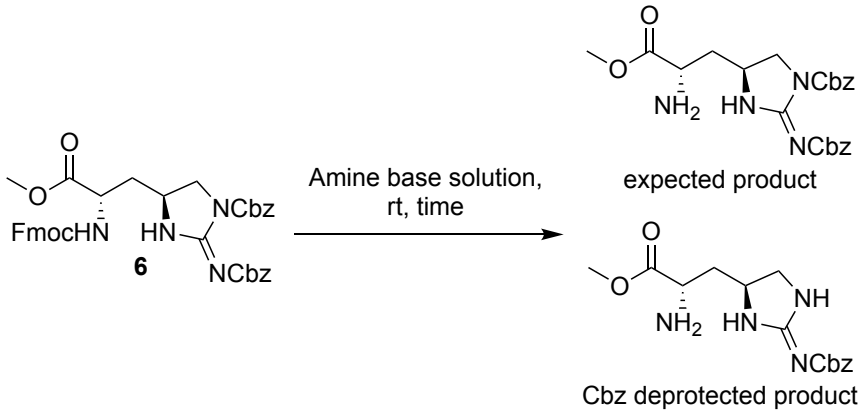

entry	base solution	time (h)	outcome
1	20% piperidine in 3:1 THF:H_2O	1	Fmoc deprotection + Cbz deprotection
2	5% piperidine in 3:1 THF:H_2O	1	Fmoc deprotection + Cbz deprotection
3	33% Et_2NH in MeCN	2	Fmoc deprotection + Cbz deprotection

Figure 4.6 and Table 4.2. Overview of the reaction conditions that were attempted for Fmoc deprotection of methyl ester **4**.

Following attempts to Fmoc deprotect Fmoc-L-*allo*-End(Cbz)$_2$-OMe before subsequent hydrolysis and Fmoc protection, I attempted to perform an acid-catalyzed hydrolysis of the methyl ester (Figure 4.7, Table 4.3). Unfortunately, all attempts to convert the starting material to Fmoc-

L-*allo*-End(Cbz)$_2$-OH under acidic conditions led to Cbz deprotection. Purification of these attempts indicated that the major product for all reactions was the Cbz deprotected Fmoc-L-*allo*-End(Cbz)-OH.

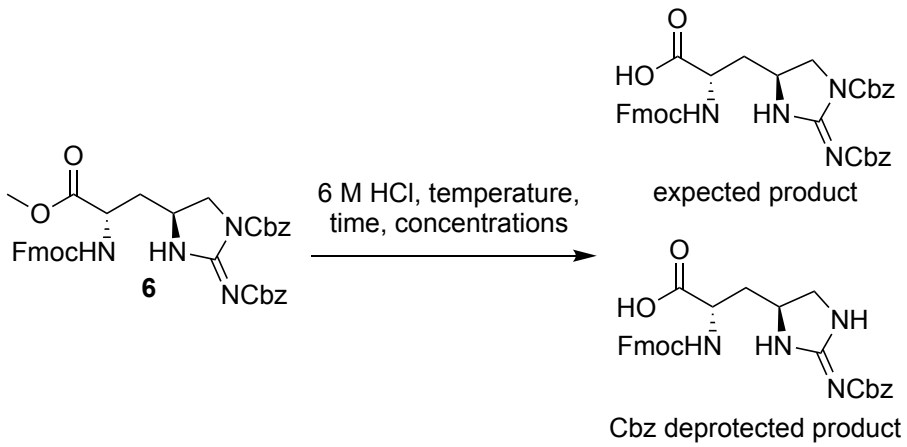

entry	temp (°C)	time (h)	starting material concentration (M)	final HCl concentration (M)	outcome
1	0 →30	24	0.1	1.5	Partial hydrolysis + loss of Cbz
2	30	24	0.1	3	Partial hydrolysis + loss of Cbz
3	30	24	0.2	1.5	Partial hydrolysis + loss of Cbz

Figure 4.7 and Table 4.3. Overview of the reaction conditions that were attempted for acid-catalyzed hydrolysis of methyl ester **4**.

With the attempts at hydrolysis in both acidic and basic conditions proving unsuccessful as well as attempts to Fmoc deprotect, new conditions needed to be tested. One recommendation for they hydrolysis was the use of trimethyltin hydroxide (Me_3SnOH). Studies have shown that Me_3SnOH can successfully hydrolyze methyl esters in the presence of both Fmoc and Cbz protecting groups.[20–24] Looking to the literature, common conditions include 5 equivalents of Me_3SnOH in 1,2-DCE at 80 °C (Figure 4.8). After 1 h, no starting material was observed and so

the reaction was worked-up to afford the crude product (Table 4.4, entry 1). Analysis of this crude product indicated successful hydrolysis, but also a large quantity of the Cbz deprotected by-product. Purification of this reaction yielded roughly 30 mg of product in a 15% yield.

Although the hydrolysis in Me_3SnOH afforded a mixture of desired product and the Cbz deprotected by-product, I believed that these reaction conditions could be improved to minimize Cbz deprotection. Through a series of optimization reactions (Table 4.4, entries 2–6), including the identification of extraction issues, I was able to obtain the final optimized conditions that consistently afforded yields ≥80%, with the ability to isolate any unreacted starting material to be resubjected to hydrolysis conditions (Table 4.4, entry 7). Now that hydrolysis conditions had been identified, the purified Fmoc-L-*allo*-End$(Cbz)_2$-OH could be incorporated into our SPPS procedure for the synthesis of teixobactin and isobactins A, B, and C.

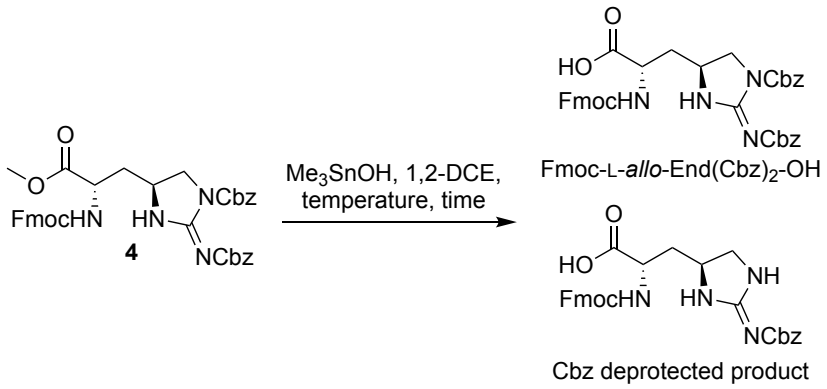

entry	Me_3SnOH equivs	temp (°C)	time (h)	outcome
1	5	80	1	Hydrolysis + Cbz deprotection
2	5	40 → 50	3	Hydrolysis + Cbz deprotection
3	6	40	4	Hydrolysis + Cbz deprotection. Issues with workup
4	4	40	4	Hydrolysis + starting material. Issues with workup
5	5	40	3.5	Hydrolysis + starting material
6	5	40	3.5	Hydrolysis + starting material
7	5	40	3	Hydrolysis + starting material

Figure 4.8 and Table 4.4. Overview of the reaction conditions that were attempted for the hydrolysis of methyl ester **4** using trimethyltin hydroxide (Me_3SnOH).

Attempts towards the synthesis of natural teixobactin

Initial synthetic attempt of natural teixobactin

While attempting to hydrolyze the methyl ester to the carboxylic acid for SPPS, I also pursued the synthesis of teixobactin. Hydrolysis using LiOH did lead to the desired product, but over the course of the reaction the carbamate side product would out compete the desired hydrolyzed product. Therefore, I attempted to hydrolyze the methyl ester using LiOH, but only allowed the reaction to occur for 15 minutes. Based on MS, there was starting material, the

hydrolyzed product, and the carbamate side product. Although these other products were present, these impurities theoretically should not cause any problems in the synthesis of the desired product, just possibly lead to less loading of the desired carboxylic acid.

With the mixture in hand, I loaded 2-chlorotrityl chloride resin following our standard SPPS protocol. The resin was allowed to load for eight hours before the any unreacted sites on the resin were capped with MeOH. I proceeded to synthesize the peptide following the standard SPPS protocol for our teixobactin analogues, but with the additional hydrogenation of the Cbz groups on the *allo*-End before the TFA global deprotection.[17,19] After global deprotection, the peptide was ether precipitated and the pellet was resuspended in a 30% MeCN in H_2O. The peptide was then frozen and lyophilized to obtain the dry, crude powder.

Analysis of the crude lyophilized peptide by MALDI MS revealed a mixture of products, with two of the identified masses corresponding to the desired product and a peptide with a $[M+H]^+$ of 1129. This mass corresponds to an Ile deletion in the peptide (Figure 4.9A). Analytical RP-HPLC analysis revealed several small peaks and one major peak (Figure 4.9B and C). Preparative purification of the peptide was then performed, and fractions were collected and analyzed by MALDI MS and analytical HPLC. Based on the data obtained, the major peak present in the crude analytical trace was associated Ile deletion peptide. Although there are three possible Ile that could have led to this product, I hypothesized that Ile_{11} was the deletion leading to this major impurity. This is because the esterification is sensitive to steric hinderance, and I hypothesized that the *allo*-End and the Cbz protecting groups would cause increased steric hinderance.

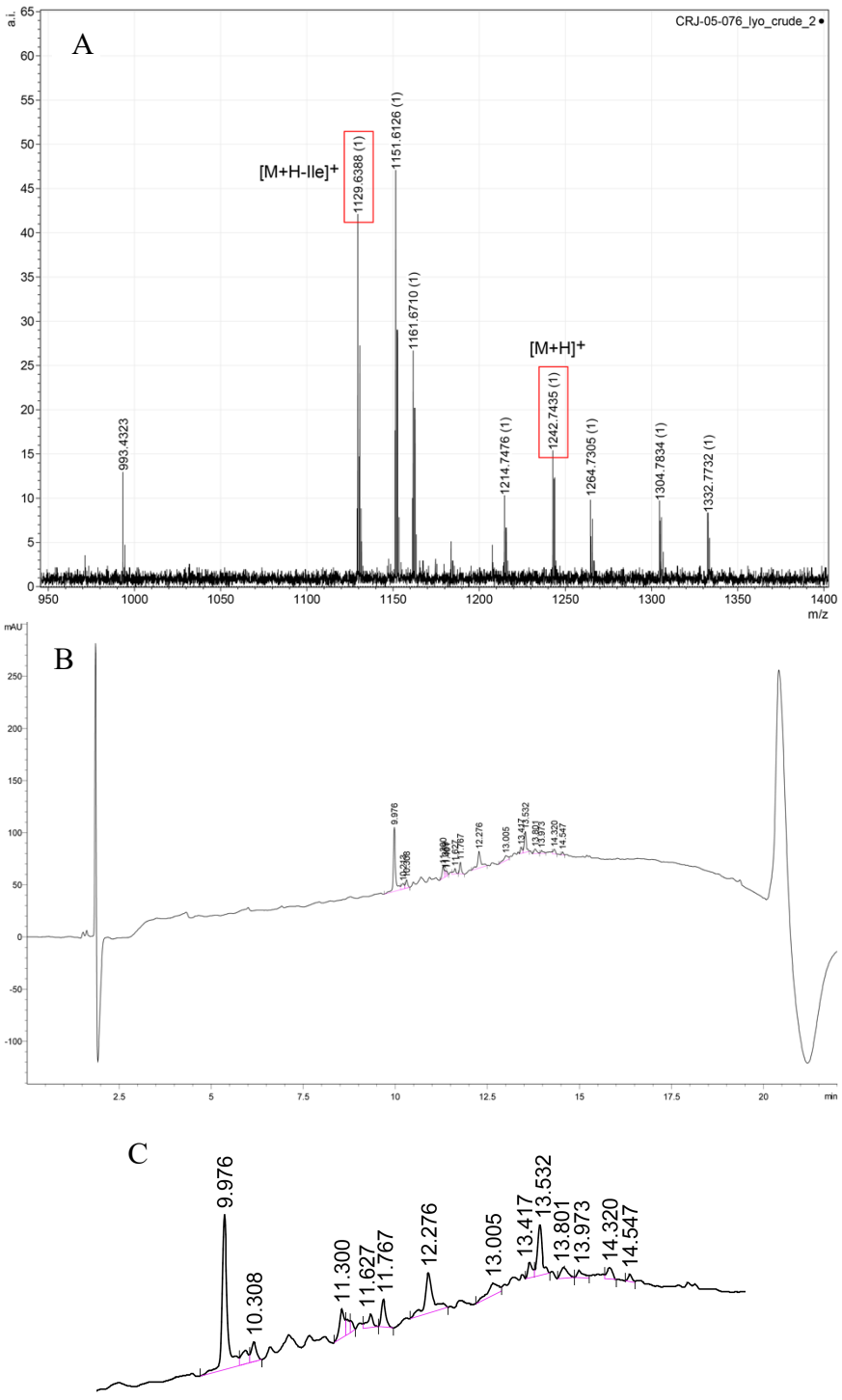

Figure 4.9. Data for CRJ-05-076, initial synthetic attempt of natural teixobactin. (A) MALDI MS spectrum of crude lyophilized peptide labeled with the $[M+H]^+$ of the desired product and Ile deletion product. (B) Analytical RP-HPLC trace of the crude lyophilized peptide. (C) Expansion of analytical RP-HPLC trace in B.

Second synthetic attempt of natural teixobactin

Upon the second attempt at synthesizing natural teixobactin I had discovered the trimethyl tin hydroxide hydrolysis conditions for Fmoc- L-*allo*-End(Cbz)$_2$-OMe. Therefore for this attempt, I loaded purified Fmoc-L-*allo*-End(Cbz)$_2$-OH onto 2-chlorotrityl chloride resin. I followed the same procedure for the synthesis of this batch of teixobactin as I had previously performed for CRJ-05-076. The MALDI MS and analytical RP-HPLC trace of the crude material for this peptide was similar to CRJ-05-076, with the major peak corresponding to an Ile deletion (Figure S4.1). Purification attempts to isolate and identify which peak in the analytical trace corresponded to the desired product were unsuccessful.

Attempts towards the synthesis of the isobactins

The synthesis of natural teixobactin has already been completed and wasn't the goal of this project, so at this point we decided instead to pursue the synthesis of the isobactins. I have consistently seen that synthesis of isobactin A analogues leads to the highest yields and lowest epimerization of Ile$_{11}$ during the esterification. I hypothesis that the *O*-acyl bond occurring so early in the synthesis of this prodrug helps break up aggregation on resin, leading to a cleaner synthesis and less sterics, allowing for facile esterification of Ile$_{11}$. With this guiding hypothesis, I began to pursue the synthesis of isobactin A.

Initial synthetic attempt of isobactin A

Following the standard SPPS protocol for the synthesis of isobactin A, I loaded purified Fmoc-L-*allo*-End(Cbz)$_2$-OH onto resin and synthesized the peptide as usual. After full deprotection of the peptide, I lyophilized the crude peptide for analysis by MALDI MS and RP-

HPLC. MALDI MS of the crude peptide showed the presence of the desired peptide mass and no mass associated with the Ile deletion, although, there were many other masses present in the spectrum (Figure 4.10A). Analysis of the peptide by analytical RP-HPLC revealed dozens of peaks (Figure 4.10B). Although there were dozens of impurities, I still attempted to purify the peptide and attempt to determine which peak in the analytical trace corresponded to the desired product. These attempts unfortunately proved unsuccessful as I could only obtain fractions containing my desired mass, but these fractions had multiple, small peaks.

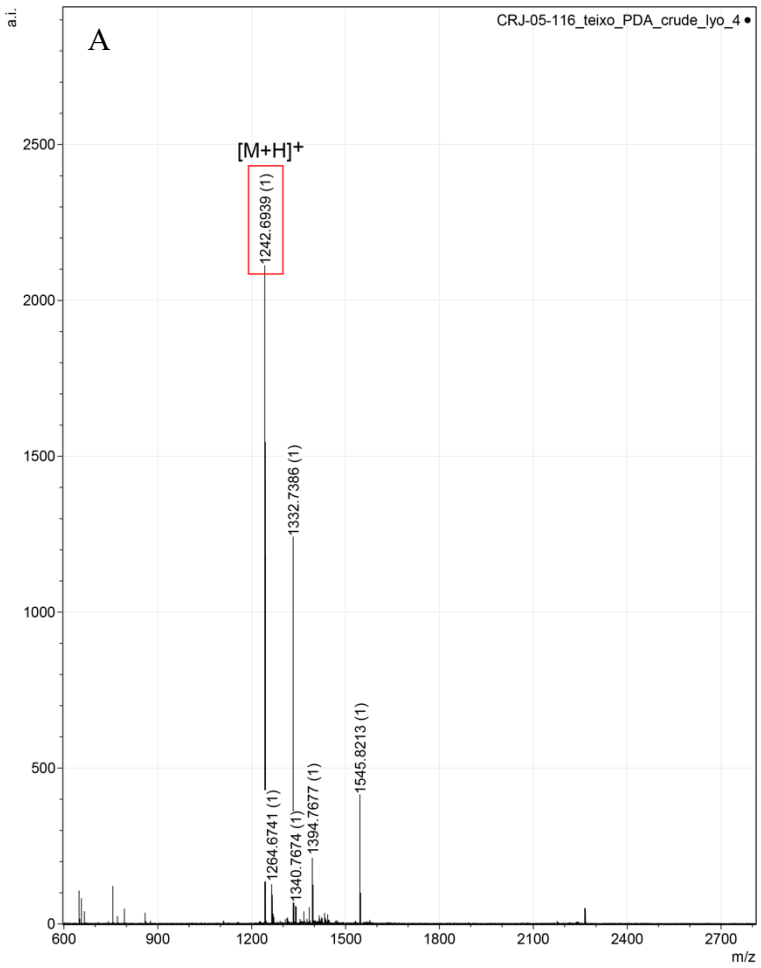

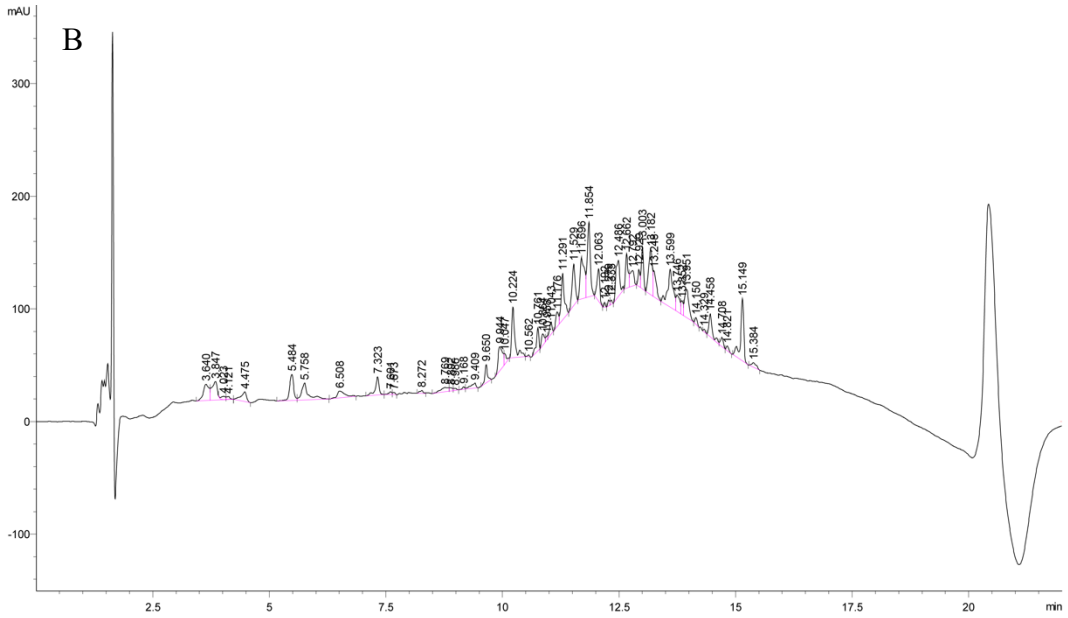

Figure 4.10. Data for CRJ-05-116, initial synthetic attempt of isobactin A. (A) MALDI MS spectrum of crude lyophilized peptide labeled with the $[M+H]^+$ of the desired product. (B) Analytical RP-HPLC trace of the crude lyophilized peptide.

I hypothesized that the loading of *allo*-End$_{10}$ onto resin was the cause for the formation of dozens of impurities. In the attempts to hydrolyze methyl ester **4** to the carboxylic acid, I had determined that the use of 20% piperidine, and even 5% piperidine, to Fmoc deprotect the peptide led to the loss of a Cbz protecting group on the cyclic guanidine sidechain (Figure 4.6, Table 4.2). As I had previously determined that piperidine could lead to Cbz deprotection, I hypothesized the formation of dozens of impurities was caused by the Cbz deprotection of the *allo*-End residue on resin and coupling of amino acids onto this deprotected amine. The deprotection of the *allo*-End sidechain could occur at any point in the linear synthesis of the peptide, therefore leading to many possible addition products. Analysis of the masses seen in the crude peptide in MALDI MS did reveal impurities that corresponded to additions of one or more amino acid, further supporting my hypothesis.

Re-routing the synthesis of isobactin A

As the attempts at loading Fmoc-L-*allo*-End(Cbz)$_2$-OH onto resin led to dozens of products and with my hypothesis of Cbz deprotection occurring during the SPPS, I decided to re-route the synthesis to minimize these impurities. This re-route of the synthesis was to load Ala$_9$ onto resin instead of *allo*-End$_{10}$ and then couple in the *allo*-End$_{10}$ after the esterification of Ile$_{11}$ and before cleavage from resin. Therefore, I began the synthesis by loading Ala$_9$ onto resin and synthesizing the peptide following the procedure for the isobactins. After the esterification of Ile$_{11}$, Fmoc deprotection afforded the free amine. The Fmoc-L-*allo*-End(Cbz)$_2$-OH building block was then coupled onto Ile$_{11}$ before Fmoc deprotection, cleavage from resin, and macrocyclization. Once cyclized, the peptide was hydrogenated to remove the Cbz protecting groups followed by TFA global deprotection to remove all other protecting groups. The deprotected peptide was then ether precipitated to remove TFA before the peptide was resuspended in a water/acetonitrile solution, frozen, and lyophilized.

Analysis of the crude, lyophilized peptide was done to ascertain purity and verify the desired product was present. MALDI MS of the crude peptide revealed the desired peptide was synthesized, but also revealed that a peptide impurity with a $[M+H]^+$ of 1088 (Figure 4.11A). This mass corresponds to an *allo*-End deletion in the peptide. Analytical RP-HPLC showed the presence of multiple small peaks and one major peak (Figure 4.11B). Purification of the crude peptide on the Biotage and analysis of the fractions by RP-HPLC and MALDI MS revealed that the major peak corresponded to the *allo*-End$_{10}$ deletion product. The poor coupling of *allo*-End$_{10}$ onto Ile$_{11}$ could be due to sterics and therefore, I reattempted the synthesis of isobactin A and adjusting a few conditions with the goal to minimize *allo*-End deletion.

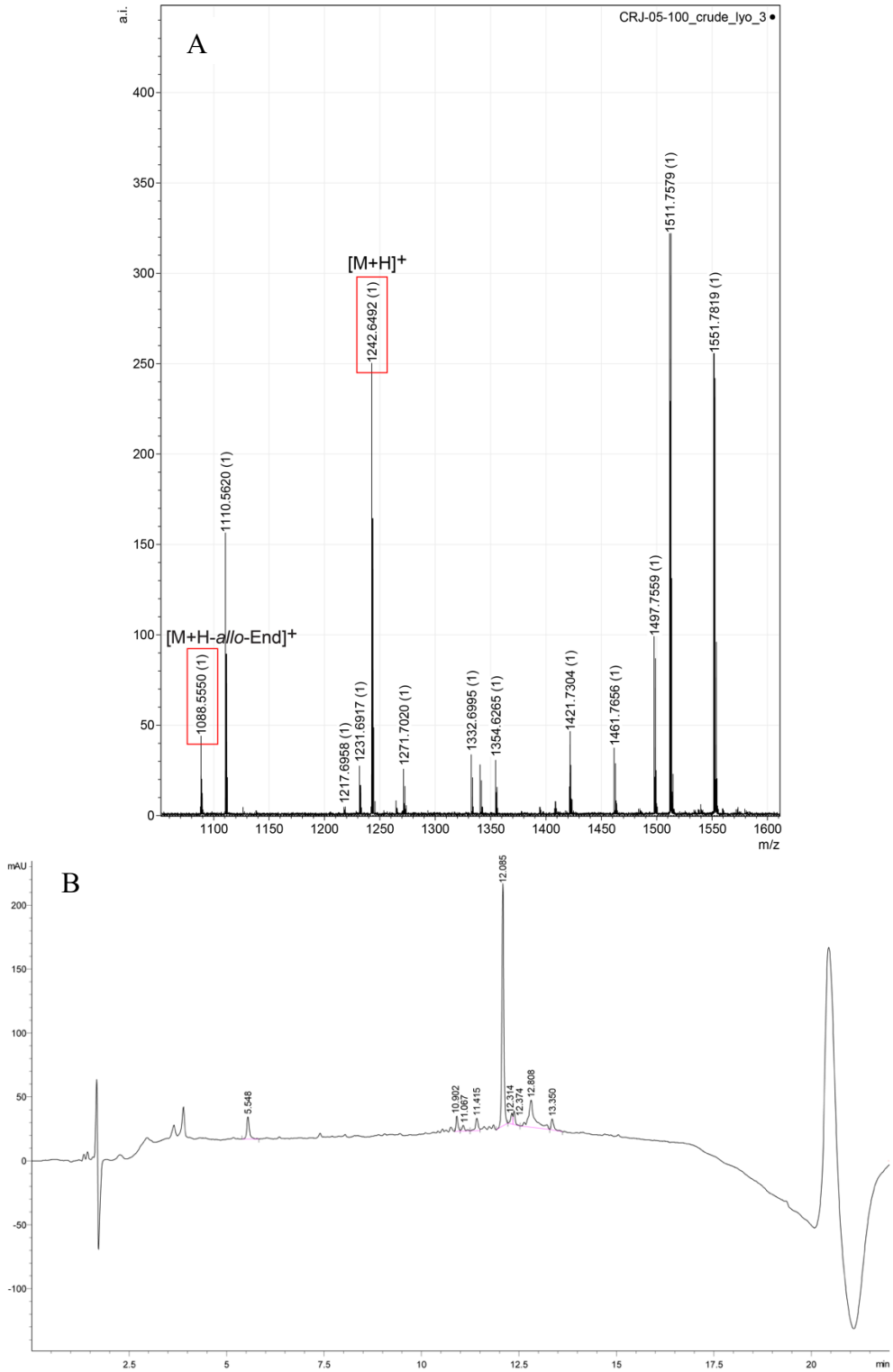

Figure 4.11. Data for CRJ-05-100, the re-routing of the synthesis of isobactin A. (A) MALDI MS spectrum of crude lyophilized peptide labeled with the $[M+H]^+$ of the desired product and *allo*-End deletion product. (B) Analytical RP-HPLC trace of the crude lyophilized peptide.

Attempts to improve the synthesis of isobactin A

I began by following the same procedure for the loading and synthesis of the linear peptide as CRJ-05-100. Once Ile_{11} was esterified, I then continued to the coupling of *allo*-End_{10}. Standard coupling time of amino acids for teixobactin synthesis is 30 minutes, but as the previous attempt to couple the *allo*-End_{10} was poor, I hypothesized allowing a longer coupling time would allow for a higher yield. Our lab has also discovered that using stronger coupling agents, such as a combination of HATU and HOAt allows for more facile coupling of difficult amino acids.[25] Therefore, for the coupling I not only extended the coupling time from 30 min to 120 min, but I also utilized a mixture of HATU and HOAt instead of HCTU as my coupling agents.

After coupling for two hours, I completed the peptide as usual with cleavage from resin, solution-phase cyclization, deprotections, and lyophilization of the crude peptide. Analysis of the crude peptide by RP-HPLC and MALDI MS, again revealed the major product was the *allo*-End deletion peptide (Figure S4.2). Attempts at purifications to isolate the product that was present was unsuccessful and I was not able to fully determine which peak in the analytical RP-HPLC trace corresponded to my desired product.

Attempted synthesis of isobactins A, B, and C using Tentagel resin

I continued to hypothesize that sterics may be playing a role in the poor coupling of *allo*-End_{10} in my attempts to synthesis isobactin A. Therefore, in attempts to reduce sterics and allow for more complete coupling of the *allo*-End residue, I turned to the use of a different resin. Standardly, our lab uses 2-chlorotrityl chloride resin for the synthesis of our peptides, but the esterification and coupling of *allo*-End can face high sterics due to the proximity of these steps to the polystyrene resin bead. Therefore, I wanted to attempt the synthesis using TentaGel resin. This

resin still uses the chlorotrityl chloride group but attaches this moiety to the polystyrene bead through a PEG linker. I hypothesized this would allow for further separation of the loading site of the resin to the polystyrene resin bead, hopefully reducing sterics faced by the coupling of *allo*-End_{10} onto Ile_{11}.

The synthesis of the peptide followed the same procedure as CRJ-05-100, but with the use of TentaGel resin instead of 2-chlorotrityl chloride resin. The lyophilized crude peptide was again analyzed by MALDI MS, with the desired mass, the *allo*-End deletion mass, and a handful of other masses being present (Figure 4.12A). Analytical RP-HPLC of the crude peptide showed two peaks each making up about 22% of the sample (Figure 4.12B). One of these peaks corresponded to the *allo*-End_{10} deletion peptide as I had already determined the retention time of the product. The hopes were that the other peak corresponded to my desired peptide and therefore purifications were attempted to isolate the desired product. After multiple rounds of preparative RP-HPLC purifications, I was unable to successfully isolate the desired product. All fractions that contained the desired mass also contained impurities and none of these peaks corresponded to the retention time hypothesized to be the product (Figure S4.3).

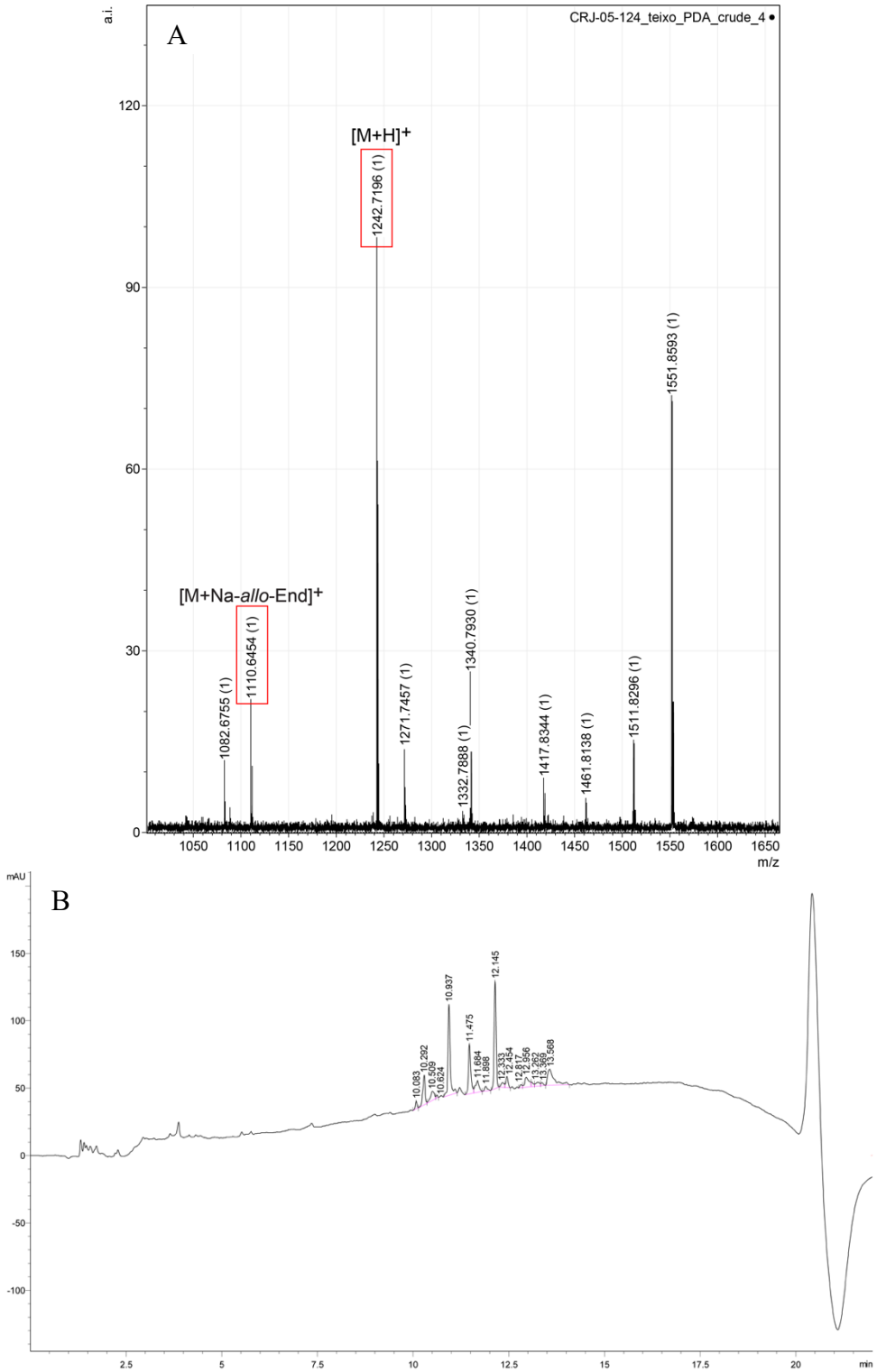

Figure 4.12. Data for CRJ-05-124, isobactin A. (A) MALDI MS spectrum of crude lyophilized peptide labeled with the $[M+H]^+$ of the desired product and the $[M+Na]^+$ of the *allo*-End deletion product. (B) Analytical RP-HPLC trace of the crude lyophilized peptide.

At the same time I was synthesizing isobactin A using TentaGel resin, I also attempted the syntheses of isobactins B and C on TentaGel resin. These peptides were synthesized followed the same procedure as CRJ-05-124. The analytical RP-HPLC seemed promising, but upon purification attempts of these peptides I was also unable to isolate any desired product or determine which peak in the analytical RP-HPLC traces corresponded to the product (Figures S4.4 and S4.5).

CONCLUSIONS

Teixobactin is a promising peptide antibiotic candidate with potent antibiotic activity against Gram-positive bacteria. However, the gel formation of teixobactin limits the preclinical development of teixobactin. *O*-Acyl isopeptide prodrugs, termed isobactins, of teixobactin analogues have shown to successfully delay gel formation and exhibit improved solubility in aqueous conditions. Although these isobactin prodrug analogues of teixobactin could be promising drug candidates on their own, none are as active as teixobactin itself. Therefore, the synthesis of teixobactin prodrugs, isobactins A, B, and C may be even superior drug candidates that circumvent the propensity of teixobactin to form gels in the aqueous conditions needed for intravenous administration. In this chapter I explored my attempts at the hydrolysis of Fmoc-L-*allo*-End(Cbz)$_2$-OMe to Fmoc-L-*allo*-End(Cbz)$_2$-OH for the incorporation into our SPPS protocol and my synthetic attempts at teixobactin and isobactins A, B, and C. Unfortunately, even with Fmoc-L-*allo*-End(Cbz)$_2$-OH in hand, none of the approaches in the synthesis of the isobactins have been successful.

REFERENCES AND NOTES

1. Ling, L. L.; Schneider, T.; Peoples, A. J.; Spoering, A. L.; Engels, I.; Conlon, B. P.; Mueller, A.; Schäberle, T. F.; Hughes, D. E.; Epstein, S.; Jones, M.; Lazarides, L.; Steadman, V. A.; Cohen, D. R.; Felix, C. R.; Fetterman, K. A.; Millett, W. P.; Nitti, A. G.; Zullo, A. M.; Chen, C.; Lewis, K. A New Antibiotic Kills Pathogens without Detectable Resistance. *Nature* **2015**, *517*, 455–459.

2. Karas, J. A.; Chen, F.; Schneider-Futschik, E. K.; Kang, Z.; Hussein, M.; Swarbrick, J.; Hoyer, D.; Giltrap, A. M.; Payne, R. J.; Li, J.; Velkov, T. Synthesis and Structure−activity Relationships of Teixobactin. *Annals of the New York Academy of Sciences* **2020**, *1459*, 86–105.

3. Jad, Y. E.; Acosta, G. A.; Naicker, T.; Ramtahal, M.; El-Faham, A.; Govender, T.; Kruger, H. G.; de la Torre, B. G.; Albericio, F. Synthesis and Biological Evaluation of a Teixobactin Analogue. *Org. Lett.* **2015**, *17*, 6182–6185.

4. Yang, H.; Chen, K. H.; Nowick, J. S. Elucidation of the Teixobactin Pharmacophore. *ACS Chem. Biol.* **2016**, *11*, 1823–1826.

5. Parmar, A.; Iyer, A.; Prior, S. H.; Lloyd, D. G.; Goh, E. T. L.; Vincent, C. S.; Palmai-Pallag, T.; Bachrati, C. Z.; Breukink, E.; Madder, A.; Lakshminarayanan, R.; Taylor, E. J.; Singh, I. Teixobactin Analogues Reveal Enduracididine to Be Non-Essential for Highly Potent Antibacterial Activity and Lipid II Binding. *Chem. Sci.* **2017**, *8*, 8183–8192.

6. Parmar, A.; Lakshminarayanan, R.; Iyer, A.; Mayandi, V.; Leng Goh, E. T.; Lloyd, D. G.; Chalasani, M. L. S.; Verma, N. K.; Prior, S. H.; Beuerman, R. W.; Madder, A.; Taylor, E. J.; Singh, I. Design and Syntheses of Highly Potent Teixobactin Analogues against Staphylococcus Aureus, Methicillin-Resistant Staphylococcus Aureus (MRSA), and Vancomycin-Resistant Enterococci (VRE) in Vitro and in Vivo. *J. Med. Chem.* **2018**, *61*, 2009–2017.

7. Jin, K.; Po, K. H. L.; Kong, W. Y.; Lo, C. H.; Lo, C. W.; Lam, H. Y.; Sirinimal, A.; Reuven, J. A.; Chen, S.; Li, X. Synthesis and Antibacterial Studies of Teixobactin Analogues with Non-Isostere Substitution of Enduracididine. *Bioorganic & Medicinal Chemistry* **2018**, *26*, 1062–1068.

8. Shukla, R.; Medeiros-Silva, J.; Parmar, A.; Vermeulen, B. J. A.; Das, S.; Paioni, A. L.; Jekhmane, S.; Lorent, J.; Bonvin, A. M. J. J.; Baldus, M.; Lelli, M.; Veldhuizen, E. J. A.; Breukink, E.; Singh, I.; Weingarth, M. Mode of Action of Teixobactins in Cellular Membranes. *Nat Commun* **2020**, *11*, 2848.

9. Shukla, R.; Lavore, F.; Maity, S.; Derks, M. G. N.; Jones, C. R.; Vermeulen, B. J. A.; Melcrová, A.; Morris, M. A.; Becker, L. M.; Wang, X.; Kumar, R.; Medeiros-Silva, J.; van Beekveld, R. A. M.; Bonvin, A. M. J. J.; Lorent, J. H.; Lelli, M.; Nowick, J. S.;

MacGillavry, H. D.; Peoples, A. J.; Spoering, A. L.; Ling, L. L.; Hughes, D. E.; Roos, W. H.; Breukink, E.; Lewis, K.; Weingarth, M. Teixobactin Kills Bacteria by a Two-Pronged Attack on the Cell Envelope. *Nature* **2022**, *608*, 390–396.

10. Atkinson, D. J.; Naysmith, B. J.; Furkert, D. P.; Brimble, M. A. Enduracididine, a Rare Amino Acid Component of Peptide Antibiotics: Natural Products and Synthesis. *Beilstein J Org Chem* **2016**, *12*, 2325–2342.

11. Tsuji, S.; Kusumoto, S.; Shiba, T. Synthesis of Enduracididine, A Component Amino Acid of Antibiotic Enduracidin. *Chemistry Letters* **1975**, *4*, 1281–1284.

12. Sanière, L.; Leman, L.; Bourguignon, J.-J.; Dauban, P.; Dodd, R. H. Iminoiodane Mediated Aziridination of α-Allylglycine: Access to a Novel Rigid Arginine Derivative and to the Natural Amino Acid Enduracididine. *Tetrahedron* **2004**, *60*, 5889–5897.

13. Olson, D. E.; Su, J. Y.; Roberts, D. A.; Du Bois, J. Vicinal Diamination of Alkenes under Rh-Catalysis. *J. Am. Chem. Soc.* **2014**, *136*, 13506–13509.

14. Peoples, A.; Hughes, D.; Ling, L.; Millett, W.; Nitti, A.; Spoering, A.; Steadman, V.; Chiva, J.-Y.; Lazarides, L.; Jones, M.; Poullennec, K.; Lewis, K.; Epstein, S. Novel Depsipeptide and Uses Thereof, June 12, 2014.

15. Craig, W.; Chen, J.; Richardson, D.; Thorpe, R.; Yuan, Y. A Highly Stereoselective and Scalable Synthesis of L-Allo-Enduracididine. *Org. Lett.* **2015**, *17*, 4620–4623.

16. Giltrap, A. M.; Dowman, L. J.; Nagalingam, G.; Ochoa, J. L.; Linington, R. G.; Britton, W. J.; Payne, R. J. Total Synthesis of Teixobactin. *Org. Lett.* **2016**, *18*, 2788–2791.

17. Zong, Y.; Fang, F.; Meyer, K. J.; Wang, L.; Ni, Z.; Gao, H.; Lewis, K.; Zhang, J.; Rao, Y. Gram-Scale Total Synthesis of Teixobactin Promoting Binding Mode Study and Discovery of More Potent Antibiotics. *Nat Commun* **2019**, *10*, 3268.

18. Gangathade, N.; Nayani, K.; Bukya, H.; Mainkar, P. S.; Chandrasekhar, S. Scalable Synthesis of L-Allo-Enduracididine: The Unusual Amino Acid Present in Teixobactin. *Synlett* **2021**, *32*, 1465–1468.

19. Jones, C. R.; Guaglianone, G.; Lai, G. H.; Nowick, J. S. Isobactins: O-Acyl Isopeptide Prodrugs of Teixobactin and Teixobactin Derivatives. *Chem. Sci.* **2022**, *13*, 13110–13116.

20. Nicolaou, K. C.; Estrada, A. A.; Zak, M.; Lee, S. H.; Safina, B. S. A Mild and Selective Method for the Hydrolysis of Esters with Trimethyltin Hydroxide. *Angewandte Chemie International Edition* **2005**, *44*, 1378–1382.

21. Gao, B.; Chen, S.; Hou, Y. N.; Zhao, Y. J.; Ye, T.; Xu, Z. Solution-Phase Total Synthesis of Teixobactin. *Org. Biomol. Chem.* **2019**, *17*, 1141–1153.

22. Horn, A.; Kazmaier, U. Stereoselective Synthesis of a Protected Side Chain of Callipeltin A. *Org. Lett.* **2022**, *24*, 7072–7076.

23. Li, Y.; Miller, S. J. Chemoenzymatic Synthesis of Each Enantiomer of Orthogonally Protected 4,4-Difluoroglutamic Acid: A Candidate Monomer for Chiral Brønsted Acid Peptide-Based Catalysts. *J. Org. Chem.* **2011**, *76*, 9785–9791.

24. Hänchen, A.; Rausch, S.; Landmann, B.; Toti, L.; Nusser, A.; Süssmuth, R. D. Alanine Scan of the Peptide Antibiotic Feglymycin: Assessment of Amino Acid Side Chains Contributing to Antimicrobial Activity. *ChemBioChem* **2013**, *14*, 625–632.

25. Guaglianone, G.; Kreutzer, A. G.; Nowick, J. S. Chapter Five - Synthesis and Study of Macrocyclic β-Hairpin Peptides for Investigating Amyloid Oligomers. In *Methods in Enzymology*; Petersson, E. J., Ed.; Synthetic and Enzymatic Modifications of the Peptide Backbone; Academic Press, 2021; Vol. 656, pp 123–168.

Supporting Information for Chapter 4:

Efforts Towards the Synthesis of Teixobactin and Isobactins A, B, and C

Table of Contents

Supplementary figures

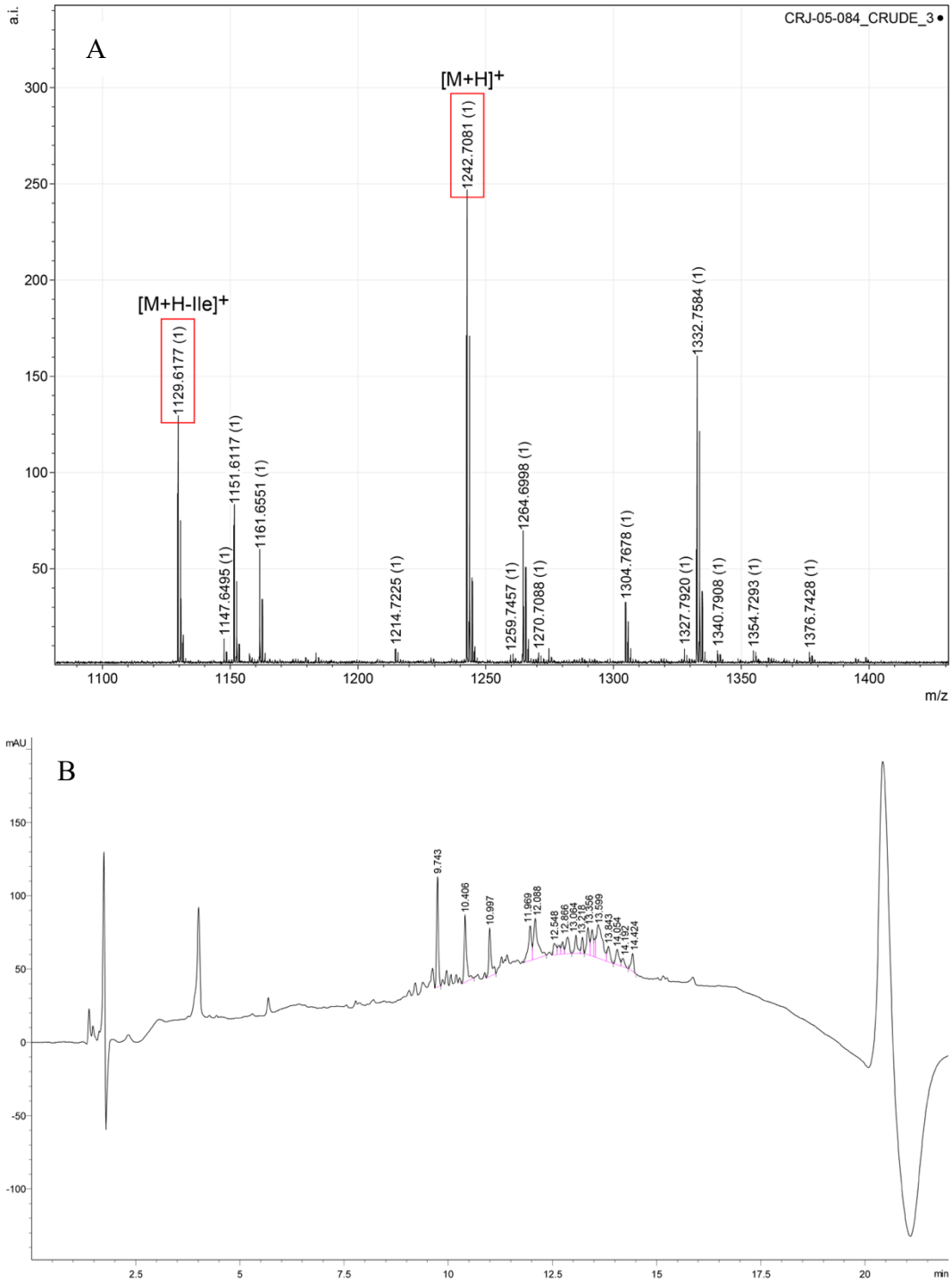

Figures S4.1. Data for CRJ-05-084 – natural teixobactin. (A) MALDI MS spectrum of crude lyophilized peptide labeled with the $[M+H]^+$ of the desired peptide product and Ile deletion peptide product. (B) Analytical RP-HPLC trace of the crude lyophilized peptide.

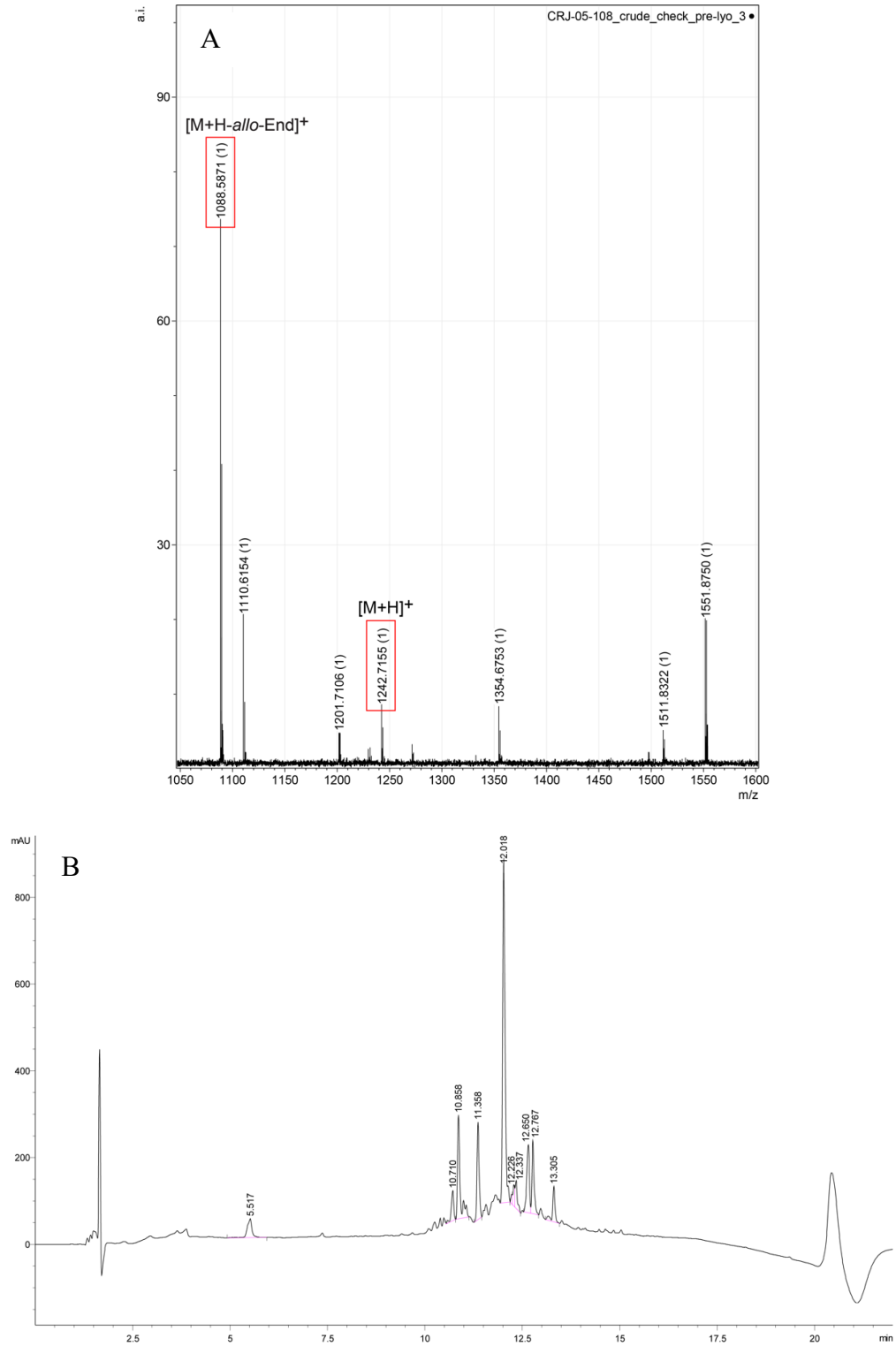

Figures S4.2. Data for CRJ-05-108 – isobactin A. (A) MALDI MS spectrum of crude lyophilized peptide labeled with the $[M+H]^+$ of the desired peptide product and *allo*-End deletion product. (B) Analytical RP-HPLC trace of the crude lyophilized peptide.

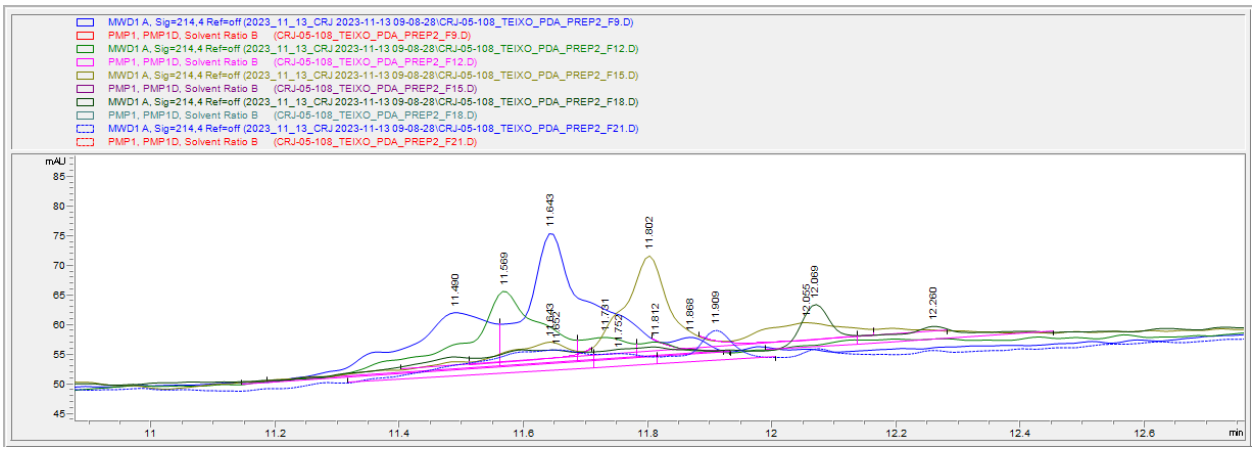

Figures S4.3. Overlay of fractions from preparative purification of CRJ-05-124 that all contained desired mass by MALDI MS.

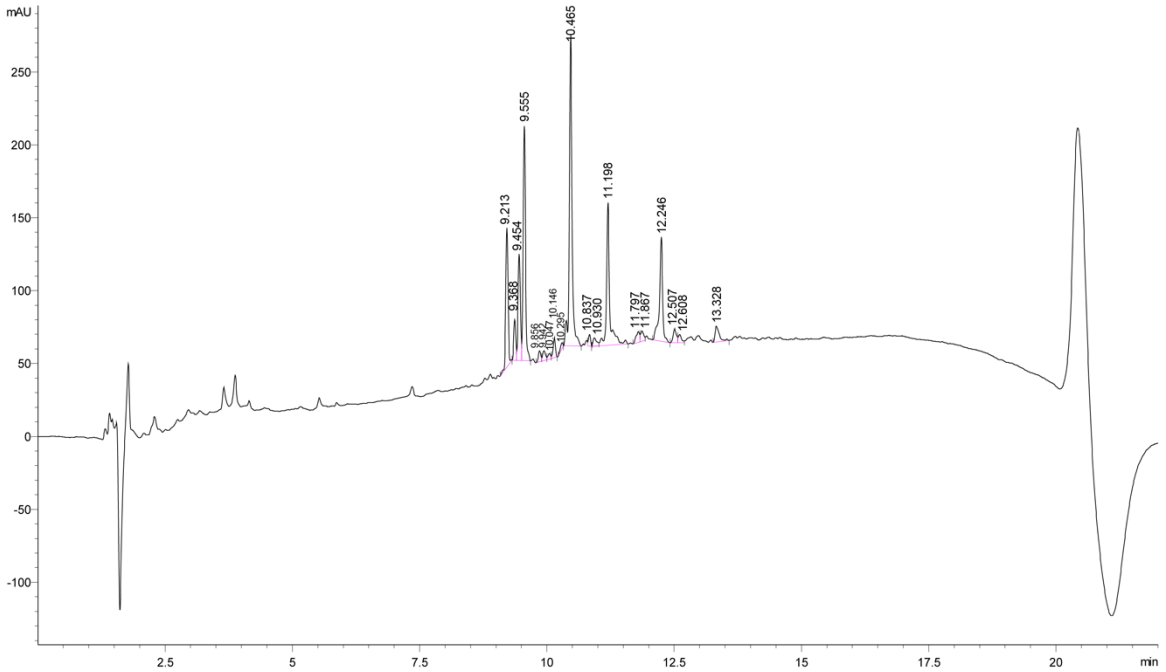

Figures S4.4. Data for CRJ-05-132 – isobactin B. Analytical RP-HPLC trace of the crude lyophilized peptide.

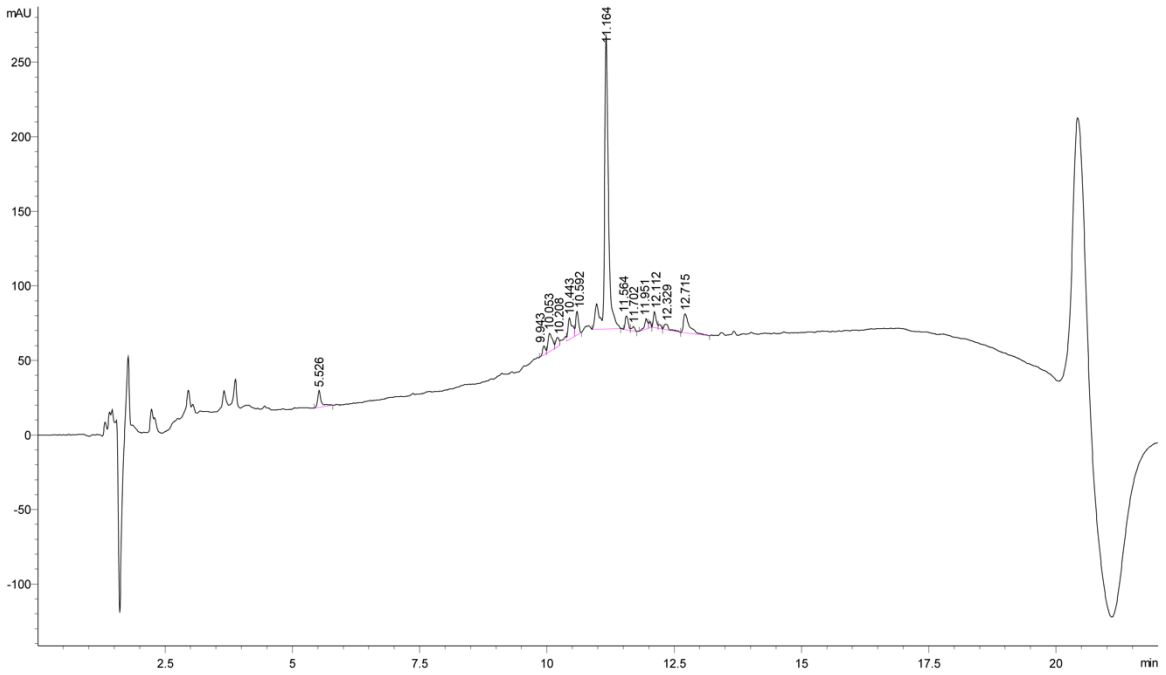

Figures S4.5. Data for CRJ-05-140 – isobactin C. Analytical RP-HPLC trace of the crude lyophilized peptide.

General Synthetic Procedures

General synthetic procedure for entries 1–6 in Table 4.1:

Methyl ester **4** (200 mg, 0.296 mmol, 1 equiv.) was added to a scintillation vial charged with a stir bar and dissolved in 0.75 mL THF. LiOH or KOH (3 equiv.) was dissolved in 0.25 mL H_2O and added to methyl ester **4**. The reaction was either performed on ice or at room temperature. After 1 h, the reaction was quenched with 1 mL of 1 M HCl. For entries 1–3 the products were not isolated, but the reaction mixtures were tracked and analyzed through LC-MS. The mass of these products corresponded to the starting material as no hydrolysis was observed for these products. For entries 4–6, the reactions were analyzed by LC-MS after quenching of the reaction and then carried on to the Fmoc protection described below.

General synthetic procedure for Fmoc protection of entries 4–6 in Table 4.1:

To solution was cooled to 0 °C using an ice bath and Fmoc-OSu (1.1 equiv.) dissolved in 1 mL THF was added followed by $NaHCO_3$ (5 equiv.). The reaction mixture was stirred on ice for 1 h, warmed to room temperature, and stirred for an additional 23 hours. The reaction was placed on ice and acidified to a pH of 3 with 1 M HCl. The material was concentrated by rotary evaporation to remove all THF. The resulting suspension was diluted with 10 mL EtOAc and transferred to a separatory funnel and the organic layer was collected; the aqueous layer was then extracted with EtOAc (2 x 10 mL). The combined organic layer was then dried with Na_2SO_4, decanted, and concentrated by rotary evaporation to a white solid. The crude material was analyzed by LC-MS and the mass corresponding to the Fmoc-deprotected carboxylic acid was observed. Products were not further purified, isolated, and analyzed.

General synthetic procedure for entries 1–3 in Table 4.2:

Methyl ester **4** (200 mg, 0.296 mmol, 1 equiv.) was added to a scintillation vial charged with a stir bar and dissolved in the corresponding solvent (3:1 THF:H_2O or MeCN) and cooled to 0 °C using an ice bath. To the cooled solution the corresponding base (piperidine or diethylamine) was added at the correct percentage. The products were not isolated, but the reaction mixtures were tracked through LC-MS. The appearance of the desired Fmoc-deprotected mass and the Cbz-deprotected mass were observed in all entries. Any attempts to subject to LiOH hydrolysis or Fmoc-protection following the above procedures led to no desired product as observed by LC-MS. Products were not further purified, isolated, and analyzed.

General synthetic procedure for entries 1–3 in Table 4.3:

Methyl ester **4** (100 mg, 0.148 mmol, 1 equiv.) was added to a scintillation vial charged with a stir bar and dissolved in either 0.74 mL or 0.19 mL THF and heated to 30 °C using an oil bath. To the reaction mixture, 6 M HCl (0.74 mL or 0.56 mL) was added dropwise, and the reaction was stirred for 24 h. The THF was removed from the reaction by rotary evaporation and the resulting suspension was transferred to a separatory funnel using 10 mL H_2O and the aqueous layer was washed with EtOAc (3 x 15 mL). The combined organic layer was then dried with Na_2SO_4, decanted, and concentrated by rotary evaporation to a yellow solid. The product was purified via flash chromatography in 12:1:1:0.5 EtOAc:MeOH:acetone:H_2O. The fractions were analyzed by TLC, indicating three distinct products. The fractions corresponding to each spot by TLC were combined and concentrated by rotary evaporation to afford white solids. Each product was analyzed by LC-MS to determine corresponding mass of each product and yields were calculated. It was determined that the major product from all entries was the Cbz-deprotected carboxylic acid. Products were not further analyzed.

General synthetic procedure for entries 1–7 in Table 4.4:

Methyl ester **4** (200 mg, 0.296 mmol, 1 equiv.) and Me_3SnOH (5 equiv.) were added to a 25-mL round bottom flask charged with a stir bar and dissolved in 1,2-DCE (6 mL) and heated to 40 °C using an oil bath. The reaction was then placed under N_2 atmosphere and allowed to stir. The reaction mixture was concentrated by rotary evaporation and the resulting material was resuspended in 15 mL EtOAc and transferred to a separatory funnel. The organic layer was then washed with 0.01 M $KHSO_4$ (2 x 15 mL) followed by brine (1 x 15 mL). The organic layer was then dried over Na_2SO_4, decanted, and concentrated by rotary evaporation to afford a white solid. The product was purified via flash chromatography (elution with 5:95 CH_3OH:CH_2Cl_2) to afford Fmoc-L-*allo*-End$(Cbz)_2$-OH as a white solid. Product was verified by LC-MS.